

NASA TECHNICAL  
MEMORANDUM

NASA TM X- 53453

July, 1966

NASA TM X-53453

FACILITY FORM 602	N 67-21520	
	(ACCESSION NUMBER)	(THRU)
	13 243 R 22/21	1
	(PAGES)	(CODE)
	TMX-53453	15
	(NASA CR OR TMX OR AD NUMBER)	(CATEGORY)

THE FABRICATION OF BERYLLIUM VOLUME VI:  
JOINING TECHNIQUES FOR BERYLLIUM ALLOYS

By R. F. Williams and S. E. Ingels

Manufacturing Research and Technology Division  
Manufacturing Engineering Laboratory

Available to NASA Offices, NASA  
Centers, and NASA Contractors  
Only.

NASA

*George C. Marshall  
Space Flight Center,  
Huntsville, Alabama*

~~\_\_\_\_\_~~  
~~\_\_\_\_\_~~  
~~\_\_\_\_\_~~



NASA-GEORGE C. MARSHALL SPACE FLIGHT CENTER

---

TECHNICAL MEMORANDUM X-53453

---

THE FABRICATION OF BERYLLIUM - VOLUME VI.

JOINING TECHNIQUES FOR BERYLLIUM ALLOYS

By R. F. Williams and S. E. Ingels

The other Volumes of Technical Memorandum X-53453 are:

- Vol. I.      A Survey of Current Technology
- Vol. II.     Forming Techniques for Beryllium Alloys
- Vol. III.    Metal Removal Techniques for Beryllium Alloys
- Vol. IV.     Surface Treatments for Beryllium Alloys
- Vol. V.      Thermal Treatments for Beryllium Alloys

MANUFACTURING ENGINEERING LABORATORY

## ACKNOWLEDGEMENT

The work accomplished to generate the information enclosed in this report was performed under Contract NAS8-11798 by Large Space Vehicle Programs, Space Systems Division, Lockheed Missiles and Space Company. The program encompasses the development and documentation of needed new manufacturing techniques and fabrication methods suitable for the application of beryllium and beryllium alloys in space flight vehicle structures.

Mr. R. F. Williams, NASA Advanced Manufacturing Programs, was the Project Manager of this effort under the management of Mr. S. T. Hart, Jr., Manager, NASA Advanced Development Programs, Lockheed Missiles and Space Company. The work was performed under the technical direction of Mr. S. E. Ingels, assisted by Mr. C. Fruth in preparation of the final report.



## TABLE OF CONTENTS (Cont'd)

	Page
4. Specimen Preparation . . . . .	218
5. Results and Discussion. . . . .	221
6. Diffusion and Bonding- Conclusions and Rec- ommendations . . . . .	226
SECTION IV. CONCLUSIONS AND RECOMMENDATIONS . . . . .	228
A. Mechanical Fasteners . . . . .	229
B. Adhesive Bonding . . . . .	229
C. Brazing . . . . .	230
D. Diffusion Bonding . . . . .	230
REFERENCES . . . . .	232

## LIST OF ILLUSTRATIONS

Figure	Title	Page
1.	Drill Fixture Consisting of Interchangeable Bases and Plates. Drilled Segments of One Specimen . . . . .	6
2.	Type I Joint Configuration - Nominal Dimensions . . . . .	10
3.	Type IA Specimens - Huckbolt Fasteners . . . . .	16
4.	Type IA Specimen - Tensile Test . . . . .	17
5.	Type IA Specimens - Typical Failure Mode . . . . .	18
6	Type IA Load-Deflection Curve - Specimen 201A-5. Note Slight Indication of Yield. . . . .	19
7.	Type IB Specimens - Jo-bolt Fasteners . . . . .	21
8.	Type IB Specimens - Tensile Test . . . . .	22
9.	Specimen 201B-2 Still Sustaining a Load of 4500 lbs. after Two Fasteners Had Sheared at 8220 lbs. . . . .	23
10.	Type IB Specimens - Typical Failure Mode . . . . .	25
11.	Type IB Load-Deflection Curve - Specimen 201B-5 . . . . .	26
12.	Type IC Specimens - 0.030-Inch Material - Cherry Blind Rivets . . . . .	27

# TABLE OF CONTENTS

	Page
SECTION I. INTRODUCTION . . . . .	1
SECTION II. GENERAL . . . . .	2
SECTION III. JOINING METHODS . . . . .	3
A. Mechanical Fasteners . . . . .	3
1. Introduction . . . . .	3
2. Specimen Preparation . . . . .	4
3. Type I Lap Joints	
Single Row Fasteners . . . . .	8
a. Type IA Huckbolts . . . . .	9
b. Type IB Jo-bolts . . . . .	15
c. Type IC - Cherry	
Blind Rivets . . . . .	24
d. Type ID Beryllium	
Rivets . . . . .	30
e. Type IE "Lockalloy"	
Rivets . . . . .	47
f. Type IF - Combina-	
tion Adhesive Bonding	
and Cherry Blind Rivets . . . . .	57
4. Type II Lap Joints - Double	
Row Fasteners . . . . .	60
a. Type IIA - Huckbolts . . . . .	70
b. Type IIB - Jo-bolts . . . . .	74
c. Type IIC - Cherry	
Blind Rivets . . . . .	74
d. Type IID - Beryllium	
Rivets . . . . .	84
e. Type IIE - "Lockalloy"	
Rivets . . . . .	92
f. Type IIF - Combination	
Adhesive Bonding and	
Cherry Blind Rivets . . . . .	97
5. Type III Lap Joints - Re-	
duced Sections . . . . .	105
a. Type IIIA - Huckbolts . . . . .	109
b. Type IIIB - Jo-bolts . . . . .	118

# TABLE OF CONTENTS (Cont'd)

	Page
c. Type IIIC - Cherry Blind Rivets . . . . .	122
d. Type IIID - Countersunk Beryllium Rivets . . . . .	122
6. Type IVA Lap Joints - Reduced Sections with Eccentric Joints . . . . .	134
a. Type IVA - Huckbolts . .	134
b. Type IVB - Jo-bolts . .	143
c. Type IVC - Cherry Blind Rivets . . . . .	149
d. Type IVD - Beryllium Rivets . . . . .	155
7. Mechanical Fasteners - Conclusions . . . . .	161
B. Adhesive Bonding. . . . .	163
1. Introduction . . . . .	163
2. Specimen Preparation. . . . .	165
3. Results and Discussion . . . . .	184
4. Adhesive Bonding - Conclusions and Recommendations . . . . .	188
C. Brazing . . . . .	189
1. Introduction . . . . .	189
2. Low Temperature Zinc Brazing . . . . .	190
a. Experimental Procedures .	190
b. Results and Discussion . .	196
3. Medium Temperature Alloy Brazing. . . . .	199
a. Plating Investigation - Substrate for Brazing . .	203
b. Experimental Procedures .	206
c. Results and Discussion . .	211
4. Brazing Conclusions and Recommendations . . . . .	211
D. Diffusion Bonding . . . . .	215
1. Introduction. . . . .	215
2. Background. . . . .	216
3. Experimental Procedures . . .	218

# LIST OF ILLUSTRATIONS (Cont'd)

Figure	Title	Page
13.	Type IC Specimen - 0.030-Inch Material - Tensile Test . . . . .	28
14.	Type IC Specimen - 0.060-Inch Material - Tensile Test . . . . .	29
15.	Type IC Specimens - 0.030-Inch Material - Typical Failure Mode . . . . .	31
16.	Type IC Specimens - 0.060-Inch Material - Typical Failure Mode . . . . .	32
17.	Type IC Load-Deflection Curve - Specimen 201C-7. Note Load Reversal . . . . .	33
18.	Rivet Configurations - Beryllium and "Lockalloy" . . . . .	34
19.	Rivet Installation - Instron Test Machine . . . . .	37
20.	Thermal Gradient in Beryllium Specimens During Installation of Beryllium Rivets . . . . .	39
21..	Type ID Specimen - Installed Beryllium Rivet . . . . .	40
22.	Type ID Specimens - 0.030-Inch Material - Beryllium Rivets . . . . .	41
23.	Type ID Specimen - 0.030-Inch Material - Tensile Test . . . . .	42
24.	Type ID Specimen - 0.060-Inch Material - Tensile Test . . . . .	43

# LIST OF ILLUSTRATIONS (Cont'd)

Figure	Title	Page
25.	Type ID Specimens - 0.030-Inch Material - Typical Failure Mode . . . . .	44
26.	Type ID Specimens - 0.060-Inch Material - Typical Failure Mode . . . . .	45
27.	Type ID Load-Deflection Curve - Specimen 201D-3. Note Linear Trace. . . . .	46
28.	Thermal Gradient in Beryllium Specimens During Installation of "Lockalloy" Rivets . . . .	49
29.	Type IE Specimen - Installed "Lockalloy" Rivet. Note Smooth Grain Orientation. . . . .	51
30.	Type IE Specimens - 0.030-Inch Material - "Lockalloy" Rivets . . . . .	52
31.	Type IE Specimen - 0.030-Inch Material - Tensile Test . . . . .	53
32.	Type IE Specimens - 0.030-Inch Material - Typical Failure Mode . . . . .	54
33.	Type IE Specimens - 0.060-Inch Material - Typical Failure Mode . . . . .	55
34.	Type IE Load-Deflection Curve - Specimen 201E-2 . . . . .	56
35.	Type IF Specimens - 0.030-Inch Material - Adhesive Bonding and Cherry Blind Rivets . . .	58
36.	Type IF Specimens - 0.060-Inch Material - Adhesive Bonding and Cherry Blind Rivets . . .	59

# LIST OF ILLUSTRATIONS (Cont'd)

Figure	Title	Page
37.	Type IF Specimens - 0.030-Inch Material - Typical Failure Mode . . . . .	61
38.	Type IF Specimens - 0.060-Inch Material - Typical Failure Mode . . . . .	62
39.	Type II Joint Configuration - Nominal Dimensions . . . . .	65
40.	Type IIA Specimens - Huckbolt Fasteners . . .	71
41.	Type IIA Specimen - Tensile Test . . . . .	72
42.	Type IIA Specimens - Typical Failure Mode. . . . .	73
43.	Type IIB Specimens - Jo-bolt Fasteners . . .	75
44.	Type IIB Specimen - Tensile Test . . . . .	76
45.	Type IIB Specimens - Typical Failure Mode . . . . .	77
46.	Type IIC Specimens - 0.060-Inch Material - Cherry Blind Rivets. . . . .	79
47.	Type IIC Specimen - 0.030-Inch Material - Tensile Test . . . . .	80
48.	Type IIC Specimen - 0.060-Inch Material - Tensile Test . . . . .	81
49.	Type IIC Specimens - 0.030-Inch Material - Typical Failure Mode . . . . .	82
50.	Type IIC Specimens - 0.060-Inch Material - Typical Failure Mode . . . . .	83

# LIST OF ILLUSTRATIONS (Cont'd)

Figure	Title	Page
51.	Type IIC Load-Deflection Curve -Specimen 202C-6. Note Load Reversal. . . . .	85
52.	Type IID Specimens - 0.006-Inch Material - Beryllium Rivets. Note Original and Upset Head Configurations. . . . .	86
53.	Type IID Specimens - 0.060-Inch Material - Beryllium Rivets . . . . .	87
54.	Type IID Specimen - 0.030-Inch Material - Tensile Test . . . . .	89
55.	Type IID Specimens - 0.030-Inch Material - Typical Failure Mode . . . . .	90
56.	Type IID Specimens - 0.060-Inch Material - Typical Failure Mode . . . . .	91
57.	Type IID Load-Deflection Curve - Specimen 202D-6. Note Lack of Yield Indication. . . . .	93
58.	Type IIE Specimens - 0.060-Inch Material - "Lockalloy" Rivets . . . . .	94
59.	Type IIE Specimen - 0.030-Inch Material - Tensile Test . . . . .	95
60.	Type IIE Specimen - 0.060-Inch Material - Tensile Test . . . . .	96
61.	Type IIE Specimens - 0.030-Inch Material - Typical Failure Mode . . . . .	98
62.	Type IIE Specimens - 0.060-Inch Material - Typical Failure Mode. Note "Clean" Shearing of the Rivets. . . . .	99



## LIST OF ILLUSTRATIONS (Cont'd)

Figure	Title	Page
63.	Type IIE Load-Deflection Curve - Specimen 202E-8 . . . . .	100
64.	Type IIF Specimens - 0.030-Inch Material- Adhesive Bonding and Cherry Blind Rivets. Note Radial Cracks at Rivet in Specimen 202F-2 . . . . .	101
65.	Type IIF Specimens - 0.060-Inch Material - Adhesive Bonding and Cherry Blind Rivets . . .	102
66.	Type IIF Specimen - 0.030-Inch Material - Tensile Test. Note Bond Failure . . . . .	103
67.	Type IIF Specimen - 0.060-Inch Material - Tensile Test. Note Bond Failure and Rivet "Tilting." . . . . .	104
68.	Type IIF Specimens - 0.060-Inch Material - Typical Failure Mode . . . . .	106
69.	Type IIF Specimens - 0.060-Inch Material - Typical Failure Mode. . . . .	107
70.	Type IIF Load-Deflection Curve - Specimen 202F-10 . . . . .	108
71.	Type III Joint Configuration - Nominal Dim- ensions . . . . .	111
72.	Type IIIA Specimens - Huckbolt Fasteners . . .	115
73.	Type IIIA Specimen - Tensile Test. . . . .	116
74.	Type IIIA Specimens - Typical Failure Mode. Note Secondary Fractures into the 0.060-Inch Section. . . . .	117

# LIST OF ILLUSTRATIONS (Cont'd)

Figure	Title	Page
75.	Type IIIB Specimens - Jo-bolt Fasteners . . .	119
76.	Type IIIB Specimen - Tensile Test. . . . .	120
77.	Type IIIB Specimens - Typical Failure Mode . . . . .	121
78.	Type IIIC Specimens - Cherry Blind Rivets. . . . .	123
79.	Type IIIC Specimen - Tensile Test . . . . .	124
80.	Type IIIC Specimens - Typical Failure Mode . . . . .	125
81.	Type IIID Specimens - Beryllium Rivets . . .	126
82.	Type IIID Specimen - Beryllium Rivet Installation. Note Full Deformation of Center Rivet into the 60° Countersunk Hole. . . . .	128
83.	Type IIID Specimens - Countersunk Beryl- lium Rivets. Rivets Ground Flush on Both Sides. . . . .	129
84.	Type IIID Specimen - Countersunk Beryl- lium Rivets. Close-up of Flush Ground Rivets . . . . .	130
85.	Type IIID Specimen - Double Countersunk Beryllium Rivet. . . . .	131
86.	Type IIID Specimen - Tensile Test. . . . .	132
87.	Type IIID Specimens - Typical Failure Mode . . . . .	133

# LIST OF ILLUSTRATIONS (Cont'd)

Figure	Title	Page
88.	Type IIID Load-Deflection Curve - Specimen 203D-5 Double Flush Counter-Sunk Beryllium Rivets. Note Load Release Point. . . . .	135
89.	Type IIID Load-Deflection Curve - Specimen 203D-4. Double Countersunk Beryllium Rivets - "As Forged" - not Flush Ground . . .	136
90.	Type IV Joint Configuration - Nominal Dimensions . . . . .	138
91.	Type IVA Specimens - Huckbolt Fasteners . . .	142
92.	Type IVA Specimen - Tensile Test . . . . .	144
93.	Type IVA Specimens - Typical Failure Mode . . . . .	145
94.	Type IVB Specimens - Jo-bolt Fasteners . . .	146
95.	Type IVB Specimen - Tensile Test . . . . .	147
96.	Type IVB Specimens - Typical Failure Mode . . . . .	148
97.	Type IVC Specimens - Cherry Blind Rivets . . . . .	150
98.	Type IVC Specimen - Tensile Test . . . . .	151
99.	Type IVC Specimens - Typical Failure Mode . . . . .	152
100.	Type IVC Specimens - Typical Failure Mode . . . . .	153
101.	Type IVC Load-Deflection Curve - Specimen 204C-3. Note Load Reversal. . . . .	154

# LIST OF ILLUSTRATIONS (Cont'd)

Figure	Title	Page
102.	Type IVD Specimens - Countersunk Beryllium Rivets "As Forged" Rivet Heads . . . . .	156
103.	Type IVD Specimens - Countersunk Beryllium Rivets. Rivets Ground Flush on Both Sides . . . . .	157
104.	Type IVD Specimens - Countersunk Beryllium Rivets. Close-up of Flush Ground Rivets . . . . .	158
105.	Type IVD Specimen - "As Forged" Beryllium Rivets - Tensile Test. . . . .	159
106.	Type IVD Specimens - Typical Failure Mode . . . . .	160
107.	Type IVD Load-Deflection Curve - Specimen 204D-3. Note Lack of Yield Indication . .	162
108.	Adhesive Bonded Joint Configuration - Nominal Dimensions . . . . .	168
109.	Adhesive Bonded Joints - Test Summary . . .	170
110.	Completed 0.020-Inch Segments - Ready for Cleaning and Bonding . . . . .	174
111.	Assembly Fixture and One Shim. Five Specimens May be Bonded Simultaneously . . . .	176
112.	First Step in the Assembly of Adhesive Bonded Test Specimens . . . . .	177
113.	Second Step in the Assembly of Adhesive Bonded Test Specimens . . . . .	178

# LIST OF ILLUSTRATIONS (Cont'd)

Figure	Title	Page
114.	Third Step in the Assembly of Adhesive Bonded Test Specimens . . . . .	180
115.	Bonding Fixture and Assembled Test Specimens in Vacuum Bag . . . . .	181
116.	Adhesive Bonded Specimens . . . . .	182
117.	Test Fixture and Adhesive Bonded Specimen . .	183
118.	Reinforced 0.060-Inch Test Specimens with an Unreinforced 0.120-Inch Test Specimen. . .	185
119.	Adhesive Bonded Specimen - Tensile Test . . .	186
120.	Adhesive Bonded Specimens - FM-1000 Adhesive - 0.120-Inch Material - Typical Failure Mode . . . . .	187
121.	Contact Angle at Junction - Zinc on Beryllium -200X. Nickel-Copper-Zinc-Beryllium Interface . . . . .	193
122.	Plated Beryllium Cross-Section - 200X Nickel-Copper-Zinc-Beryllium Interface . . . . .	193
123.	Zinc-Beryllium Interface - 1040X . . . . .	195
124.	Zinc-Beryllium Interface - 1040X. . . . .	195
125.	Zinc Brazed Lap Shear Joint - Test Specimen . . . . .	197
126.	Zinc Brazed Lap Shear Joint - Approximately 14X . . . . .	200
127.	Zinc-Beryllium Interface - Sound Braze Area - 1040X . . . . .	201

# LIST OF ILLUSTRATIONS (Cont'd)

Figure	Title	Page
128.	Zinc-Beryllium Interface - Discontinuous Braze Area - 1040X . . . . .	202
129.	Beryllium and Stainless Steel Test Seg- ments . . . . .	207
130.	Brazing Fixture and Lap Gage . . . . .	209
131.	Brazing Fixture and Specimen Segments. Lap Gage in Use . . . . .	210
132.	Plated Beryllium - Ready for Brazing - 1000X . . . . .	214
133.	Beryllium-to-Beryllium Solid-State Diffusion 500X . . . . .	214
134.	Thermal-Mechanical Characteristics of Hot- Pressed QMV Beryllium Block . . . . .	219
135.	Diffusion Bonded QMV Beryllium Test Speci- mens . . . . .	223
136.	Specimen A - Beryllium Solid-State Diffusion Bonded at 1112°F - 500X . . . . .	224
137.	Specimen A - Showing Products of the Inter- facial Reaction between Beryllium and Copper - 3000X . . . . .	225
138.	Specimen A - Adjacent Bonded and Unbonded Areas . . . . .	227

# LIST OF TABLES

Table	Title	Page
I.	Chemical Analysis and Mechanical Properties - Material for Single Row Mechanical Fastener Specimens . . . . .	7
II.	Fasteners - Type and Ultimate Single Shear Strength . . . . .	8
III.	Type I Specimens - Test Summary . . . . .	11
IV.	Steel Development Samples - Beryllium Rivets . . . . .	36
V.	Steel Development Samples - "Lockalloy" Rivets . . . . .	48
VI.	Chemical Analysis and Mechanical Properties - Material for Double Row Mechanical Fastener Specimens . . . . .	63
VII.	Type II Specimens - Test Summary . . . . .	66
VIII.	Chemical Analysis and Mechanical Properties - Material for Type III Mechanical Joints . . .	100
IX.	Type III Specimens (1) - Test Summary . . . . .	112
X.	Chemical Analysis and Mechanical Properties - Material for Type IV Mechanical Joints . . . .	137
XI.	Type IV Specimens (1) - Test Summary . .	139
XII.	Cure Cycles and Shear Strengths - Selected Adhesives . . . . .	164

# LIST OF TABLES (Cont'd)

Table	Title	Page
XIII.	Chemical Analyses and Mechanical Properties - Material for Adhesive Bonded Specimens . . . . .	166
XIV.	Adhesive Bonded Specimens - Failure Modes . . . . .	169
XV.	Brazed Specimens - Low Temperature Zinc Brazing - Test Summary . . . . .	198
XVI.	Brazed Specimens - Lap Shear Brazes on Nickel Plated Beryllium - Test Summary . . . . .	212
XVII.	Time - Temperature - Pressure Cycles - Diffusion Bonded Beryllium . . . . .	221



# TECHNICAL MEMORANDUM X-53453

## THE FABRICATION OF BERYLLIUM - VOLUME VI.

### JOINING TECHNIQUES FOR BERYLLIUM ALLOYS

#### SECTION I. INTRODUCTION

The objectives of this task are the investigation, development, and documentation of the beryllium fabrication operations classified as "Joining" in the Beryllium Fabrication Methods Development Program Plan.

For many years the full realization of the potential advantages of beryllium in the fabrication of aerospace vehicle structures was delayed pending the ready availability of sheet material and structural shapes, such as extrusions and forgings, in sizes compatible with design requirements. The desired beryllium sheet material and structural shapes are now available, but the lack of suitable production joining techniques and processes still inhibits the wide adoption of beryllium in the fabrication of large space vehicle structures.

Although several potentially suitable joining methods were investigated and evaluated, the mechanical fastener method of joining beryllium to itself or to other material is considered to be most applicable to routine production operations. The several types of mechanical fasteners selected for this study, and used in assembling the test specimens in both single and double row configurations, included:

- a. NAS 2006-V4 Huckbolts
- b. NAS 1671-3 Jo-bolts
- c. MS 20600-M5 Cherry Blind Rivets
- d. Beryllium Rivets
- e. "Lockalloy" Rivets



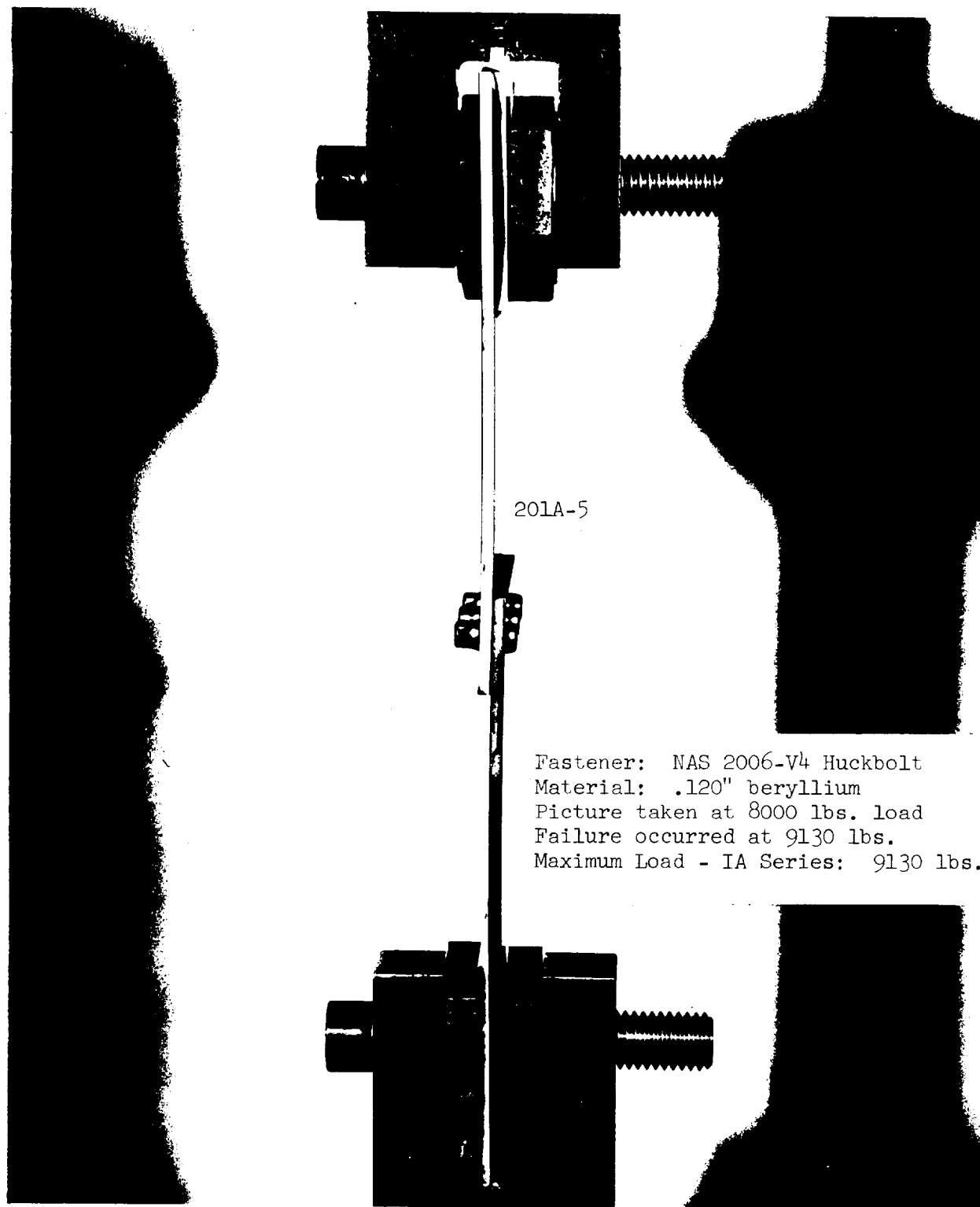


FIGURE 4. TYPE IA SPECIMEN - TENSILE TEST

Except for items d and e, all of the fasteners were high-strength 6 AC-4V, A286 steel, and monel materials.

The accomplishment of this task, directed toward the development of both engineering and production information and data was divided into logical sub-tasks as follows:

1. Mechanical Fasteners, including combination bonding and riveting.
2. Adhesive Bonding.
3. Brazing.
4. Diffusion bonding.

## SECTION II. GENERAL

The material utilized in the accomplishment of the tasks included in this phase of the program was purchased either from The Brush Beryllium Company of Cleveland, Ohio, or from The Beryllium Corporation of Reading, Pennsylvania. The cross-rolled sheet was purchased in accordance with the specification requirements and contained the following minimum specified material properties:

- |               |              |
|---------------|--------------|
| a. $F_{tu}$   | - 70,000 psi |
| b. $F_{ty}$   | - 50,000 psi |
| c. Elongation | - 5%         |

The vacuum hot-pressed block material, used in machining the diffusion bonding specimens, was purchased in accordance with the specification requirements; the minimum specified material properties are:

- |               |              |
|---------------|--------------|
| a. $F_{tu}$   | - 40,000 psi |
| b. $F_{ty}$   | - 30,000 psi |
| c. Elongation | - 1%         |

The beryllium and Lockalloy rod material from which the rivets were machined was procured in accordance with the vendor's specifications. The vendor's certified material properties data is included in the discussion of the individual tasks.

Either the standard manufacturing procedures, or the fabrication techniques developed during the course of this program, were utilized in the fabrication of all of the test specimens. The results obtained during this investigation therefore, can be considered representative of the results that would be obtained during normal production operations.

Due to the many facets of this task, the several joining techniques and configurations are reported separately.

### SECTION III. JOINING METHODS

During this phase of the program, several types of fasteners, joint configurations, and joining methods were investigated to augment previously developed data (References 2 and 5) and to develop finite data in new areas not previously investigated. The principle effort was directed toward the testing and evaluation of both high-strength blind fasteners, and lightweight hot-upset beryllium and "Lockalloy" fasteners. Other joining methods including adhesive bonding, a combination of adhesive bonding and riveting, brazing, and diffusion bonding were investigated at a lower level of effort.

All technical data, descriptive material, illustrations, discussions and conclusions are presented for each joining category.

#### A. MECHANICAL FASTENERS

1 Introduction. The single lap shear type of joint was selected for this investigation. This joint not only is the most widely used configuration in aerospace structures, but it also is subjected to the most severe loading conditions. Four basic configurations, utilizing several different fasteners in both single and double row patterns, were selected to provide a basis for the evaluation of their relative efficiencies. Tabulated pertinent

dimensions, and sketches are included in the individual type group sections.

The loading of a lap joint introduces eccentricity and joint rotation which results in the failure of the joint at loads less than the capacity of a joint that has a straight load path. This joint rotation is clearly illustrated in Figures 8 and 14. The considerable "tilting" of the fastener that occurs as the ultimate load is approached also is clearly evident. This "tilting" induces localized bending stress in the beryllium in addition to that caused by the eccentricity, so that in most cases, the beryllium fails due to the combined tension, bending and bearing stresses at the fasteners. The net tension stress at the fasteners has been included in the tabulated joint test data for comparison. This value was simply computed as the ultimate load divided by the net tension area; any bending stress was neglected. In the development of an efficient joint design, the tensile and bearing strength of the material should be balanced with the fastener shear strength. Due to the unavoidable eccentricity of the lap joint, this derived net tensile stress usually will be less than the tensile yield strength of the material itself.

In order to compare and evaluate the relative efficiencies of lap shear joints with either single or double rows of identical fasteners, both types were included in this investigation. A 10,000-pound capacity "Instron" research tensile testing machine with autographic recording was used during the initial testing phase of these joints.

Due to the limited capacity of the "Instron" machine, a 60,000-pound capacity "Riehle" hydraulic tensile testing machine was used for testing the joints fabricated of heavier gage materials and high-strength fasteners. Special vise grips, in lieu of loading pins, were utilized to avoid the failure of the test specimens in the loading pin holes

2. Specimen Preparation. Current standard production methods were utilized for the production of the test specimen components. The layout of the test specimens was oriented so that both segments of a given specimen were cut in the same direction in order to aid in the reduction of data scatter; i.e., longitudinal-to-longitudinal and transverse-to-transverse segments were joined

together. All of the segments were identified during the initial layout on full-size vellum sheets and this identification was maintained throughout the program. The layout, including the identifying numbers, was transferred to the sheet material, and the parts were cut to size on the precision abrasive cut-off saw.

The pairs of segments then were "tornetically" drilled in a special drill fixture consisting of two interchangeable bases and three interchangeable drill plates. The selection of the desired combination of base and drill plate permitted the preparation of all of the mechanical fastener test specimens with a minimum of tooling. The bases, drill plates, and the two segments of a drilled specimen are illustrated in Figure 1. The use of this fixture also assured the proper alignment of the fasteners, and the subsequent control of the load path during the testing operations.

Due to the normal cutting tolerance, all of the panel segments were not precisely the same width. However, these minor dimensional differences were not considered to be critical in the fabrication and assembly of the specimens and, therefore, no additional costly steps were taken to machine the matching segments to identical dimensions. However, the exact dimensions were utilized in the calculations of the net stresses. Either the net cross-sectional area of the beryllium segment that failed was used or, if only the fasteners failed, the lesser of the net cross-sectional areas of the two beryllium segments was used. Thus, the calculated strengths of the various types of joints will be conservative.

The 0.750-inch diameter loading pin hole was pilot drilled in the drill jig, as may be seen in Figure 1, and subsequently was enlarged in the EDM (Electrical Discharge Machining) machine.

Because local stress concentrations must be eliminated, a micrometer stop countersink was used to chamfer all holes 45 degrees by 0.015 inch on one side to provide the necessary clearance for the head-to-shank radius of the fasteners. After the mechanical operations were completed, all of the beryllium parts were etched in a solution consisting of 3 percent HF (hydrofluoric acid) and 45 percent  $\text{HNO}_3$  (nitric acid) to remove

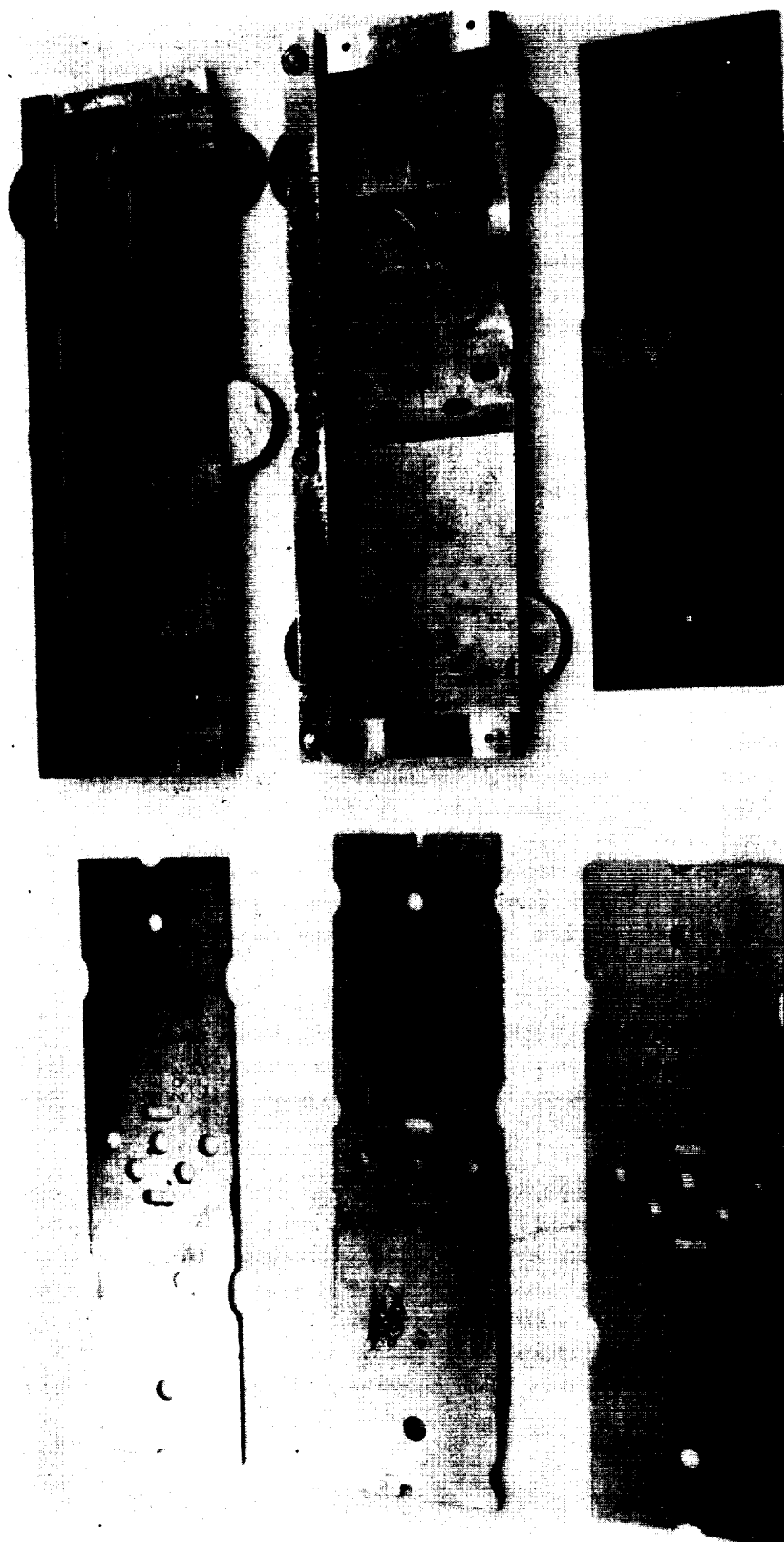


FIGURE 1. DRILL FIXTURE CONSISTING OF INTERCHANGEABLE BASES AND PLATES. DRILL SEGMENTS OF ONE SPECIMEN.



TABLE I  
CHEMICAL ANALYSIS AND MECHANICAL PROPERTIES - MATERIAL FOR SINGLE ROW MECHANICAL FASTENER SPECIMENS  
VENDOR DATA

Vendor: The Brush Beryllium Company  
Lot No.: 3516

CHEMICAL ANALYSIS - %

Be Assay	BeO	Fe	Si	Al	Mg	C
98.21	1.70	0.14	0.04	0.11	0.008	0.13

NOTE: Cr, Mn, Ni LESS THAN 0.04% EACH

MECHANICAL PROPERTIES

Type Joint	Gage Inch	Sheet No.	Test Direction	Fty PSI	Ftu PSI	Elongation % in 1"
IA	0.120	1064A2	L T	63,300 60,400	85,000 82,100	16 18
IA	0.120	1065A1	L T	61,400 60,300	81,100 82,100	10 18
IA	0.120	1065B1	L T	62,200 59,700	84,600 80,300	16 15
IA, IB	0.120	1066A2	L T	60,900 58,400	84,600 80,000	18 10
IC, IE, IF	0.030	1069B2	L T	61,000 60,700	79,900 81,100	10 24
IC, ID, IE, IF	0.030	1070B	L T	62,500 59,900	85,300 80,300	15 15
IC, ID, IE	0.060	1068A	L T	61,800 58,700	82,900 81,000	10 23
IF	0.060	1067B2	L T	58,600 61,100	80,200 80,200	12 18

at least 0.002 inch of material from all surfaces. This etching is mandatory for all highly stressed parts; all surface imperfections such as irregularities, micro-cracks, etc., must be removed to avoid compromising the integrity of the parts.

The double step from 0.090 inch to 0.075 inch to 0.060 inch in the Type III and Type IV parts was produced by chemical milling.

In order to provide the necessary bearing at the loading pin and to reduce the eccentricity in the joint during the testing, aluminum reinforcement plates of appropriate thicknesses were fabricated and bonded to the beryllium test segments. The reinforcement pads were bonded to the test specimens with Bloomingdale FM-1000 adhesive, cured for one hour at 350°F in a reduced atmosphere of 2.7 psia supplemented with a pressure of 25 psig in a nitrogen environment pressure chamber for a total effective pressure of 37 psi on the joint. Prior to the attachment of the reinforcement pads, all of the critical dimensions were measured and recorded for later use in the calculation of the stresses.

3. Type I Lap Joints - Single Row Fasteners. Table I presents the chemical analyses and the mechanical properties of the material procured from The Brush Beryllium Company for the fabrication, testing and evaluation of the single row configuration mechanically fastened joints. The specific utilization of each of the several sheets of material is identified by the type numbers of the specimens.

The ultimate shear strengths of the various fasteners are as follows:

TABLE II

Fasteners - Type and Ultimate Single Shear Strength

NAS 2006-V4 Huckbolt	2690 lbs.
NAS 1671-3 Jo-bolt	2265 lbs.
MS 20600-M5 Cherry Blind Rivet	1090 lbs.
Beryllium Rivet (0.159-inch Dia.)	1050 lbs.

TABLE II (Cont'd)

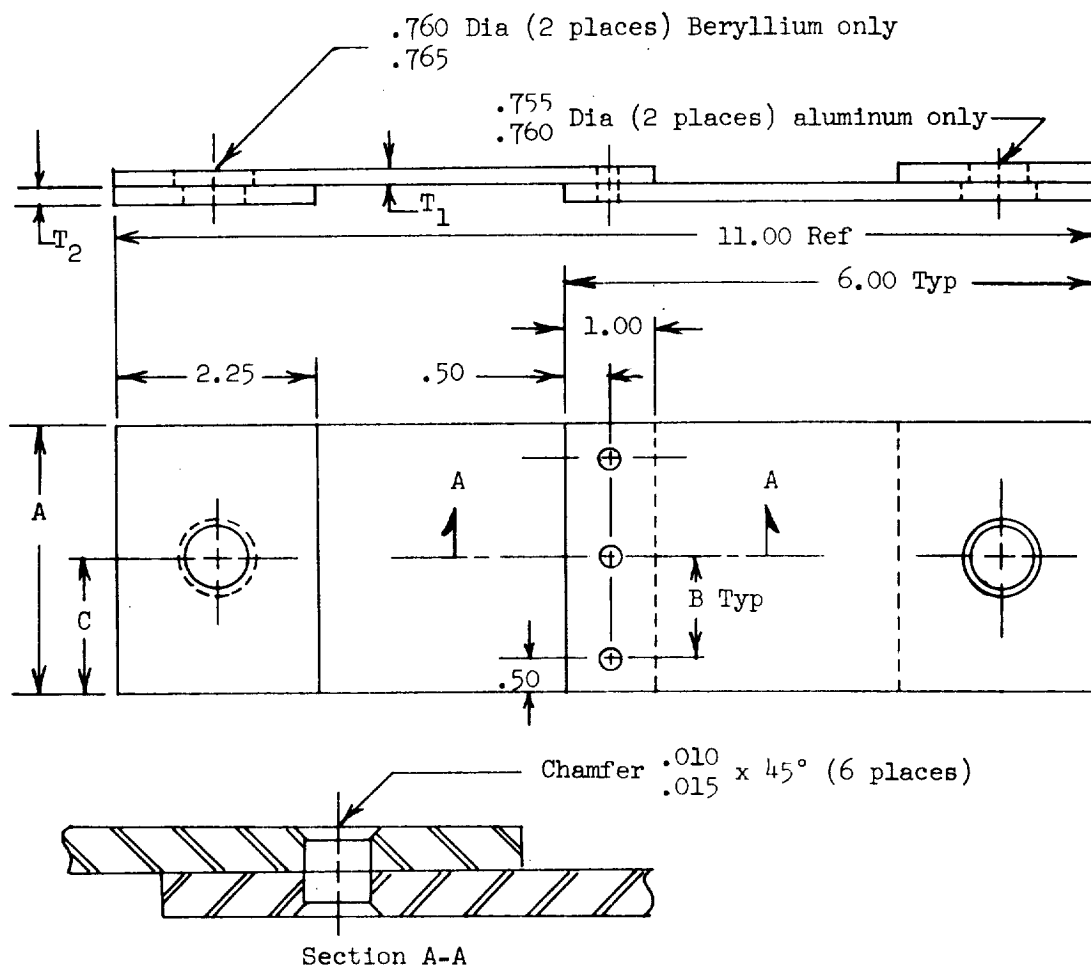
"Lockalloy" Rivet (0.159-inch Dia.) 755 lbs.

NOTE: The shear strengths of the beryllium and of the "Lockalloy" rivets which were determined during the testing of the steel development samples, will be discussed in the sections on Type ID - Beryllium Rivets, and Type ID - "Lockalloy" Rivets.

The configuration and the nominal dimensions of the "201" Type I joints are illustrated in Figure 2. A summary of the test loads, stresses, and modes of failure is presented in Table III.

a. Type IA-Huckbolts. The objective of this investigation was the evaluation of the feasibility of joining beryllium structures with high-strength blind fasteners which subject the material to an appreciable shock load at the instant of stem separation. Due to the notch sensitivity of beryllium, and the attendant susceptibility to failure during fastener installation if normal interference fits are used, a small radial clearance was provided between the fastener and the hole wall.

The diameters of ten randomly selected NAS 2006-V4 Huckbolts ranged from 0.1888 inch to 0.1891 inch; the average diameter was 0.1889 inch. As this type of fastener does not expand during installation, the fastener diameter rather than the hole diameter establishes the bearing stress. The diameters of the finished holes in the beryllium segments ranged, after etching, from 0.190 inch to 0.194 inch. However, the maximum difference in any single segment did not exceed 0.002 inch. The actual diameters of the holes were used in calculating the net tensile stress; the average diameter of the Huckbolts was used in calculating the bearing stress.



Conf.	Fastener Type	Hole Dia.	Mat'l Gage		Dimension		
			T1	T2	A	B	C
A	Huckbolt (NAS 2006-V4)	.189-.193	.12	.12	3.25	1.125	1.625
B	Jo-Bolt (NAS 1671-3)	.199-.202	.12	.12	3.25	1.125	1.625
C	Cherry Rivet (MS 20600-M5)	.158-.164	.03/.06	.03/.06	3.00	1.00	1.50
D	Beryllium Rivet	.160-.164	.03/.06	.03/.06	3.00	1.00	1.50
E	Lockalloy Rivet	.160-.164					
F	Cherry Rivet/Bonded	.158-.164					

NOTE: ALL DIMENSIONS ARE IN INCHES.

FIGURE 2. TYPE I JOINT CONFIGURATION - NOMINAL DIMENSIONS

TABLE III  
TYPE I SPECIMENS - TEST SUMMARY

Specmn No.	Sheet Thkns	Area (in <sup>2</sup> )(2)		Ult Load (PSI)	Fasteners		Tension Stress (PSI)		Avg Bearing Stress at Fastrs(PSI) (3)(14)	Notes
		Full Sectn	At Fastrs		No.	lbs/Fastr (4)	Full Sectn (13)	Net Sectn at Holes (12)		
201A-1	0.1265	SAMPLE - NOT TESTED		TESTED	3					5
201A-2	0.1225	0.4103	0.3409	8820	3	2940	21,356	25,872	123,012	8
201A-3	0.1270	0.4000	0.3292	8860	3	2953	22,150	26,914	127,628	8
201A-4	0.1275	0.4111	0.3379	8960	3	2987	21,795	26,517	124,496	7
201A-5	0.1225	0.4157	0.3418	9130	3	3043	21,963	26,712	126,332	8
201B-1	0.1220	0.3293	0.3197	8470	3	2823	21,591	26,494	116,282	10
201B-2	0.1230	0.3928	0.3192	8375	3	2792	21,321	26,237	115,454	10
201B-3	0.1240	SAMPLE - NOT TESTED		TESTED	3					7
201B-4	0.1230	0.3986	0.3242	8460	3	2820	21,224	26,095	115,669	10
201B-5	0.1240	0.4028	0.3277	8530	3	2843	21,177	26,030	115,677	5
201C-1	0.0326	SAMPLE - NOT TESTED		TESTED	3					7
201C-2	0.0300	0.0984	0.0827	1740	3	580	17,683	21,040	110,828	7
201C-3	0.0300	0.0894	0.0751	1825	3	608	20,414	24,301	127,622	7
201C-4	0.0310	0.0903	0.0759	1940	3	647	21,484	25,560	134,722	7
201C-5	0.0625	0.0925	0.0777	1870	3	623	20,216	24,067	125,503	9
201C-6	0.0635	0.1886	0.1588	3000	3	1000	15,907	18,892	100,671	9
201C-7	0.0640	0.1883	0.1580	3020	3	1007	16,038	19,114	99,670	9
201C-8	0.0630	0.1904	0.1599	2930	3	977	15,389	18,324	96,066	9
201C-9	0.0630	0.1896	0.1596	2960	3	987	15,612	18,546	98,339	8, 9
201C-10	0.0290	SAMPLE-NOT TESTED		TESTED	3					7
201D-1	0.0325	0.0865	0.0726	1240	3	413	14,335	17,080	89,209	5
201D-2	0.0310	SAMPLE - NOT TESTED		TESTED	3					7
201D-3	0.0315	0.0973	0.0818	1755	3	585	18,037	21,455	113,226	7
201D-4	0.0610	0.0932	0.0784	1350	3	450	14,485	17,219	91,216	7
201D-5	0.0640	0.0947	0.0796	1275	3	425	13,464	16,018	84,437	7
201D-6	0.0630	0.1826	0.1535	2590	3	863	14,184	16,873	89,003	8
201D-7	0.0630	0.1919	0.1613	3190	3	1063	16,623	19,777	104,590	10
201D-8	0.0630	0.1889	0.1590	2575	3	858	13,632	16,195	86,120	8
201D-9	0.0630	SAMPLE - NOT TESTED		TESTED	3					5
201D-10	0.0630	0.1903	0.1601	3160	3	1053	16,605	19,738	104,636	8

TABLE III (Cont.)  
TYPE I SPECIMENS - TEST SUMMARY

Specimen No.	Sheet Thkns	Area (in <sup>2</sup> )(2)		Ult Load (PSI)	Fasteners		Tension Stress (PSI)		Avg Bearing Stress at Fastrs (PSI) (3)(14)	Notes
		Full Sectn	At Fastrs		No.	lbs/Fastr (4)	Full Sectn (13)	Net Sectn at Holes (12)		
201E-1	0.0320	0.0967	0.0814	1380	3	460	14,271	16,953	90,196	7
201E-2	0.0303	0.0913	0.0768	1840	3	613	20,153	23,958	126,897	7
201E-3	0.0310	0.0932	0.0784	1345	3	448	14,431	17,156	90,878	7
201E-4		SAMPLE - NOT TESTED			3					5
201E-5	0.0280	0.0835	0.0701	1430	3	477	17,126	20,399	106,716	7
201E-6	0.0620	0.1890	0.1595	2350	3	783	12,434	14,734	79,392	10
201E-7	0.0615	0.1860	0.1565	2480	3	827	13,333	15,847	84,068	10
201E-8	0.0620	0.1832	0.1535	2425	3	808	13,237	15,798	81,650	10
201E-9	0.0620	0.1814	0.1518	2350	3	783	12,955	15,481	79,392	10
201E-10		SAMPLE - NOT TESTED			3					5
201F-1		SHATTERED DURING ASSEMBLY - NOT REPLACED								6
201F-2	0.0310	0.0932	0.0783	1000	3	333	10,730	12,771	67,114	7, 11
201F-3	0.0280	0.0823	0.0689	1520	3	507	18,469	22,061	108,571	7, 15
201F-4	0.0300	0.0896	0.0752	1680	3	560	18,750	22,340	116,667	7, 16
201F-5		SAMPLE - NOT TESTED								5
201F-6	0.0610	0.1796	0.1505	2970	3	990	16,537	19,734	102,062	8, 17
201F-7	0.0630	0.1862	0.1561	2920	3	973	15,682	18,706	97,010	10, 18
201F-8		SAMPLE - NOT TESTED								5
201F-9	0.0615	0.1787	0.1491	2925	3	975	16,368	19,618	99,153	10, 19
201F-10	0.0635	0.1854	0.1551	2930	3	977	15,804	18,891	96,700	10, 20

### TABLE III NOTES

1. The nominal dimensions of the Type I specimens are shown in Figure 2.
2. Either the cross-sectional area of the failed segment or, if the fasteners failed, the lesser of the cross-sectional areas of the two segments is reported.
3. The 0.010-inch - 0.015-inch chamfer disregarded in the calculations.
4. The fastener shear strengths are presented in Table II.
5. Sample - not tested.
6. Fractured during assembly - not tested.
7. Failed in net tension through the fastener holes - no fastener failure.
8. Simultaneous failure of the fasteners in shear, and the material in net tension through the fastener holes.
9. Failed in full section of the beryllium segment due to severely warped material.
10. Fastener sheared prior to development of full tensile potential of the beryllium segment.
11. Fractured through rivet holes during assembly -- total load represents bond strength only.

12. Net Tension Stress:

$$\sigma_{nt} = \frac{P}{W_n t_1}$$

P = Test Load; pounds

$W_n$  = Specimen width less diameter of 3 holes; inches

$t_1$  = Beryllium thickness; inch

TABLE III NOTES (Cont.)

13. Full Section Tensile Stress:

$$\sigma_{ft} = \frac{P}{Wt_1}$$

P = Test Load; pounds  
W = Specimen width; inches  
t<sub>1</sub> = Beryllium thickness; inch

14. Average Bearing Stress:

$$\sigma_{br} = \frac{P}{Dt}$$

P = Test Load; pounds  
t = Beryllium thickness; inch

- (a) Types 201A and 201B only:  
D = Total average diameter of (3) fasteners; inch
- (b) Types 201C, 201D, 201E, and 201F only:  
D = Total diameter of (3) fastener holes; inch

15. Bond release at 1325 pounds.
16. Bond released at 1500 pounds.
17. Bond released at 1250 pounds.
18. Bond released at 800 pounds.
19. Bond released at 1200 pounds.
20. Bond released at 1300 pounds.



The segments to be joined and the fasteners were hand-held during the installation of the fasteners. A standard Huck Model 352 pneumatic "gun" was used to "pull" the Huckbolts. The completed Type IA specimens, ready for testing, are illustrated in Figure 3. Figure 4 illustrates the testing of one of the specimens in the "Instron" tensile testing machine at a constant cross-head travel rate of 0.05 inch per minute and an average loading rate of 3080 pounds per minute. The bending of the segments and the "tilting" of the fasteners is clearly visible in the illustration. In order to reduce this "tilting" at the loading pins as much as possible, shims were placed between the beryllium specimens and the "forks" of the "Instron" loading rods.

Except for specimen number 201A4, the catastrophic failure of the beryllium specimens was precipitated by the failure, in shear, of one of the fasteners. The low indicated net tensile stresses for the beryllium, therefore, can be partially attributed to the failure of the fastener before the full tensile strength of the beryllium was reached.

As discussed earlier, the primary cause of the failure of any lap joint at relatively low net tensile loads is the effect of the combined bending and tensile loads. The high bearing stress at the fasteners in this particular test joint series, plus the effect of the "tilting" of the fasteners, resulted in the failure of the joints through the fastener line as illustrated in Figure 5. The elongation of the fastener holes, visible in specimen 201A3, verified the existence of the high bearing loads. The beryllium failed in bearing at one of the loading pin holes in specimen 201A4 at a load of 8150 pounds. However, the aluminum reinforcement pad and the adhesive bond did not fail; the specimen continued to carry the load and the testing was continued without interruption to ultimate failure in the joint at 8960 pounds.

Visual inspection of a representative autographically recorded load-deflection curve, illustrated in Figure 6, clearly reveals that only minor yield, attributable to the failure in bearing, occurred in the beryllium just prior to the ultimate load failure.

b. Type IB - Jo-bolts. The objective of this investigation was the further evaluation of the feasibility of joining beryllium structures with high strength blind fasteners. The installation of Jo-bolts also subjects the material to an appreciable

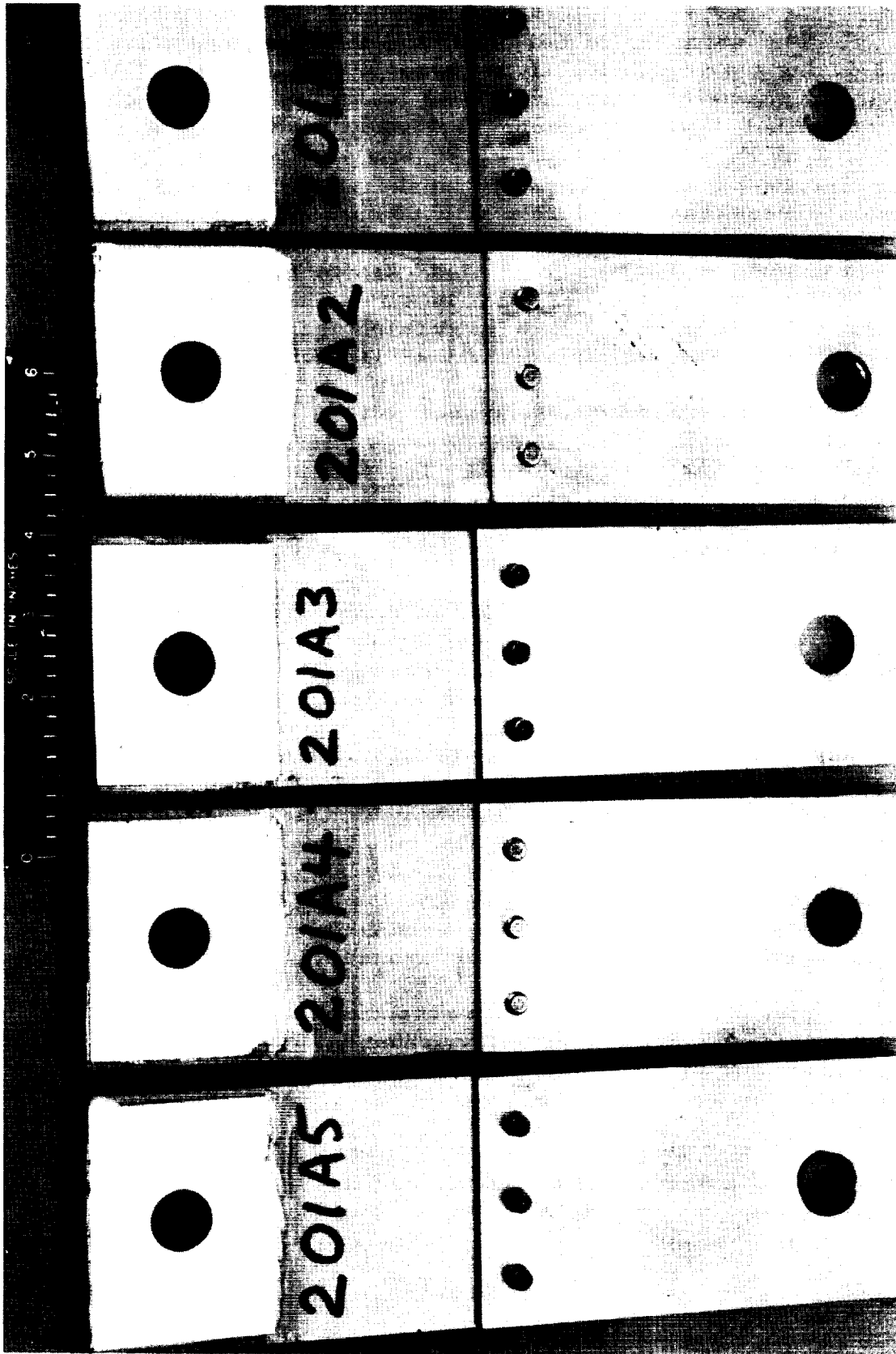


FIGURE 3. TYPE IA SPECIMENS - HUCKBOLT FASTENERS

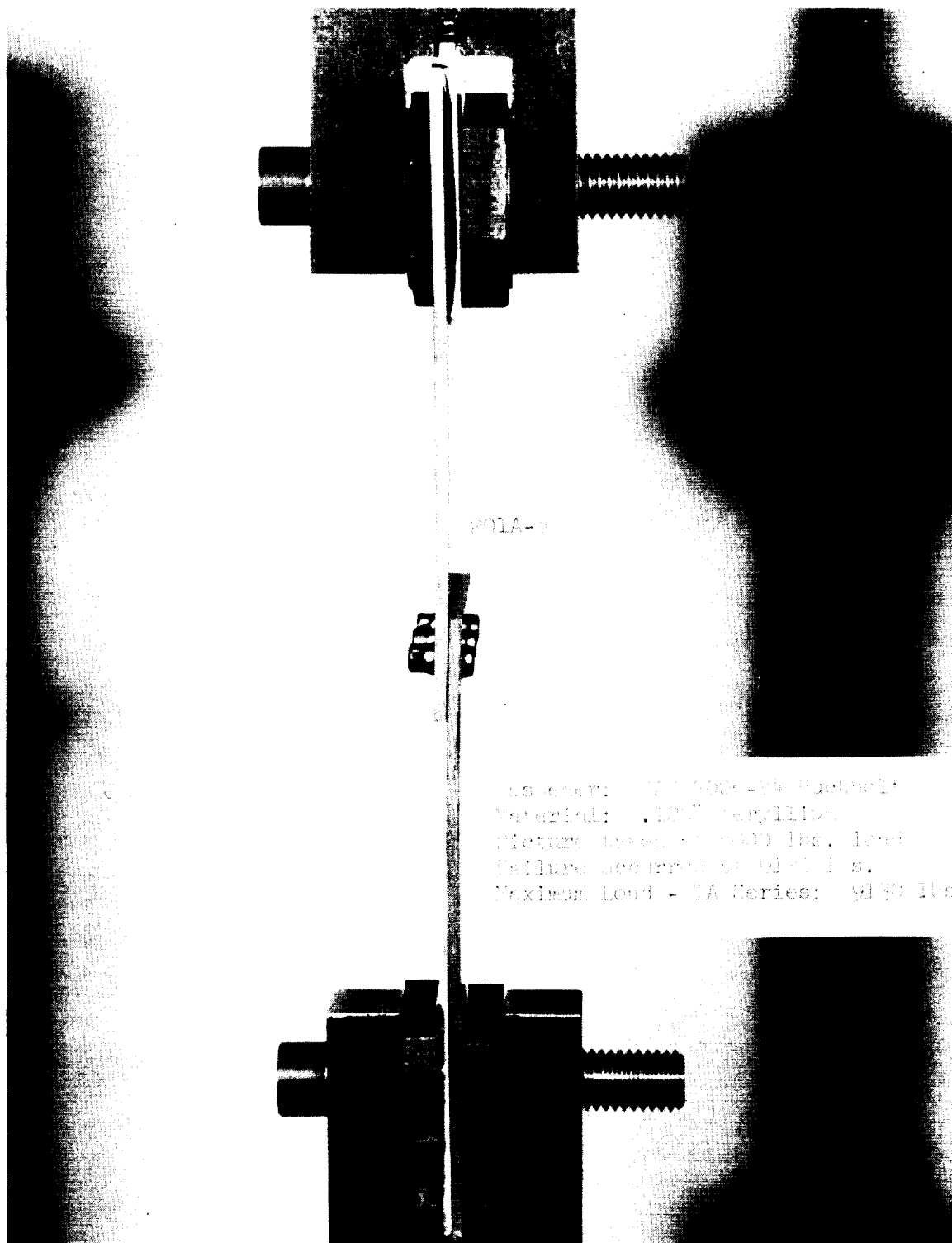


FIGURE 4. TYPE 1A SPECIMEN - TENSILE TEST

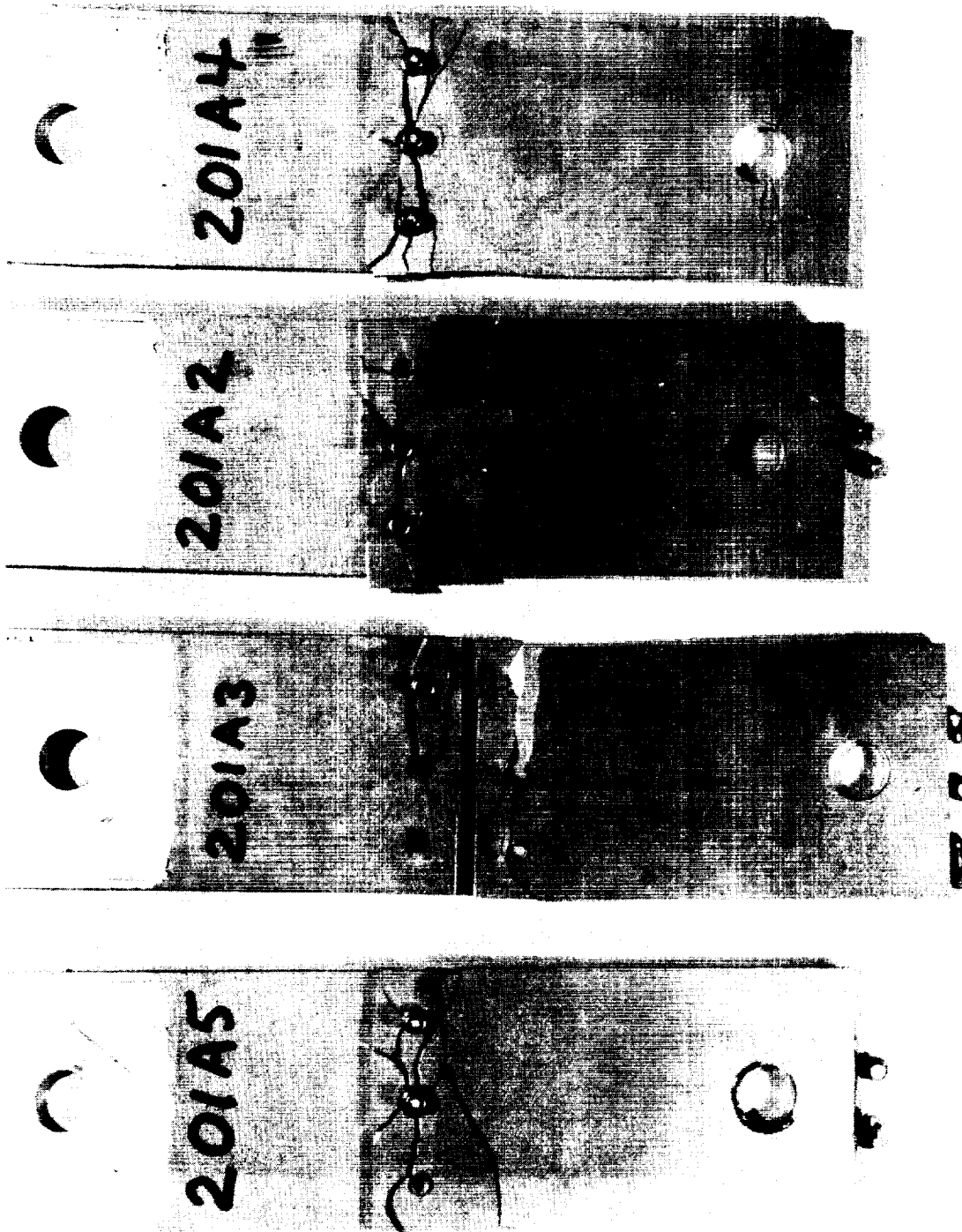


FIGURE 5. TYPE IA SPECIMENS - TYPICAL FAILURE MODE

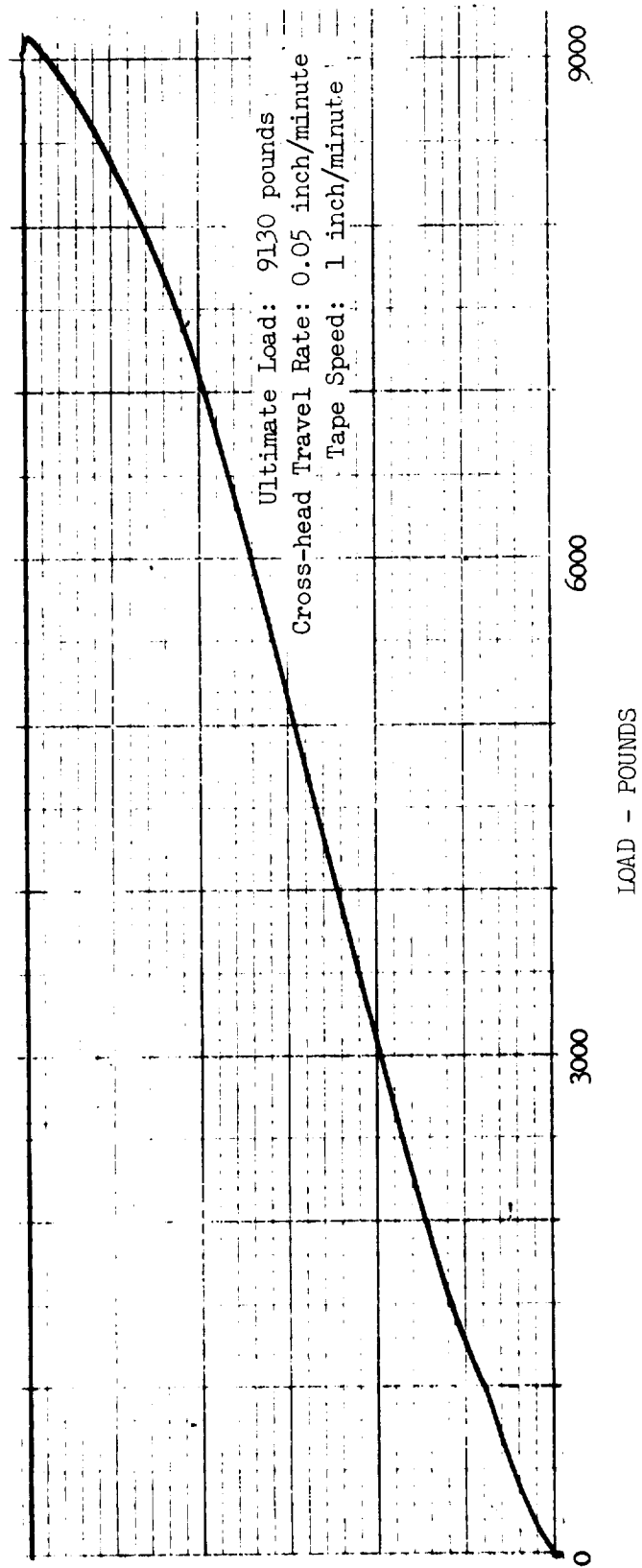


FIGURE 6. TYPE 1A LOAD-DEFLECTION CURVE - SPECIMEN 201A-5.  
NOTE SLIGHT INDICATION OF YIELD.

shock at the instant of stem separation. Again, all of the holes provided a small radial clearance between the fastener and the hole wall.

The diameters of ten randomly selected NAS 1671-3 Jo-bolts ranged from 0.1981 inch to 1.984 inches; the average diameter was 0.1982 inch. As this type of fastener does not expand during installation, the fastener diameter rather than the hole diameter establishes the bearing stress.

The diameters of the finished holes in the beryllium segments ranged, after etching, from 0.202 inch to 0.204 inch. The actual diameters of the holes were used in calculating the net tensile stress; the average diameter of the Jo-bolts was used in calculating the bearing stress.

The segments to be joined, and the fasteners, were hand-held during the installation of the fasteners. A standard Jo-bolt Model 302M/MTD302 (Torque Responsive) gun was used to install the Jo-bolts. The completed Type IB specimens, ready for testing, are illustrated in Figure 7. Figure 8 illustrates the testing of one of the Type IB specimens in the "Instron" tensile testing machine at a constant cross-head travel rate of 0.05 inch per minute and an average loading rate of 3000 pounds per minute. The bending of the segments is clearly visible in this illustration. Shims also were placed between the beryllium specimens and the "forks" of the "Instron" in order to minimize the "tilting" at the loading pins.

During the initial testing of these Type IB specimens, two (B1 and B5) failed, due to the shearing of the fasteners. The other two failed in shearing at the loading pin holes. The two panels which initially failed in the loading pin holes were retested in the "Riehle" tensile testing machine. Vise jaws, which spanned the full width of the specimens and thus assured even distribution of the load, were used for these subsequent tests. As may be noted in Table III, the ultimate load attained during the second test of one specimen (201B-2) exceeded the initial load by 155 pounds, and failed when two of the Jo-bolts sheared. The loading was discontinued before the third fastener failed, although partial shearing undoubtedly did occur as may be observed in Figure 9. The other specimen (201B-4) failed at a load 60 pounds under the original load, due to a combination of

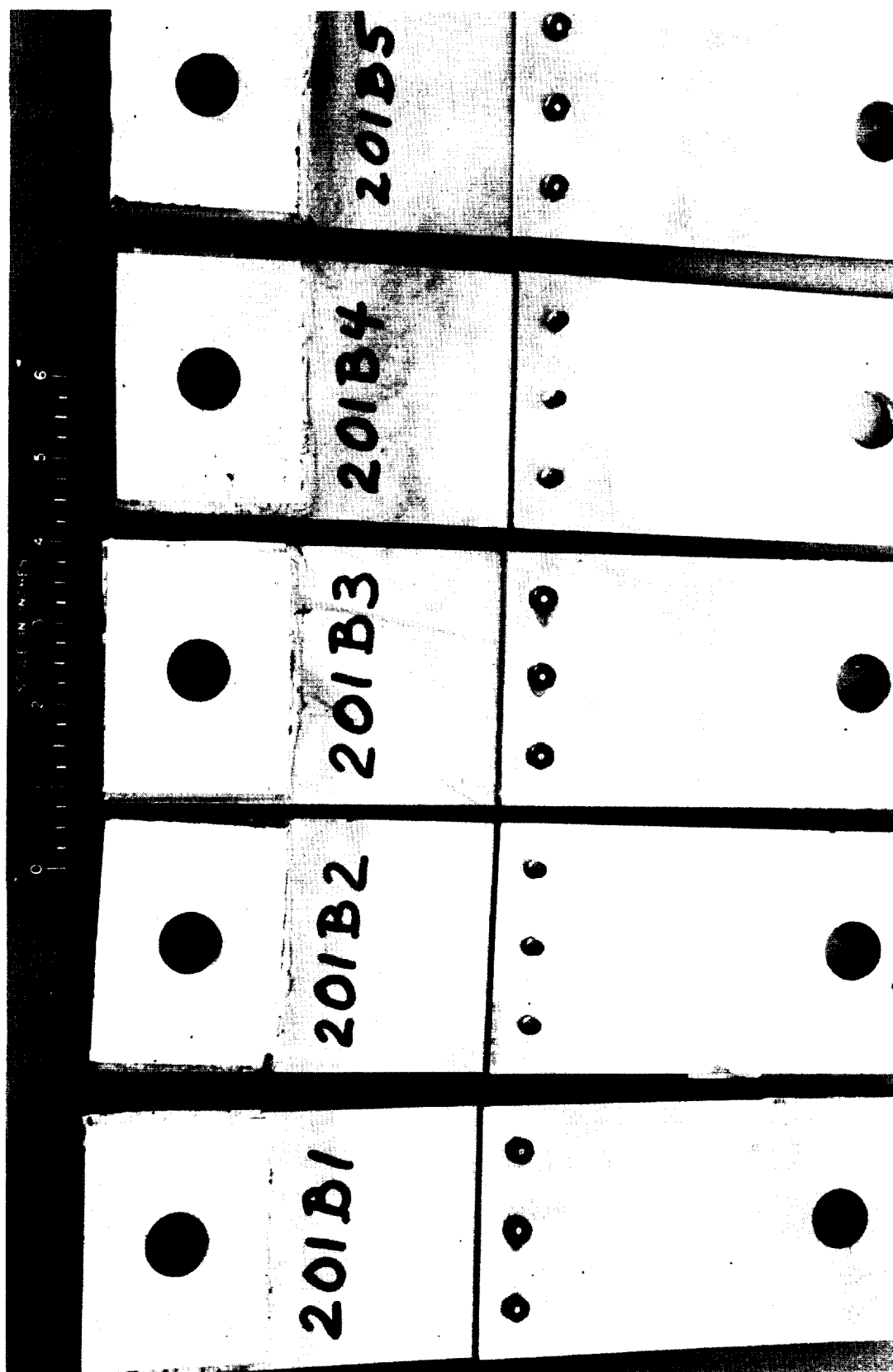
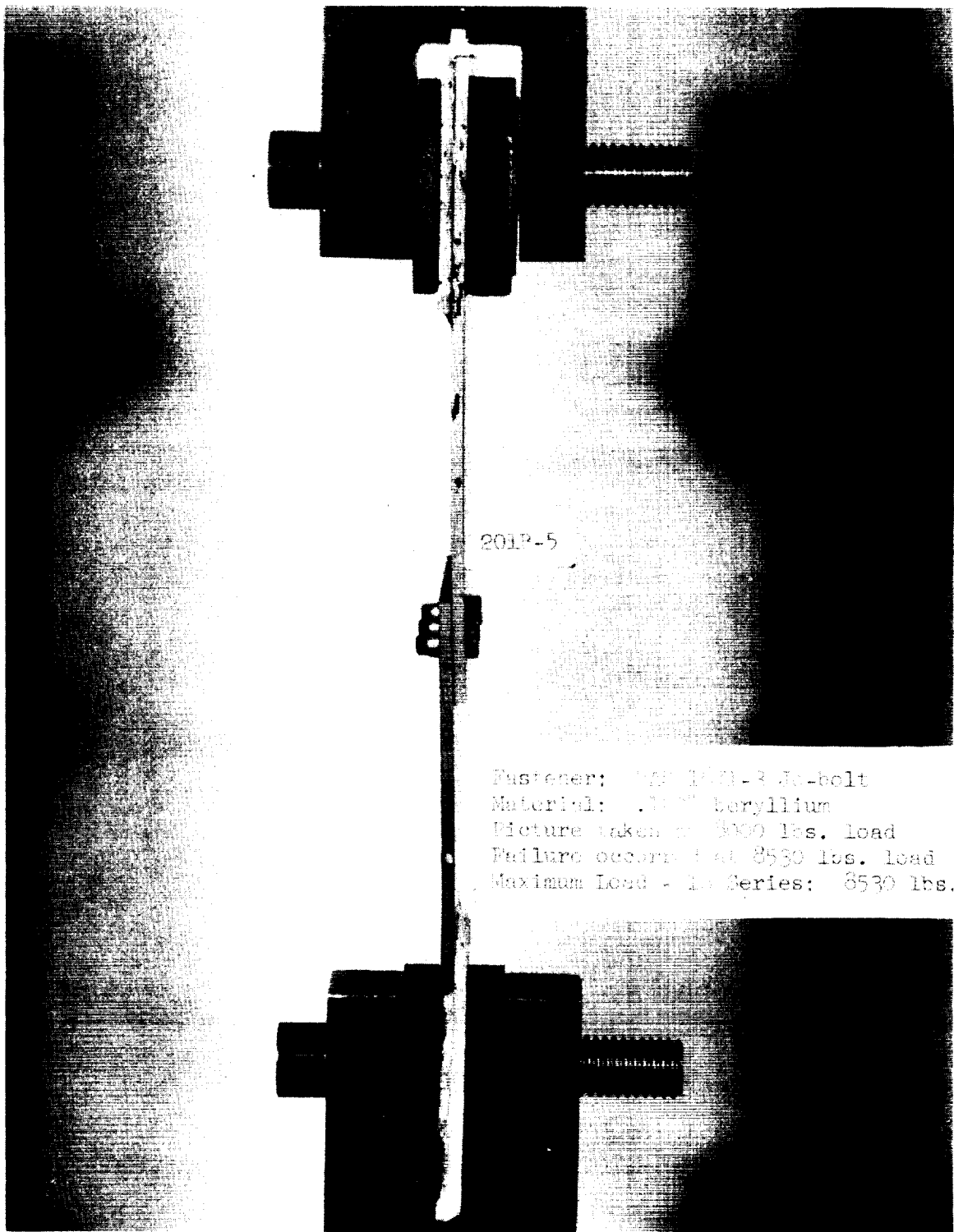


FIGURE 7. TYPE IB SPECIMENS - JO-BOLT FASTENERS





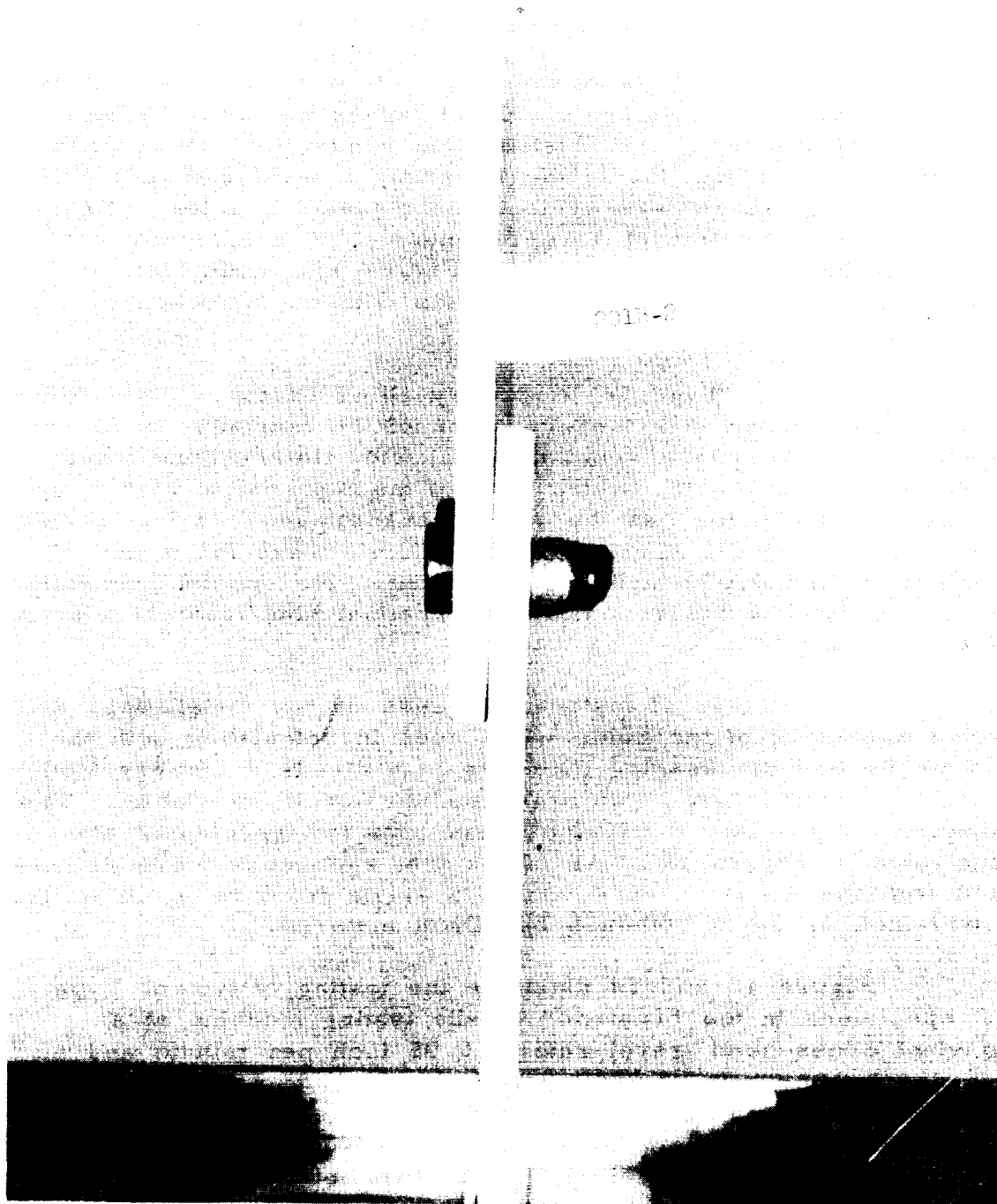


FIGURE 9. SPECIMEN 201B-2 - STILL SUSTAINING A LOAD OF 4500 LBS.  
AFTER TWO FASTENERS HAD SHEARED AT 8220 LBS.

tensile, bearing and bending stress through the fastener line.

The failure mode of the Type IB specimens was quite different from the catastrophic type of failure exhibited by the Type IA specimens. As illustrated in Figure 10, three of the four specimens failed due to the shearing of the fasteners; only minor bearing failure was evident at the fastener holes. However, visual inspection of a representative autographically recorded load-deflection curve, illustrated in Figure 11, again clearly reveals the abrupt failure at high loads with no indication of a yield point.

c. Type IC - Cherry Blind Rivets. The objective of this investigation was the evaluation of the feasibility of joining relatively thin beryllium sheet material with cherry blind rivets, such as MS 20600-M5, which subject the material to high hoop stresses in the holes, as the rivet shank expands during installation. The Type IC specimens, therefore, were fabricated of 0.030-inch and 0.060-inch gage material. No special precautions were observed to insure other than nominal hole/fastener diametrical tolerances.

As this type of fastener expands during installation, the actual diameters of the holes were used in calculating both the net tensile and the bearing stresses. A standard Cherry Model G15DB pneumatic rivet gun was used to install the rivets. The completed Type IC, 0.030-inch gage material specimens are illustrated in Figure 12. All of the test specimens were assembled with the cherry rivets without a single fracture in either the 0.030-inch or the 0.060-inch beryllium material.

Figure 13 and 14 illustrate the testing of typical Type IC specimens in the "Instron" tensile testing machine at a constant cross-head travel rate of 0.05 inch per minute and an average loading rate of 3600 pounds per minute. The typical bending of the material and the "tilting" of the fasteners is clearly visible in these illustrations. However, due to the difference in the thickness of the material in the two sets of specimens, the types of failure were quite different.

All of the 0.030-inch thick test specimens failed in the beryllium through the fastener line, at a net tensile stress significantly higher than was exhibited by the 0.060-inch thick

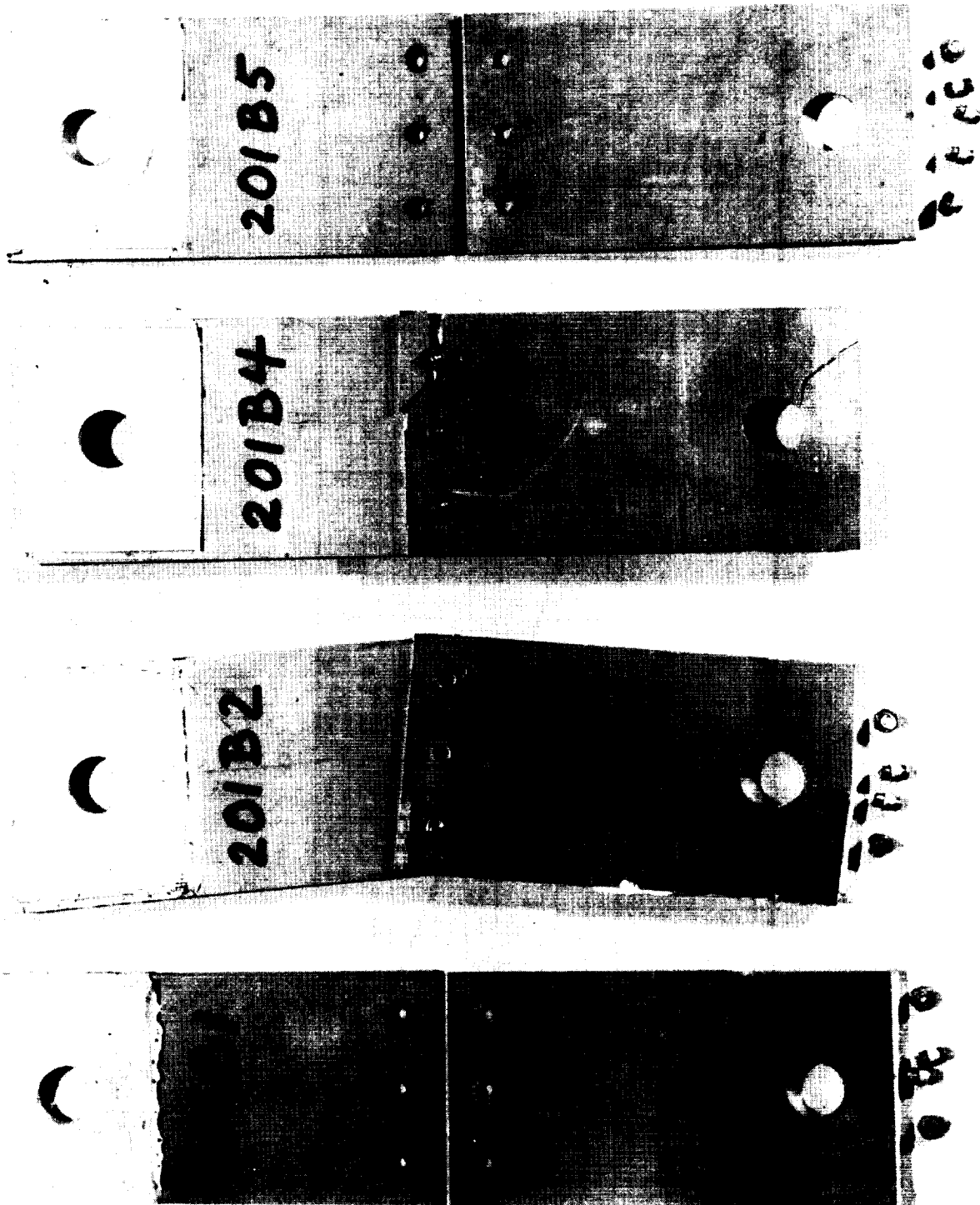


FIGURE 10 TYPE IB SPECIMENS - TYPICAL FAILURE MODE

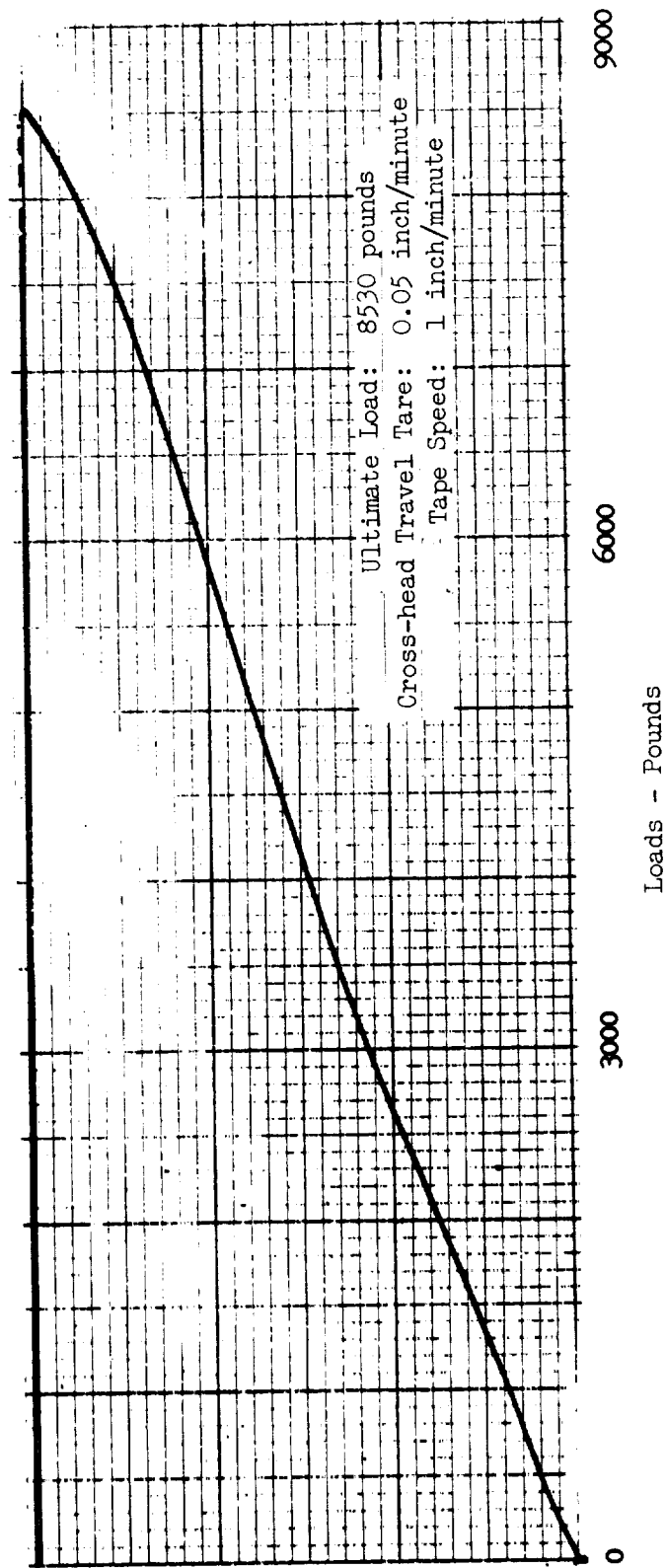
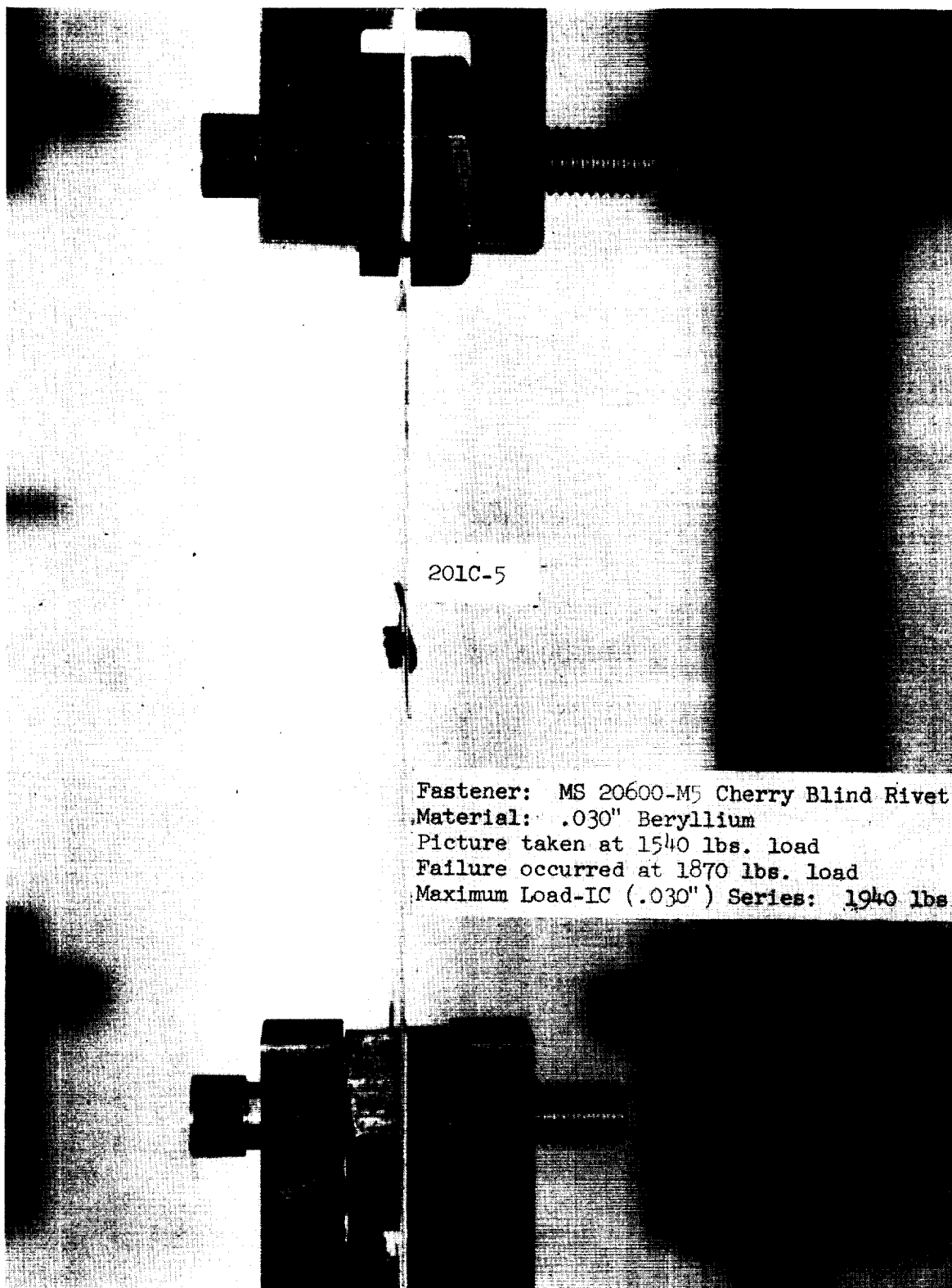


FIGURE 11. TYPE IB LOAD-DEFLECTION CURVE - SPECIMEN 201B-5



FIGURE 12. TYPE IC SPECIMENS - 0.030-INCH MATERIAL - CHERRY BLIND RIVETS



201C-5

Fastener: MS 20600-M5 Cherry Blind Rivet  
Material: .030" Beryllium  
Picture taken at 1540 lbs. load  
Failure occurred at 1870 lbs. load  
Maximum Load-IC (.030") Series: 1940 lbs.

FIGURE 13. TYPE IC SPECIMEN - 0.030-INCH MATERIAL - TENSILE TEST

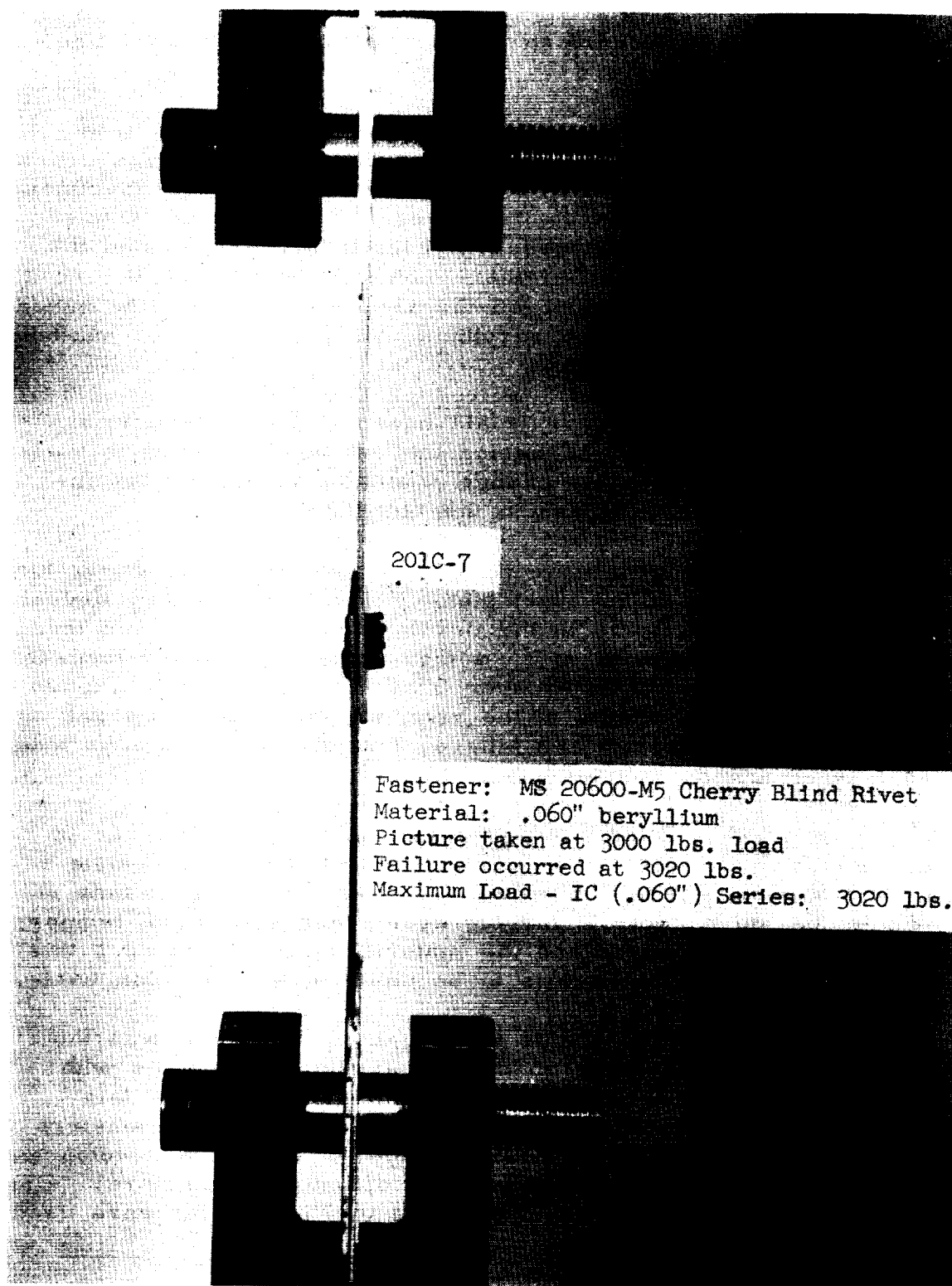


FIGURE 14. TYPE IC SPECIMEN - 0.060-INCH MATERIAL - TENSILE TEST

test specimens. The consistent failures through the rivet line are illustrated in Figure 15.

The failure mode of the 0.060-inch specimens was entirely different from that exhibited by the 0.030-inch specimens. As illustrated in Figure 16, the primary failure of the specimens was due to the failure of the fasteners. The extreme "tilting" of the joint area, clearly visible in Figure 14, precipitated the failure of the rivets; the beryllium material cut through the rivet sleeve and caused it to strip off the rivet stem. The low indicated net tensile stresses for the beryllium, therefore, can be attributed to the failure of the fasteners before the full tensile strength of the beryllium was reached. A reduction in the pitch dimension, or spacing, of the fasteners would improve the load-carrying capacity of this joint by increasing the net tensile stress in the beryllium. However, this change would be limited by the increase in the bearing stress in the beryllium.

Furthermore, the separation of the segments under load, due to the slipping of the rivet stem, not only was highly undesirable, but materially contributed to the development of the low net tensile loads. Visual inspection of an autographically recorded load-deflection curve, for specimen Number 201C-7, illustrated in Figure 17, clearly reveals the effects of the rivet slippage; the reversal of the load just prior to joint failure, but after the maximum load had been reached, indicated this effect.

d. Type ID - Beryllium Rivets. The use of beryllium rivets, rather than other types of fasteners, would result in the maximum savings in weight. However, the problems of rivet temperature control, forging cycle, and differential temperatures between the rivets and the material must be solved if this ultimate lightweight fastener is to be used on a production basis.

The objective of this investigation, therefore was the evaluation of the feasibility of joining beryllium structures with beryllium rivets. Because of the preliminary nature of this phase of the mechanical fastener program, several parameters were based upon "current best practice;" extensive development work was not undertaken to establish optimum parameters. Only two configurations of rivets, illustrated in Figure 18, were used during this investigation.



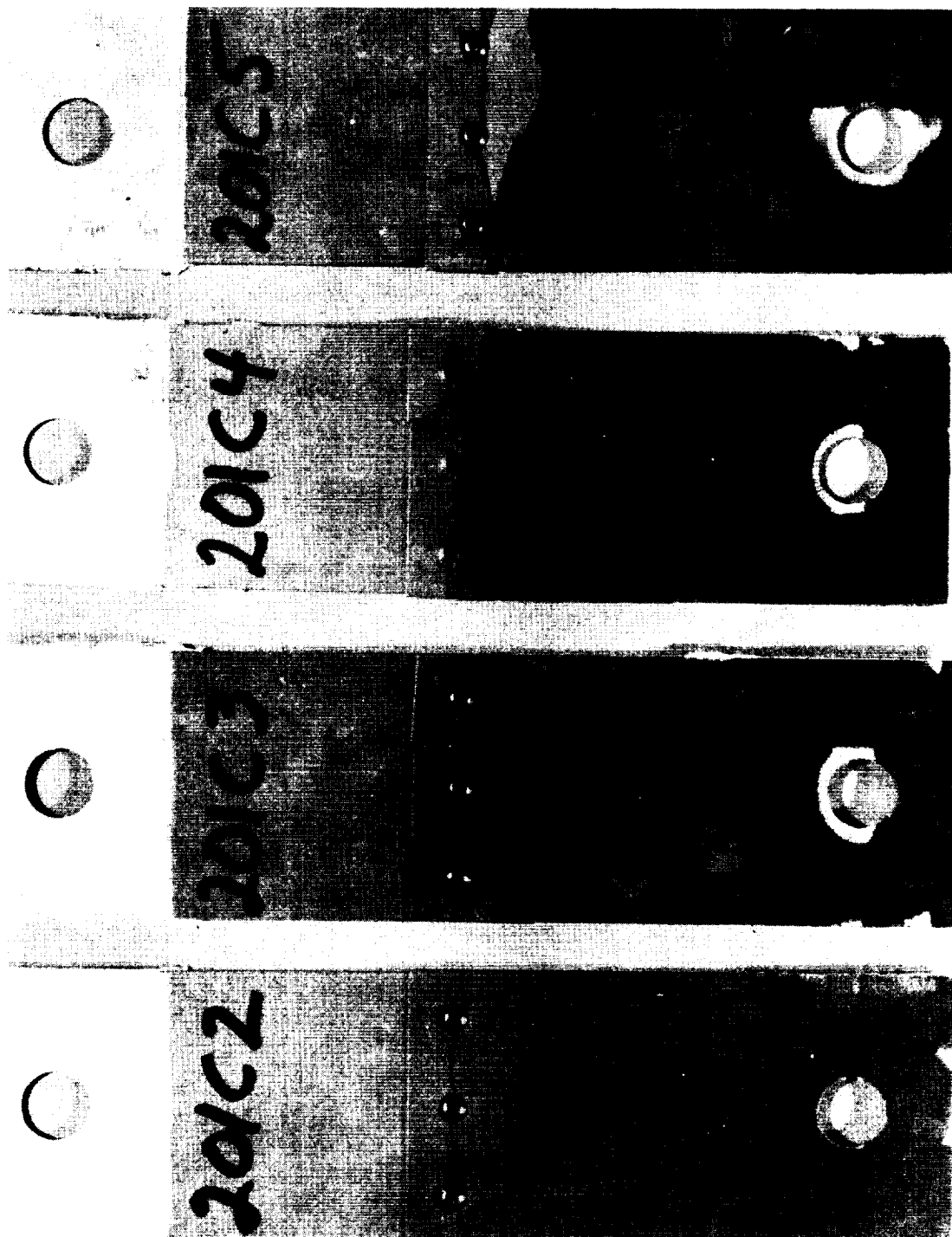


FIGURE 15. TYPE IC SPECIMENS - 0.030-INCH MATERIAL - TYPICAL FAILURE MODE

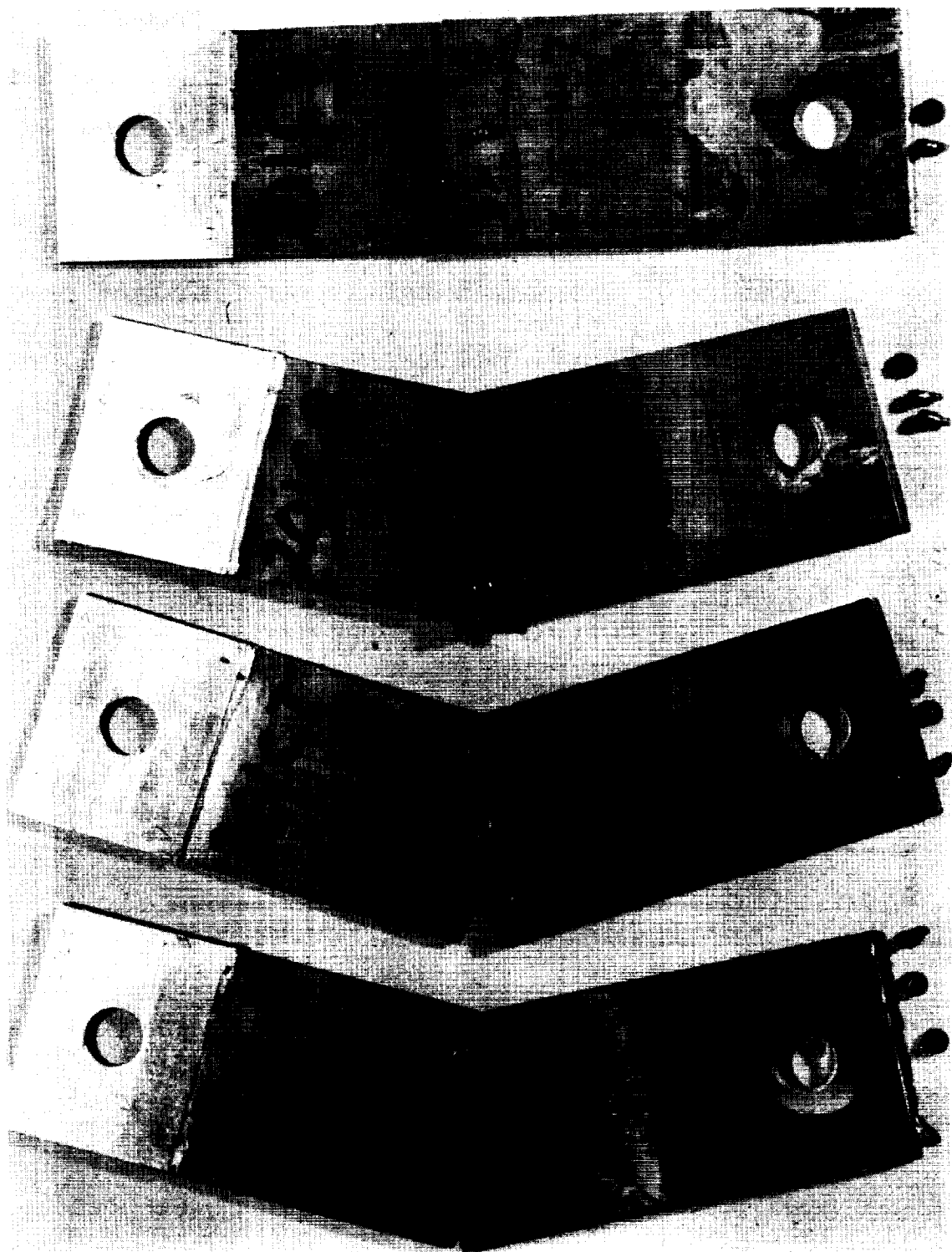


FIGURE 16. TYPE IC SPECIMENS - 0.060-INCH MATERIAL - TYPICAL FAILURE MODE

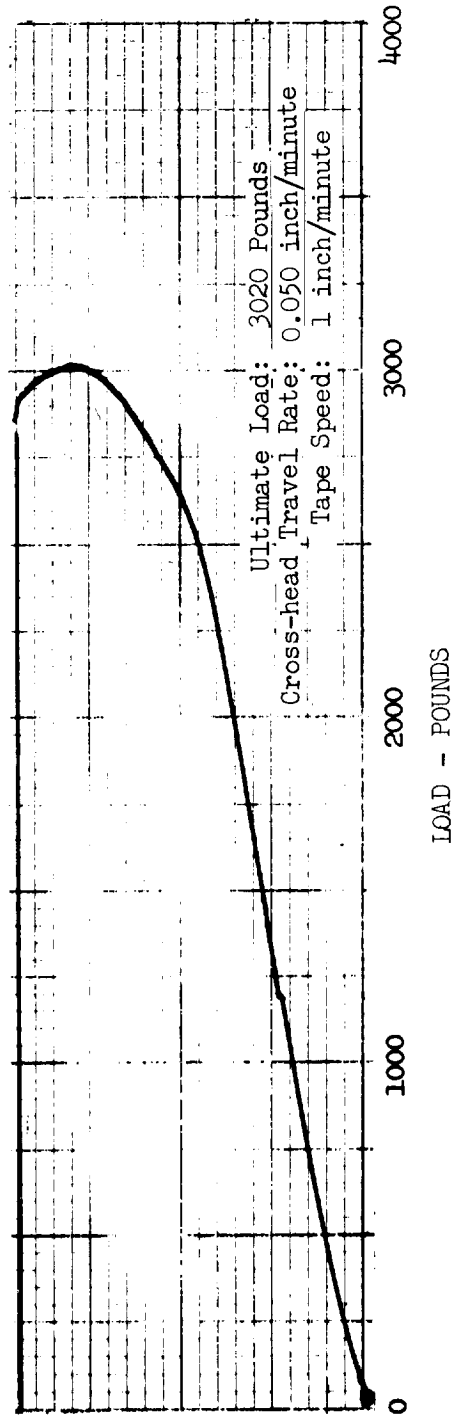
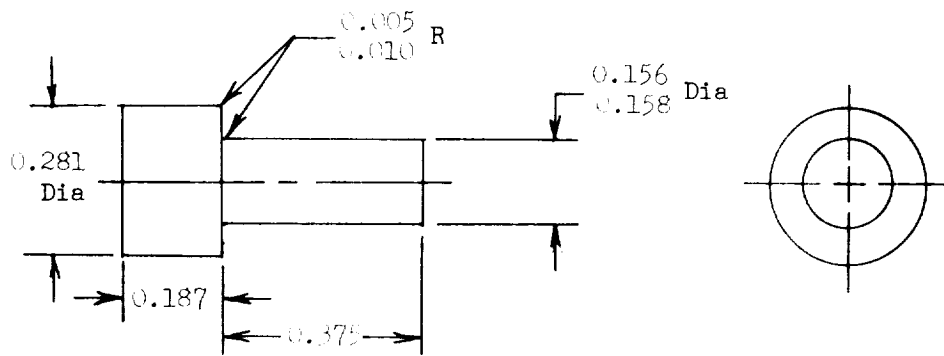
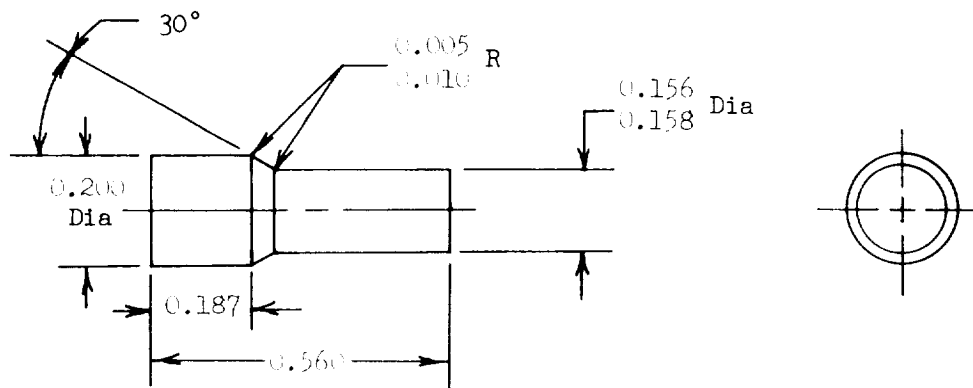


FIGURE 17. TYPE IC LOAD-DEFLECTION CURVE - SPECIMEN 201C-7.  
 NOTE LOAD REVERSAL.



Beryllium and "Lockalloy"



Beryllium

NOTES:

1. DIMENSIONS SHOWN ARE FINAL AFTER CHEMICAL ETCHING
2. AFTER MACHINING ETCH 0.006-INCH TO 0.008-INCH FROM BERYLLIUM RIVETS ONLY
3. MACHINE "LOCKALLOY" RIVETS TO FINAL DIMENSIONS
4. BREAK ALL EDGES 0.001-INCH TO 0.005-INCH RADIUS

FIGURE 18. RIVET CONFIGURATIONS - BERYLLIUM AND "LOCKALLOY"

The beryllium rivets were machined 0.008 inch over-size to permit the subsequent chemical etching of the rivets to the final dimensions; the use of the standard nitric hydrofluoric acid solution not only resulted in the removal of any induced surface damage, but reduced the machined rivets to their final net dimensions.

In order to establish the basic forging temperature and the percentage of reduction during the "upsetting" of the rivets, several test samples, consisting of 1-inch by 2-inch by 0.060-inch steel plates, were joined with one rivet and tested to determine the relative shear strengths. Two trial forging temperatures, 750°F and 1350°F, were selected for these initial trials. The rivets were cut to length and faced to provide a protrusion of approximately 0.150 inch prior to the "upsetting" operation.

"Upsetting" the rivets at the lower temperature of 750°F resulted in extensive radial cracks in the upset head, and deformation of the rivet above the material, rather than within the hole itself; the ultimate result was loose rivets. Increasing the forging temperature to 1350°F resulted in the complete elimination of the radial cracking, and the proper expansion of the rivet within the hole; the fits within the hole were uniformly tight. In addition, it was determined during this experimental work that a 10 to 15 percent reduction in the height of the upset head portion of the rivet yielded the best results.

A low-voltage (0-6 volts), high-current (0-1000 amperes) power supply was used for the resistance heating of the rivets. The power leads were attached to the opposing René 41 steel mandrels. The lower mandrel was fixed; the upper mandrel was attached to the cross-head of the 10,000-pound capacity "Instron" research tensile testing machine.

Temperature control was maintained by means of thermocouple feedback to a fast response recorder-controller. The thermocouple was attached to the upper protruding section of the rivet (to be upset), and an initial light load of approximately 20 pounds was applied to hold the rivet and the panel assembly firmly in place during the heating of the rivet.

At the 1350°F forging temperature, the most effective cross-head rate was 0.05 inch per minute. During the "upsetting"

of the rivet, the applied force increased rapidly to approximately 5000 pounds. This rapid increase was due both to the forging action on the rivet and the heat loss from the rivet into the beryllium segments as the metal-to-metal contact became more intimate.

The test results of the steel development samples were as follows:

TABLE IV

Steel Development Samples - Beryllium Rivets

<u>Rivet Material</u>	<u>Forging Temp - °F</u>	<u>Single Shear Range - PSI</u>
Be	750	45,000-46,000
Be	1350	57,000-57,500

On the basis of this limited data, 1350°F was selected as the "upsetting" temperature for the beryllium rivets. Figure 19 illustrates the "Instron" research tensile testing machine, the heating equipment, and the instrumentation utilized for the assembly of the Type ID beryllium riveted specimens.

During the "upsetting" of the rivets, the temperature gradient in the beryllium segments was measured by means of thermocouples temporarily attached at several points.

Visual inspection of the temperature data, plotted as a function of distance from the centerline of the rivet, reveals that the temperature gradient in the beryllium material is nearly linear from the edge of the rivet head. The slight variations are believed due to slight variations in the contact resistance during the heating of the rivets. A contributing factor in the successful installation of the beryllium rivets, therefore, was believed to be the relatively high temperature of the beryllium segments adjacent to the rivet which locally improved the ductility of the material and minimized the effect of induced hoop stresses. As no test specimens failed

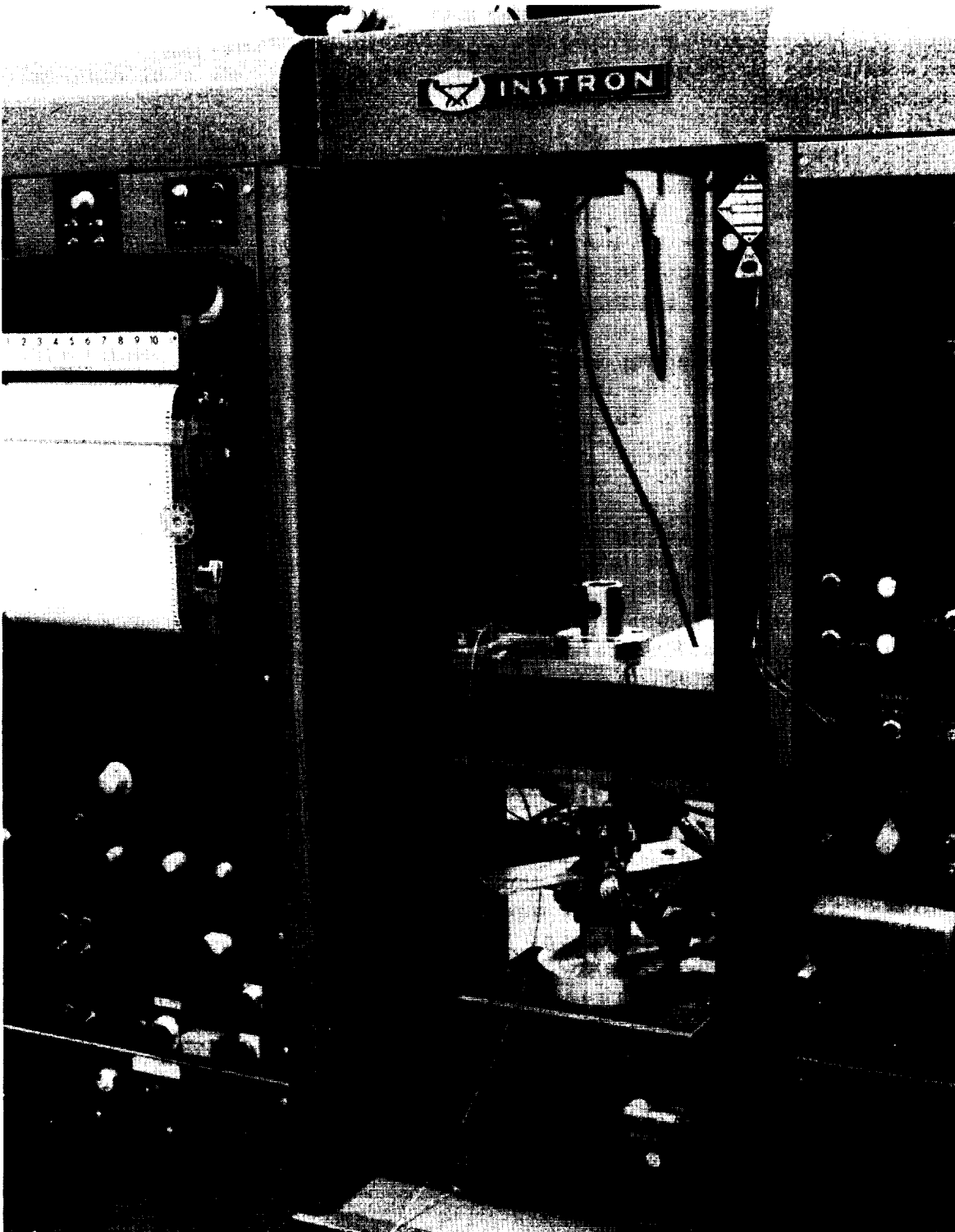


FIGURE 19. RIVET INSTALLATION - INSTRON TEST MACHINE

during the riveting operation, the verification of this conclusion is assumed. This data is graphically presented in Figure 20.

Macro and micro sections of an installed beryllium rivet are illustrated in Figure 21. The lack of any indication of damage should be noted.

The completed Type ID, 0.030-inch gage material specimens are illustrated in Figure 22. All of the test specimens were assembled with beryllium rivets without a single fracture in either the 0.030-inch or the 0.060-inch beryllium material. Figure 23 and 24 illustrate the testing of typical Type ID specimens in the "Instron" tensile testing machine.

Constant loading rates of 2000 and 2500 pounds per minute were used during the testing of the 0.030-inch and the 0.060-inch specimens, respectively. The typical bending of the material and the "tilting" of the fasteners is clearly visible in these illustrations. However, no rivet "slipping," or separation of the panel segments at the rivet line, is evident. Due to the difference in the thickness of the material in the two sets of specimens, the types of failure were quite different.

All of the 0.030 inch-thick test specimens failed in the beryllium, through the fastener line, due to a combination of high bending and bearing stress through the holes. There was no evidence of rivet failure. The consistent failures through the rivet line are illustrated in Figure 25.

The failure mode of the 0.060-inch specimens was entirely different from that exhibited by the 0.030-inch specimens. As illustrated in Figure 26, the failure of the specimens was precipitated by the shearing of the beryllium rivets, which usually occurred as the separation of one or both heads from the shank. It may be concluded, therefore, that the "tilting" of the fasteners also added a tension moment to the rivets which resulted in a greatly increased local stress at the rivet head-shank transition.

Because of the high modulus of both the rivets and the specimen segments, the failures were of the catastrophic type. Visual inspection of a representative autographically recorded load-deflection curve, illustrated in Figure 27, clearly reveals the lack of indication of yield; the trace is nearly linear.



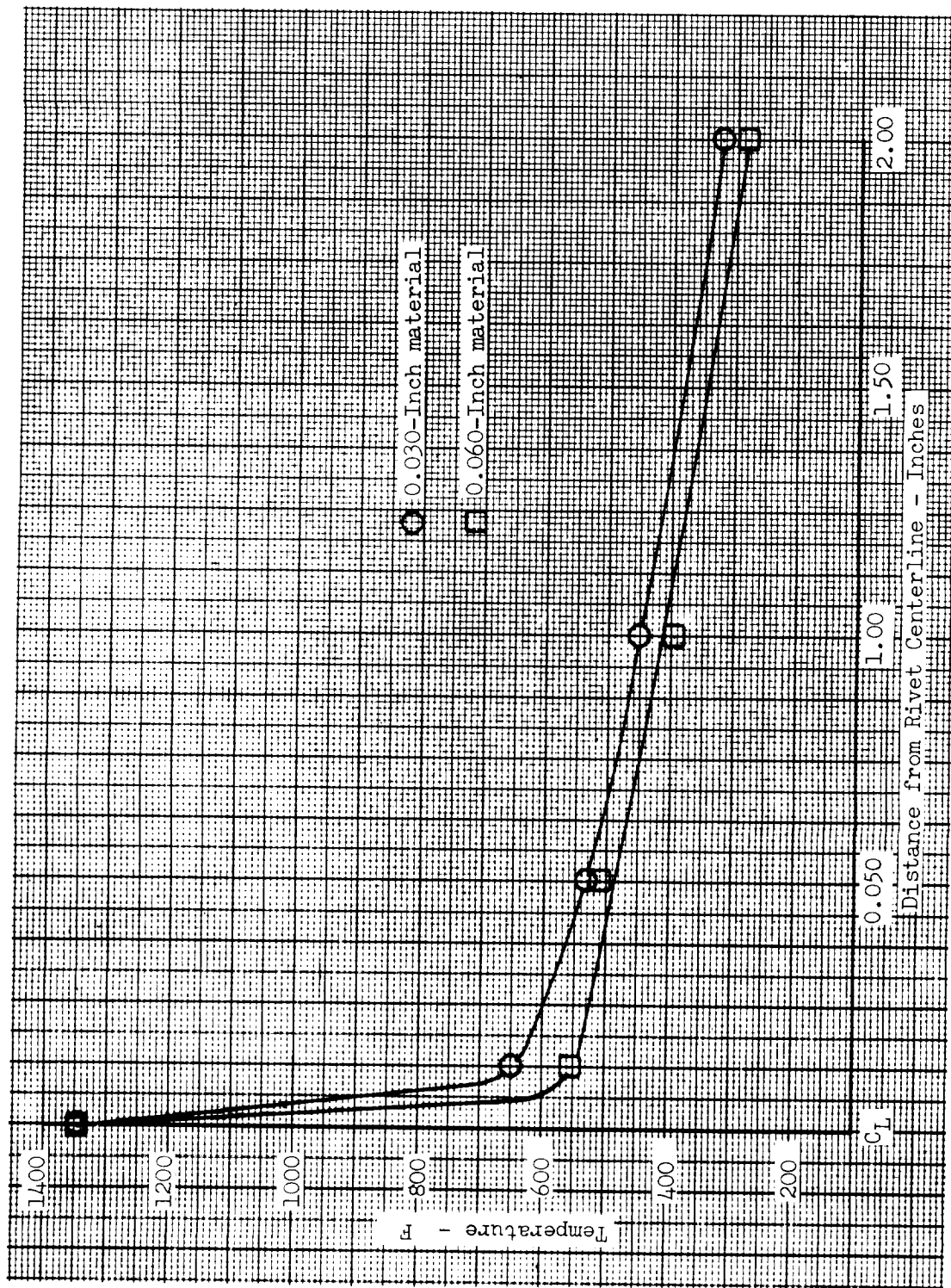
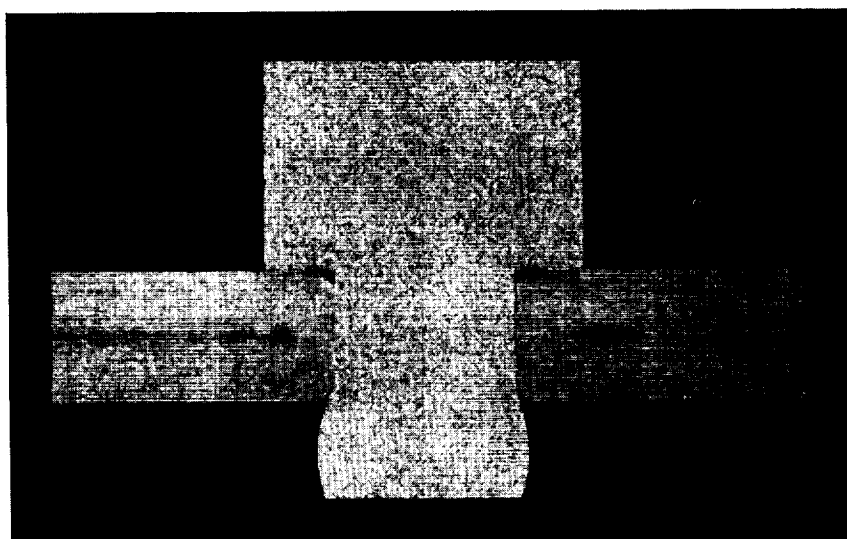


FIGURE 20. THERMAL GRADIENT IN BERYLLIUM SPECIMENS DURING INSTALLATION OF BERYLLIUM RIVETS



Beryllium Riveted Joint - 10X

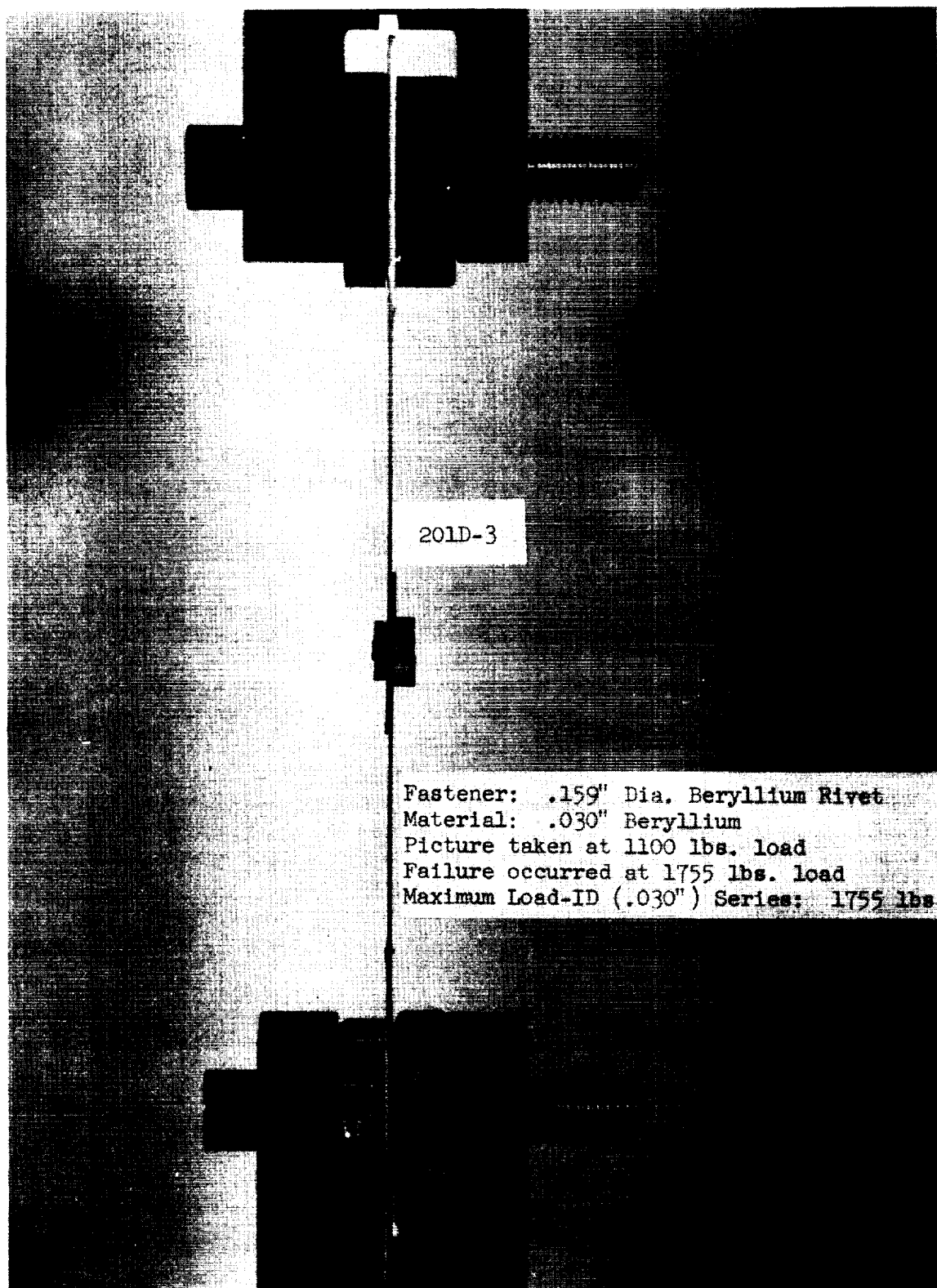


Intersection of Beryllium Sheets and Rivet - 100X

FIGURE 21. TYPE ID SPECIMEN - INSTALLED BERYLLIUM RIVET



FIGURE 22. TYPE ID SPECIMENS - 0.030-INCH MATERIAL - BERYLLIUM RIVETS



201D-3

Fastener: .159" Dia. Beryllium Rivet  
Material: .030" Beryllium  
Picture taken at 1100 lbs. load  
Failure occurred at 1755 lbs. load  
Maximum Load-ID (.030") Series: 1755 lbs.

FIGURE 23. TYPD ID SPECIMEN - 0.030-INCH MATERIAL - TENSILE TEST

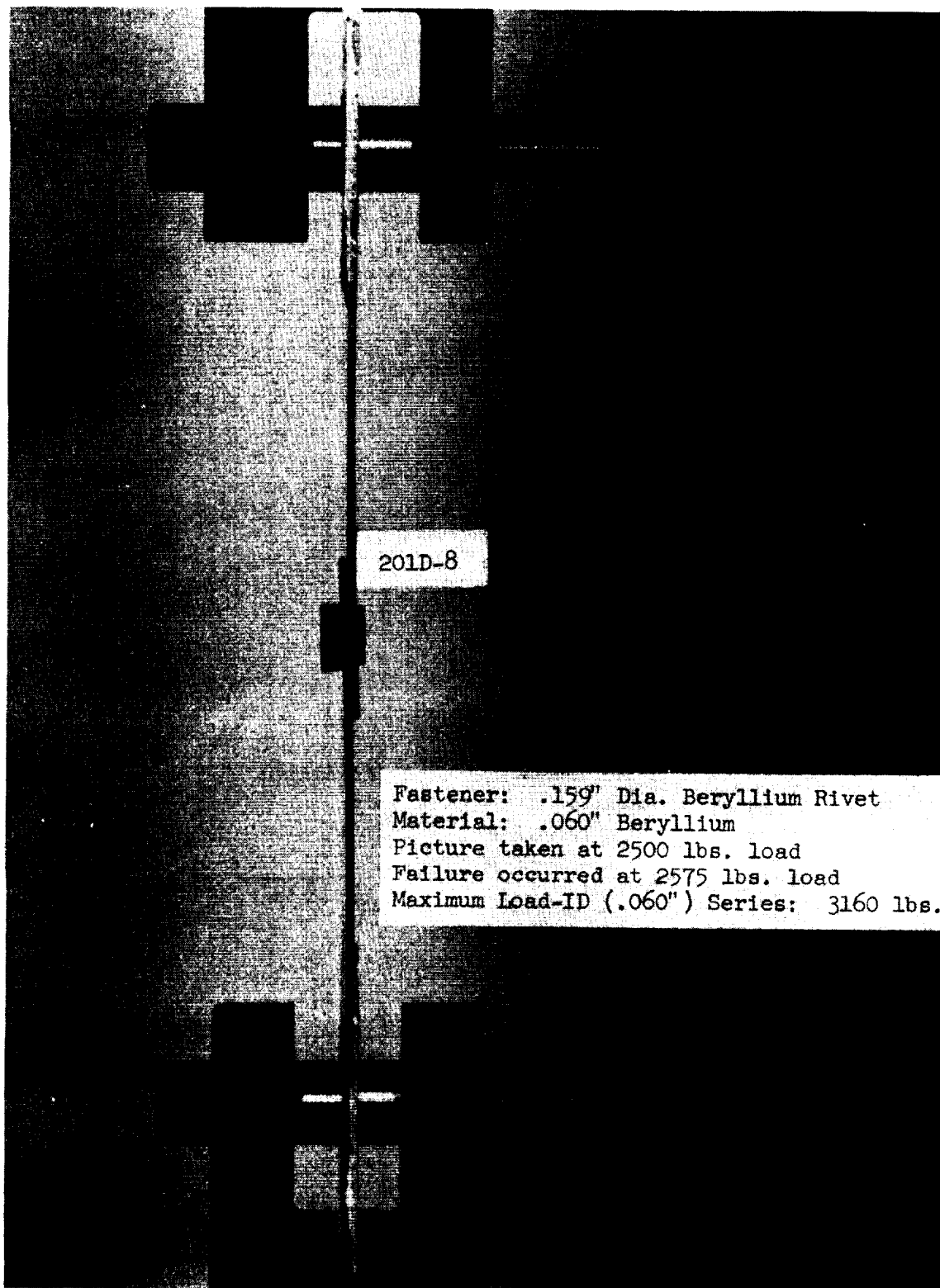


FIGURE 24. TYPE ID SPECIMEN - 0.060-INCH MATERIAL - TENSILE TEST



FIGURE 25. TYPE ID SPECIMENS - 0.030-INCH MATERIAL - TYPICAL FAILURE MODE

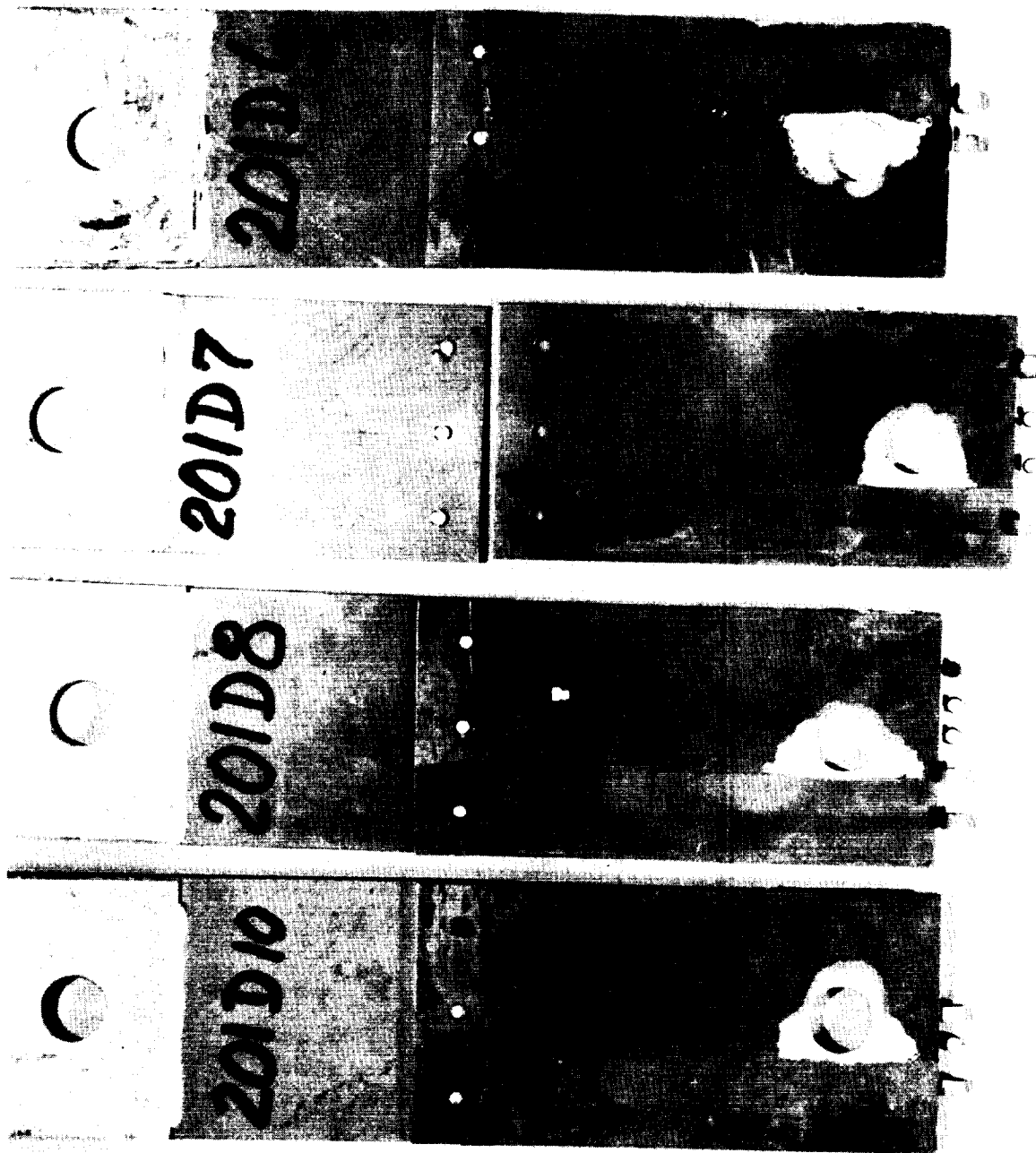


FIGURE 26. TYPE ID SPECIMENS - 0.060-INCH MATERIAL - TYPICAL FAILURE MODE

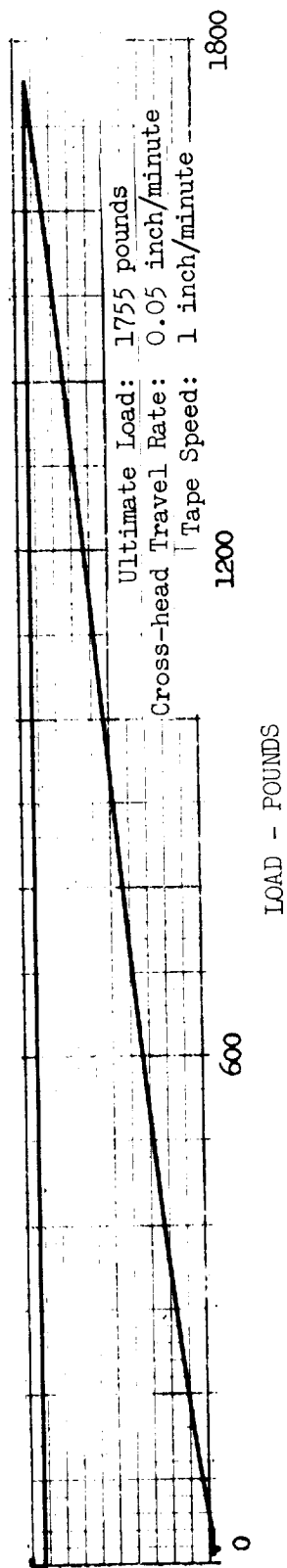


FIGURE 27. TYPE ID LOAD-DEFLECTION CURVE - SPECIMEN 20LD-3.  
NOTE LINEAR TRACE.



e. Type IE - "Lockalloy" Rivets. The use of "Lockalloy" as the rivet material results in fasteners nearly as light in weight as beryllium rivets. In addition, the somewhat lower modulus and greater ductility of "Lockalloy" at room temperature should afford a more efficient fastener than "unalloyed" beryllium.

The objectives of this investigation, therefore, were the evaluation of the feasibility of joining beryllium structures with "Lockalloy" rivets, and the comparison of the characteristics of the "Lockalloy" and beryllium rivets. Therefore, in order to permit the direct comparison of the results, dimensionally identical rivets and test joints were utilized. The configuration of the "Lockalloy" rivets is illustrated in Figure 18.

The "Lockalloy" rivets were machined to net final dimensions. Because of the machining characteristics of this material, the etching operation was not deemed necessary and, therefore, was omitted.

The establishment of the basic forging temperature and of the percentage of reduction during the "upsetting" of the rivets was accomplished in the same manner as with the beryllium rivets. Several steel test samples again were prepared, joined with one rivet, and tested to determine the relative shear strengths. Two trial forging temperatures, 400°F and 1000°F, were selected for these initial trials. The rivets were cut to length, faced to provide a protrusion of approximately 0.150 inch prior to the "upsetting" operation.

Forging the "Lockalloy" rivets at the lower temperature of 400°F produced extensive radial cracks in the upset head. The forging temperature then was increased to 1000°F, which did not completely eliminate the radial cracking problem, although the condition was greatly reduced. The 10 percent reduction in the height of the protruding end of the rivet again was found to yield the best results.

The same equipment and procedure used during the developmental work on the beryllium riveted joints was used for the fabrication of the "Lockalloy" riveted steel test specimens, except that the "upsetting" of the "Lockalloy" rivets was performed at 700 pounds pressure and a controlled rate of 0.005 inch per

minute.

The test results of the steel development samples were as follows:

TABLE V

Steel Development Samples - "Lockalloy" Rivets

<u>Rivet Material</u>	<u>Forging Temp - °F</u>	<u>Single Shear Range - PSI</u>
"Lockalloy"	400	39,000-40,000
"Lockalloy"	1000	39,000-40,000

On the basis of this limited data, 1000°F was selected as the forging temperature for the "Lockalloy" rivets. Figure 19 illustrates the "Instron" tensile testing machine, the heating equipment, and the instrumentation utilized for the assembly of the Type IE "Lockalloy" riveted specimens.

During the upsetting of the rivets, the temperature gradient in the beryllium segments was measured by means of thermocouples temporarily attached at several points.

Visual inspection of the temperature data, plotted as a function of distance from the centerline of the rivet, reveals that the temperature gradient in the beryllium material is almost linear from the edge of the rivet head. The slight variations are believed due to slight variations in the contact resistance during the heating of the rivets. A contributing factor in the successful installation of the "Lockalloy" rivets, therefore, is believed due to the relatively high temperature of the beryllium segments adjacent to the rivet, as all of the test specimens were successfully joined without failure. The temperature gradient data is graphically presented in Figure 28.

However, it was noted that several rivets, after they had cooled to room temperature, were loose in the holes

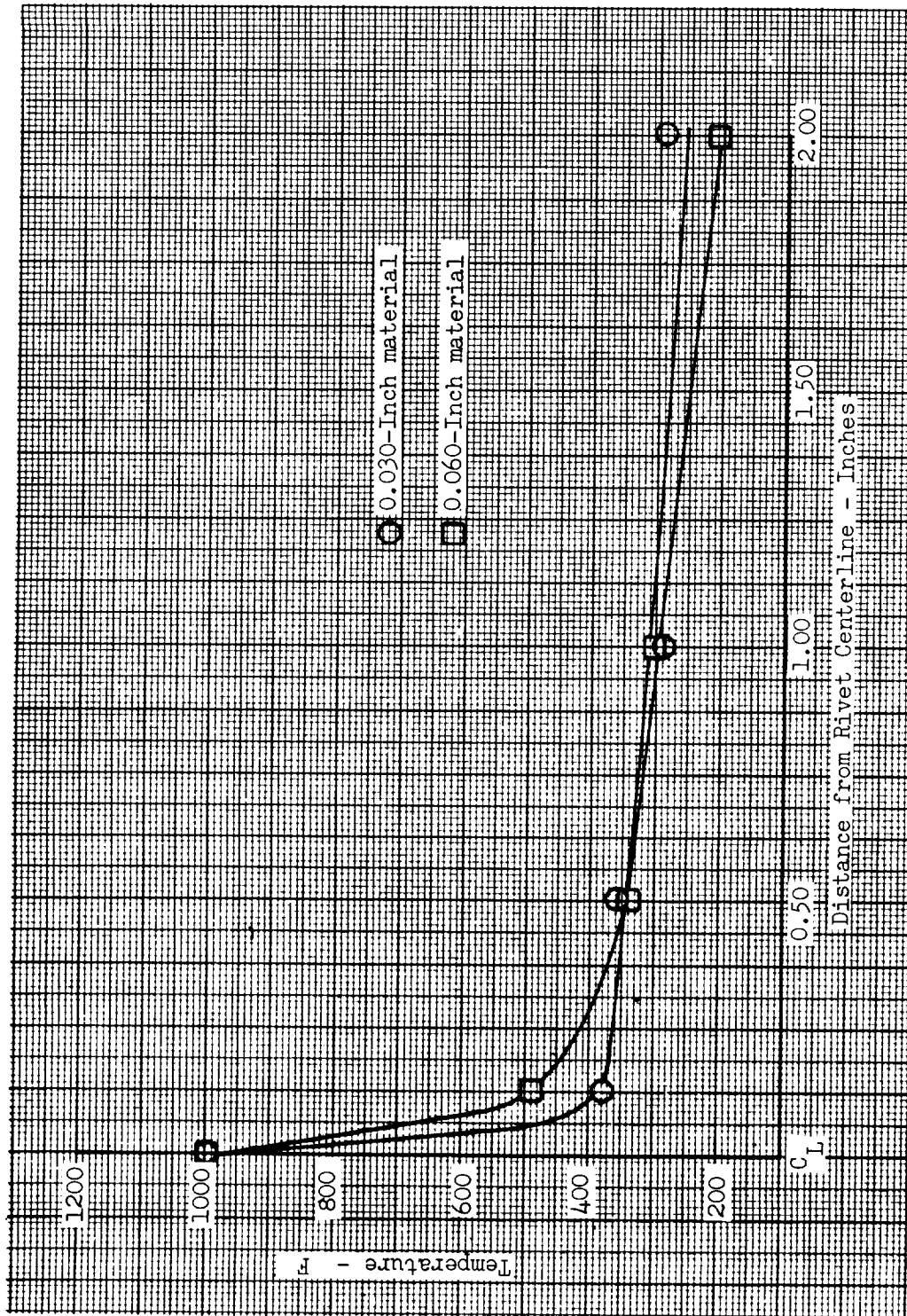


FIGURE 28. THERMAL GRADIENT IN BERYLLIUM SPECIMENS DURING INSTALLATION OF "LOCKALLOY" RIVETS

and could be rotated "by hand." These rivets were "re-stuck" to increase the shank diameter and thus completely fill the hole prior to the initiation of testing operations. Macro and micro sections of an installed "Lockalloy" rivet are illustrated in Figure 29.

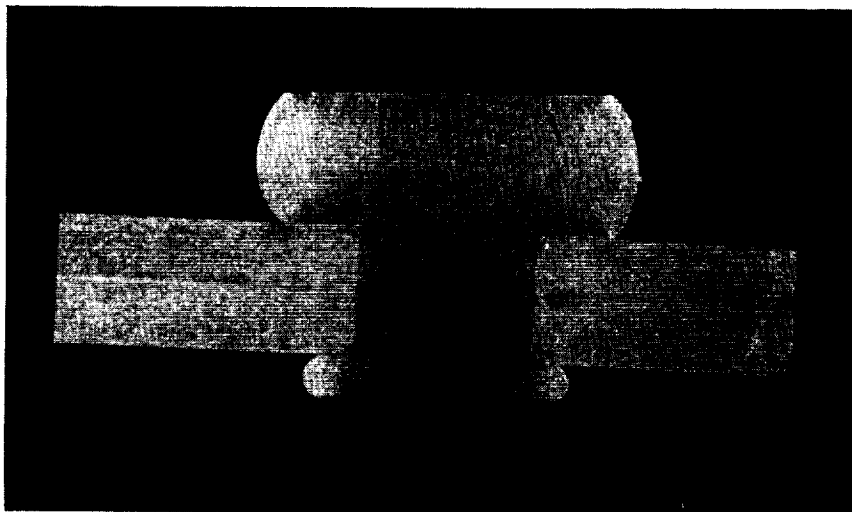
The completed Type IE, 0.030-inch gage material specimens are illustrated in Figure 30. All of the test specimens were assembled with the "Lockalloy" rivets without a single fracture in either the 0.030-inch or the 0.060-inch beryllium material. Figure 31 illustrates the testing of a typical Type IE specimen in the "Instron" tensile testing machine.

Constant loading rates of 1800 and 2300 pounds per minute were used during the testing of the 0.030-inch and the 0.060-inch specimens, respectively. Again, due to the difference in the thickness of the material in the two sets of specimens, the types of failure were quite different.

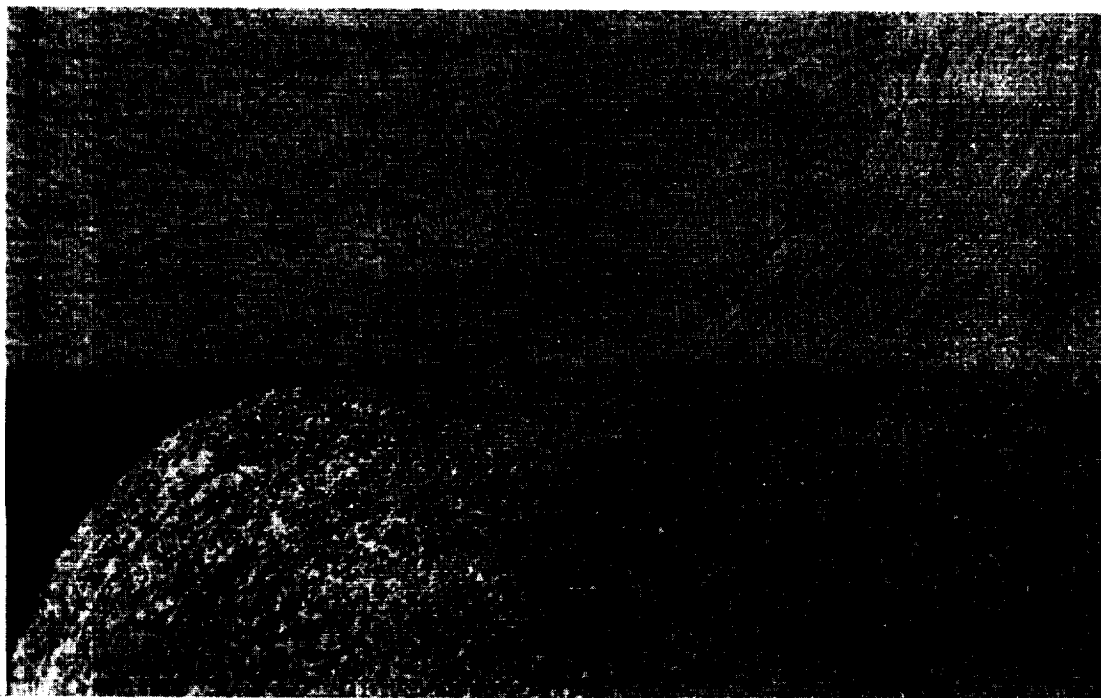
As occurred during the testing of the "beryllium riveted" specimens, all of the 0.030-inch thick test specimens failed in the beryllium, through the fastener line, due to a combination of high tensile and bearing stresses compounded by bending stresses. There was no evidence of rivet failure. The consistent failures through the rivet line are illustrated in Figure 32.

The failure mode of the 0.060-inch specimens was entirely different from that exhibited by the 0.030-inch specimens. As illustrated in Figure 33, the failure of the specimens was due to the shearing of the "Lockalloy" rivets. It should be specifically noted that all of the "Lockalloy" rivets failed in shear at the joint interface, not at the rivet head-shank transition as occurred with the beryllium rivets. Visual comparison of the failed rivets, illustrated in Figures 26 (beryllium) and 33 ("Lockalloy"), clearly reveals the difference in the two types of failure. This difference is believed due to the greater ductility and lower notch sensitivity of the "Lockalloy" rivet material.

Visual inspection of a representative autographically recorded load-deflection curve, illustrated in Figure 34, reveals a slight indication of yield, an improvement over the linear characteristic displayed by the beryllium specimen illustrated in Figure 27.



"Lockalloy" Riveted Joint - 10X

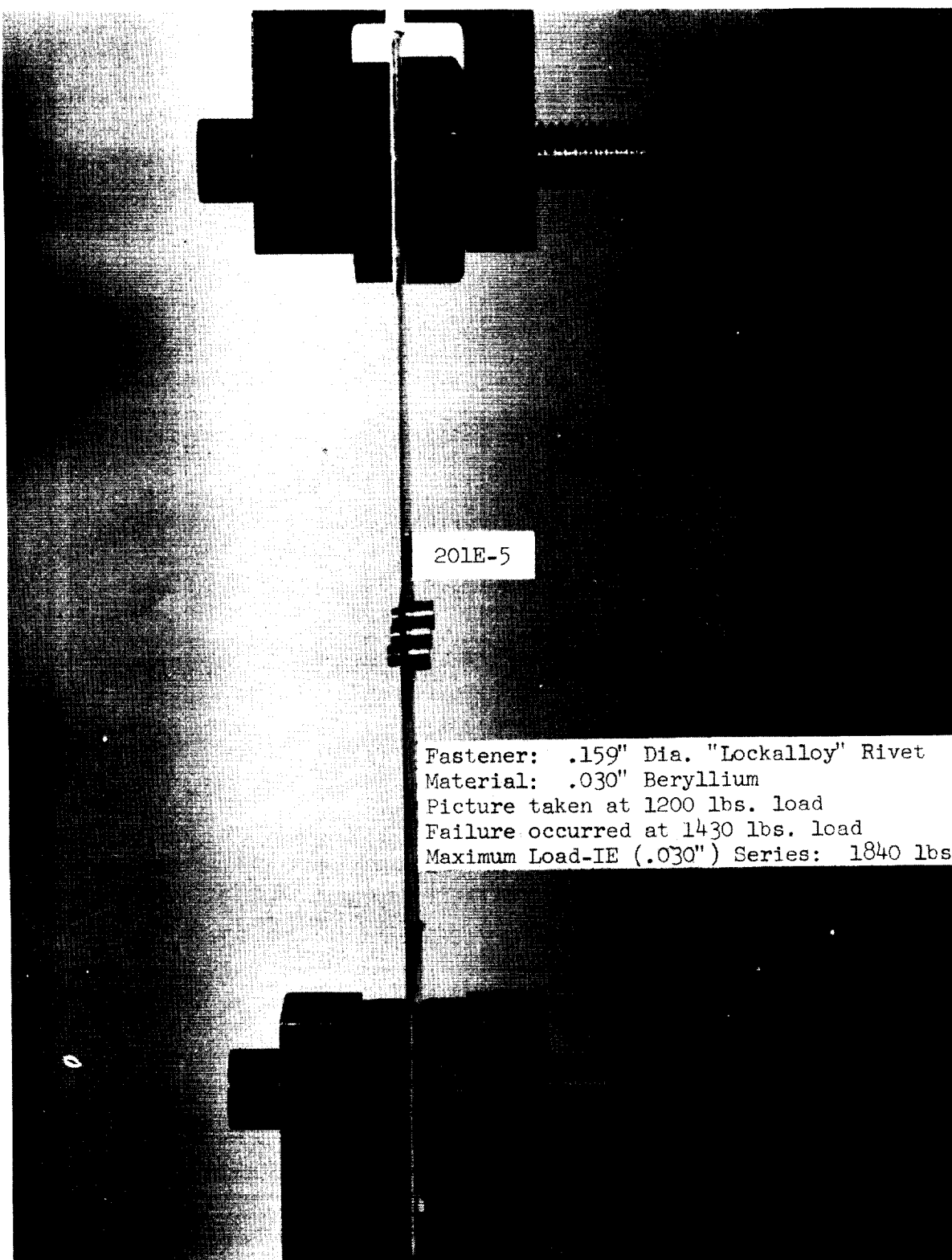


Bottom of "Lockalloy" Rivet - 100X

FIGURE 29. TYPE IE SPECIMEN - INSTALLED "LOCKALLY" RIVET.  
NOTE SMOOTH GRAIN ORIENTATION.



FIGURE 30. TYPE IE SPECIMENS - 0.030-INCH MATERIAL - "LOCKALLOY" RIVETS



201E-5

Fastener: .159" Dia. "Lockalloy" Rivet  
Material: .030" Beryllium  
Picture taken at 1200 lbs. load  
Failure occurred at 1430 lbs. load  
Maximum Load-IE (.030") Series: 1840 lbs.

FIGURE 31. TYPE IE SPECIMEN - 0.030-INCH MATERIAL - TENSILE TEST

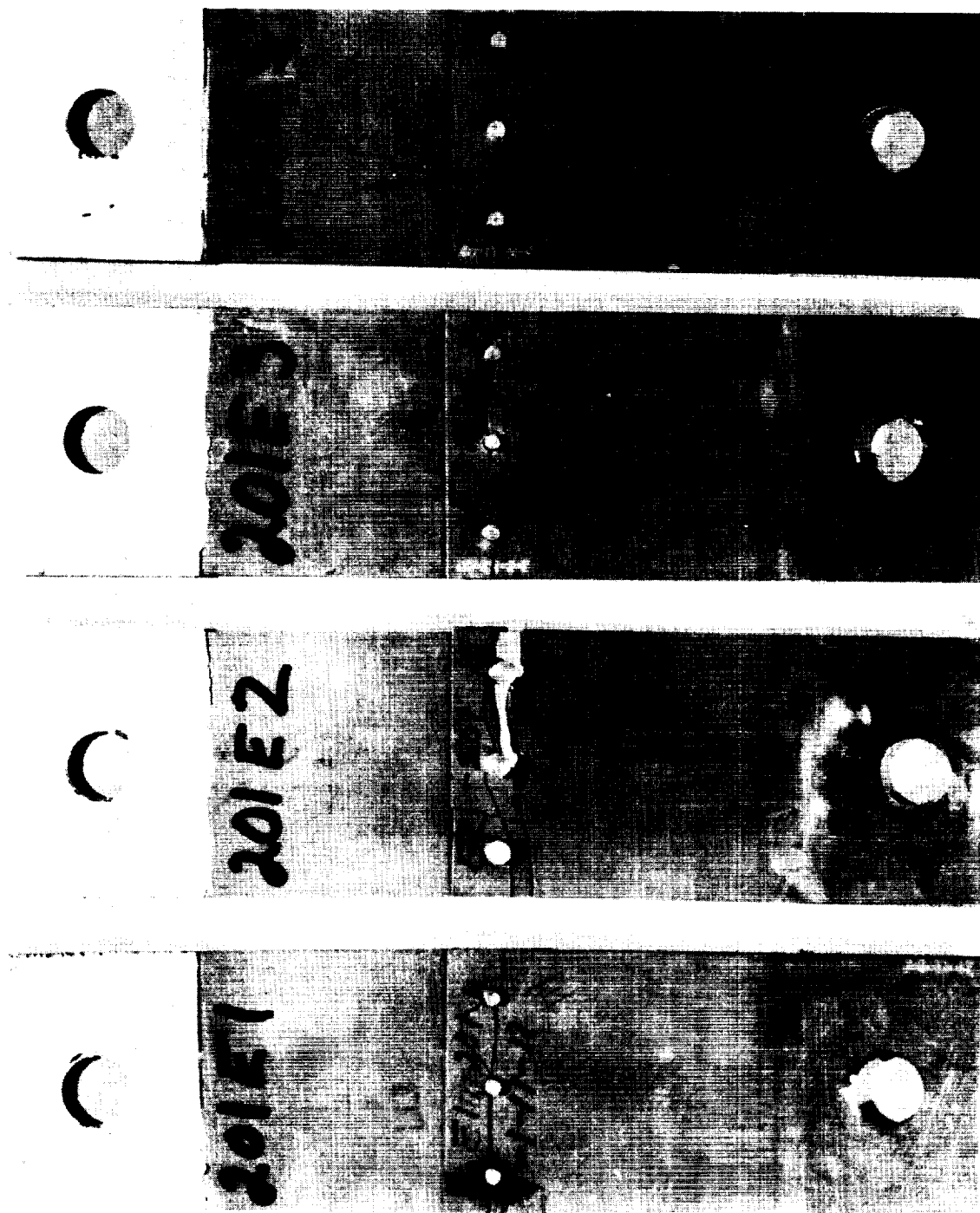


FIGURE 32. TYPE IE SPECIMENS - 0.030-INCH MATERIAL - TYPICAL FAILURE MODE



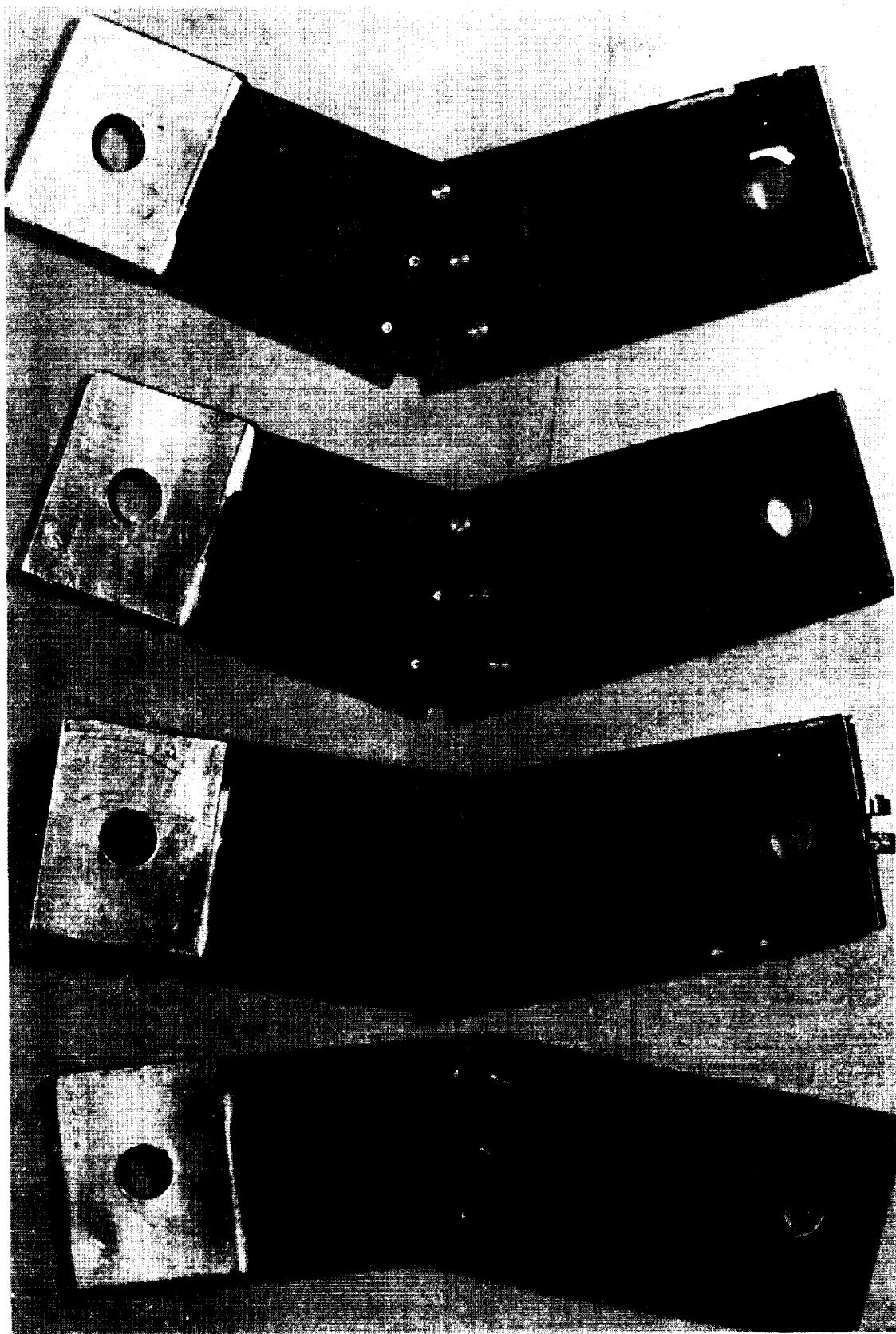


FIGURE 33. TYPE IE SPECIMENS - 0.060-INCH MATERIAL - TYPICAL FAILURE MODE

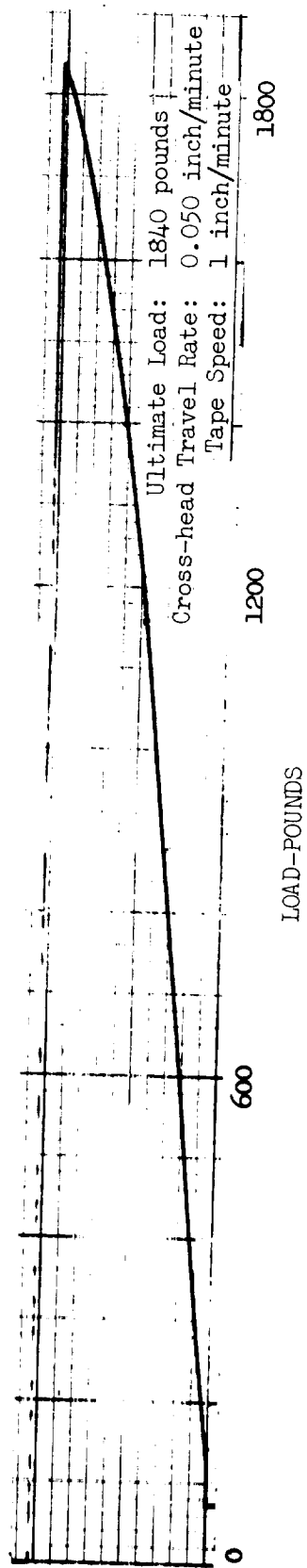


FIGURE 34. TYPE IE LOAD-DEFLECTION CURVE - SPECIMEN 201E-2

f. Type IF - Combination Adhesive Bonding and Cherry Blind Rivets. Due to the load concentration at the mechanical fasteners, and the notch sensitivity of beryllium at room temperature, the combination of adhesive bonding and riveting should result in the fabrication of improved mechanical joints. The distribution of the load-carrying capacity of the adhesive bond at room temperature, and the increased ductility and reduced notch sensitivity of beryllium at higher temperatures, should result in improved joint efficiency throughout the normally anticipated "working" temperature range for beryllium structures.

The objective of this limited investigation was the evaluation of the feasibility of the combination joining method. As the scope of the program is limited, only one adhesive was tested. The use of cherry blind rivets permitted a direct comparison of the characteristics of the two types of joints, i.e., identical mechanical fasteners with and without adhesive bonding.

In order to obtain the maximum comparative data, one of the bonding materials tested during the "Adhesive Bonding" phase of this program, Epon VI (Shell Chemical Company), was selected for this task.

The faying surfaces of the specimens were prepared and the adhesive applied in accordance with the procedure outlined in the section on Adhesive Bonding. The rivets then were installed as outlined previously in the section on Type IC - Cherry Blind Rivets.

The completed Type IF specimens are illustrated in Figures 35 and 36. Two of the joints, fabricated of 0.030-inch material, failed during the installation of the rivets. This was due to the localized distortion of the beryllium around the hole caused by the displacement of the bonding material as the rivet was "set." These failures are clearly illustrated in Figure 35. No failures occurred during the assembly of the 0.060-inch specimens.

A constant loading rate of 2500 pounds per minute was used during the testing of the specimens. Due to the failure during assembly, specimen 201F1 was not tested. Specimen 201F2, also cracked during assembly, was tested to failure; the specimen failed in the beryllium, through the fastener line, as anticipated. Specimen 201F3 failed initially by "peeling" of

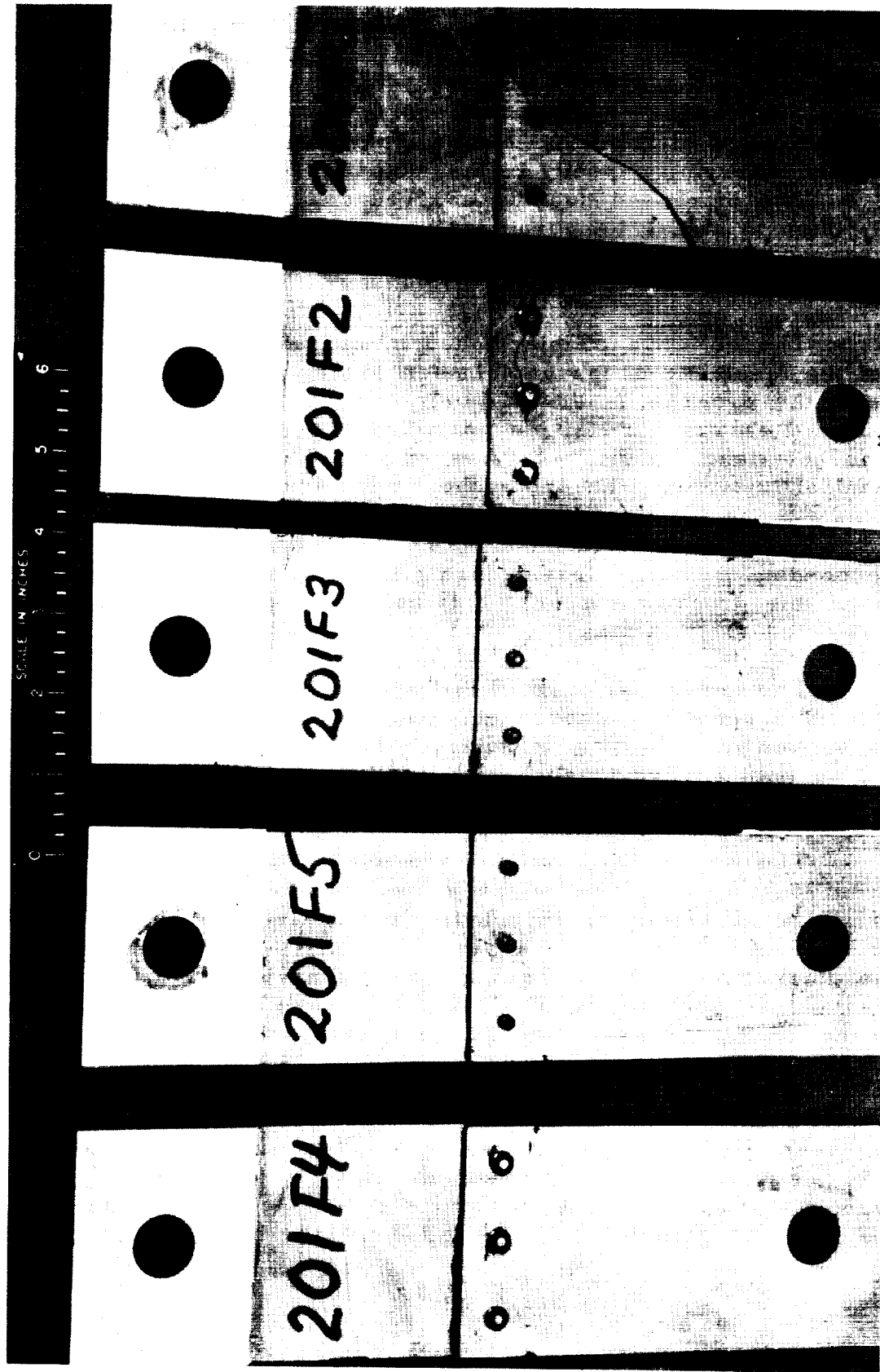


FIGURE 35. TYPE IF SPECIMENS - 0.030-INCH MATERIAL - ADHESIVE BONDING AND CHERRY BLIND RIVETS

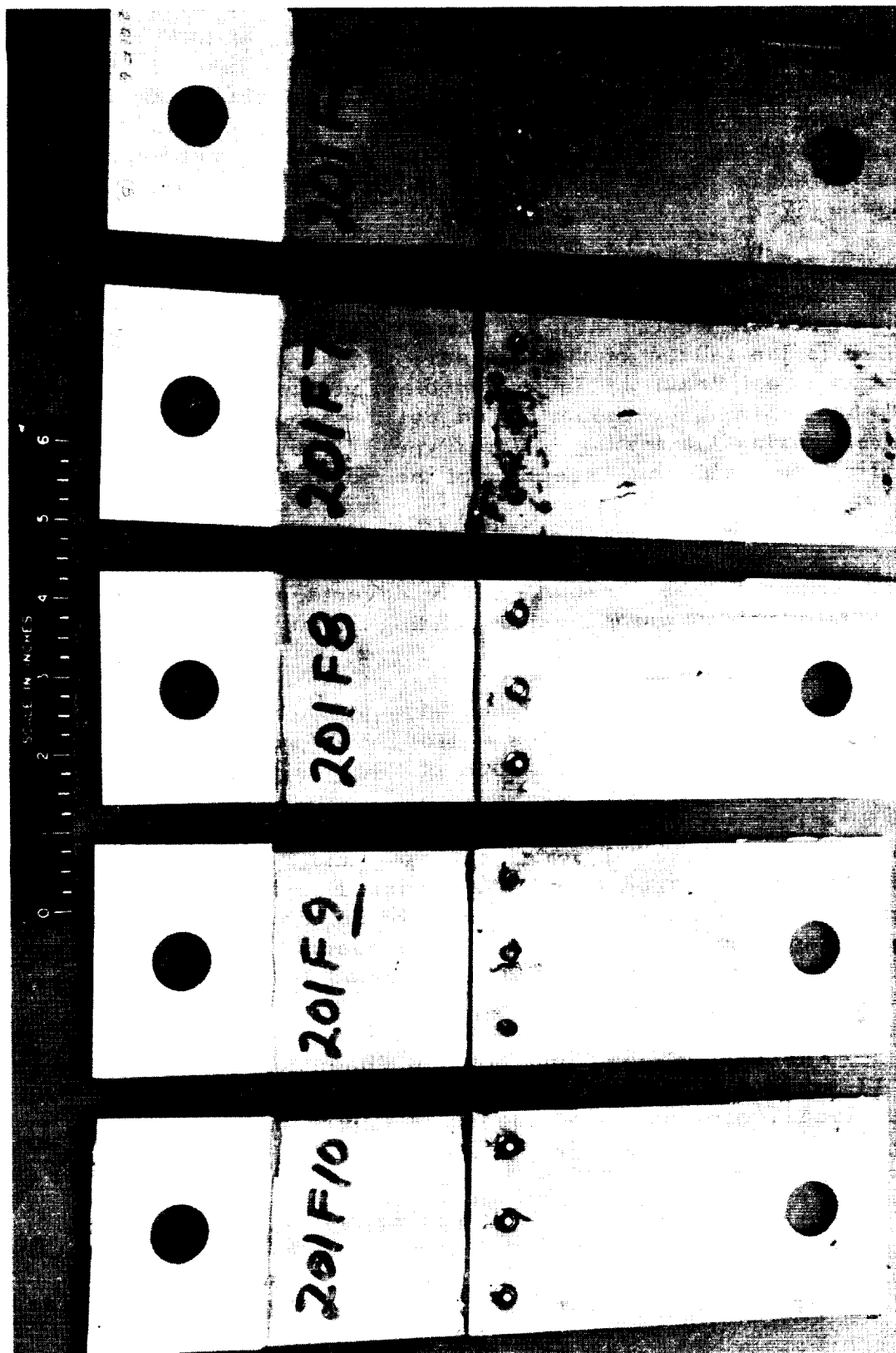


FIGURE 36. TYPE IF SPECIMENS - 0.060-INCH MATERIAL - ADHESIVE BONDING AND CHERRY BLIND RIVETS

the adhesive, followed by bearing failure at one of the loading pin holes, at a load of 1680 pounds. Retesting of this specimen, substituting vise jaws for the pin connections, resulted in failure in the beryllium through the fastener line. Specimen 201F4 failed in the beryllium, through the fastener line, due to the combination of high bearing and bending stresses, subsequent to the early failure of the bond. The failed specimens are illustrated in Figure 37.

The failure mode of the 0.060-inch specimens, was entirely different from that exhibited by the 0.030-inch specimens. As illustrated in Figure 38, the primary failure of the specimens was due to the failure of the fasteners. The "tilting" of the joint area precipitated the failure of the rivets; the rivet collars were sheared and the stems pulled out in the same manner as occurred during the testing of the Type IC joints; the joint configurations, with the exception of the adhesive bonding, were identical.

A comparison of the test results, presented in Table III, clearly indicates the lack of any advantage accruing from the incorporation of the adhesive bonding in the mechanically fastened joint.

The utilization of a higher strength adhesive may result in improved joint characteristics. However, such an extensive investigation is not within the scope of this program.

#### 4. Type II Lap Joints - Double Row Fasteners.

Table VI presents the chemical analyses and mechanical properties of the material procured from The Brush Beryllium Company for the fabrication, testing, and evaluation of the double-row configuration, mechanically fastened joints. The specific utilization of each of the several sheets of material is identified by the type numbers of the specimens.

The configuration and nominal dimensions of the "202" Type II joints are illustrated in Figure 39. A summary of the test loads, stresses, and modes of failure is presented in Table VII.

The preparation of the Type II specimens and the

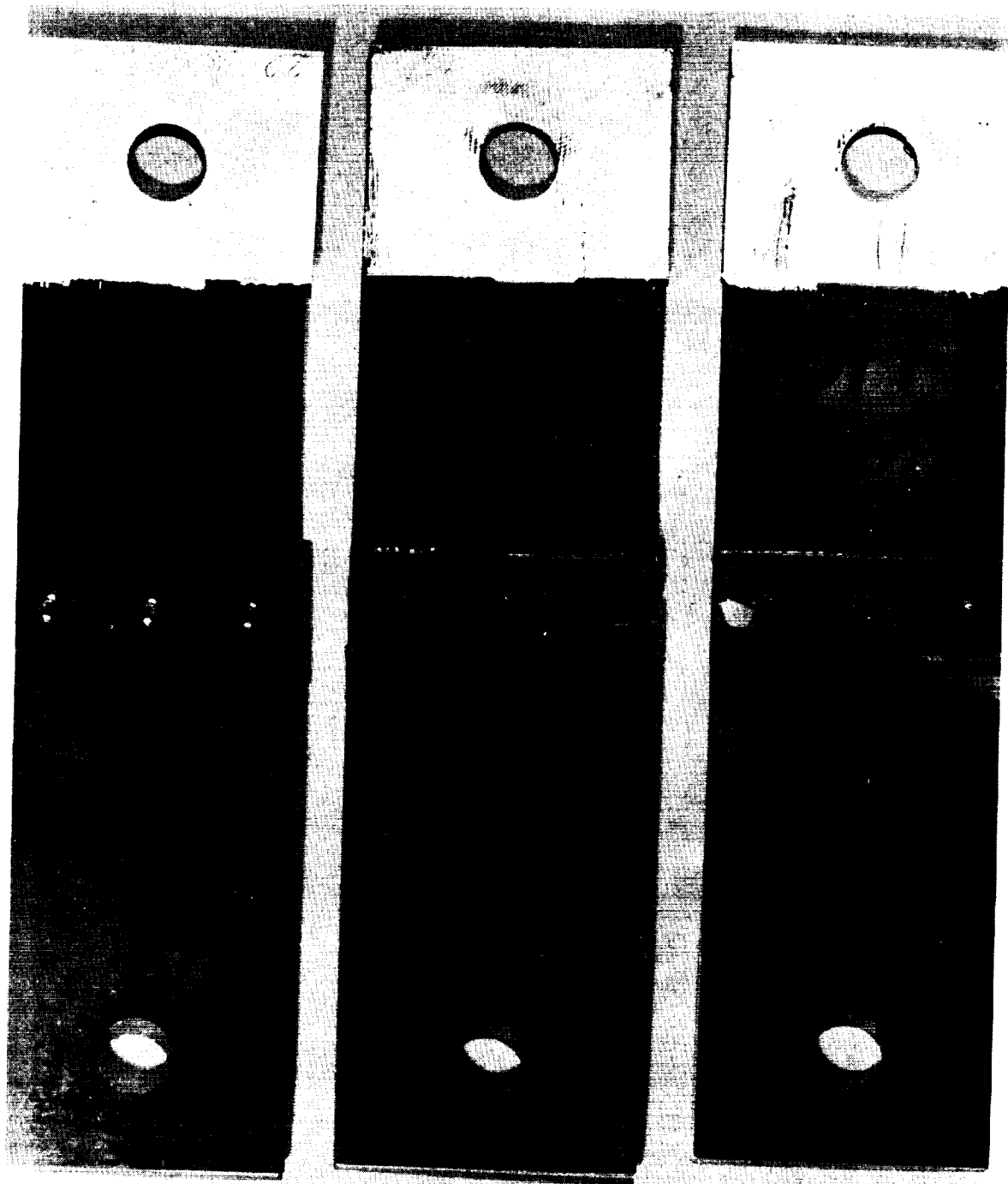


FIGURE 37. TYPE IF SPECIMENS - 0.030-INCH MATERIAL - TYPICAL FAILURE MODE

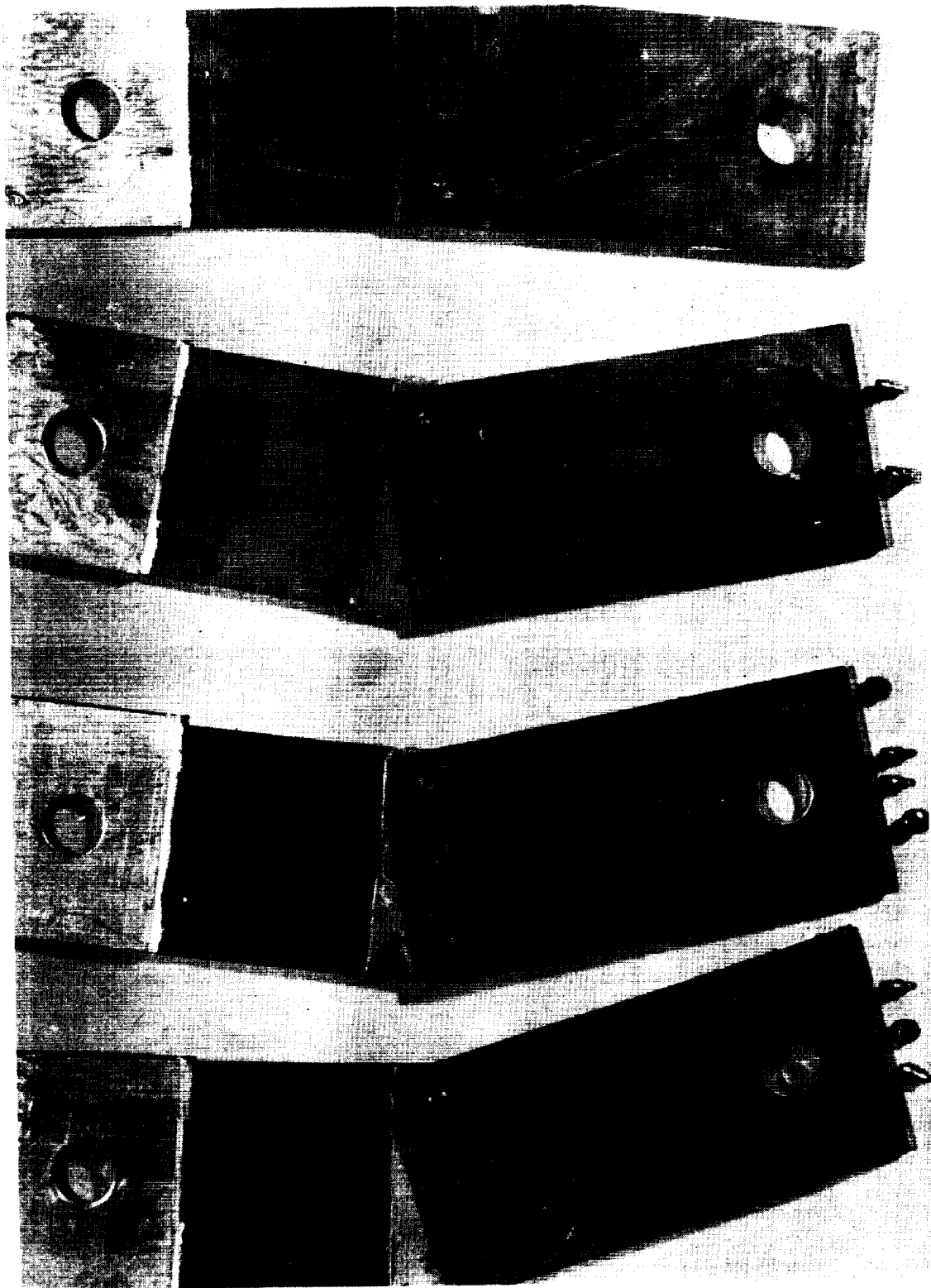


FIGURE 38. TYPE IF SPECIMENS - 0.060-INCH MATERIAL - TYPICAL FAILURE MODE



TABLE VI  
CHEMICAL ANALYSIS AND MECHANICAL PROPERTIES - MATERIAL FOR DOUBLE-ROW MECHANICAL FASTENER SPECIMENS  
Vendor: The Brush Beryllium Company

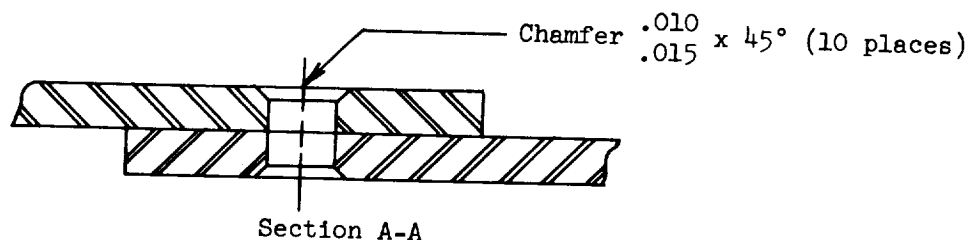
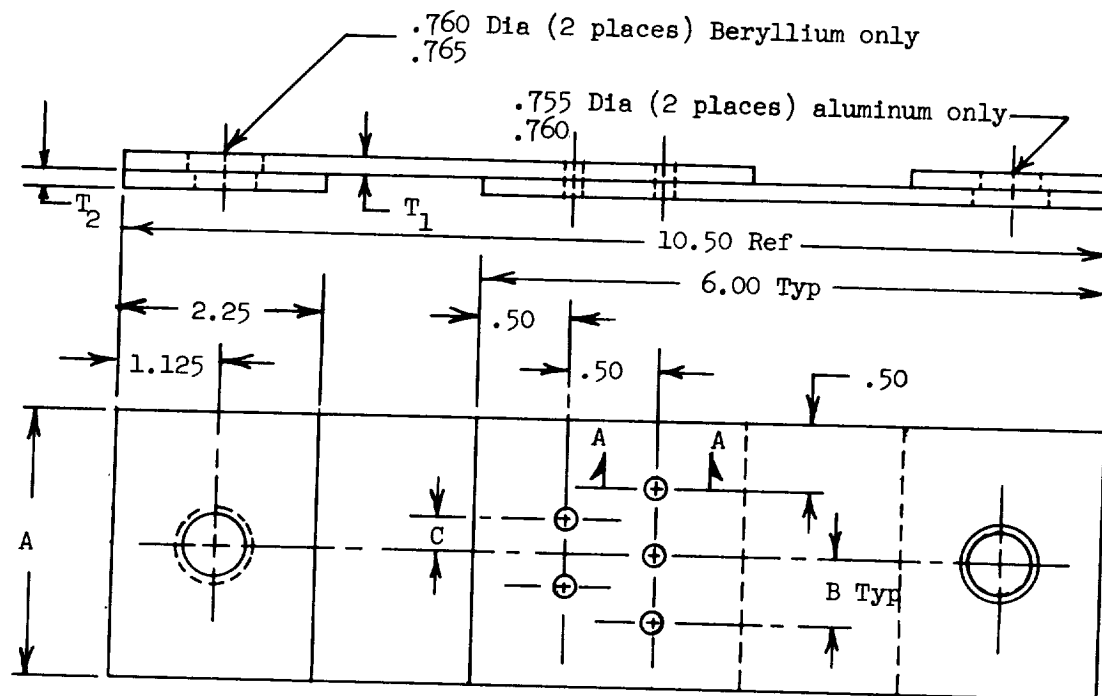
CHEMICAL ANALYSIS - %							
Lot No.	Be Assay	BeO	Fe	Si	Al	Mg	C
3516	98.21	1.70	0.14	0.04	0.11	0.008	0.13
2469	98.50	1.83	0.12	0.03	0.008	0.009	0.10
9967	98.29	1.66	0.138	0.05	0.095	0.011	0.12
1033	98.19	1.60	0.129	0.045	0.07	0.021	0.11

NOTE: Cr, Mn, Ni LESS THAN 0.04% EACH

TABLE VI (Cont.)

## Mechanical Properties

Type Joint	Gage Inch	Lot No.	Sheet No.	Test Direction	Fty PSI	Ftu PSI	Elongation % in 1-Inch
IIA, IIB	0.120	3516	1066A1	L T	60,900 58,400	84,600 80,000	18 10
IIB	0.120	3516	1065B1	L T	62,200 59,700	84,600 80,300	16 15
IIIC, IID, IIE, IIF	0.030	3516	1069B2	L T	61,000 60,700	79,900 81,100	10 24
IIF	0.030	3516	1070B	L T	62,500 59,900	85,300 80,300	15 15
IIF	0.030	3516	1070A	L T	62,500 59,900	85,300 80,300	15 15
IIIC, IID	0.060	3516	1067B2	L T	58,600 61,100	80,200 80,200	12 18
IIIE, IIF	0.060	3516	1067A2	L T	58,600 61,100	80,200 80,200	12 18
IIIE	0.060	2469	734	L T	51,300 50,300	79,700 70,000	16.5 6.5
IIIE	0.060	9967	447B	L T	57,400 58,100	78,300 86,200	11.5 14
IIIE	0.060	1033	456A	L T	56,700 54,900	81,100 74,000	12.8 12.8
IIIE	0.060	3516	1068A	L T	61,800 58,700	82,900 81,000	10 23
IIF	0.060	3516	1067B1	L T	58,600 61,100	80,200 80,200	12 18



Conf.	Fastener Type	Hole Dia.	Mat'l Gage		Dimension		
			T1	T2	A	B	C
A	Huckbolt (NAS 2006-V4)	.189-.193	.12	.12	3.25	1.125	.56
B	Jo-bolt (NAS 1671-3)	.199-.202	.12	.12	3.25	1.125	.56
C	Cherry Rivet (MS 20600-M5)	.158-.164	.03/.06	.03/.06	3.00	1.00	.50
D	Beryllium Rivet	.160-.164					
E	Lockalloy Rivet	.160-.164					
F	Cherry Rivet/Bonded	.158-.164					

NOTE: ALL DIMENSIONS ARE IN INCHES.

FIGURE 39. TYPE II JOINT CONFIGURATION - NOMINAL DIMENSIONS

TABLE VII

## TYPE II SPECIMENS - TEST SUMMARY

Specmn No.	Sheet Thkns	Area (in <sup>2</sup> )(2)		Ult Load (PSI)	Fasteners		Tension Stress (PSI)		Avg Bearing Stress at Fastrs(PSI) (3)(19)	Notes
		Full Sectn	At Fastrs		No.	lbs/Fastr (4)	Full Sectn (17)	Net Sectn at Holes (18)		
202A-1	0.1255	0.4071	0.3348	11,450	5	2290	28,126	34,200	96,584	7
202A-2		SAMPLE - NOT TESTED								5
202A-3	0.1260	0.4095	0.3369	13,250	5	2650	32,357	39,329	111,326	7
202A-4	0.1255	0.4129	0.3387	12,700	5	2540	30,758	37,496	107,128	7
202A-5	0.1260	0.4095	0.3373	11,960	5	2392	29,206	35,458	100,487	7
202B-1	0.1250	0.4089	0.3350	13,750	5	2750	33,627	41,045	110,986	8
202B-2	0.1215	0.3934	0.3212	12,950	5	2590	32,918	40,318	107,540	7
202B-3	0.1230	0.3996	0.3261	13,520	5	2704	33,834	41,460	110,901	7
202B-4	0.1280	0.4146	0.3386	11,925	5	2385	28,763	35,219	93,994	7
202B-5		SAMPLE - NOT TESTED								5
202C-1	0.0306	0.0912	0.0764	2,750	5	550	30,154	35,995	111,789	7
202C-2		ONE SEGMENT SEVERELY CRACKED DURING ASSEMBLY								6
202C-3	0.0284	0.0839	0.0748	2,620	5	524	31,228	35,013	115,929	7
202C-4	0.0330	0.0990	0.0781	2,940	5	588	29,697	37,639	112,342	7
202C-5		SAMPLE - NOT TESTED								5
202C-6	0.0600	0.1798	0.1512	4,640	5	928	25,806	30,688	97,275	10
202C-7		SAMPLE - NOT TESTED								5
202C-8	0.0600	0.1799	0.1511	4,700	5	940	26,126	31,105	97,917	10
202C-9	0.0600	0.1800	0.1514	4,650	5	930	25,833	30,713	97,484	10
202C-10	0.0600	0.1795	0.1509	4,600	5	920	25,627	30,484	96,639	10
202D-1	0.0275	0.0818	0.0686	790	5	158	9,658	11,516	35,908	7
202D-2	0.0326	0.0981	0.0824	2,260	5	452	23,038	27,411	86,656	7, 11
202D-3	0.0296	0.0887	0.0745	1,425	5	285	16,065	21,564	60,177	7, 11
202D-4	0.0312	0.0943	0.0794	1,610	5	322	17,073	20,277	64,737	7, 11
202D-5		SAMPLE - NOT TESTED								5
202D-6	0.0585	0.1755	0.1475	3,350	5	670	19,088	22,712	71,765	8
202D-7	0.0595	0.1789	0.1505	4,630	5	926	25,880	30,764	97,886	8
202D-8	0.0590	0.1770	0.1487	2,180	5	436	12,316	14,660	46,186	7, 11
202D-9	0.0585	0.1755	0.1476	2,030	5	406	11,567	13,753	43,656	7, 11
202D-10		SAMPLE - NOT TESTED								5

TABLE VII (Cont.)  
TYPE II SPECIMENS - TEST SUMMARY

Specmn No.	Sheet Thkns	Area (in <sup>2</sup> )(2)		Ult Load (PSI)	Fasteners		Tension Stress (PSI)		Avg Bearing Stress at Fastrs(PSI) (3)(19)	Notes
		Full Sectn	At Fastrs		No.	lbs/Fastr (4)	Full Sectn (17)	Net Sectn at Holes (18)		
202E-1	0.0297	0.0890	0.0747	2,000	5	400	22,472	26,774	84,282	7
202E-2	0.0306	0.0917	0.0770	1,920	5	384	20,938	24,929	78,240	7
202E-3	0.0290	0.0869	0.0728	2,210	5	442	25,432	30,349	94,566	7
202E-4	0.0293	0.0879	0.0739	2,025	5	405	23,038	27,402	86,612	7, 11
202E-5		SAMPLE - NOT TESTED								5
202E-6	0.0620	0.1869	0.1574	3,610	5	722	19,315	22,935	73,240	10
202E-7		SAMPLE - NOT TESTED								5
202E-8	0.0620	0.2438	0.2143	3,675	5	735	15,074	17,149	74,559	10
202E-9	0.0610	0.1821	0.1530	3,720	5	744	20,428	24,314	76,701	10
202E-10	0.0625	0.1870	0.1572	3,670	5	734	19,626	23,346	73,858	10
202F-1	0.0300	0.0910	0.0766	1,650	5	330	18,132	21,540	68,750	9
202F-2	0.0290	0.0853	0.0713	1,225	5	245	14,361	17,181	54,688	6, 7, 12
202F-3	0.0310	0.0929	0.0781	2,750	5	550	29,602	35,211	110,968	9
202F-4	0.0315	0.0946	0.0794	1,580	5	316	16,702	19,899	62,698	9
202F-5		BADLY FRACTURED DURING ASSEMBLY								6
202F-6	0.0610	0.1821	0.1528	4,900	5	980	26,908	32,068	100,410	8, 13
202F-7		SAMPLE - NOT TESTED								5
202F-8	0.0610	0.1830	0.1539	4,430	5	886	24,208	28,785	91,340	10, 14
202F-9	0.0610	0.1828	0.1539	4,680	5	936	25,602	30,409	97,116	10, 15
202F-10	0.0605	0.1807	0.1516	4,880	5	976	27,006	32,190	100,702	10, 16

## TABLE VII NOTES

1. The nominal dimensions of the Type II specimens are shown in Figure 39.
2. Either the cross-sectional area of the failed segment or, if the fasteners failed, the lesser of the cross-sectional areas of the two segments is reported.
3. The 0.010-inch - 0.015-inch chamfer disregarded in the calculations.
4. The fastener shear strengths are presented in Table II.
5. Sample - not tested.
6. Fractured during assembly - not tested.
7. Failed in net tension through the fastener holes - no fastener failure.
8. Simultaneous failure of the fasteners in shear, and the material in net tension through the fastener holes.
9. Failed in full section of the beryllium segment, due to severely warped material.
10. Fasteners sheared prior to development of full tensile potential of the beryllium segment.
11. Short radial cracks occurred at one hole prior to assembly.
12. Bond released at 1000 pounds.
13. Bond released at 2580 pounds.
14. Bond released at 1850 pounds.
15. Bond released at 2500 pounds.
16. Bond released at 2000 pounds.

# TABLE VII NOTES (Cont'd)

## 17. Full section Tensile Stress:

$$\sigma_{nt} = \frac{P}{Wt_1}$$

P = Test Load; pounds

W = Specimen width; inches

$t_1$  = Beryllium thickness; inch

## 18. Net Tension Stress

$$\sigma_{nt} = \frac{P}{W_n t_1}$$

P = Test Load; pounds

$W_n$  = Special width less diameter of 3 holes on common centerline; inches

$t_1$  = Beryllium thickness; inch

## 19. Average Bearing Stress:

$$\sigma_{br} = \frac{P}{Dt}$$

P = Test Load; pounds

t = Beryllium thickness; inch

(a) Types 202A and 202B only:

D = Total average diameter of (5) fasteners; inch

(b) Types 202C, 202D, 202E, and 202F only:

D = Total diameter of (5) fastener holes; inch

installation of the fasteners were accomplished with the same procedures utilized for the assembly of the Type I specimens. In all cases, the difference was in the basic configuration; five fasteners were installed in two staggered rows versus three fasteners installed in a single row.

The testing of the double-row configuration lap joints provided the bases for the direct comparison of the joint efficiencies, and the evaluation of the reductions in the local bearing loads at the fasteners, in relation to the proportional increases gained in the net tensile loads.

a. Type IIA - Huckbolts. The assembly of the Type IIA specimens, utilizing the procedures discussed in the section on Type IA - Huckbolts, was accomplished without incident. All of the specimens were assembled without any indication of fracture in the beryllium, even though additional fasteners were installed at a decreased pitch dimension. The completed Type IIA specimens, ready for testing, are illustrated in Figure 40. Figure 41 illustrates the testing of one of the specimens in the "Riehle" hydraulic tensile testing machine at a constant loading rate of 2500 pounds per minute. It may be noted that, although the typical bending of the material and the "tilting" of the fasteners are clearly visible in the illustration, the magnitudes are significantly less than occurred during the testing of Type IA - Single Row Fastener specimens.

The failure mode of the Type IIA specimens was quite similar to that exhibited by the Type IA specimens except that the failures of the specimens were not precipitated by the shearing of the fasteners. The high bearing stress at the fasteners in this joint series, plus the effect of the bending stress, resulted in the failure of the joints in net tension in the beryllium material through the fastener lines, as illustrated in Figure 42.

A comparison of the results of the tensile tests of the two series of joint specimens (Type IA - Single Row Fasteners, and Type IIA - Double Row Fasteners) clearly reveals the advantage of the staggered double row fastener configuration. The installation of the additional fasteners, which reduced the bearing stresses, resulted in a 46 percent increase in the net tensile stress in the beryllium material; thus, the overall result was a substantially more efficient joint.





FIGURE 40. TYPE IIA SPECIMENS - HUCKBOLT FASTENERS

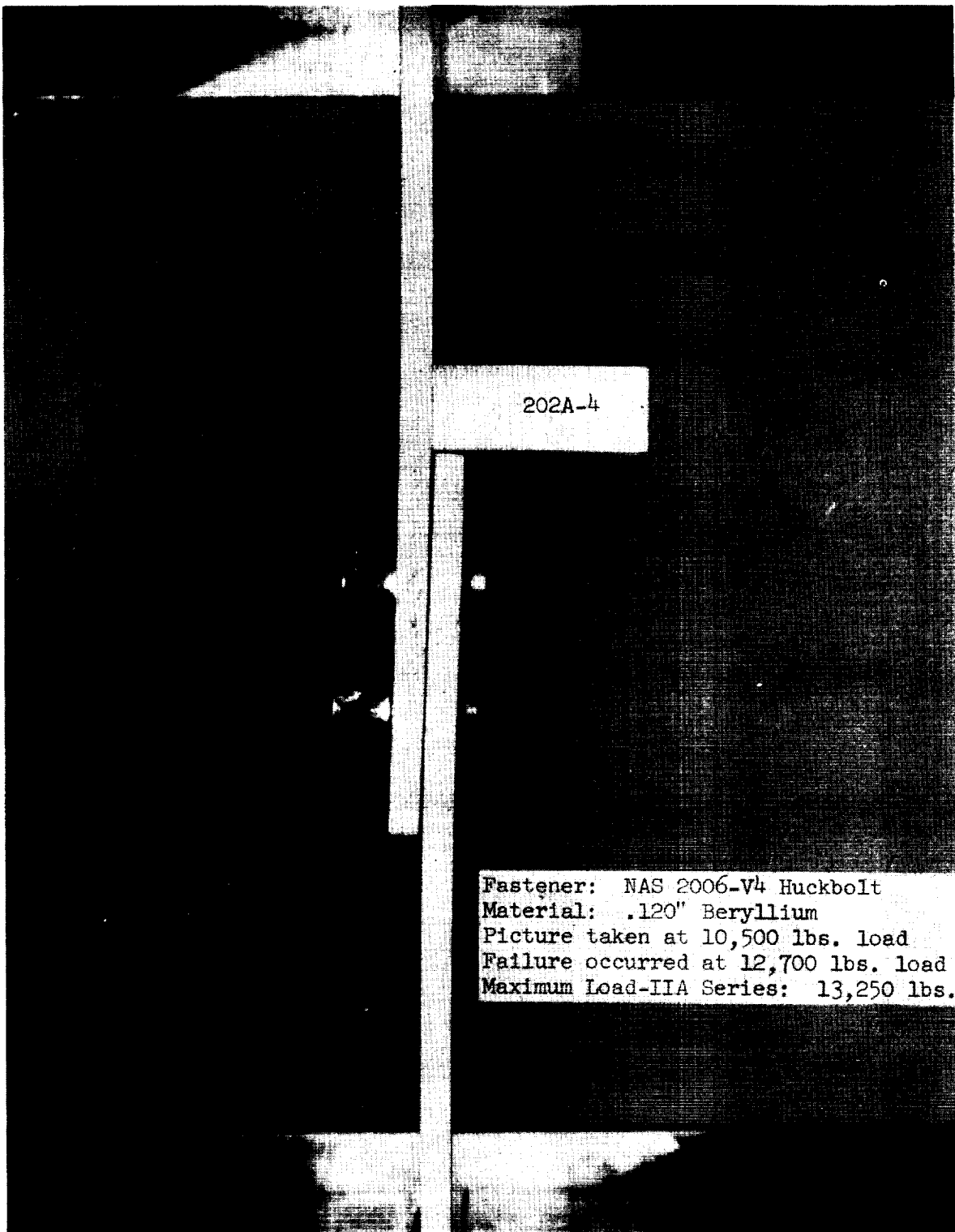


FIGURE 41. TYPE IIA SPECIMEN - TENSILE TEST.

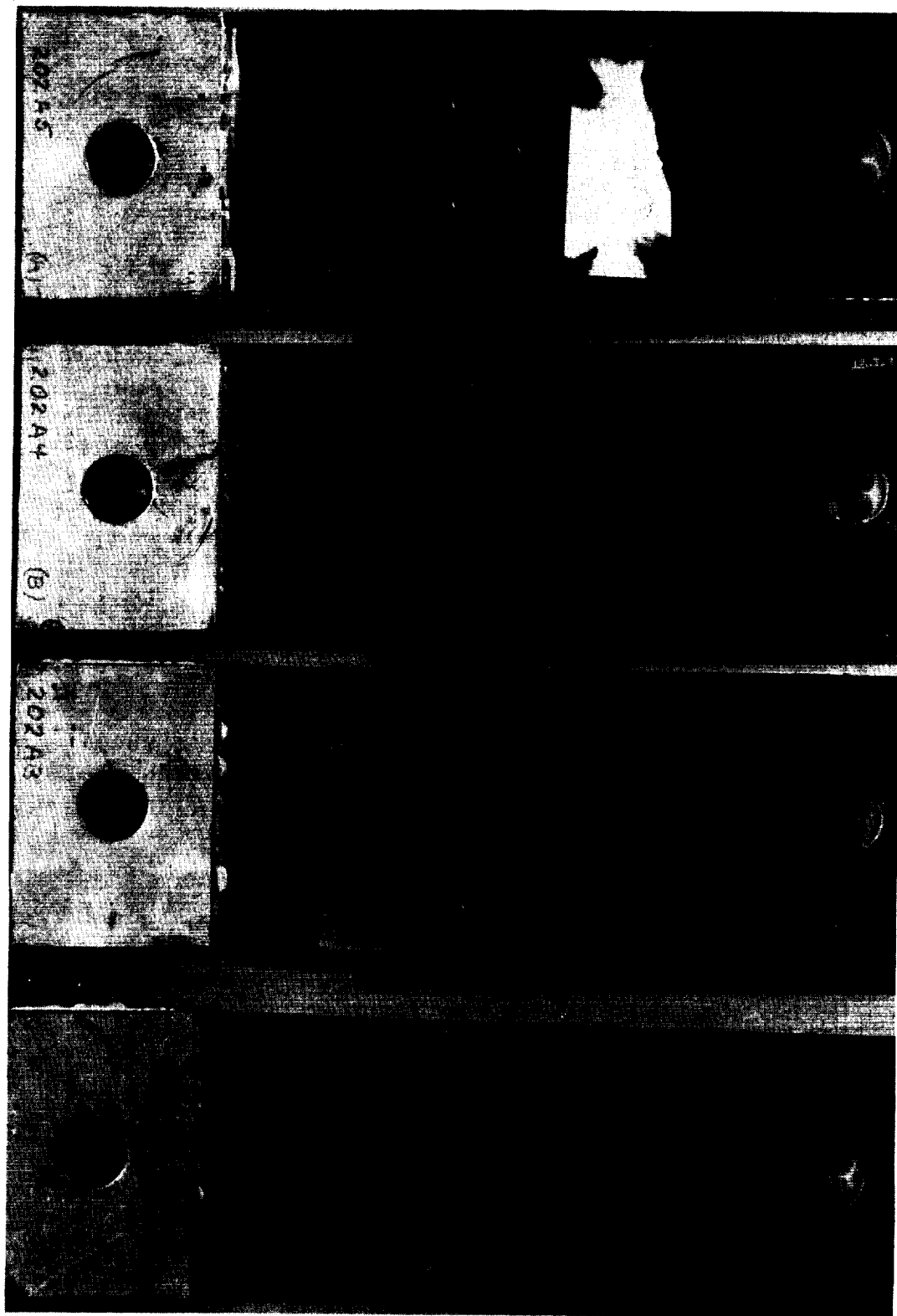


FIGURE 42. TYPE IIA SPECIMENS - TYPICAL FAILURE MODE

b. Type IIB - Jo-bolts. The assembly of the Type IIB specimens, utilizing the procedures discussed in the section on Type IB Jo-bolts, was accomplished without incident. The completed Type IIB specimens, ready for testing, are illustrated in Figure 43.

During the initial testing of specimen 202B-2 in the "Wiedman-Baldwin" tensile test machine, the beryllium failed in bearing at one of the loading pin holes at a load of 11,150 pounds. The retesting of this specimen and the testing of the balance of the Type IIB series were performed in the "Riehle" tensile testing machine. The vise grips, which spanned the full width of the specimens and thus assured even distribution of the load, were used for these tests. Figure 44 illustrates the testing of one of the specimens in the "Riehle" hydraulic tensile testing machine at a constant loading rate of 2500 pounds per minute. Again, it may be noted that although the typical bending of the material and the "tilting" of the fasteners are clearly visible in the illustration, the magnitudes, even at the higher load, are less than occurred during the testing of the Type IB - Single Row Fastener specimens.

The failure mode of the Type IIB specimens was quite similar to that exhibited by the Type IIA (Huckbolt) specimens; and quite different from that exhibited by the Type IB - Single Row Fastener Specimens which failed due to the shearing of the fasteners. The combined effect of the high bearing stress at the fasteners and the bending stress in the material resulted in the failure of the joints in net tension in the beryllium material through the fastener lines as illustrated in Figure 45.

A comparison of the results of the tensile tests of the two series of joint specimens (Type IB - Single Row Fasteners, and Type IIB - Double Row Fasteners) again verifies the advantage of the staggered double row fastener configuration. The 60 percent increase in the net tensile stress in the beryllium material clearly emphasized the substantial improvement in the efficiency of the joint.

c. Type IIC - Cherry Blind Rivets. During the assembly of these specimens utilizing the standard procedures discussed in the section on Type IC - Cherry Blind Rivets, one of the 0.030-inch gage material specimens (202C-2) cracked from

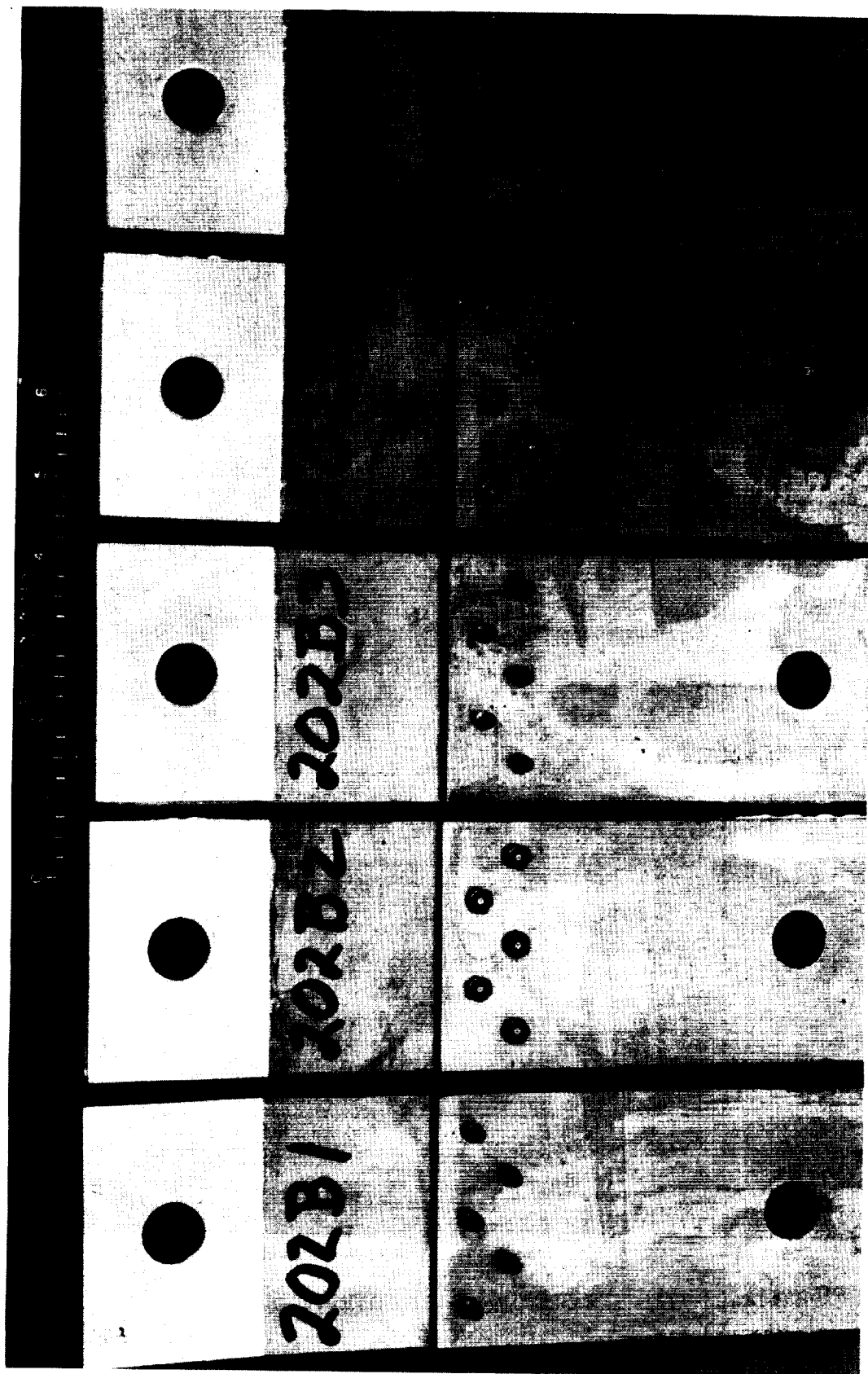
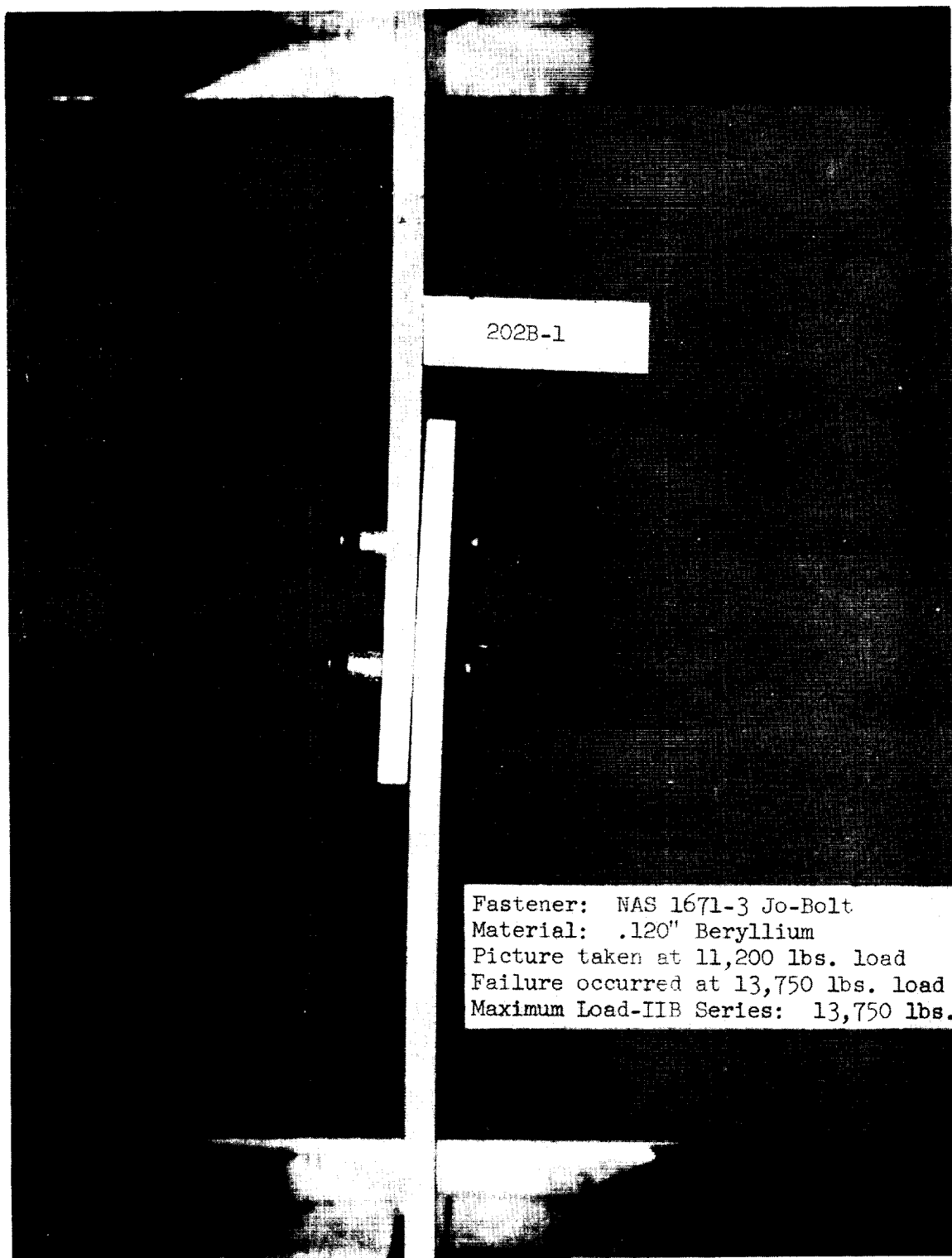


FIGURE 43. TYPE IIB SPECIMENS - JO-BOLT FASTENERS



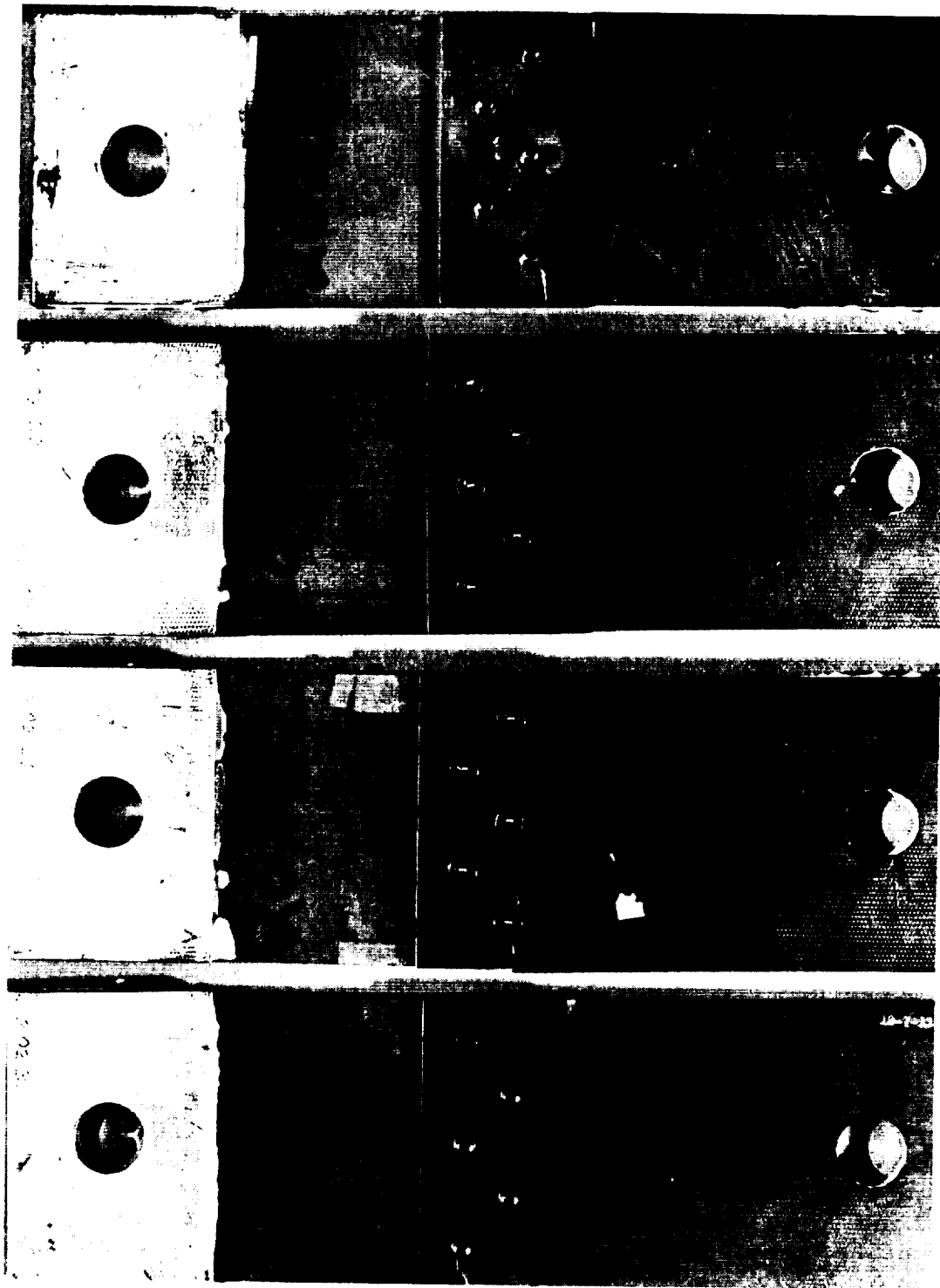


FIGURE 45. TYPE IIB SPECIMENS - TYPICAL FAILURE MODE

the rivet hole to the edge of the segment, and therefore was not tested. The balance of the specimens was assembled without incident. It is believed this failure may have occurred due to the hoop stresses developed during the installation of the fastener. This failure does serve to emphasize the danger inherent in the utilization of this type of internally expanding rivet for assembling thin gages of beryllium material. The completed Type IIC, 0.060-inch gage specimens are illustrated in Figure 46.

Figures 47 and 48 illustrate the testing of typical 0.030-inch and 0.060-inch gage specimens in the "Instron" tensile testing machine at average loading rates of 2100 and 2900 pounds per minute respectively. The typical bending of the material and the "tilting" of the fasteners is clearly visible in these illustrations.

During the initial testing of these Type IIC specimens, two of the 0.030-inch gage specimens (C1 and C3) failed in bearing at one of the loading pin holes. However, the aluminum reinforcement pad and the adhesive bond did not fail on specimen 202C-3; the specimen continued to carry the load and the testing was continued without interruption to ultimate failure through one of the rivet holes in the joint. The vise grips were used during the retesting of specimen C1 in the "Riehle" tensile testing machine.

Due to the differences in the thickness of the material in the two sets of specimens, the types of failure were quite different. However, the respective failure modes of these Type IIC specimens were identical to those exhibited by the Type IC specimens. Due to the combined effects of the high bearing stress at the fasteners and the bending stress in the material, all of the 0.030-inch thick test specimens failed in the beryllium, through the fastener line, at a net tensile stress significantly higher than was exhibited by the 0.060-inch thick specimens. The consistent failures through the rivet line are illustrated in Figure 49.

The failure mode of the 0.060-inch thick specimens was entirely different from that exhibited by the 0.030-inch specimens. As illustrated in Figure 50, the primary failure was due to the failure of the fasteners. The "tilting" of the joint area, clearly visible in Figure 48, precipitated the failure of the rivets; the beryllium material cut through the rivet sleeve and caused it to strip off the rivet stem. The resulting deformation of the rivet holes also is clearly visible in Figure 50. The lower indicated



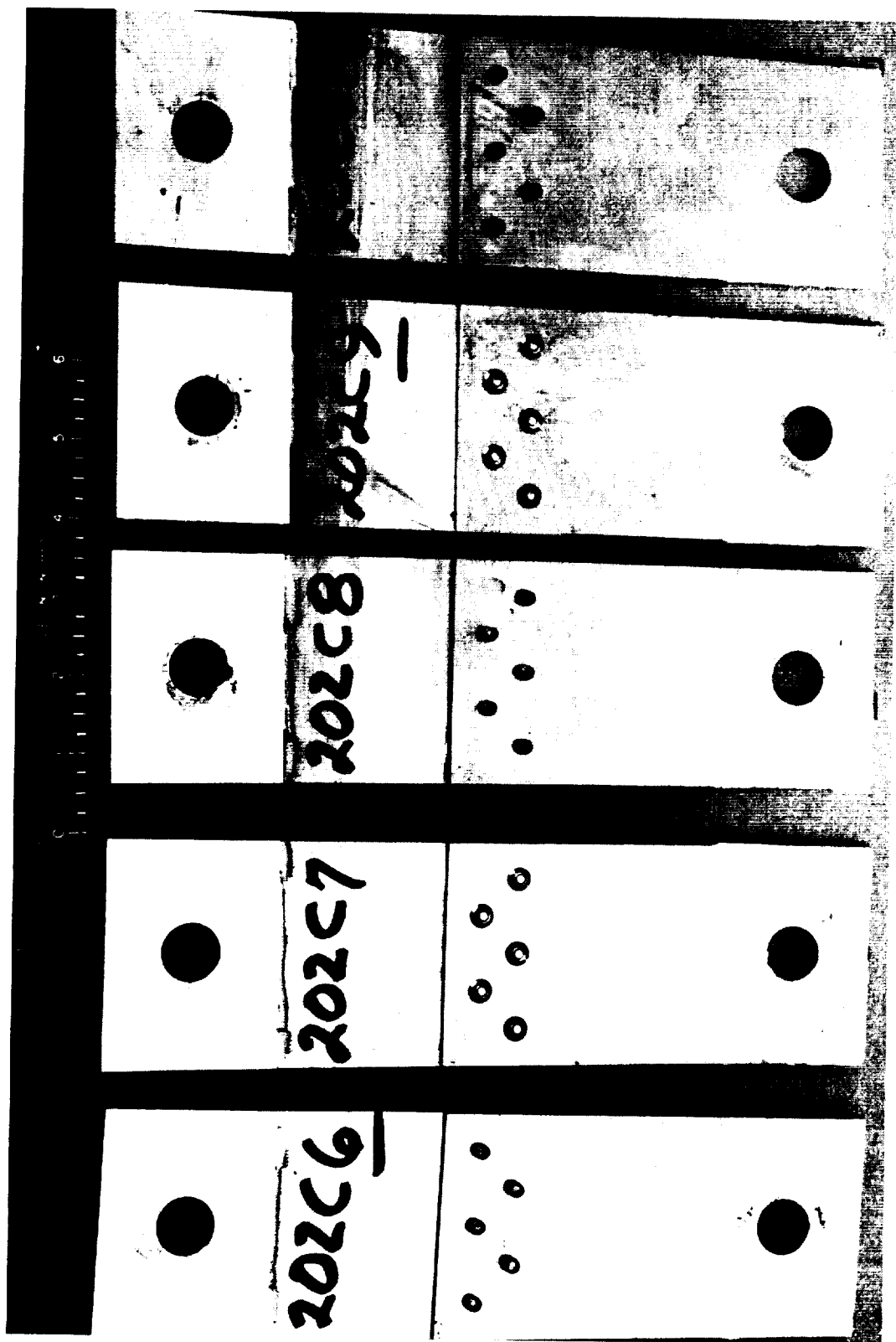
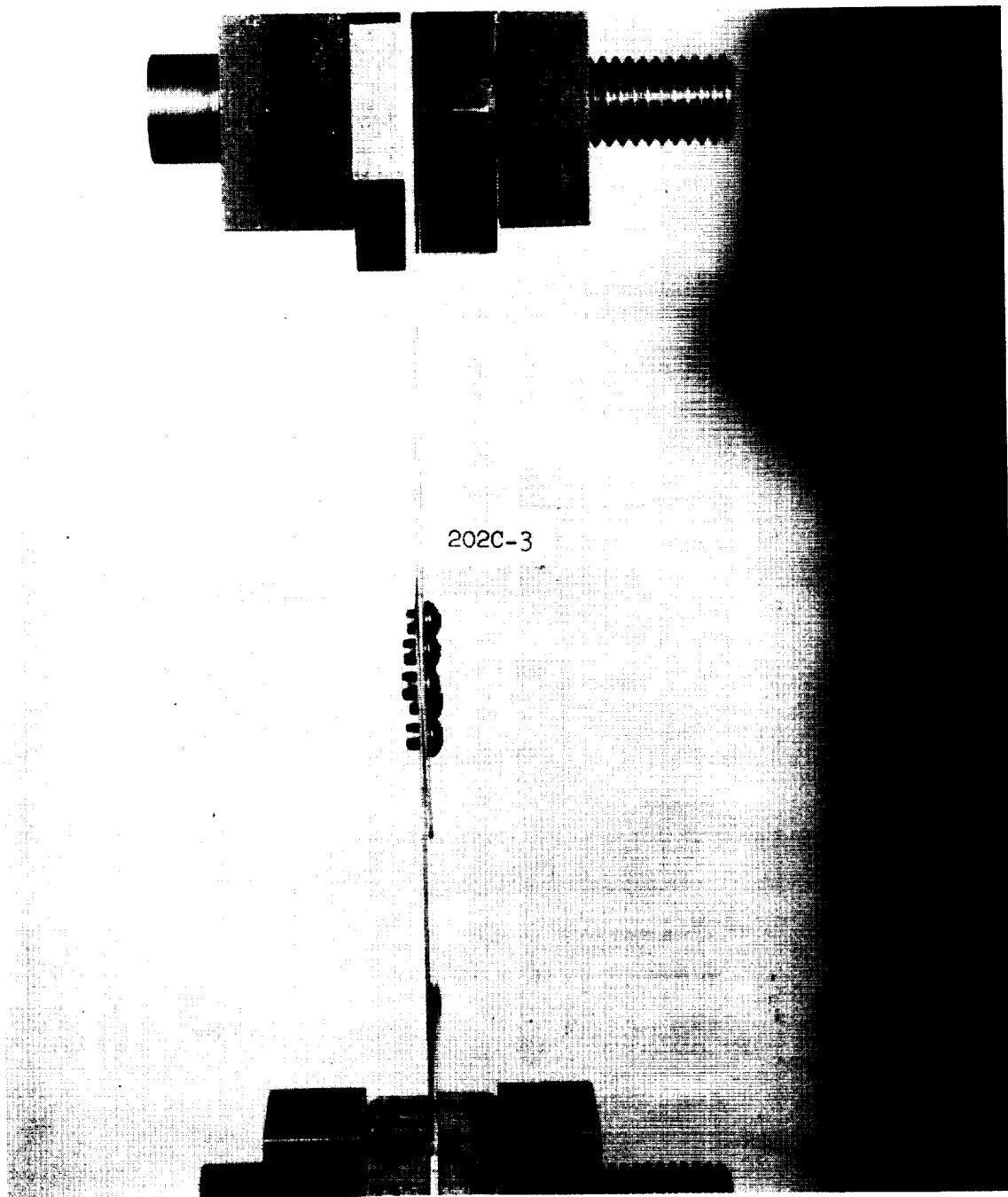
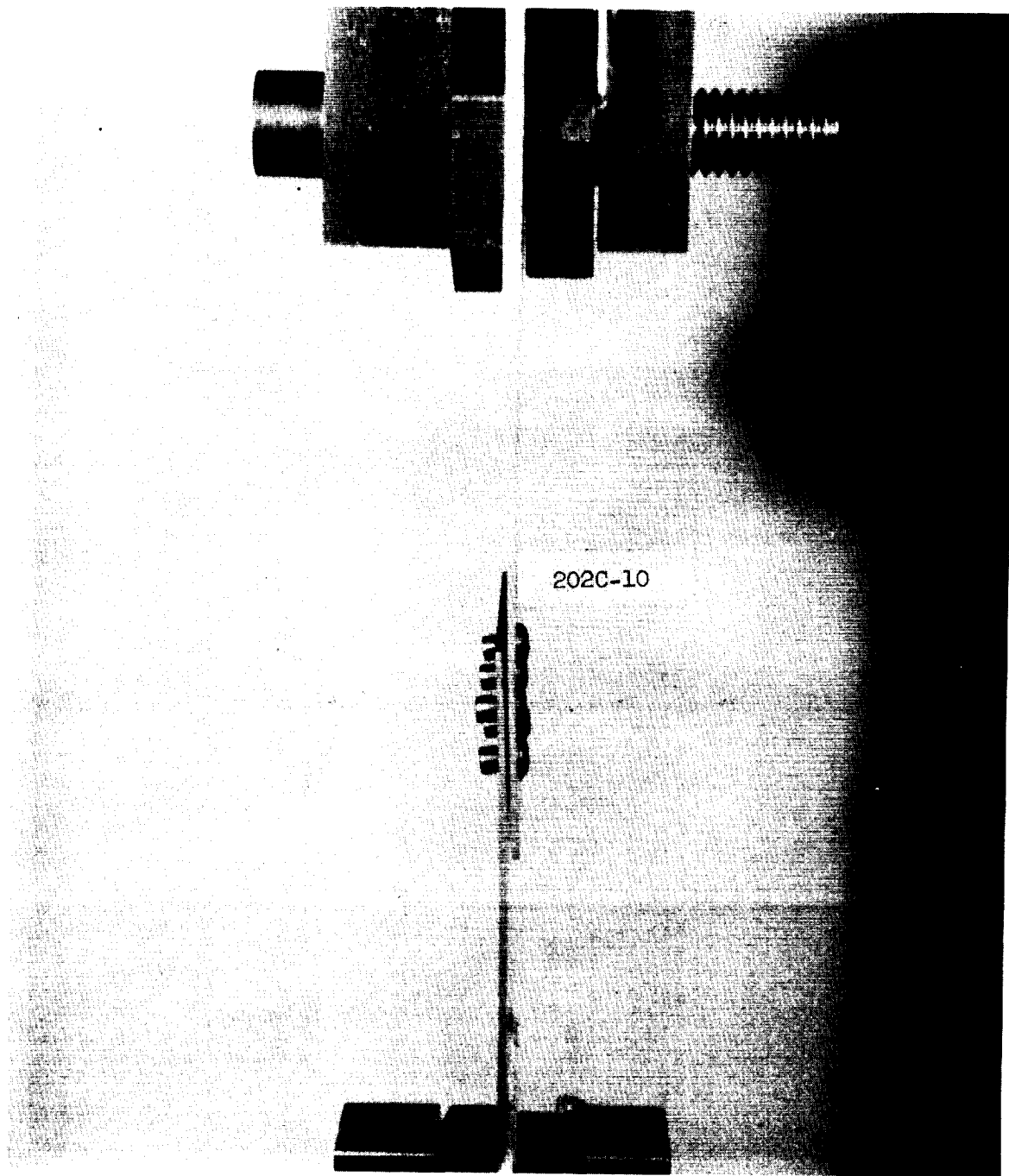


FIGURE 46. TYPE IIC SPECIMENS - 0.060-INCH MATERIAL - CHERRY BLIND RIVETS



Fastener: MS 20600-M5 Cherry Blind Rivet  
Material: .030" Beryllium  
Picture taken at 2100 lbs. load  
Failure occurred at 2620 lbs. load  
Maximum Load-IIC (.030") Series: 2940 lbs.

FIGURE 47. TYPE IIC SPECIMEN - 0.030-INCH MATERIAL - TENSILE TEST



Fastener: MS 20600-M5 Cherry Blind Rivet  
Material: .060" Beryllium  
Picture taken at 4270 lbs. load  
Failure occurred at 4600 lbs. load  
Maximum Load-IIC (.060") Series: 4700 lbs.

FIGURE 48. TYPE IIC SPECIMEN - 0.060-INCH MATERIAL - TENSILE TEST

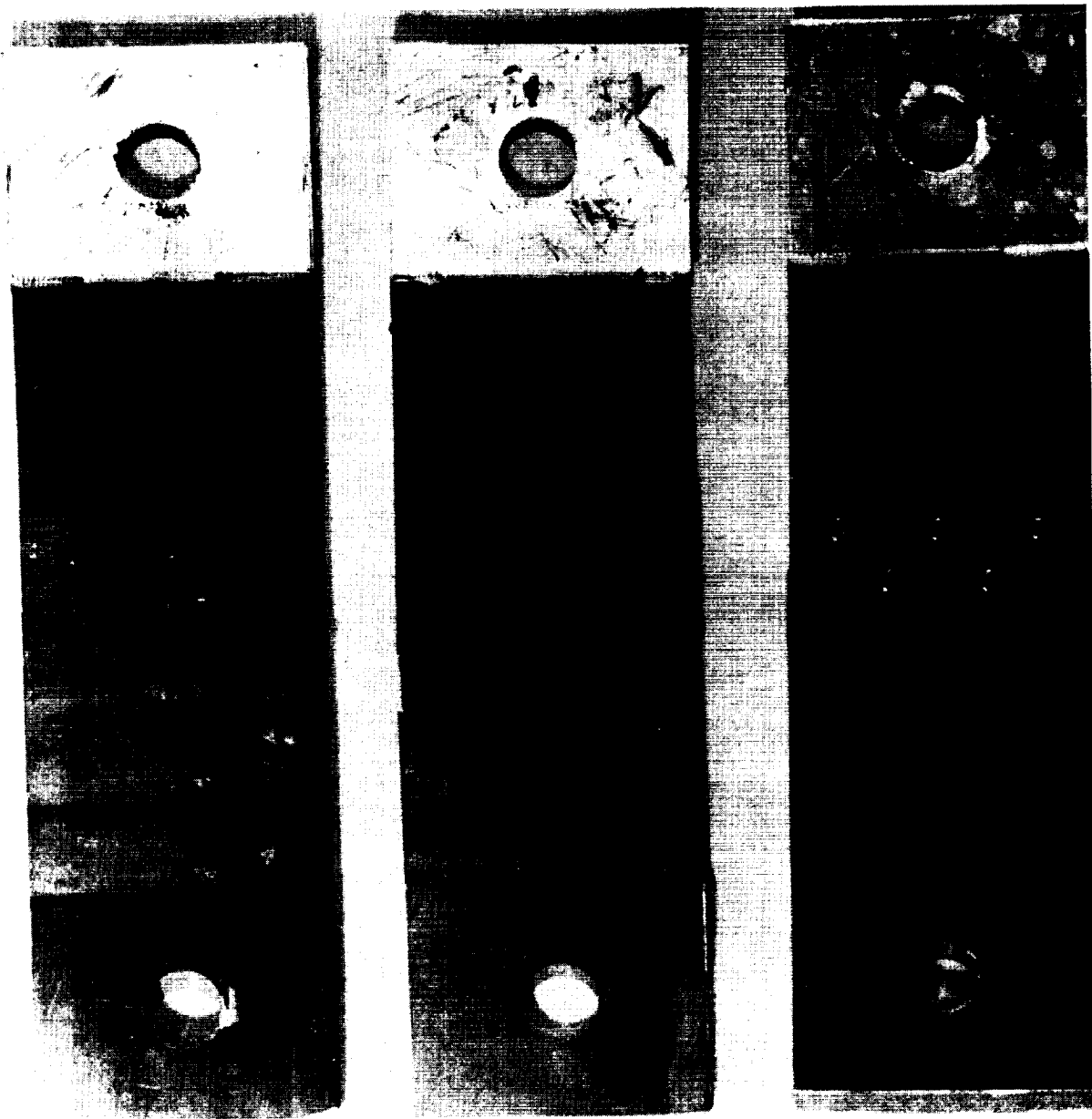


FIGURE 49. TYPE IIC SPECIMENS - 0.030-INCH MATERIAL - TYPICAL FAILURE MODE

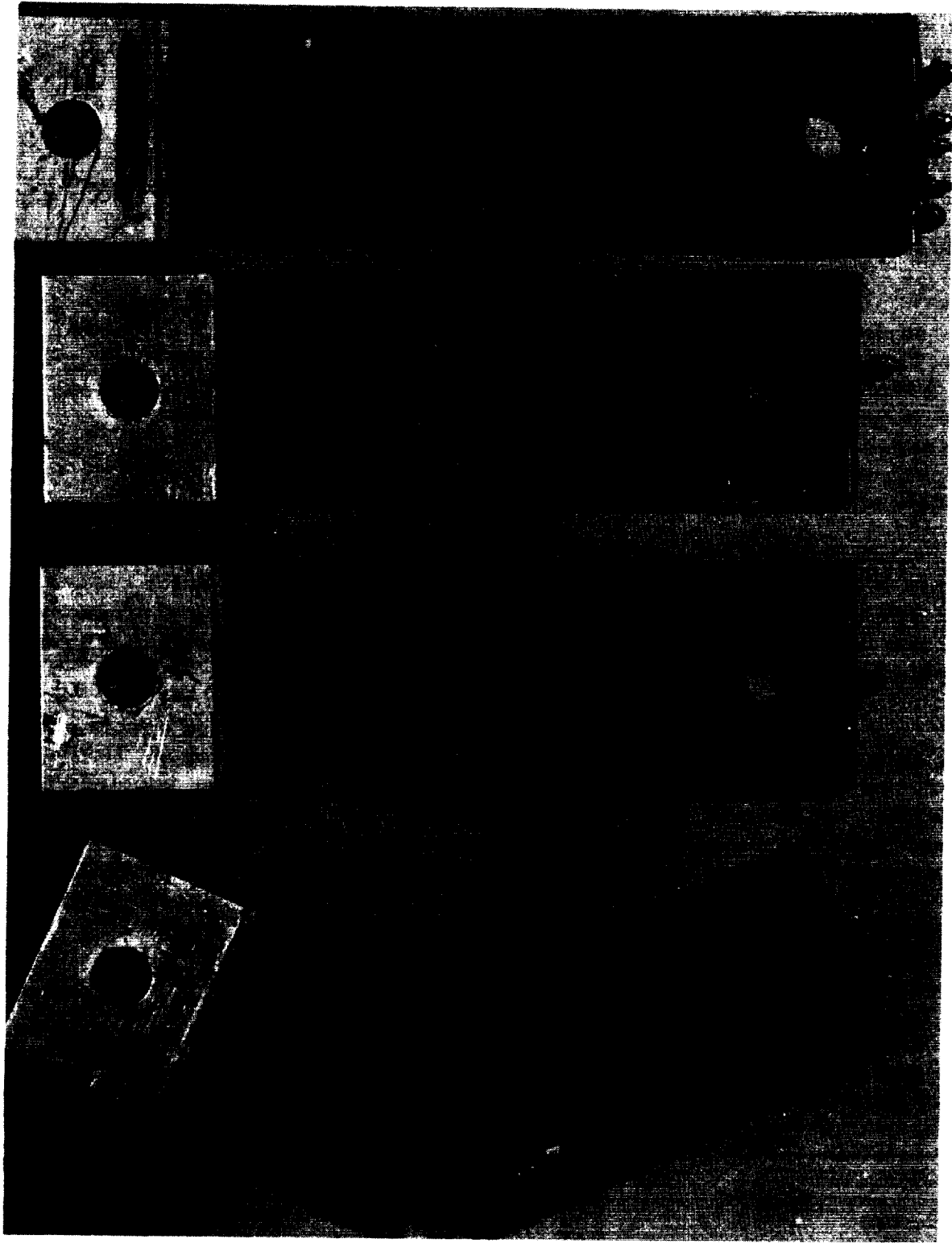


FIGURE 50. TYPE IIC SPECIMENS - 0.060-INCH MATERIAL - TYPICAL FAILURE MODE

net tensile stress for the beryllium, therefore, can be attributed to the failure of the fasteners before the full tensile strength of the beryllium was reached. Furthermore, the separation of the segments under load, due to the slipping of the rivet stem, not only was highly undesirable, but contributed materially to the development of the lower net tensile loads. Visual inspection of an autographically recorded load-deflection curve for specimen number 202C-6, illustrated in Figure 51, clearly reveals the effect of the rivet slippage; the reversal of the load just prior to the joint failure, but after the maximum load had been reached, indicated this effect.

A comparison of the results of the tensile tests of the two series of joint specimens (Type IC - Single Row Fasteners, and Type IIC - Double Row Fasteners) again clearly verifies the advantage of the staggered double row fastener configuration. The large increases of 55 and 65 percent in the net tensile stresses in the 0.030-inch and 0.060-inch gage specimens, respectively, emphasize the increased efficiency of this joint configuration.

d. Type IID - Beryllium Rivets. The objective of this investigation was the further evaluation of the relative joint efficiencies of the single and double row fastener configurations, and the determination of the failure modes at the higher loads anticipated with this fastener arrangement.

It was noted, prior to the assembly of the test specimens, that several of the beryllium segments were quite "bowed." However, as all of the test segments had been cut from "as received" material, no attempt was made to improve this condition although it was realized that the test results might be affected. In addition, an extremely fine radial crack was observed at one hole in each of two (202D-8 and 202D-9) specimens. However, the assembly of all of the test specimens, including these two, was accomplished without incident. The same procedure that had been used for assembling the single row specimens and discussed in the section on Type ID - Beryllium Rivets, was utilized. The "original" and the "upset" configurations on both ends of the rivets are illustrated in Figure 52. The completed Type IID, 0.060-inch gage specimens are illustrated in Figure 53.

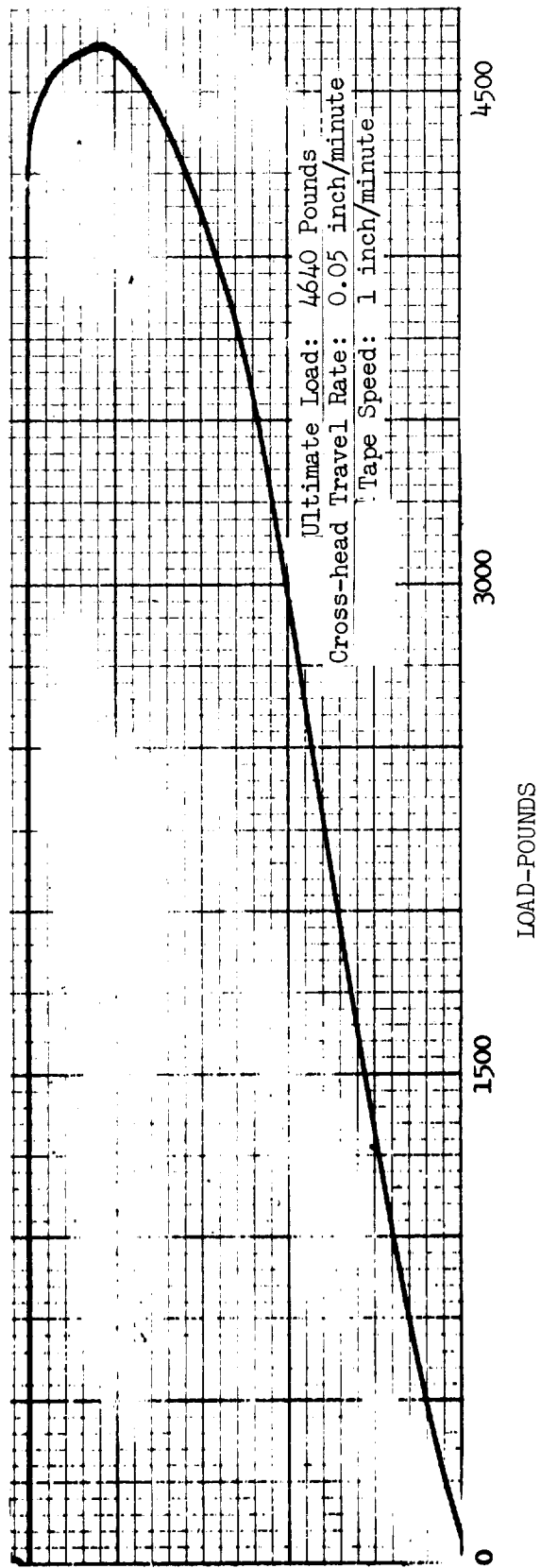


FIGURE 51. TYPE IIC LOAD-DEFLECTION CURVE - SPECIMEN 2020-6.  
NOTE LOAD REVERSAL.



FIGURE 52. TYPE IID SPECIMENS - 0.060-INCH MATERIAL - BERYLLIUM RIVETS.  
NOTE ORIGINAL AND UPSET HEAD CONFIGURATIONS.



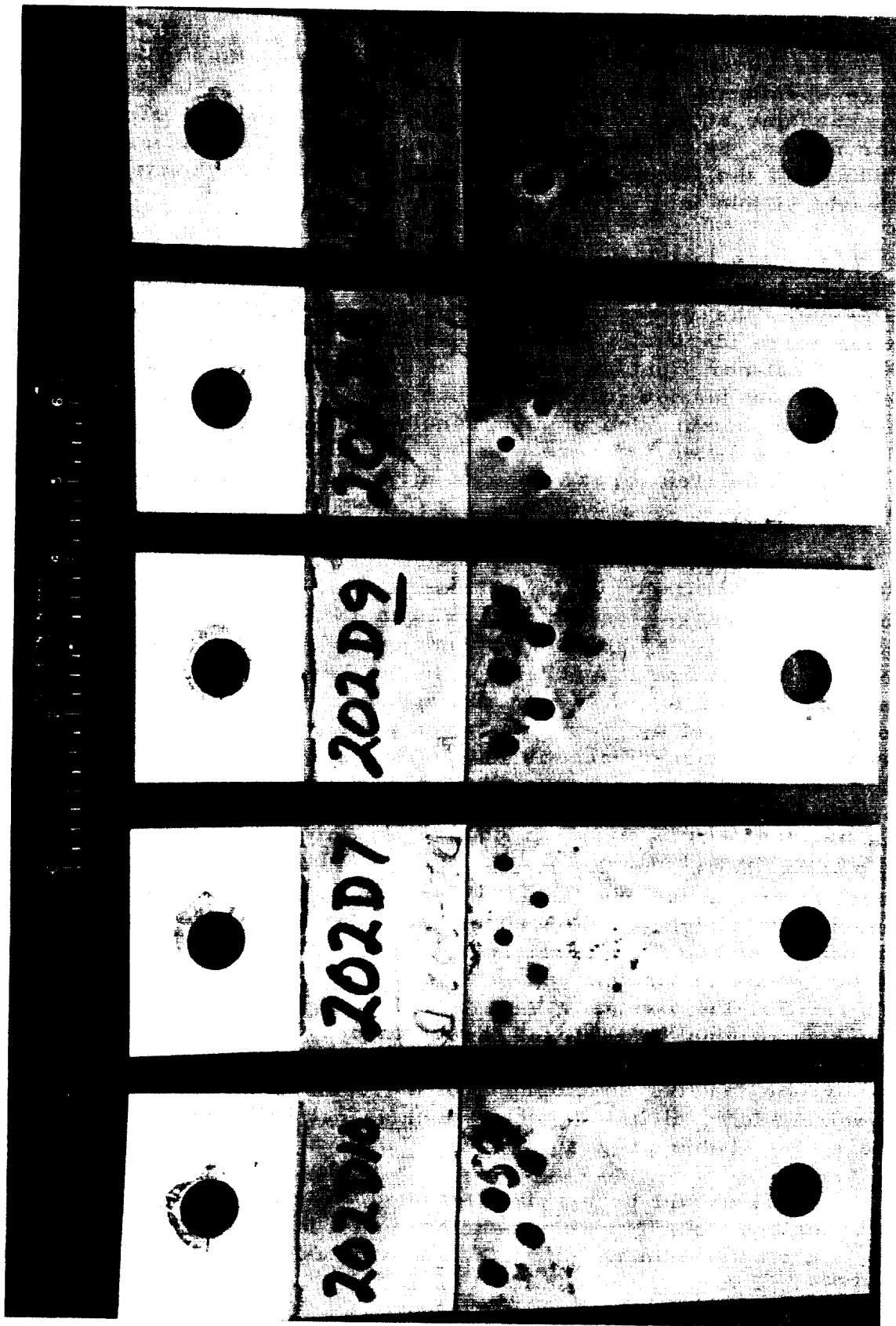


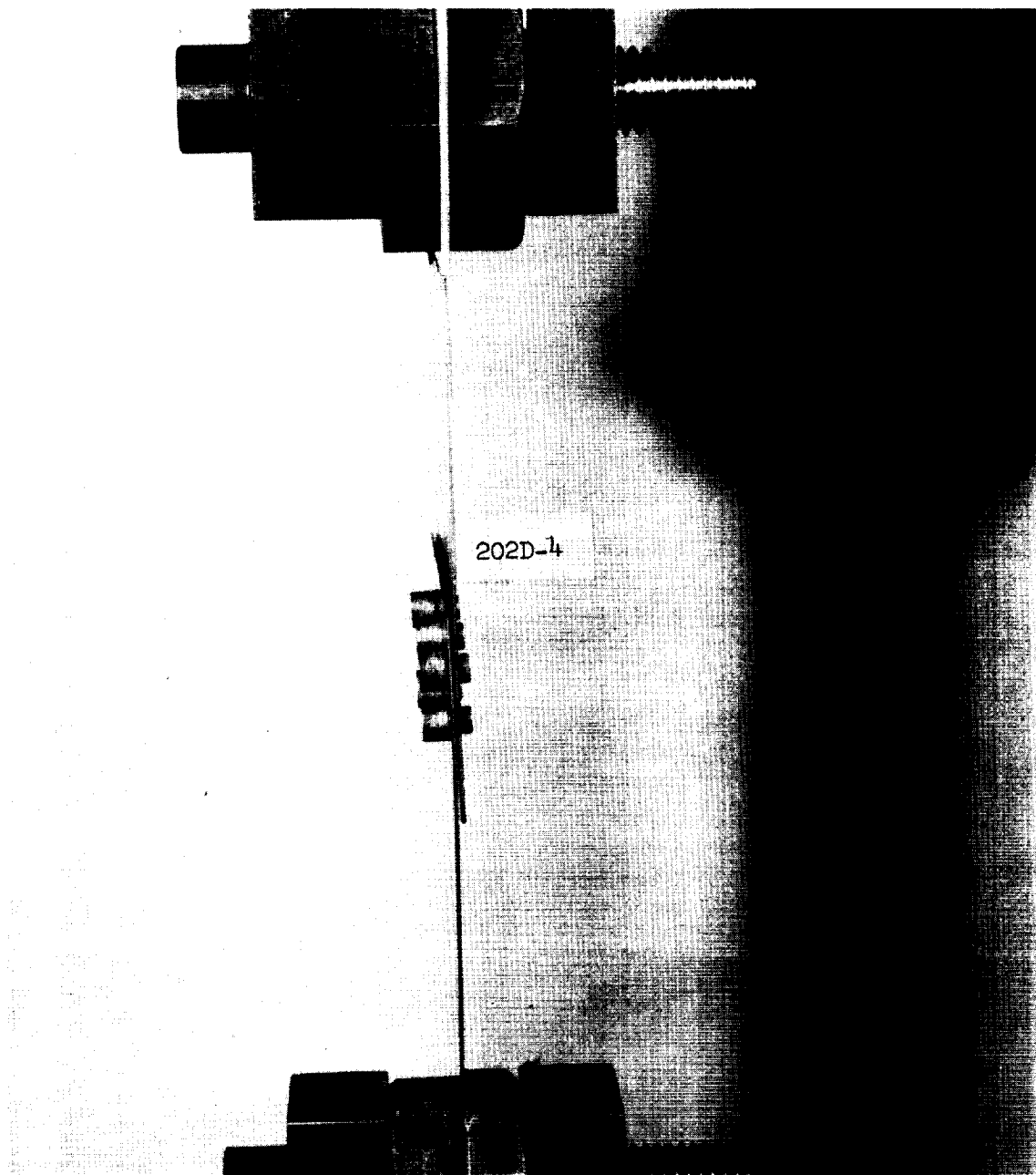
FIGURE 53 TYPE IID SPECIMENS - 0.060-INCH MATERIAL - BERYLLIUM RIVETS

The testing of both the 0.030-inch and the 0.060-inch gage specimens was accomplished in the "Instron" tensile testing machine at average loading rates of 1950 and 2800 pounds per minute, respectively. The typical bending of the material, "tilting" of the fasteners, and separation of the segments are clearly visible in Figure 54.

Due to the difference in the thickness of the material in the two sets of specimens, the types of failure were quite different. However, the respective failure modes of these Type IID specimens were identical with those exhibited by the Type ID - Single Row Fastener Specimens. All of the 0.030-inch thick specimens failed in net tension in the beryllium, through the fastener line, due to the combination of high bending and bearing stresses through the holes. There was no evidence of rivet failure. The consistent failures through one of the rivet lines are illustrated in Figure 55.

Except for the two cracked specimens (202D-8 and 202D-9) which failed at low stress levels, the failure mode of the 0.060-inch gage specimens was quite different from that exhibited by the 0.030-inch specimens. Although the ultimate failures also were in net tension in the beryllium material, the failures appear to have been precipitated by the shearing and/or tensile failure of the beryllium rivets; the rivet failures occurred as the separation of one or both of the heads from the shank. As may be noted in Figure 56 (202D-6 and 202D-7), both the original and the upset heads separated from the shank. It may be concluded, therefore, that the "tilting" of the fasteners added a tension moment to the rivets which resulted in greatly increased local stress at the rivet-shank transitions, and that the combined effect of this high tensile load and the high notch sensitivity of beryllium at room temperature may have resulted in the failure of the rivets in tension rather than in shear. As illustrated in Figure 56, the rivet shanks are still in place in the specimen, but both original and "upset" heads failed. The results of this test indicate that the head-shank geometry may be a critical factor and that the development of the optimum configuration will require additional investigation which is not believed to be within the scope of this program.

It should be specifically noted that this staggered double row fastener configuration resulted in far less improvement in the net tensile ultimate strength than was noted for the other types



Fastener: .159" Dia. Beryllium Rivet  
Material: .030" Beryllium  
Picture taken at 1500 lbs. load  
Failure occurred at 1610 lbs. load  
Maximum Load-IID (.030") Series: 2260 lbs.

FIGURE 54. TYPE IID SPECIMEN - 0.030-INCH MATERIAL - TENSILE TEST

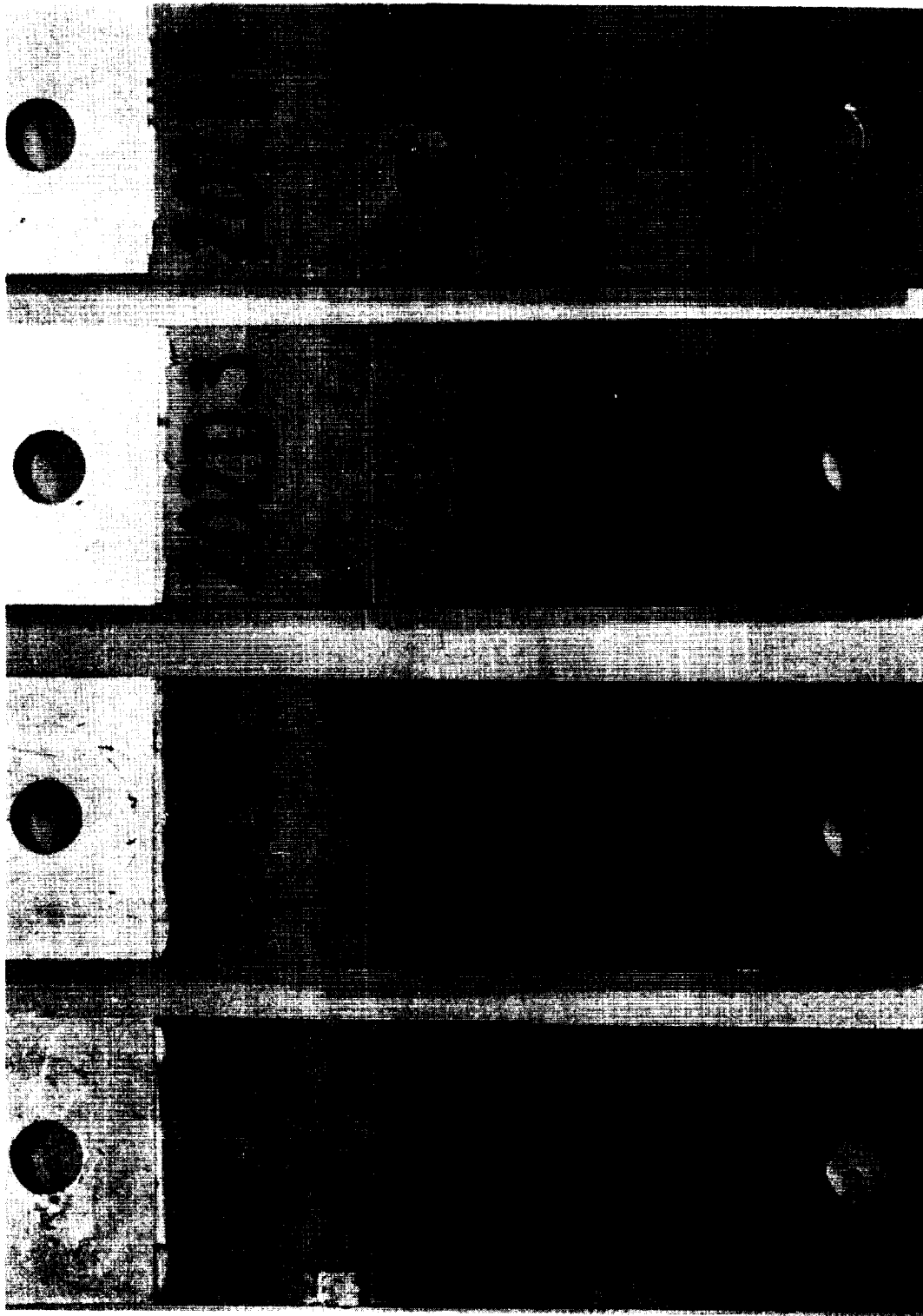


FIGURE 55. TYPE IID SPECIMENS - 0.030-INCH MATERIAL - TYPICAL FAILURE MODE

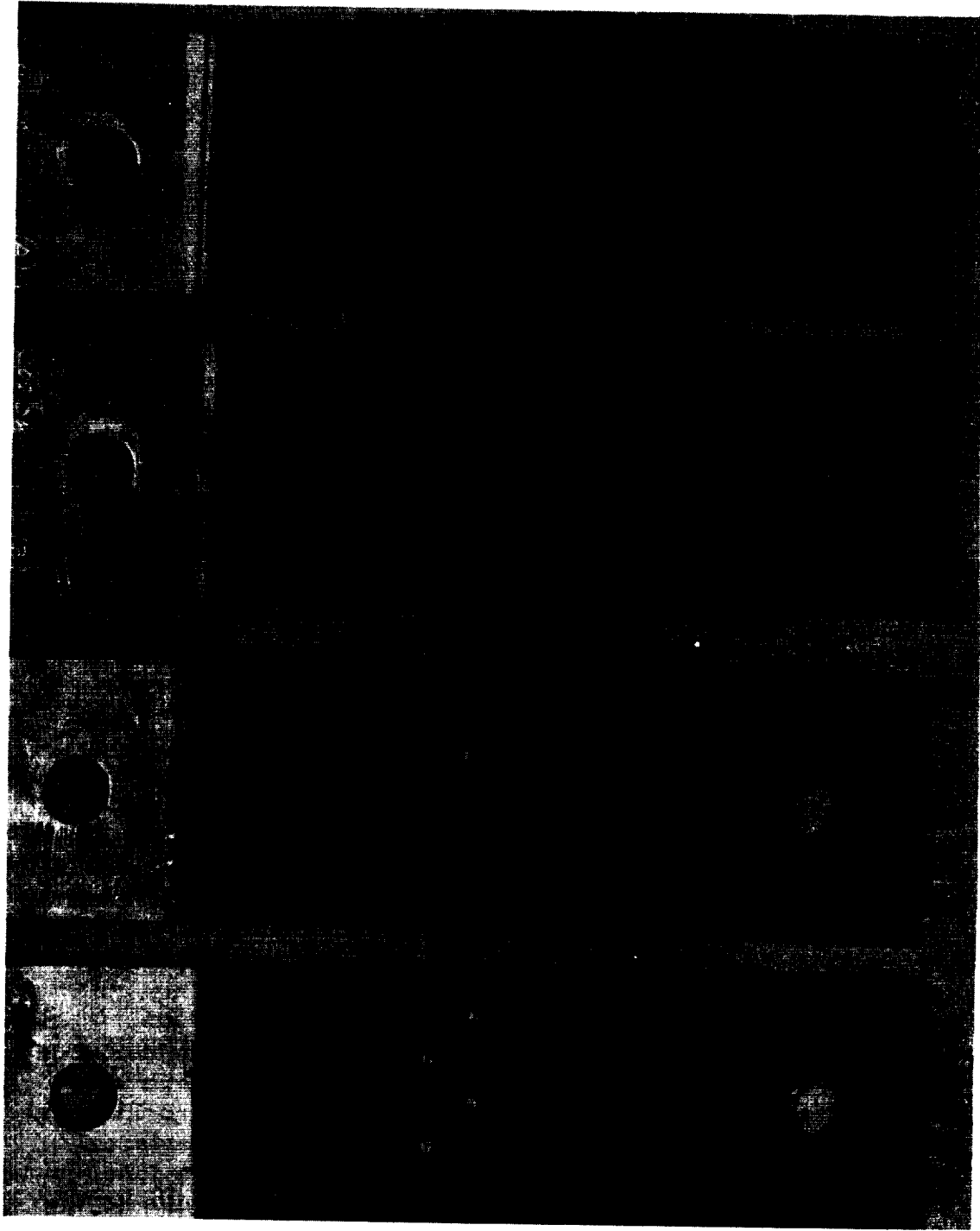


FIGURE 56. TYPE IID SPECIMENS - 0.060-INCH MATERIAL - TYPICAL FAILURE MODE

of fasteners. This is attributed to the high modulus of both the rivets and the specimen segments, the high bearing loads at the fasteners, and the lack of yield or plastic deformation in the rivets. Visual inspection of a representative autographically recorded load-deflection curve for specimen 202D-6, illustrated in Figure 57, clearly reveals the lack of indication of yield; the trace is nearly linear.

e. Type IIE - "Lockalloy" Rivets. The objectives of this test were the further investigation of the relative joint efficiencies of the single and double row fastener configurations, and the comparison of the characteristics of the "Lockalloy" and beryllium rivets. It was anticipated that the lower modulus and greater ductility of the "Lockalloy" rivets would result in more evenly distributed bearing loads and higher joint efficiency.

All of the Type IIE test specimens were assembled, utilizing the procedures discussed in the section on Type IE - "Lockalloy" Rivets, without incident. There was no indication of radial cracking in the edges of the "upset" rivet heads, looseness of the rivets in the holes, or fracture in either the 0.030-inch or the 0.060-inch gage beryllium material. The completed Type IIE, 0.060-inch gage specimens are illustrated in Figure 58.

The testing of both the 0.030-inch and the 0.060-inch gage specimens was accomplished in the "Instron" tensile testing machine at average loading rates of 1950 and 2700 pounds per minute respectively. As illustrated in Figures 59 and 60, the separation of the beryllium segments at the joint interfaces was greater than than observed for the Type IID (beryllium rivet) specimens. This is believed due to the combination of the "Lockalloy" material characteristics and the difficulty experienced in obtaining a "tight" rivet.

Due to the difference in the thickness of the material in the two sets of test specimens, the types of failure were quite different. However, the respective failure modes were identical with those exhibited by the Type IE - Single Row Fastener specimens. All of the 0.030-inch thick test specimens failed in net tension in the beryllium, through a fastener line, due to the combination of high tensile and bearing stresses compounded by the bending stresses. There was no evidence of rivet failure.

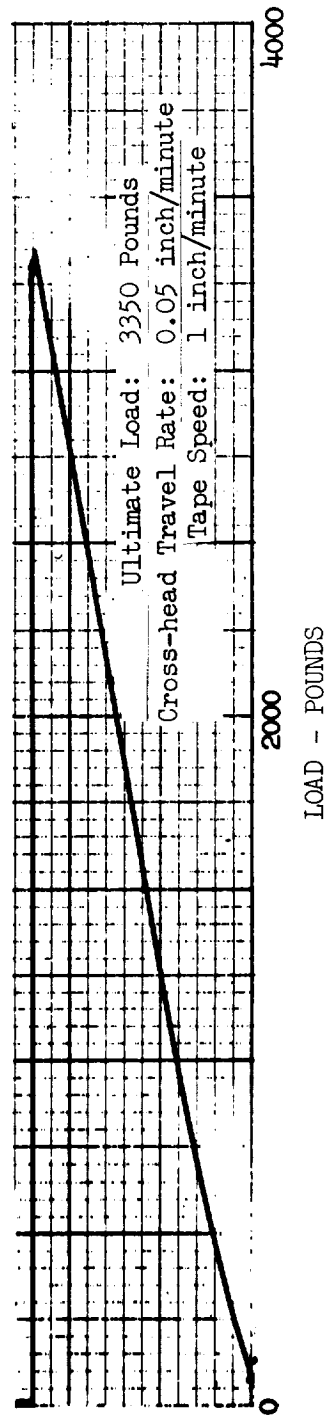


FIGURE 57. TYPE IID LOAD-DEFLECTION CURVE - SPECIMEN 202D-6.  
NOTE LACK OF YIELD INDICATION.

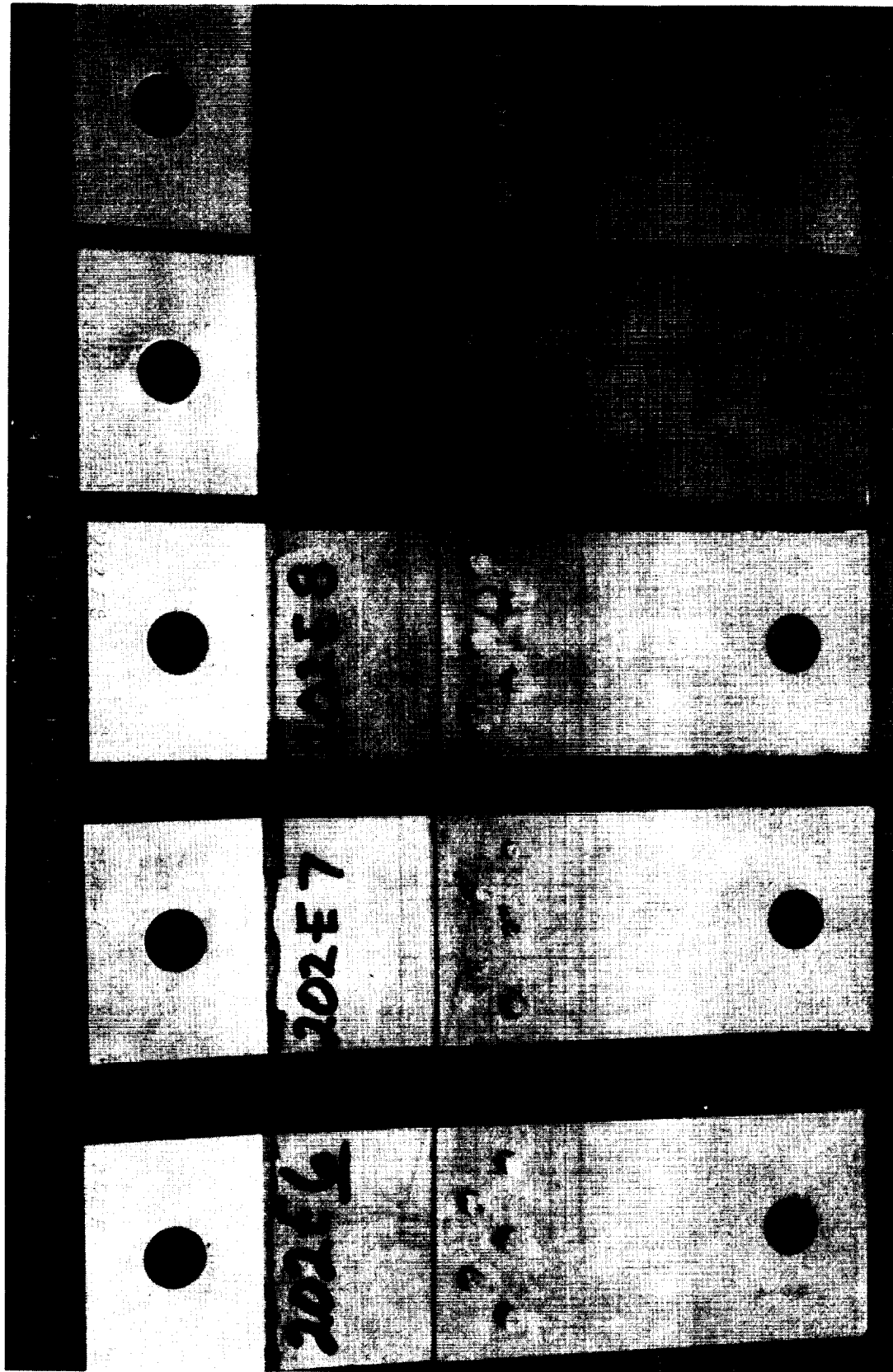
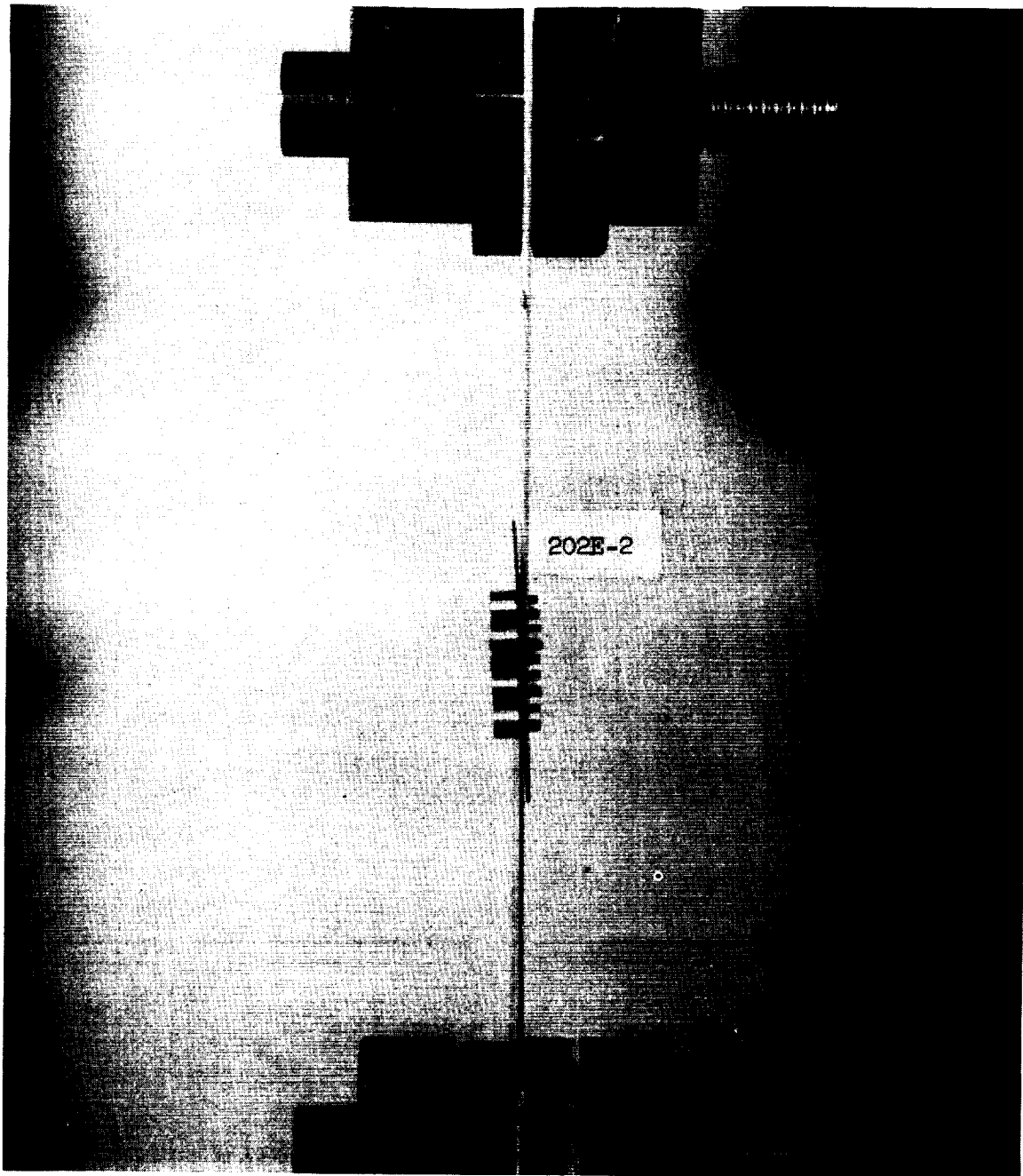


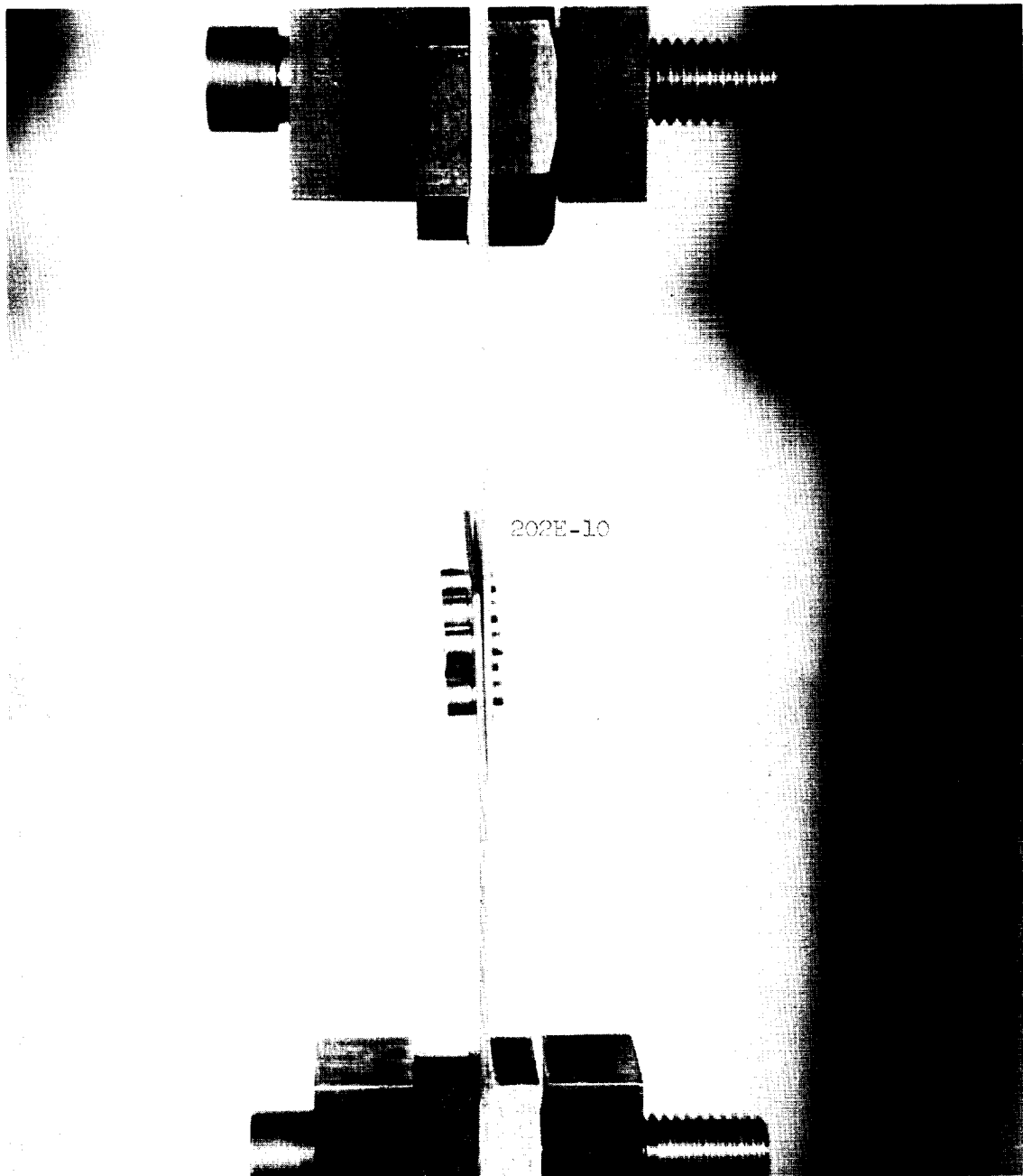
FIGURE 58. TYPE IIE SPECIMENS - 0.060-INCH MATERIAL - "LOCKALLOY" RIVETS





Fastener: .159" Dia. "Lockalloy" Rivet  
Material: .030" Beryllium  
Picture taken at 1880 lbs. load  
Failure occurred at 1920 lbs. load  
Maximum Load-IIE (.030") Series: 2210 lbs.

FIGURE 59. TYPE IIE SPECIMEN - 0.030-INCH MATERIAL - TENSILE TEST



Fastener: .159" Dia. "Lockalloy" Rivet  
Material: .060" Beryllium  
Picture taken at 3000 lbs. load  
Failure occurred at 3670 lbs. load  
Maximum Load-IIIE (.060") Series: 3720 lbs.

FIGURE 60. TYPE IIE SPECIMEN - 0.060-INCH MATERIAL - TENSILE TEST

The consistent failures are illustrated in Figure 61.

As illustrated in Figure 62, the failure of the 0.060-inch thick specimens was due to the shearing of the "Lockalloy" rivets. It should be specifically noted that all of the "Lockalloy" rivets failed in shear at the joint interface, not at the rivet head-shank transition as occurred with the beryllium rivets. The difference in the two types of failure is believed due to the greater ductility and lower notch sensitivity of the "Lockalloy" rivet material.

Visual inspection of a representative autographically recorded, load-deflection curve, illustrated in Figure 63, reveals a slight indication of yield, an improvement over the linear characteristic displayed by the beryllium curve illustrated in Figure 57. Although the full net tensile strength of the beryllium was not realized in the 0.060-inch thick specimens, the increases of 25 and 56 percent, respectively, in the net tensile stresses in the 0.030-inch and 0.060-inch gage specimens clearly emphasize the advantage of the staggered double row fastener configuration.

f. Type IIF - Combination Adhesive Bonding and Cherry Blind Rivets. During the assembly of the Type IIF specimens, utilizing the procedures discussed in the section on Type IF Specimens, one of the 0.030-inch thick specimens (202F-5) failed completely, and a second (202F-2) failed in one hole during the installation of the rivets. These failures were due to the localized distortion of the beryllium around the holes caused by the displacement of the bonding material as the rivets were "set." No failures occurred during the assembly of the 0.060-inch thick specimens. The completed Type IIF specimens, ready for test, are illustrated in Figures 64 and 65.

Figures 66 and 67 illustrate the testing of typical 0.030-inch and 0.060-inch thick specimens in the "Instron" tensile testing machine at average loading rates of 2200 and 3200 pounds per minute respectively. In all cases, the early failure of the bonded joint resulted in the entire load being assumed by the rivets. As anticipated, specimen 202F-2 failed prematurely, due to the early bond failure and the radial cracks at one of the holes. Specimen 202F-3 failed in bearing at both of the loading pin holes; this specimen withstood the highest load of the Type IIF 0.030-inch series. As little could be gained by retesting this specimen in the "Riehle" machine, it was not retested. Two of the 0.030-

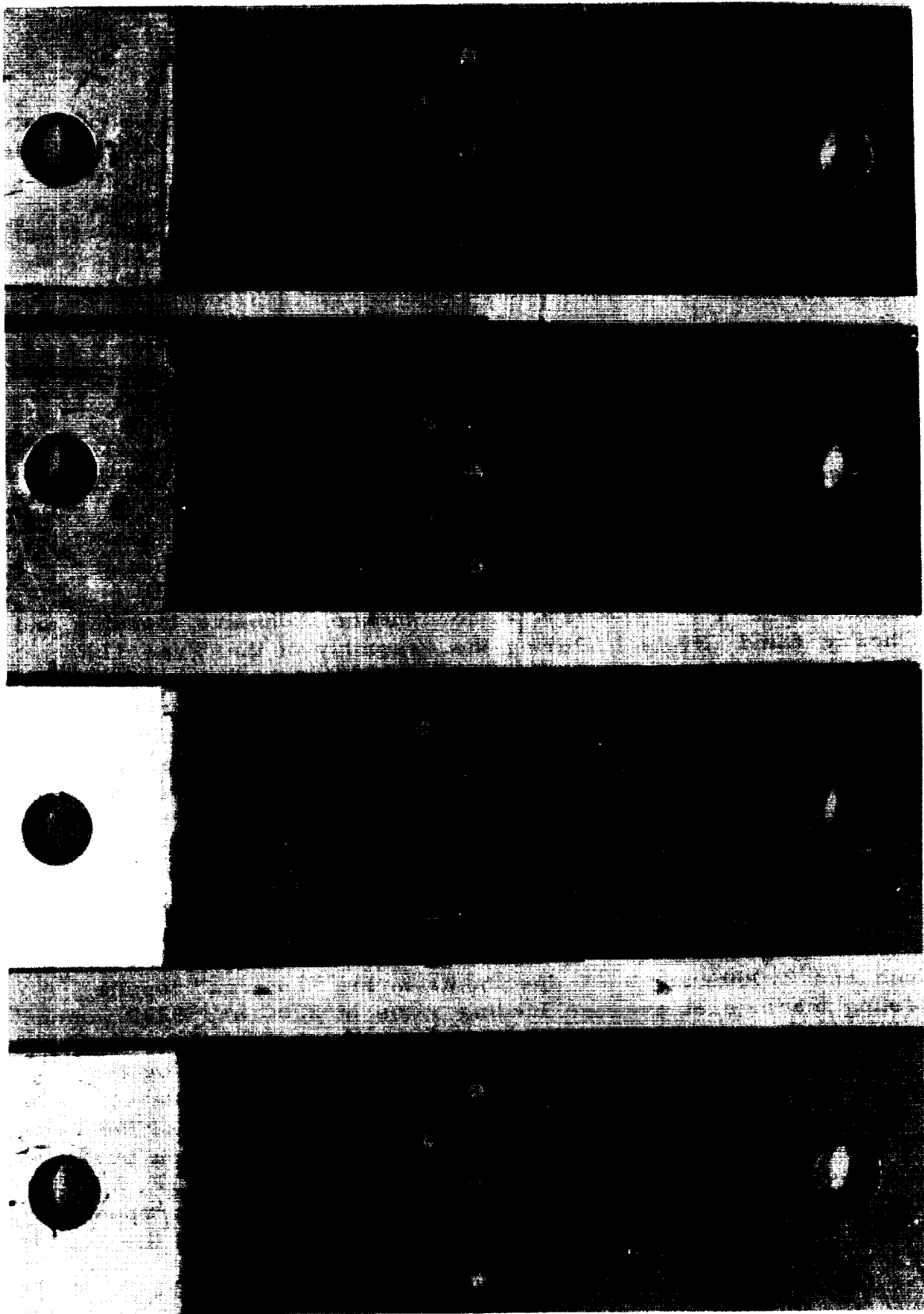


FIGURE 61. TYPE IIE SPECIMENS - 0.030-INCH MATERIAL - TYPICAL FAILURE MODE

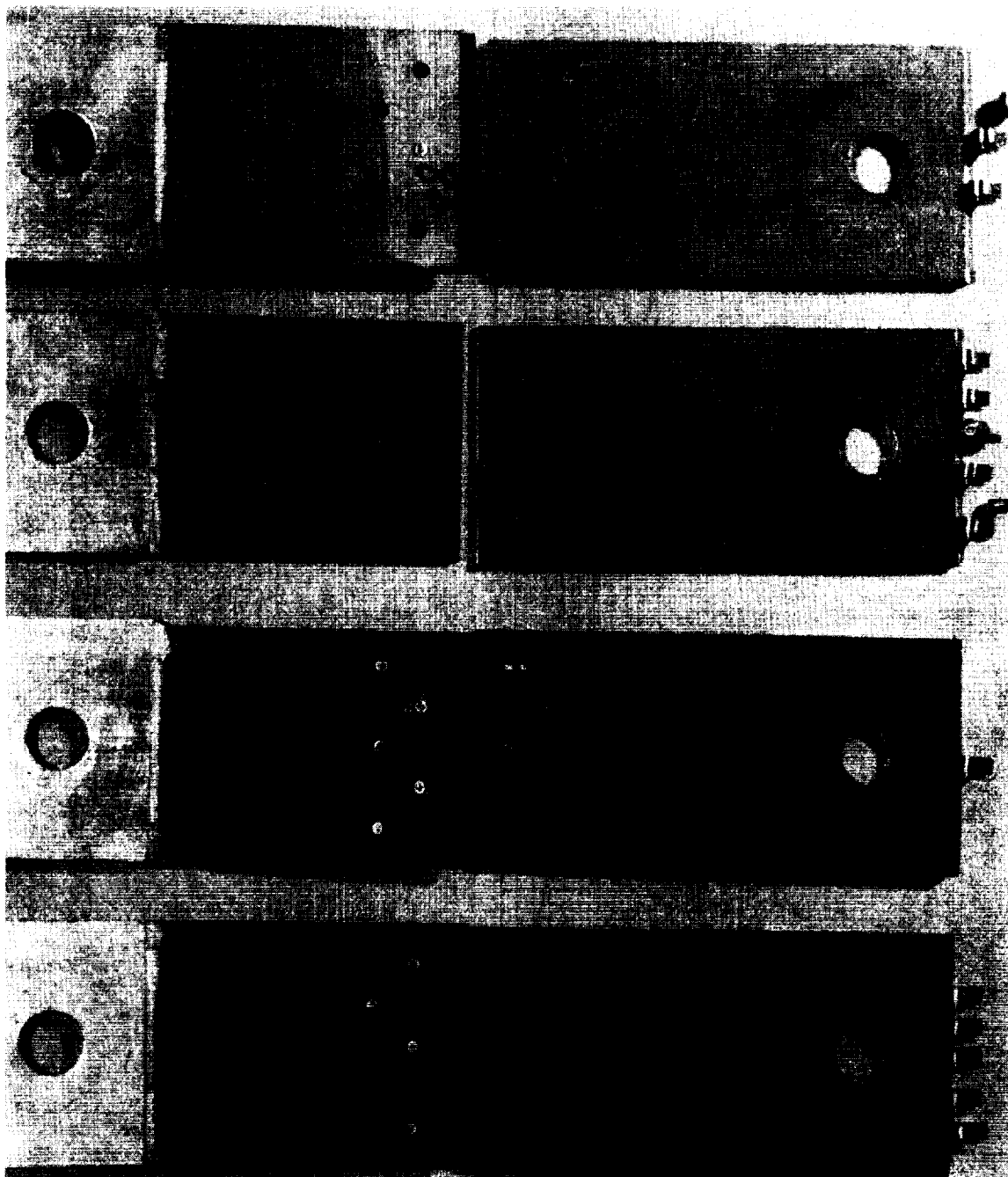


FIGURE 62. TYPE IIE SPECIMENS - 0.060-INCH MATERIAL - TYPICAL FAILURE MODE.  
NOTE "CLEAN" SHEARING OF THE RIVETS.

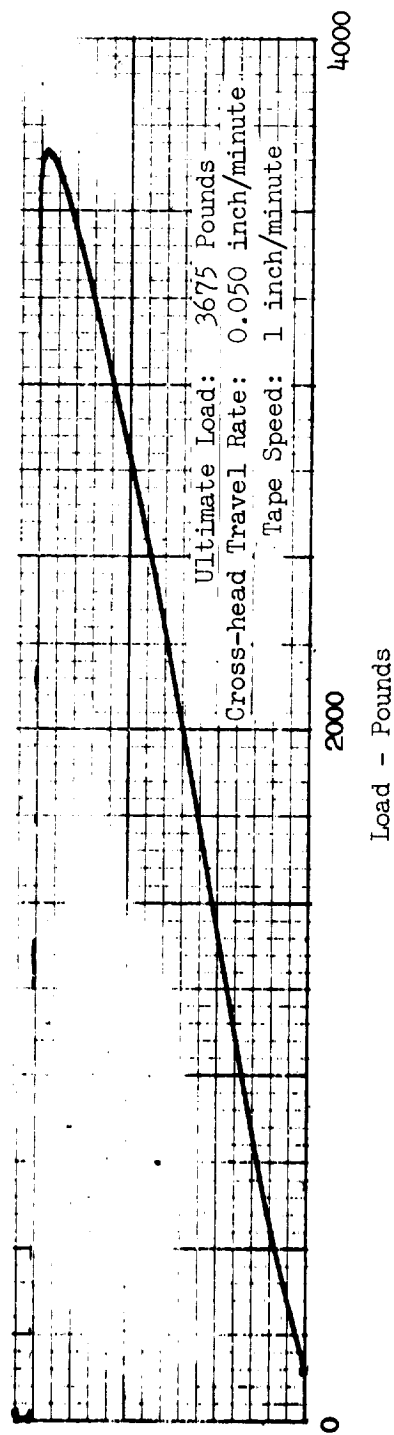


FIGURE 63. TYPE IIE LOAD-DEFLECTION CURVE - SPECIMEN 202E-8

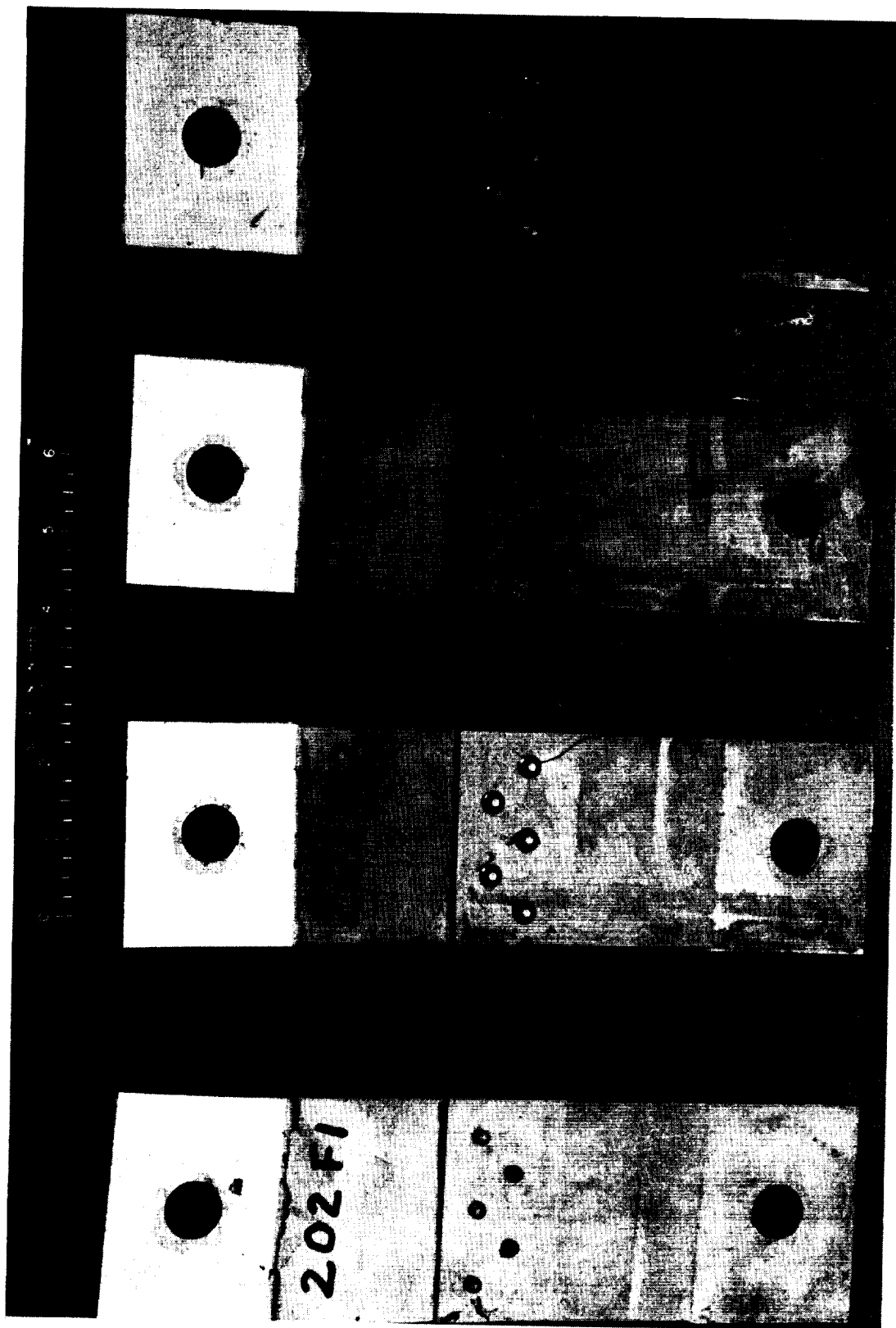


FIGURE 64. TYPE IIF SPECIMENS - 0.030-INCH MATERIAL - ADHESIVE BONDING AND CHERRY BLIND RIVETS.  
NOTE RADIAL CRACKS AT RIVET IN SPECIMEN 202F-2.

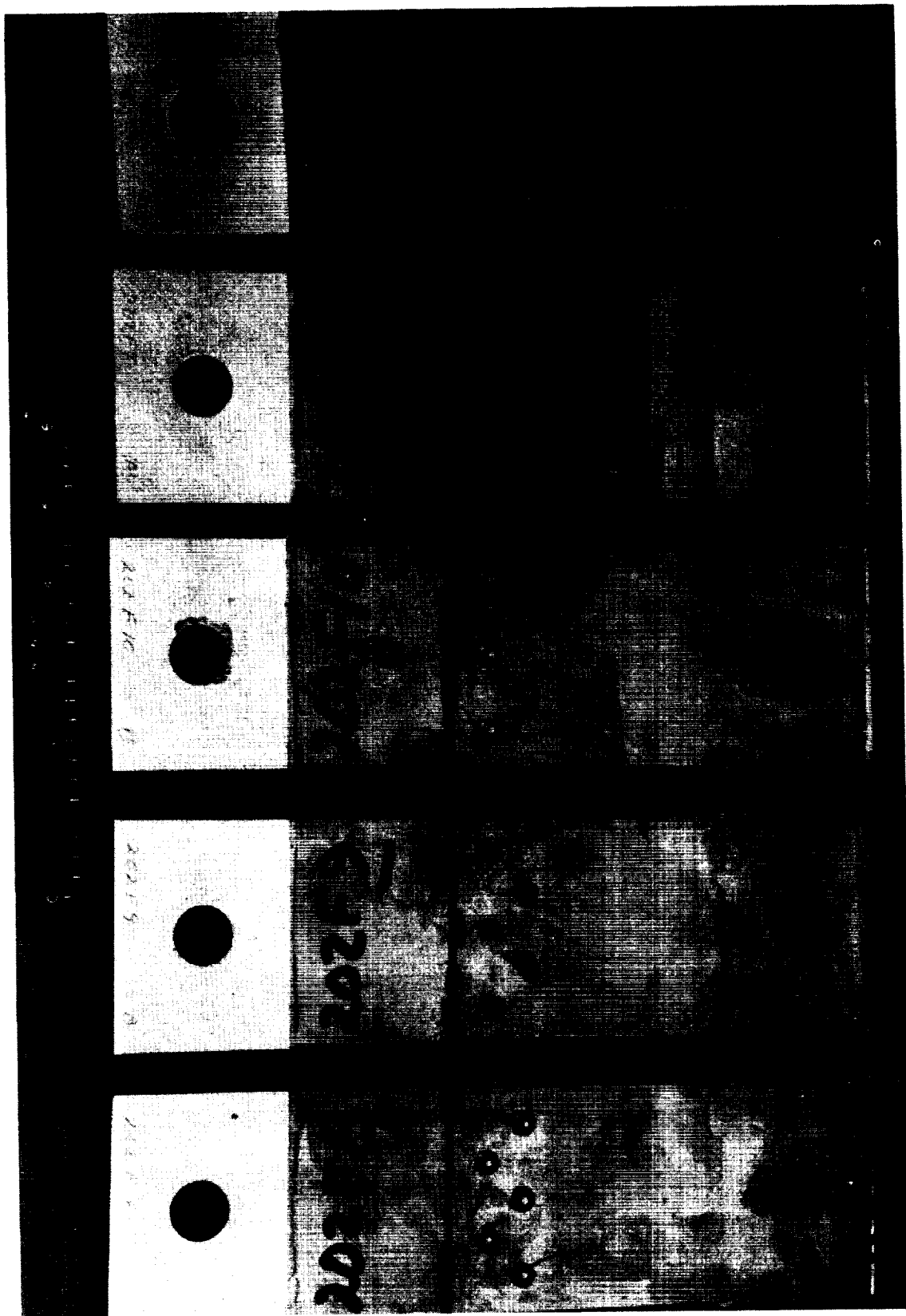
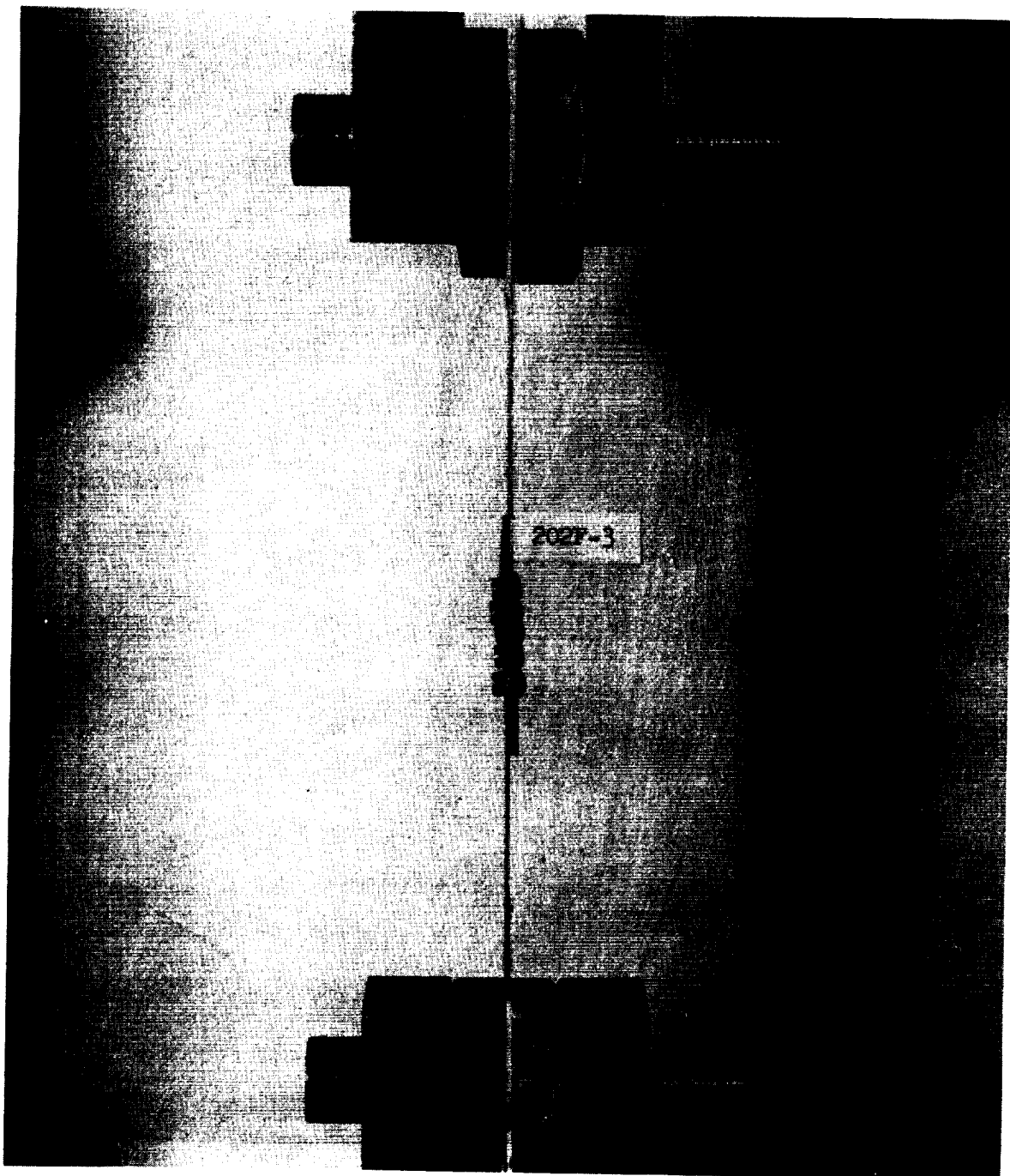


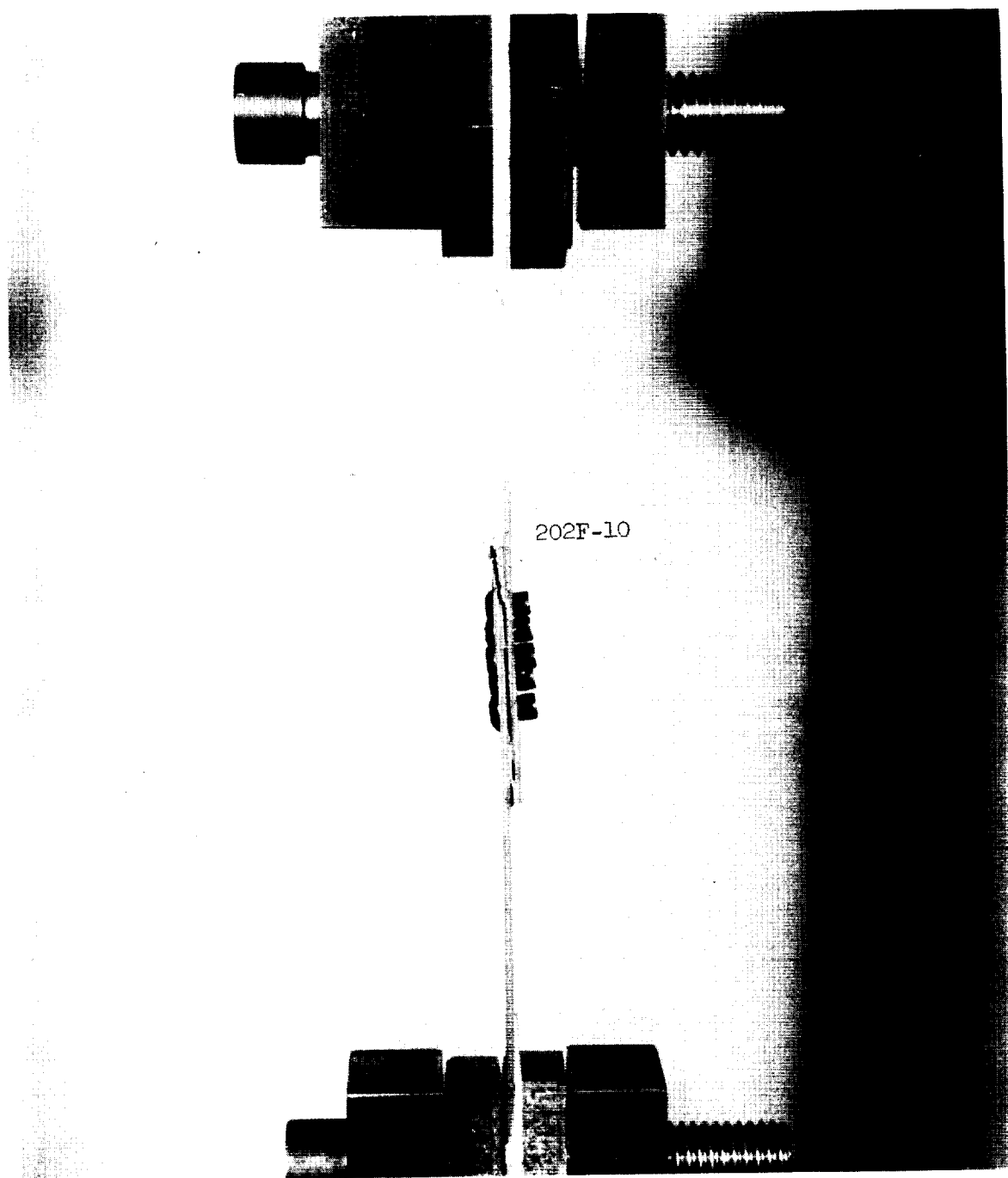
FIGURE 65. TYPE IIF SPECIMENS - 0.060-INCH MATERIAL - ADHESIVE BONDING AND CHERRY BLIND RIVETS





Fastener: Adhesive Bonding and Cherry Blind Rivet  
Material: .030" Beryllium  
Picture taken at 2220 lbs. load  
Failure occurred at 2750 lbs. load  
Maximum Load-IIF (.030") Series: 2750 lbs.

FIGURE 66. TYPE IIF SPECIMEN - 0.030-INCH MATERIAL - TENSILE TEST.  
NOTE BOND FAILURE.



Fastener: Adhesive Bonding and Cherry Blind Rivet  
Material: .060" Beryllium  
Picture taken at 4000 lbs. load  
Failure occurred at 4880 lbs. load  
Maximum Load-IIF (.060") Series: 4900 lbs.

FIGURE 67. TYPE IIF SPECIMEN - 0.060-INCH MATERIAL - TENSILE TEST.  
NOTE BOND FAILURE AND RIVET "TILTING;"

inch specimens (202F-1 and 202F-4) failed in net tension, at very low loads, in the beryllium material outside of the joint area. The failed 0.030-inch thick specimens are illustrated in Figure 68.

The failure mode of the 0.060-inch thick specimens was entirely different from that exhibited by the 0.030-inch thick specimens. As illustrated in Figure 69, the early failure of the adhesive bond was followed, in three cases, by the failure of the fasteners; the fourth specimen failed in net tension through the fastener line. The "tilting" of the joint area precipitated the failure of the rivets; the rivet collars were sheared and the stems pulled out in the same manner as occurred during the testing of the Type IF - Single Row Fastener; Combination Adhesive Bonding and Cherry Blind Rivets. The typical failure of the bond at approximately 50 percent of the ultimate load, and the failure of the first rivet are clearly illustrated in the autographically recorded load-deflection curve presented in Figure 70.

A comparison of the test results, presented in Tables III and VII, clearly indicates the lack of any advantage accruing from the incorporation of adhesive bonding in mechanically fastened joints. In fact, the ever present possibility of failure at the holes during the installation of the rivets, due to the localized distortion of the beryllium caused by the displacement of the adhesive, strongly inhibits further consideration of the combination joining method.

5. Type III Lap Joints - Reduced Sections. The objective of this investigation was the evaluation of joints in panels incorporating reduced thickness areas, and specifically the effect of reducing the stress gradient by means of an intermediate step in thickness between the joint area and the basic panel. This investigation provides practical data directly applicable in the design of minimum weight structures. Such structural designs may include panels in gages too thin to provide the normal joint strength due to insufficient bearing area.

In addition, the feasibility of joining beryllium structures with double-flush countersunk beryllium rivets was investigated. A 60-degree countersink was selected, as the use of the

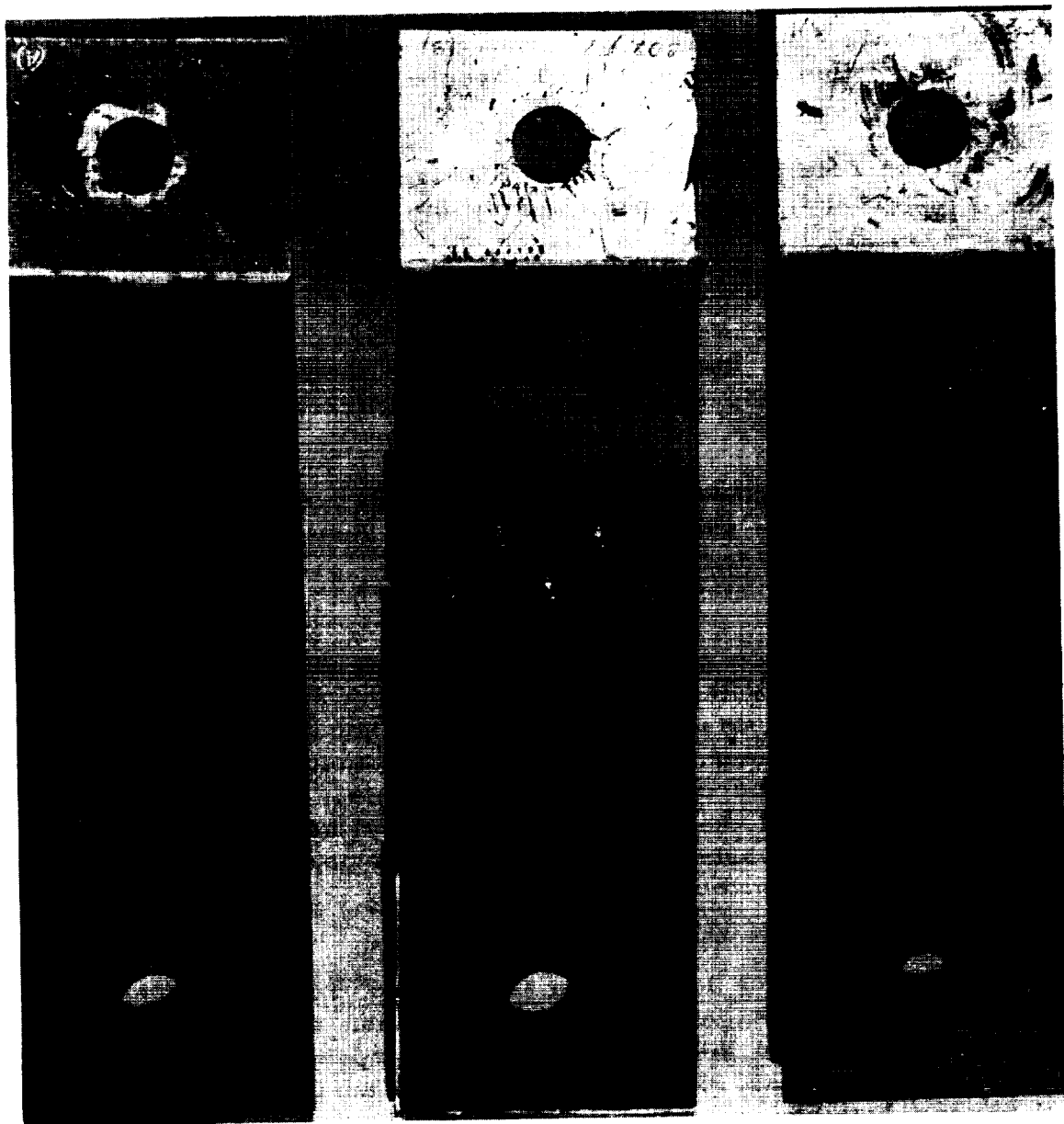


FIGURE 68. TYPE IIF SPECIMENS - 0.030-INCH MATERIAL - TYPICAL FAILURE MODES

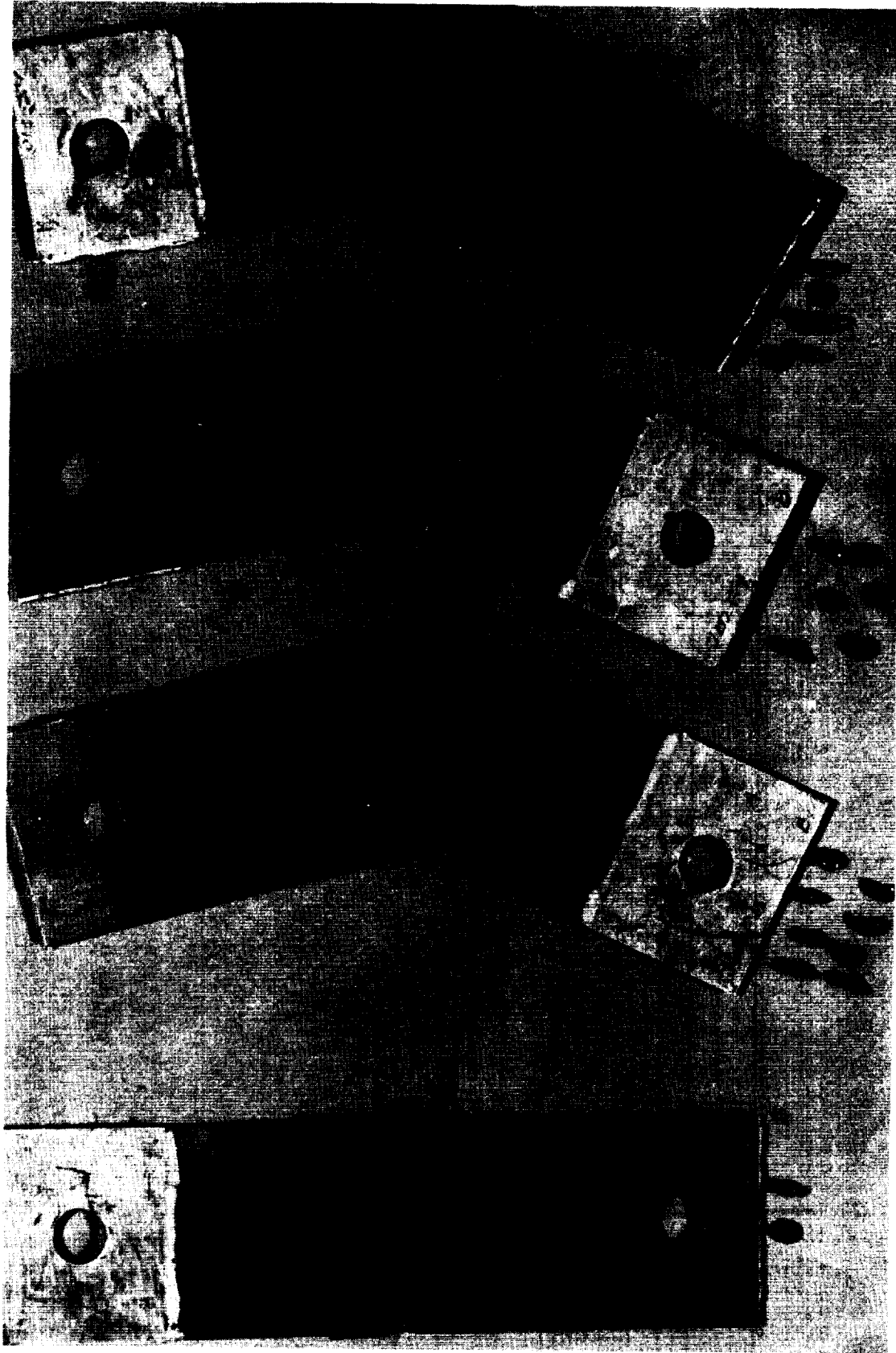


FIGURE 69. TYPE IIF SPECIMENS - 0.060-INCH MATERIAL - TYPICAL FAILURE MODE

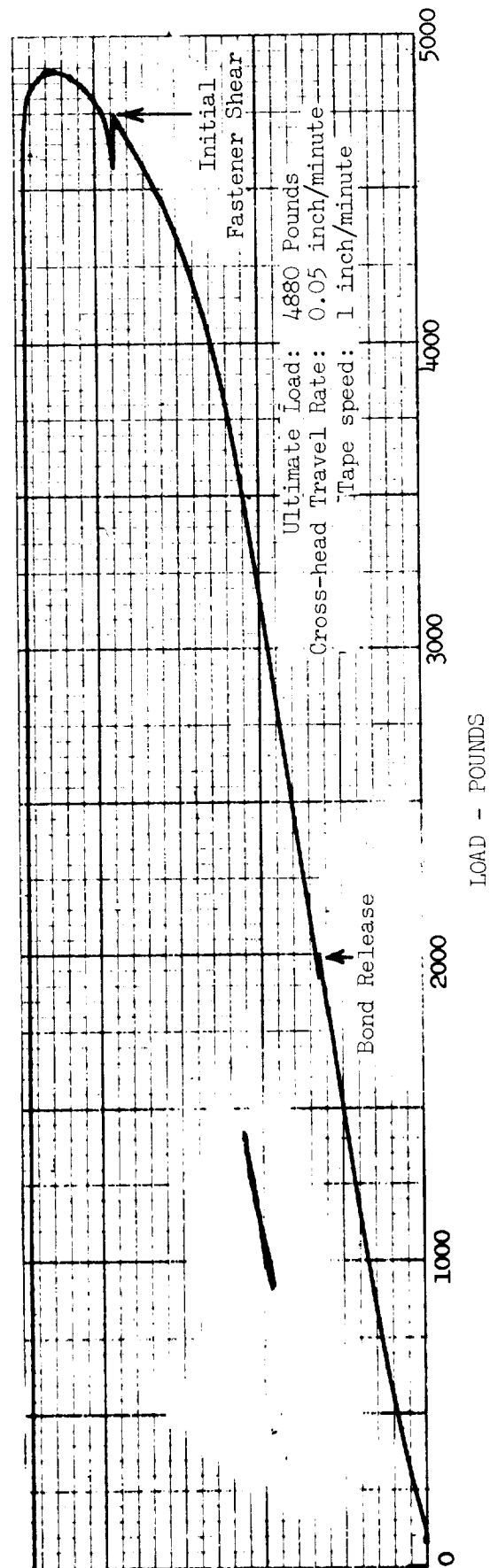


FIGURE 70. TYPE IIF LOAD-DEFLECTION CURVE - SPECIMEN 202F-10

configuration results in the development of the required clamping force without excessive rivet deformation.

Table VIII presents the chemical analysis and the mechanical properties of the material procured from The Brush Beryllium Company for the fabrication, testing, and evaluation of the Type III - Reduced Section mechanically fastened joints. The configuration and nominal dimensions of the "203" Type III joints are illustrated in Figure 71. A summary of the test loads, stresses and modes of failure is presented in Table IX.

The formation of the reduced thickness sections (steps) in the Type III test segments was accomplished by successive chemical milling operations. The subsequent preparation of the specimens and the installation of the fasteners were accomplished with the same procedures utilized for the assembly of the respective Type I and Type II specimens.

a. Type IIIA - Huckbolts. Although the thickness of the joint area was less (0.090-inch versus 0.120-inch) than the previous series assembled with Huckbolts, the assembly of the Type IIIA specimens, utilizing the procedures discussed in the section on the Type IA specimens, was accomplished without incident. The completed Type IIIA specimens, ready for testing, are illustrated in Figure 72.

The testing of the Type IIIA specimens was accomplished in the "Riehle" hydraulic tensile testing machine at a constant loading rate of 3000 pounds per minute. The typical bending of the material, "tilting" of the fasteners, and separation of the segments in the joint area are clearly visible in Figure 73.

The failure mode of the Type IIIA specimens, illustrated in Figure 74, was very similar to that exhibited by the Type IIA specimens. With one exception (203A-2), all of the specimens failed in net tension in the beryllium through a fastener line. Again, with one exception (203A-5), crack propagation extended through the 0.075-inch "step" into the basic 0.060-inch area. There was no indication of fastener failure.

A comparison of the results of the tensile tests of these Type IIIA specimens and of the Type IIA - Double Row Fastener specimens, clearly verifies the advantage of the "stepped" joint

TABLE VIII

## CHEMICAL ANALYSIS AND MECHANICAL PROPERTIES - MATERIAL FOR TYPE III MECHANICAL JOINTS

Vendor: The Brush Beryllium Company

Lot No.: 2843

Sheet No.: 992B

## CHEMICAL ANALYSIS - %

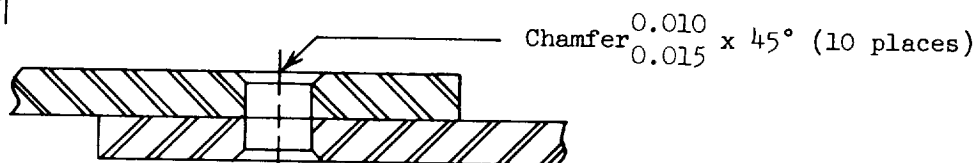
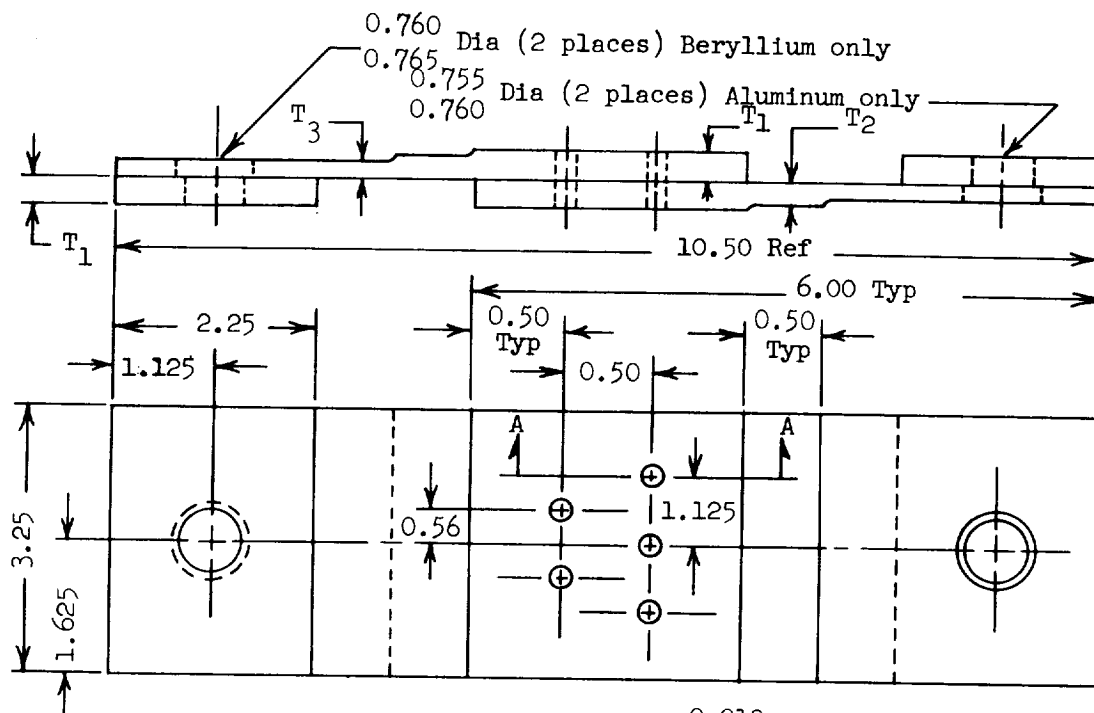
Be Assay	BeO	Fe	Si	Al	Mg	C
98.80	1.64	0.12	0.03	0.09	0.01	0.09

NOTE: Cr, Mn, Ni LESS THAN 0.040%

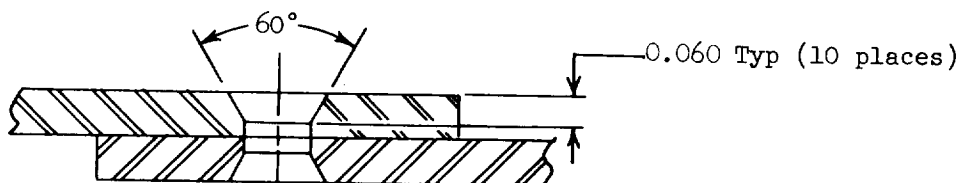
## MECHANICAL PROPERTIES

Type Joint	Gage Inch	Test Direction	Fty PSI	Ftu PSI	Elongation % in 1"
IIIA, IIIB, IIIC, IIID	0.090	L	55,200	80,500	25.0
		T	54,800	80,000	17.0





Section A-A Conf. A, B, and C



Section A-A Conf. D only

Conf.	Fastener Type	Hole Dia.	Mat'l. Gage		
			T1	T2	T3
A	Huckbolt (NAS 2006-V4)	0.189-0.193	0.090	0.075	0.060
B	Jo-bolt (NAS 1671-3)	0.199-0.202	0.090	0.075	0.060
C	Cherry Rivet (MS 20600-M5)	0.158-0.164	0.090	0.075	0.600
D	Beryllium Rivet	0.160-0.164	0.090	0.075	0.060

NOTE: ALL DIMENSIONS ARE IN INCHES.

FIGURE 71. TYPE III JOINT CONFIGURATION - NOMIAL DIMENSIONS

TABLE IX  
TYPE III SPECIMENS (1) - TEST SUMMARY

Specimen No.	Sheet Thickness			Area (in <sup>2</sup> ) (2)			Load (lbs.)		Tension Stress (PSI)				Avg. Bearing Stress at Fasteners	(10) Notes	
				Full Section			Ultimate	Per. (3) Fastener	t <sub>1</sub> (8)	t <sub>2</sub> (8)	t <sub>3</sub> (8)	Net at Holes (9)			
	t <sub>1</sub>	t <sub>2</sub>	t <sub>3</sub>	t <sub>1</sub>	t <sub>2</sub>	t <sub>3</sub>									
203A-1	0.0945	0.0760	0.0630	0.3065	0.2465	0.2043	0.2497	10,875	2,175	35,481	44,118	53,231	43,552	121,781	5
203A-2	0.0955	0.0770	0.0650	0.3109	0.2506	0.2116	0.2536	10,640	2,128	34,223	42,458	50,284	41,956	118,960	5
203A-3	0.0970	0.0780	0.0650	0.3156	0.2538	0.2115	0.2574	11,320	2,264	35,868	44,602	53,522	43,978	123,581	5
203A-4	SAMPLE - NOT TESTED														4
203A-5	0.0960	0.0750	0.0640	0.3114	0.2433	0.2076	0.2555	9,775	1,955	31,390	40,177	47,065	38,258	107,773	5
203B-1	0.0945	0.0755	0.0630	0.3067	0.2451	0.2045	0.2500	10,175	2,035	33,176	41,514	49,756	40,700	108,591	5
203B-2	0.0960	0.0760	0.0640	0.3114	0.2465	0.2076	0.2540	9,450	1,890	30,347	38,337	45,520	37,205	99,265	5
203B-3	0.0950	0.0755	0.0640	0.3082	0.2449	0.2076	0.2515	9,960	1,992	32,317	40,670	47,977	39,602	105,732	5
203B-4	SAMPLE - NOT TESTED														4
203B-5	0.0950	0.0760	0.0640	0.3086	0.2468	0.2079	0.2518	10,175	2,035	32,971	41,228	48,942	40,409	108,015	5
203C-1	SAMPLE - NOT TESTED														4
203C-2	0.0950	0.0760	0.0630	0.3083	0.2466	0.2044	0.2630	5,825	1,165	18,894	23,621	28,498	22,148	77,152	6
203C-3	0.0940	0.0750	0.0520	0.3055	0.2438	0.2015	0.2604	6,070	1,214	19,869	24,897	30,124	23,310	80,718	6
203C-4	0.0935	0.0740	0.0630	0.3039	0.2405	0.2048	0.2593	6,025	1,205	19,826	25,052	29,419	23,236	81,090	6
203C-5	0.0940	0.0740	0.0620	0.3048	0.2400	0.2011	0.2599	6,040	1,208	19,816	25,167	30,035	23,240	80,749	6
203D-1	SAMPLE - NOT TESTED														4, 7
203D-2	0.0930	0.0730	0.0610	0.3019	0.2370	0.1980	0.2572	3,880	776	12,852	16,371	19,596	15,097	52,221	6, 7
203D-3	0.0920	0.0730	0.0620	0.2976	0.2362	0.2006	0.2540	4,710	942	15,827	19,941	23,480	18,543	64,432	6
203D-4	0.0910	0.0730	0.0630	0.2944	0.2362	0.2038	0.2510	4,720	944	16,033	19,983	23,160	18,805	64,746	5
203D-5	0.0920	0.0750	0.0620	0.2975	0.2426	0.2005	0.2536	4,075	815	13,697	16,797	20,324	16,069	55,746	6, 7

## TABLE IX NOTES

1. The nominal dimensions of the Type III specimens are shown in Figure 71.
2. Either the cross-sectional area of the failed segment or, if the fasteners failed, the lesser of the cross-sectional areas of the two segments is reported.
3. The fastener shear strengths are presented in Table II.
4. Sample - not tested.
5. Failed in net tension through the fastener holes - no fastener failure.
6. Fasteners sheared prior to development of full tensile potential of the beryllium segment.
7. Rivets ground flush on both sides.
8. Full Tension Stress:

$$\sigma_{ft} = \frac{P}{Wt}$$

P = Test Load; pounds

W = Specimen width; inches

t = Local beryllium thickness; inch

9. Net Tension Stress:

$$\sigma_{nt} = \frac{P}{W_n t_1}$$

P = Test Load; pounds

$W_n$  = Specimen width less diameter of 3 holes on common centerline; inches

TABLE IX NOTES (Cont.)

$t_1$  = Beryllium thickness at Fastener Area; inch

10. Average Bearing Stress:

$$\sigma_{br} = \frac{P}{Dt_1}$$

P = Test Load; pounds

$t_1$  = Beryllium thickness at Fastener Area; inch

(a) Types 203A and 203B only:

D = Total average diameter of (5) fasteners; inch.

(b) Types 203C and 203D only:

D = Total diameter of (5) fastener holes; inch.

(c) Type 203D only:

Projected hole diameter utilized in computation of bearing area (60° countersink ignored).

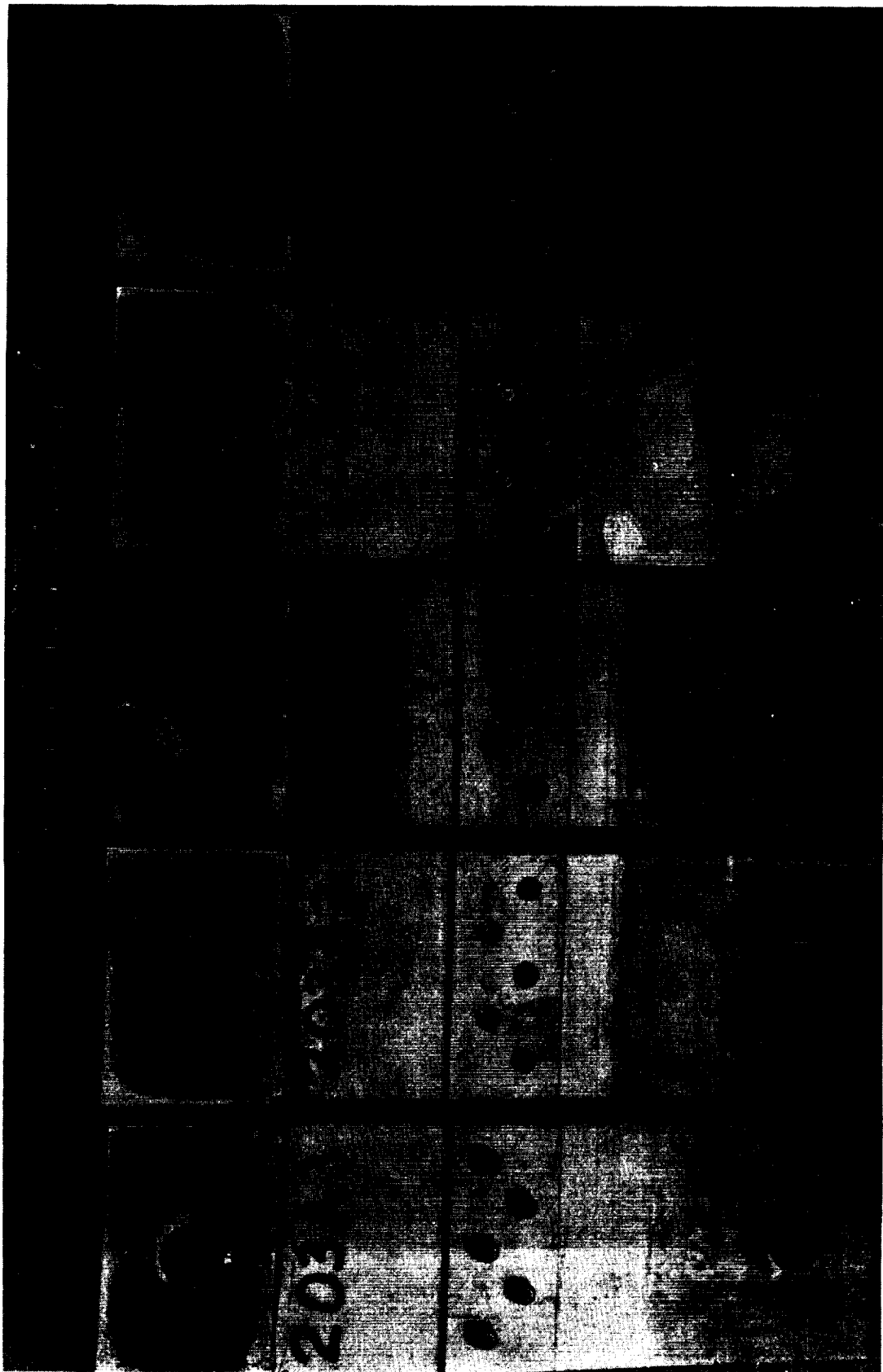


FIGURE 72. TYPE IIIA SPECIMENS - HUCKBOLT FASTENERS

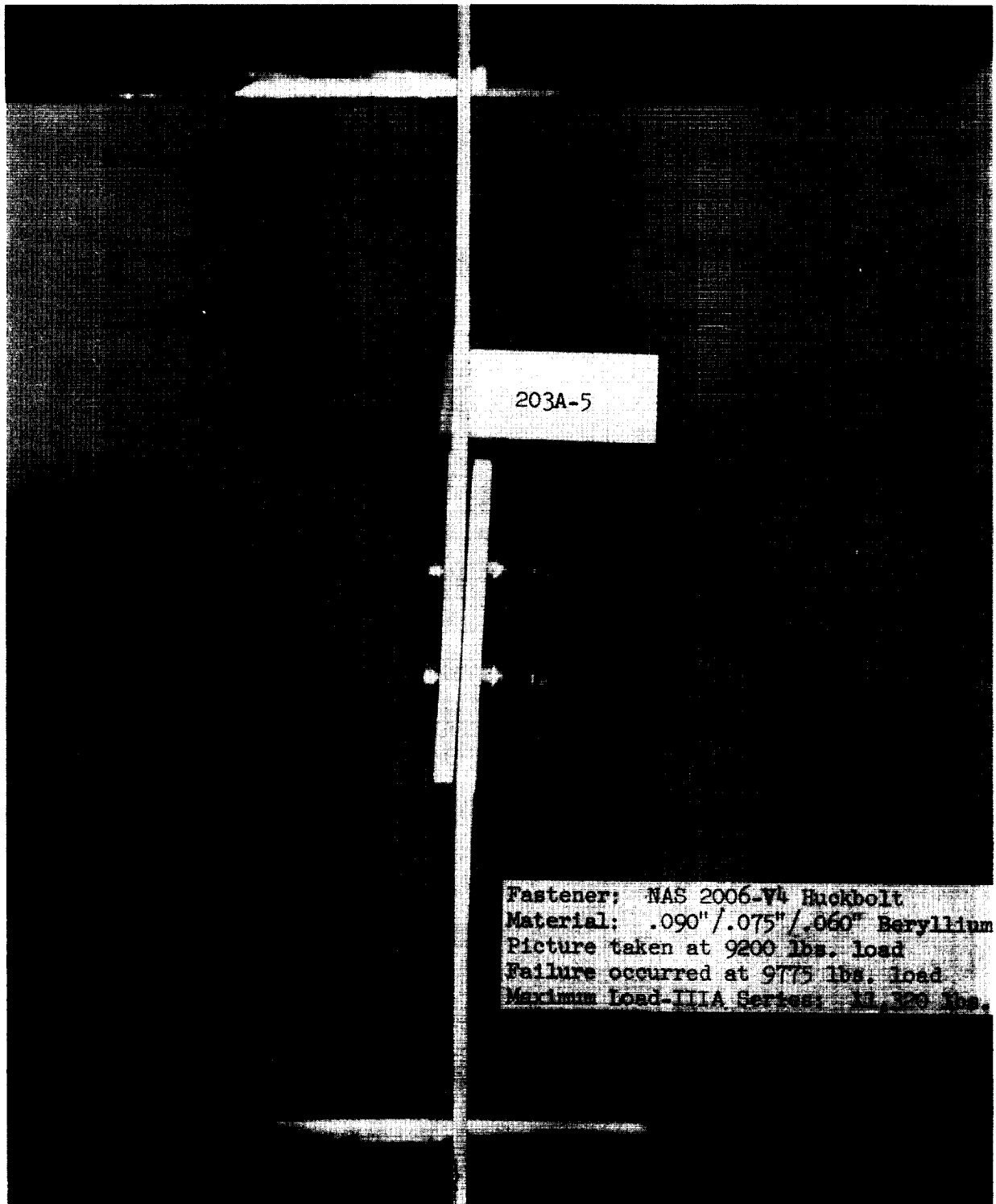


FIGURE 73. TYPE IIIA SPECIMEN - TENSILE TEST

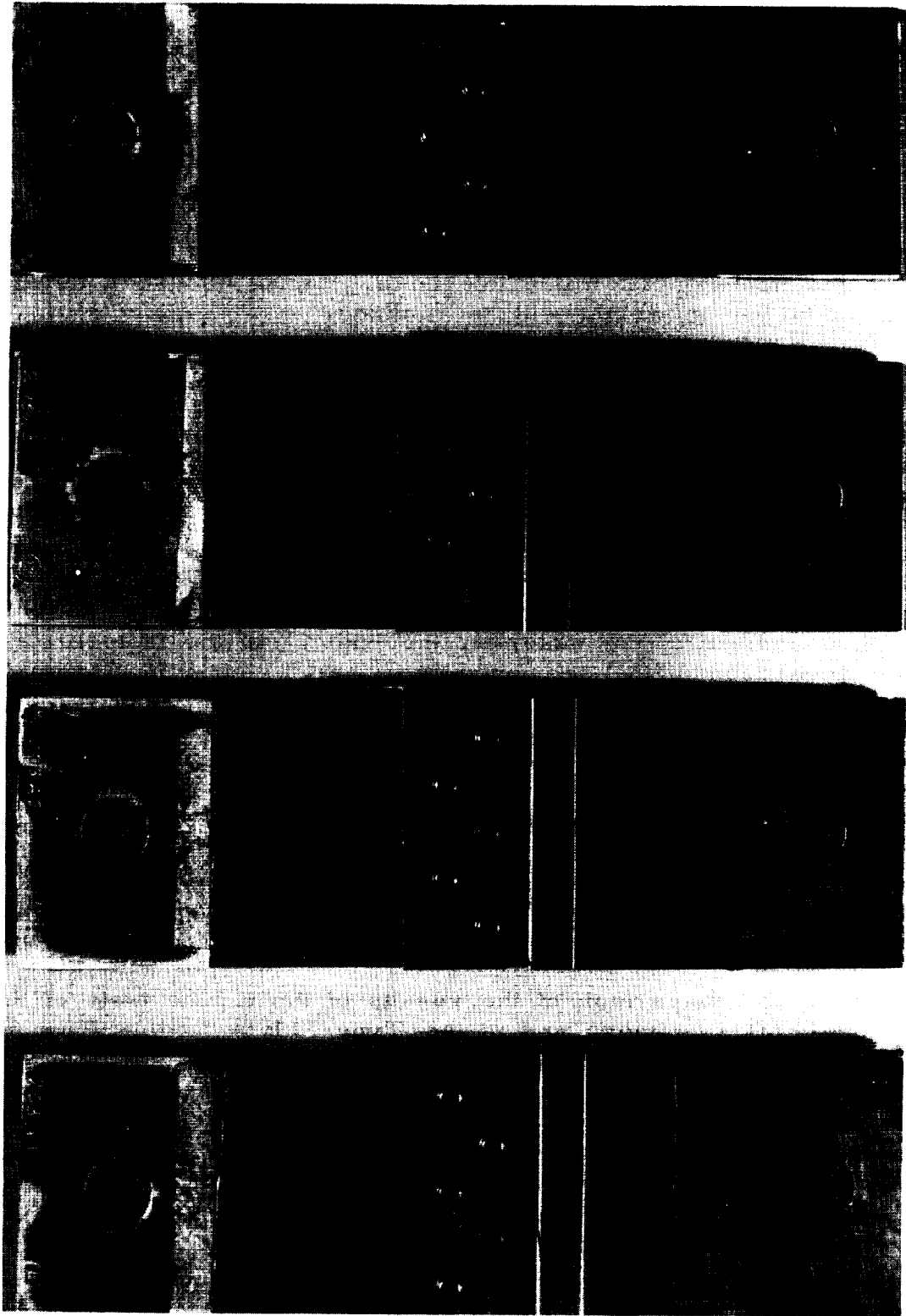


FIGURE 74. TYPE IIIA SPECIMENS - TYPICAL FAILURE MODE.  
NOTE SECONDARY FRACTURES INTO THE 0.060-INCH SECTION.

configuration. Although the thickness of the material in the joint area itself was 0.090 inch rather than 0.120 inch, the average ultimate load was reduced only approximately 16 percent, and the net tensile and bearing stresses were significantly increased.

It may be concluded, therefore, that the thickness of the basic area of a structural panel loaded in tension may be substantially reduced, and that other parameters such as the buckling requirements and fabrication capabilities tend to establish the minimum allowable thickness. In all cases, a substantial reduction in weight will be realized.

b. Type IIIB - Jo-bolts. The assembly of the Type IIIB specimens, utilizing the procedures discussed in the section on Type IB - Jo-bolts, was accomplished without incident. The completed Type IIIB specimens, ready for testing, are illustrated in Figure 75.

The testing of all of the Type IIIB specimens was accomplished in the "Riehle" hydraulic tensile testing machine at a constant loading rate of 2500 pounds per minute. The typical bending of the material, the "tilting" of the fasteners, and the separation of the segments are clearly visible in Figure 76.

Although the loads were slightly less, the failure mode of the Type IIIB specimens was quite similar to that exhibited by the Type IIIA (Huckbolt) specimens. The combined effect of the high bearing stress at the fasteners and the bending stress in the material resulted in the failure of the joints in net tension in the beryllium material, with crack propagation extending, with one exception, into the reduced thickness areas. As may be noted in Figure 77, there was no indication of fastener failure.

A comparison of the results of the tensile tests of these Type IIIB specimens and of the Type IIB - Double Row Fastener specimens, again verifies the advantages of the "stepped" joint configuration. The slight decrease in ultimate load is more than offset by the increases in net tensile and bearing stresses, and the permissible reduction in panel thickness results in substantial savings in weight.





FIGURE 75. TYPE IIIB SPECIMENS - JO-BOLT FASTENERS

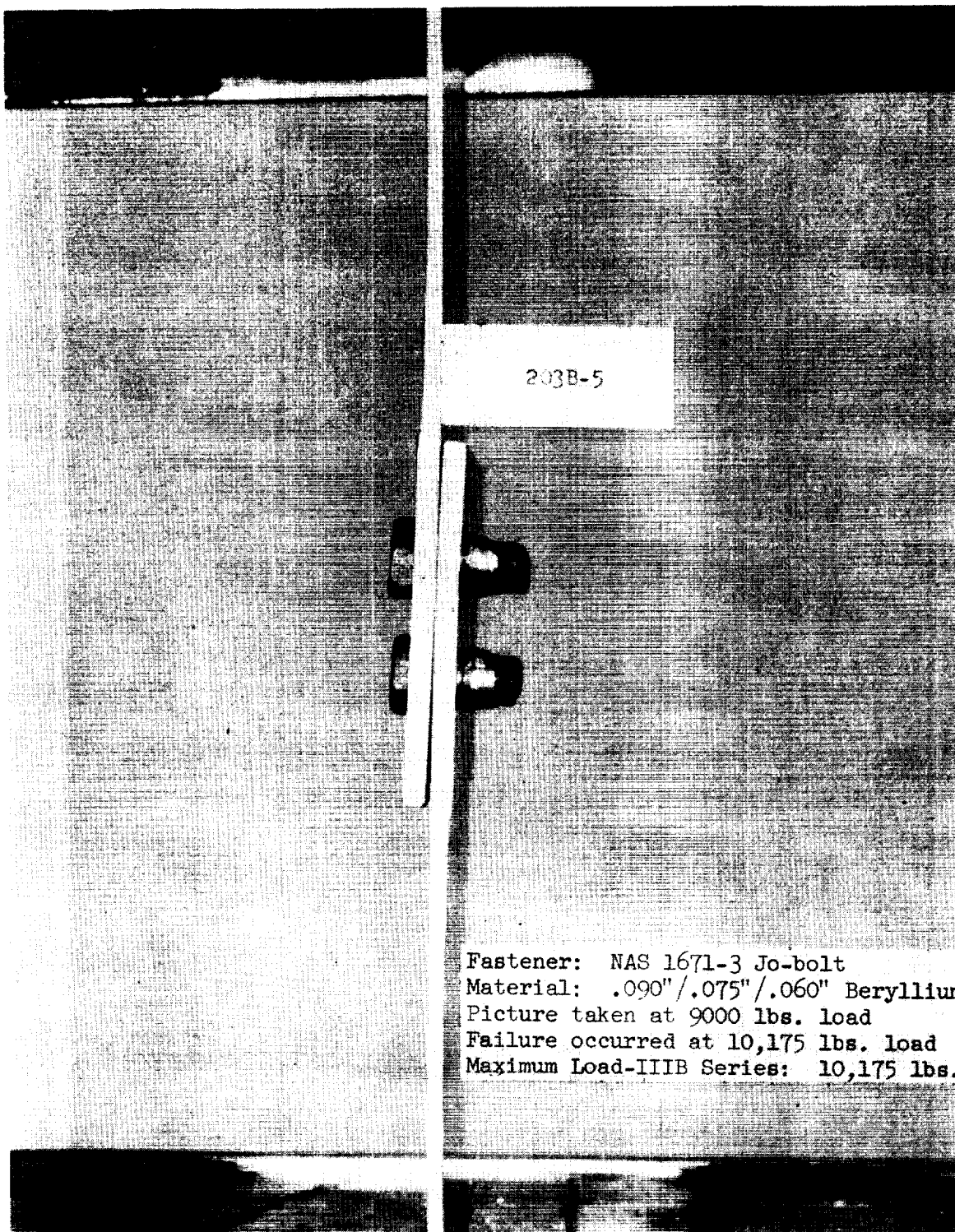


FIGURE 76. TYPE IIIB SPECIMEN - TENSILE TEST

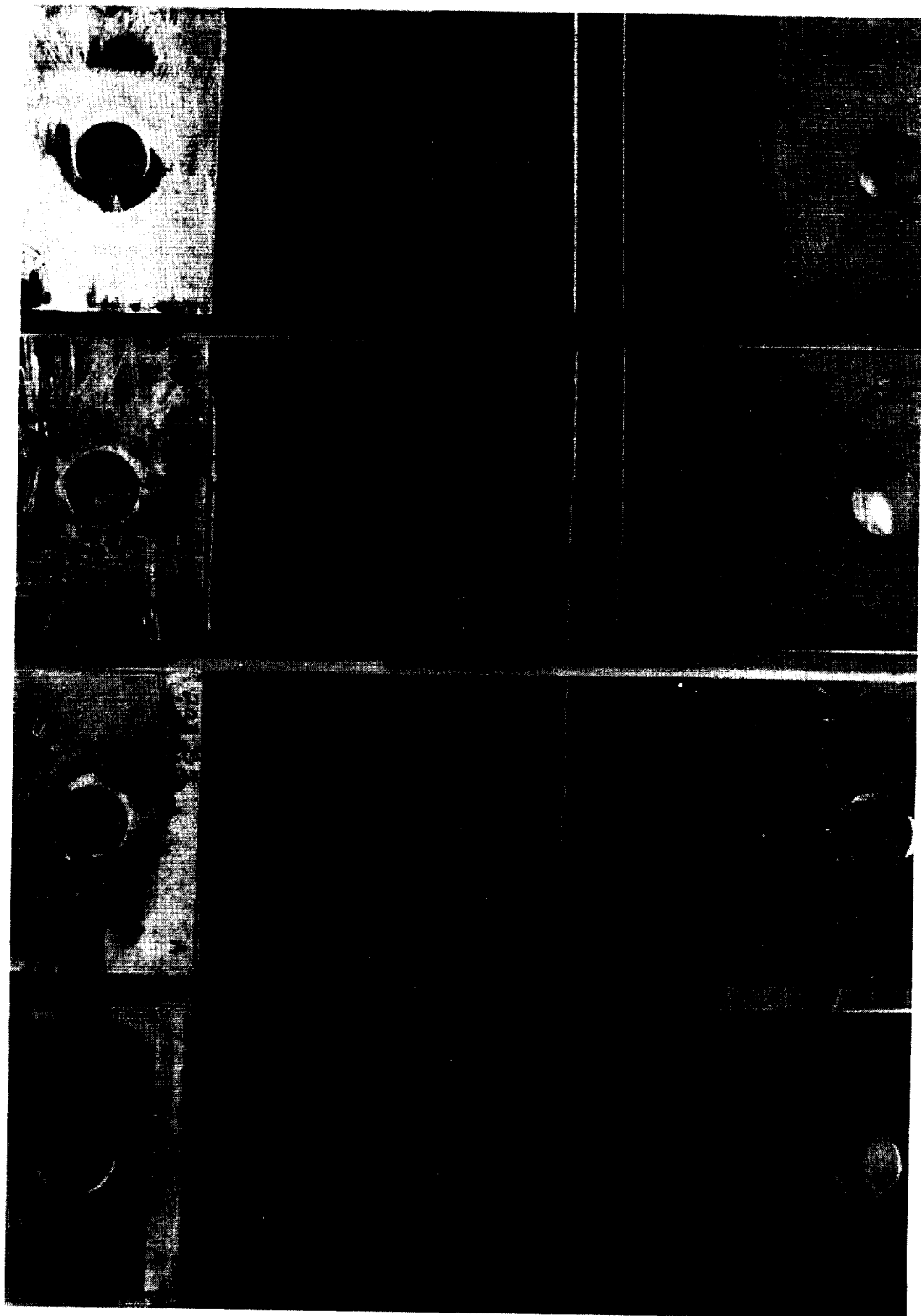


FIGURE 77. TYPE IIIB SPECIMENS - TYPICAL FAILURE MODE

c. Type IIIC - Cherry Blind Rivets. The assembly of the Type IIIC specimens, utilizing the procedures discussed in the section on Type IC - Cherry Blind Rivets was accomplished without incident. The completed Type IIIC specimens, ready for testing, are illustrated in Figure 78.

During the initial testing of the first two specimens in the "Instron" tensile testing machine, the beryllium failed in bearing at one of the loading pin holes at loads of 4530 and 5500 pounds respectively. The retesting of these specimens, and the testing of the balance of the Type IIIC specimens, were performed on the "Riehle" tensile testing machine. The vise grips, which spanned the full width of the specimens and thus assured even distribution of the load, were used for these tests. Figure 79 illustrates the testing of one of the specimens in the "Riehle" tensile testing machine at a constant loading rate of 2500 pounds per minute. The typical bending of the material, "tilting" of the fasteners, and separation of the test segments are clearly evident. This picture, taken almost at the instant of ultimate failure, is of particular interest as the shearing of the fasteners appears to have started.

The failure mode of the Type IIIC specimens was entirely different from that exhibited by the Type IC and IIC specimens. As illustrated in Figure 80, the failure of the specimens was due to the shearing of the rivets. It should be specifically noted that all of the rivets failed in shear at the joint interface; the rivet shanks remained in the holes in the material rather than pulling out as occurred during the testing of the 0.060-inch thick Type IC and IIC specimens. This is believed due to the greater cross-sectional area, due to the 0.090-inch thickness, of the beryllium segments which resulted in reduced bending of the material in the fastener area and reduced net bearing stress at the fastener holes.

d. Type IIID - Countersunk Beryllium Rivets. The objective of this investigation was the determination of the feasibility of joining beryllium structures with double-flush countersunk beryllium rivets. The rivets, illustrated in Figure 18, incorporated a 60-degree taper and extended head to provide sufficient material to fill the countersink during the final forging operation. Prior to insertion into the segment holes, the rivets were cut to the required pre-determined length. Figure 81

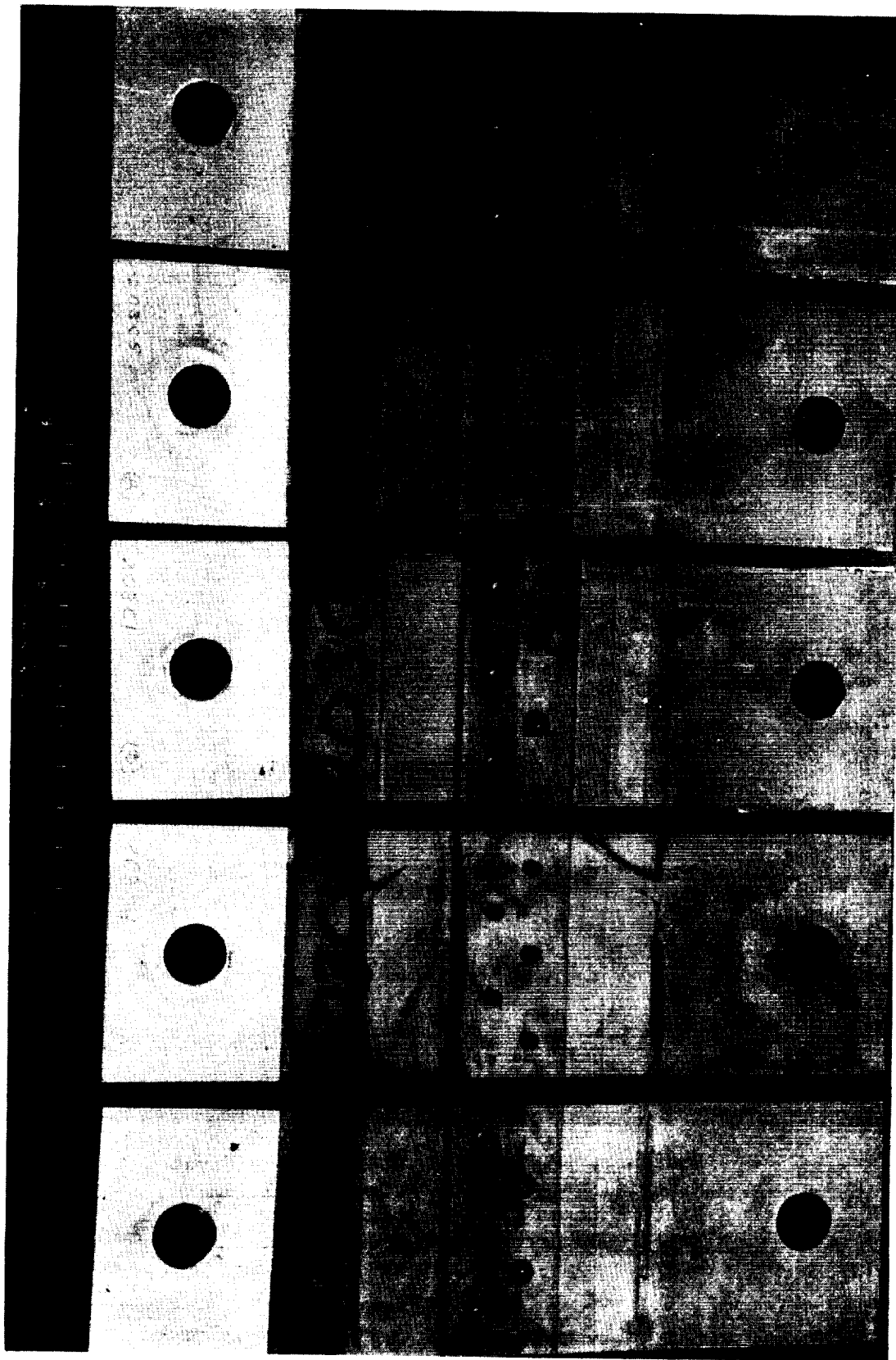
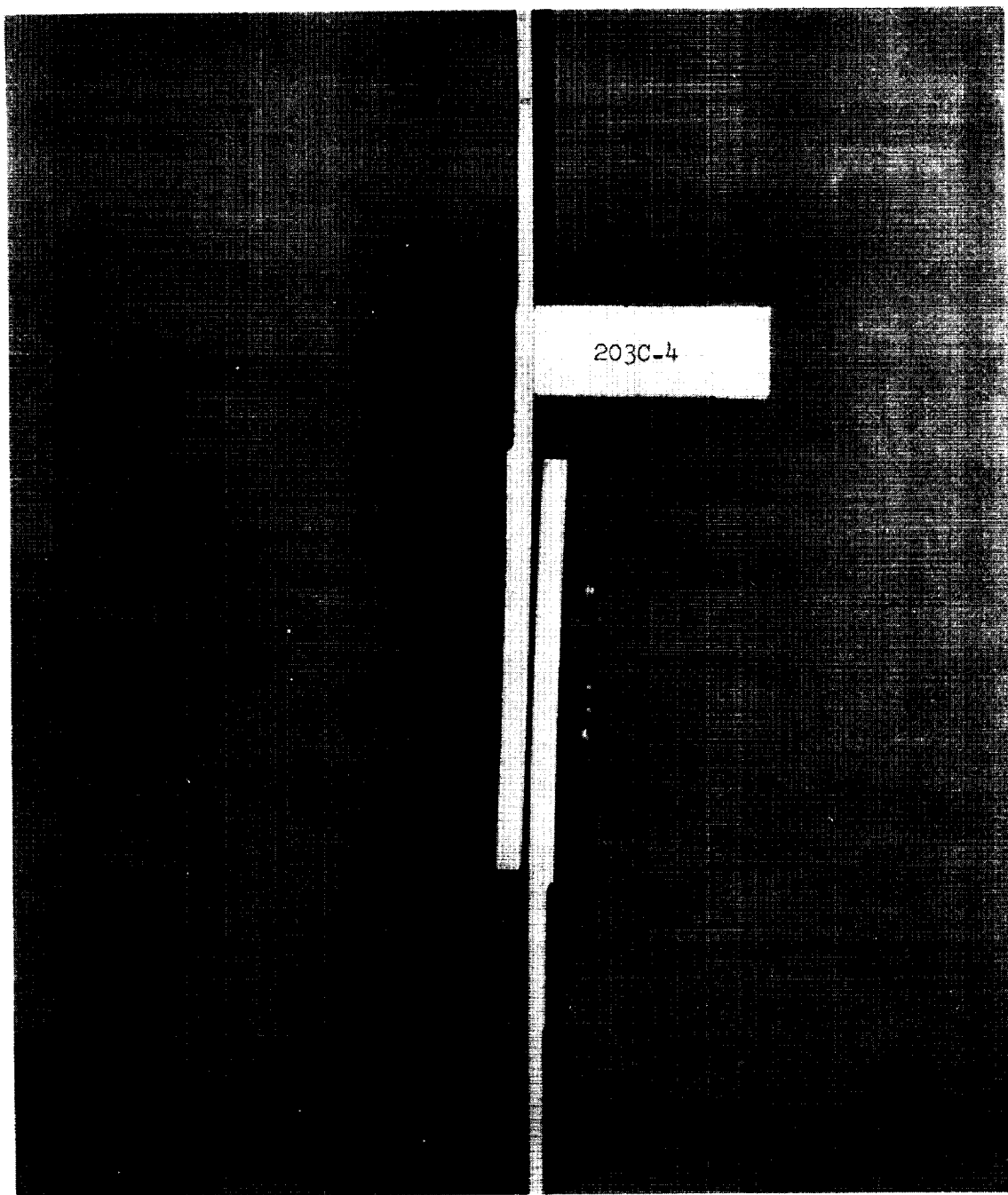


FIGURE 78 TYPE IIIC SPECIMENS - CHERRY BLIND RIVETS



Fastener: MS 20600-M5 Cherry Blind Rivet  
Material: .090"/.075"/.060" Beryllium  
Picture taken at 6000 lbs. load  
Failure occurred at 6025 lbs. load  
Maximum Load-IIIC Series: 6,070 lbs.

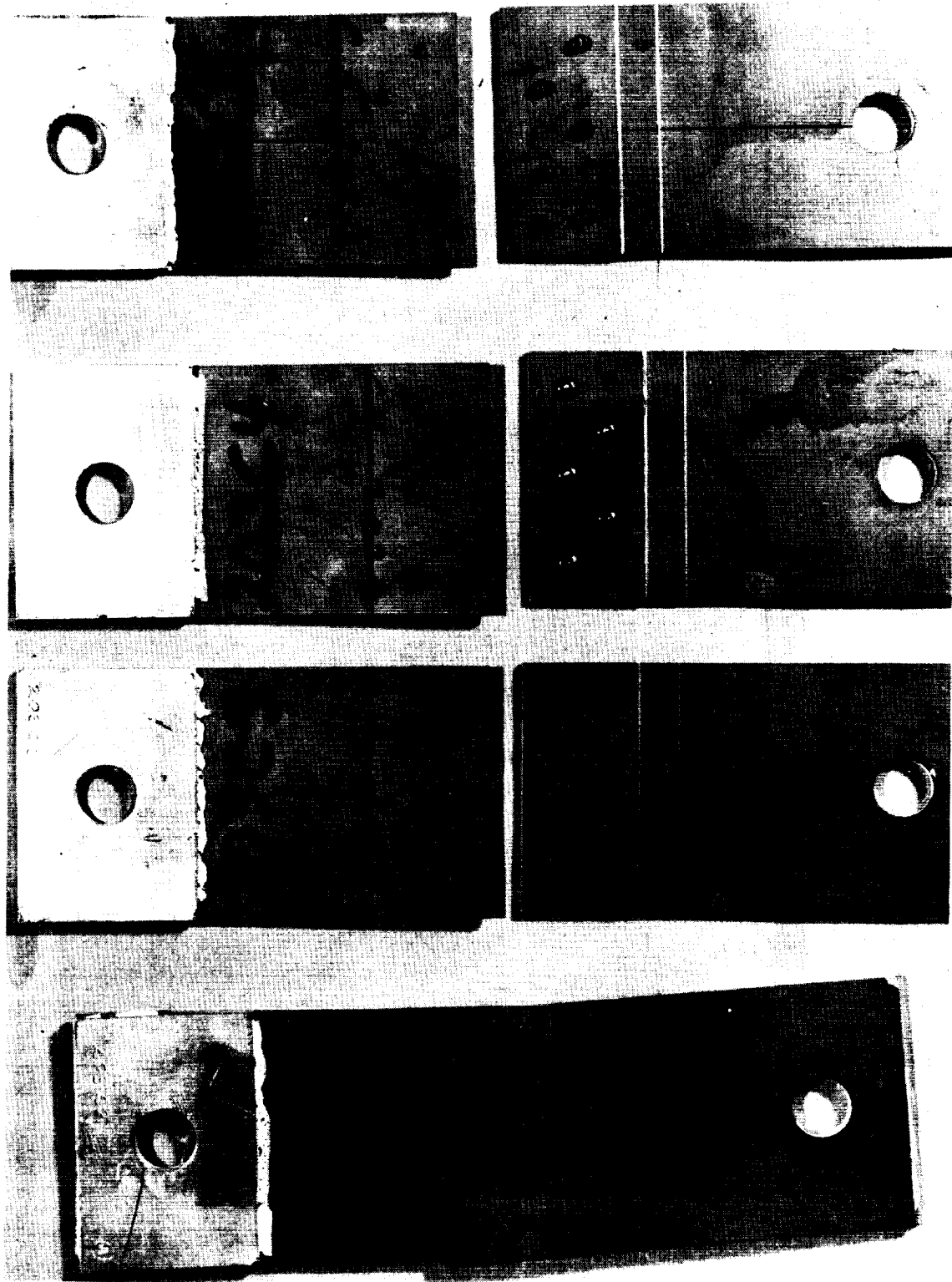
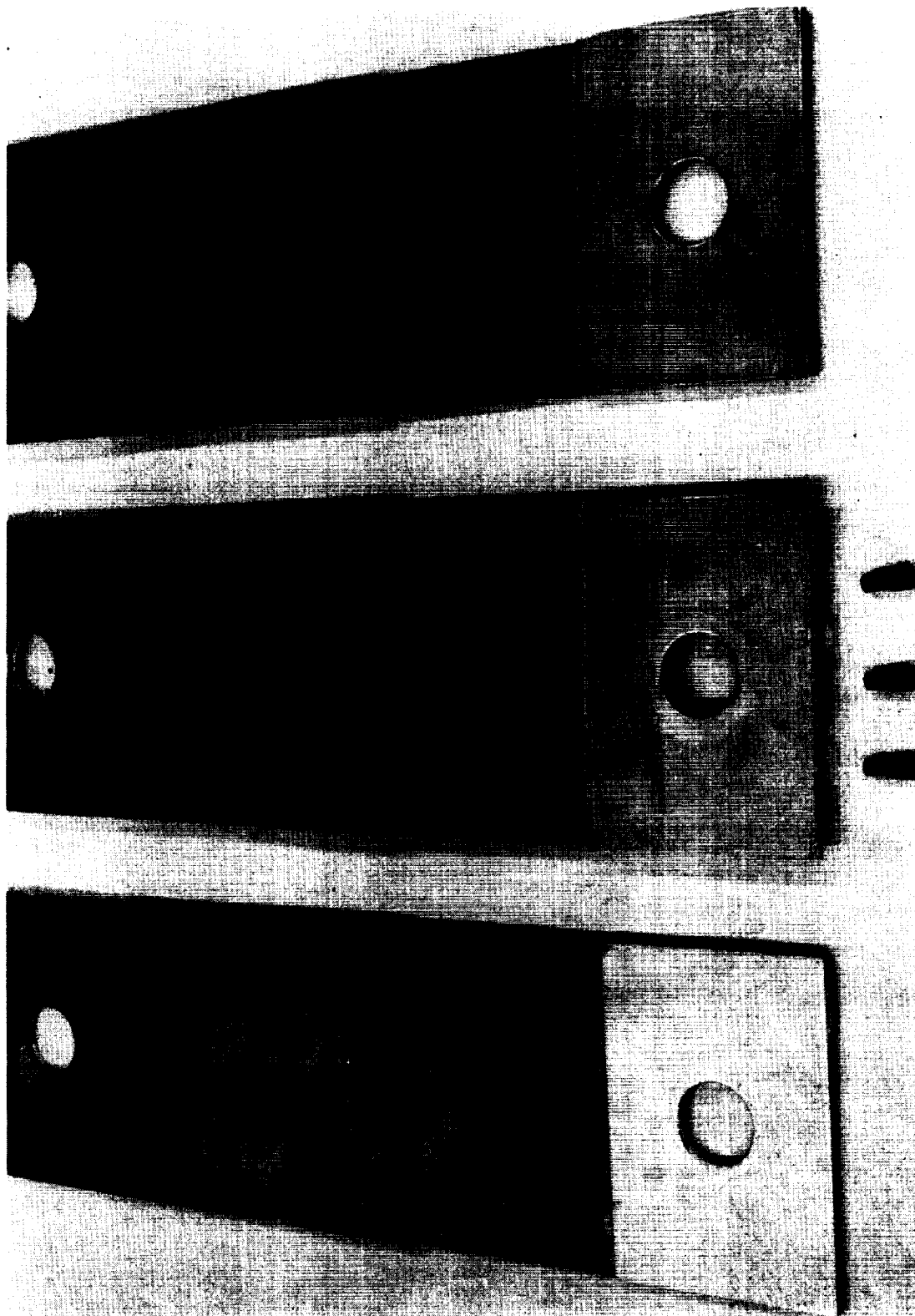


FIGURE 80 TYPE IIIIC SPECIMENS - TYPICAL FAILURE MODE



FORGED HEADS

RIVETS PRIOR TO FORGING

MANUFACTURED HEADS AFTER FORGING

FIGURE 81. TYPE IID SPECIMENS - BERYLLIUM RIVETS



illustrates the rivets prior to forging, and the final "upset" configuration of both "ends" of the rivets. A close-up view of the power leads, the heated anvils, and the actual forging operation in the "Instron" test machine is illustrated in Figure 82. The degree of "upset" of the center rivet, and the complete filling of the countersink may be noted.

Following the "forging" of the rivets, a surface grinder was used to grind the rivet heads on three of the specimens, as nearly flush with the surfaces as the slight "bowing" of the material permitted. In order to obtain comparative data, the rivet heads on the remaining two specimens (203D-3 and 203D-4) were not ground. The three "ground" completed specimens ready for testing are illustrated in Figure 83. Visual examination of a close-up of one of the specimens, illustrated in Figure 84, clearly reveals the complete filling of the countersunk holes. The shadow cast by the incompletely flush ground heads should not be mistaken for incomplete filling of the countersunk holes.

Figure 85 illustrates both macro and micro sections of one of the forged countersunk rivets prior to the flush grinding operation. The complete filling of the countersunk areas, the intimate contact of the segments, and the desirable orientation and uniformity of the grain structure in the rivet should be noted.

Figure 86 illustrates the testing of one of the specimens in the "Instron" tensile testing machine at an average loading rate of 3150 pounds per minute. Due to the decreased loads reached during the testing of these specimens, very little bending of the material or separation of the segments occurred.

As illustrated in Figure 87, the rivets in three of the specimens, including both of the "flush ground" specimens, failed in shear at the joint interface; the fourth failed in net tension in the material through one of the rivet holes.

The rivets, which had been double flush ground failed at significantly lower loads than those which had not been ground. The reason for this difference is unknown; it is possible the "as forged" rivet heads permitted slight additional rotation of the joint itself prior to failure. The investigation required to resolve this question is not believed to be within the scope of this program.



FIGURE 82. TYPE IIID SPECIMEN - BERYLLIUM RIVET INSTALLATION.  
NOTE FULL DEFORMATION OF CENTER RIVET INTO THE  
60° COUNTERSUNK HOLE.

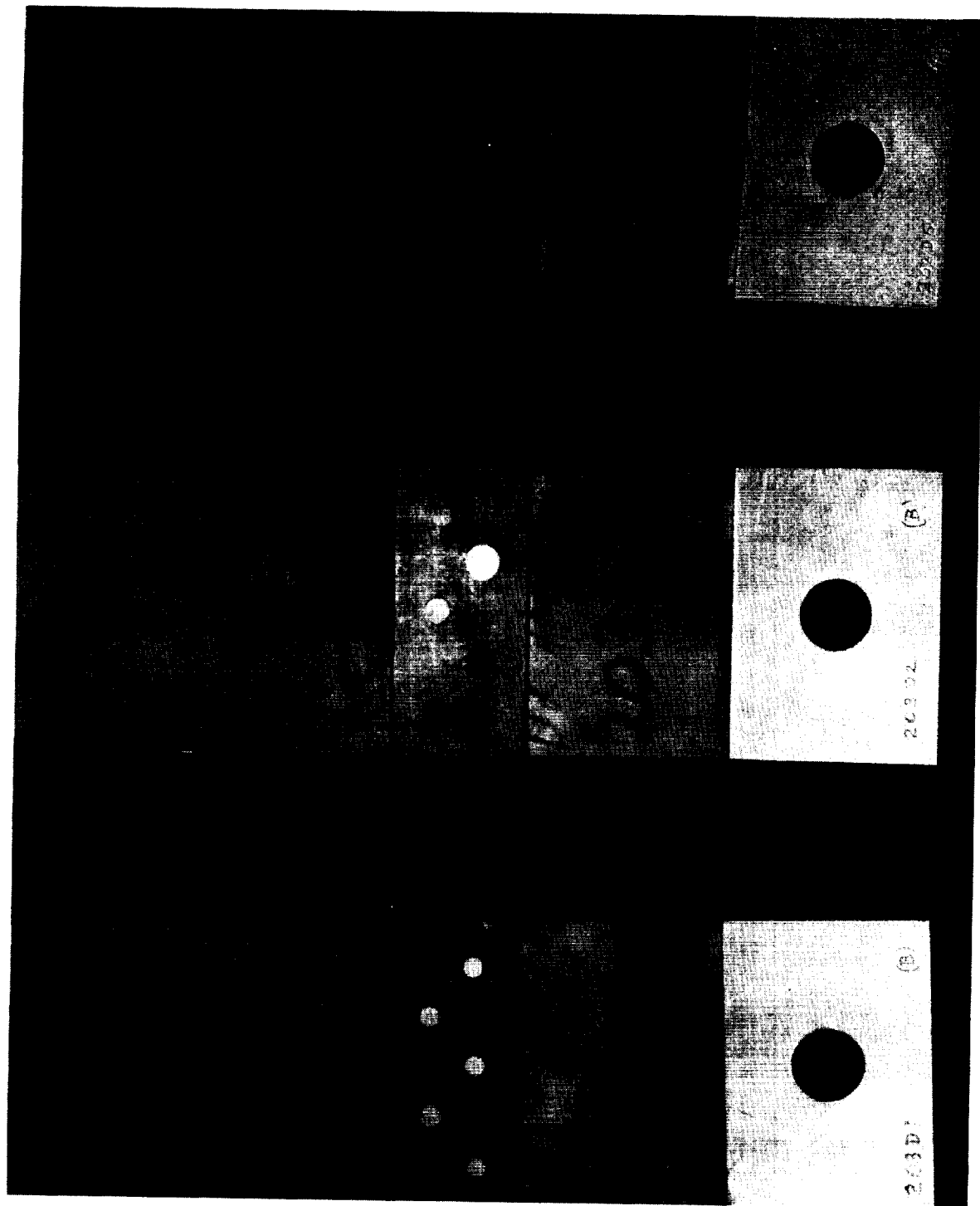


FIGURE 83. TYPE IIID SPECIMENS - COUNTERSUNK BERYLLIUM RIVETS.  
RIVETS GROUND FLUSH ON BOTH SIDES.

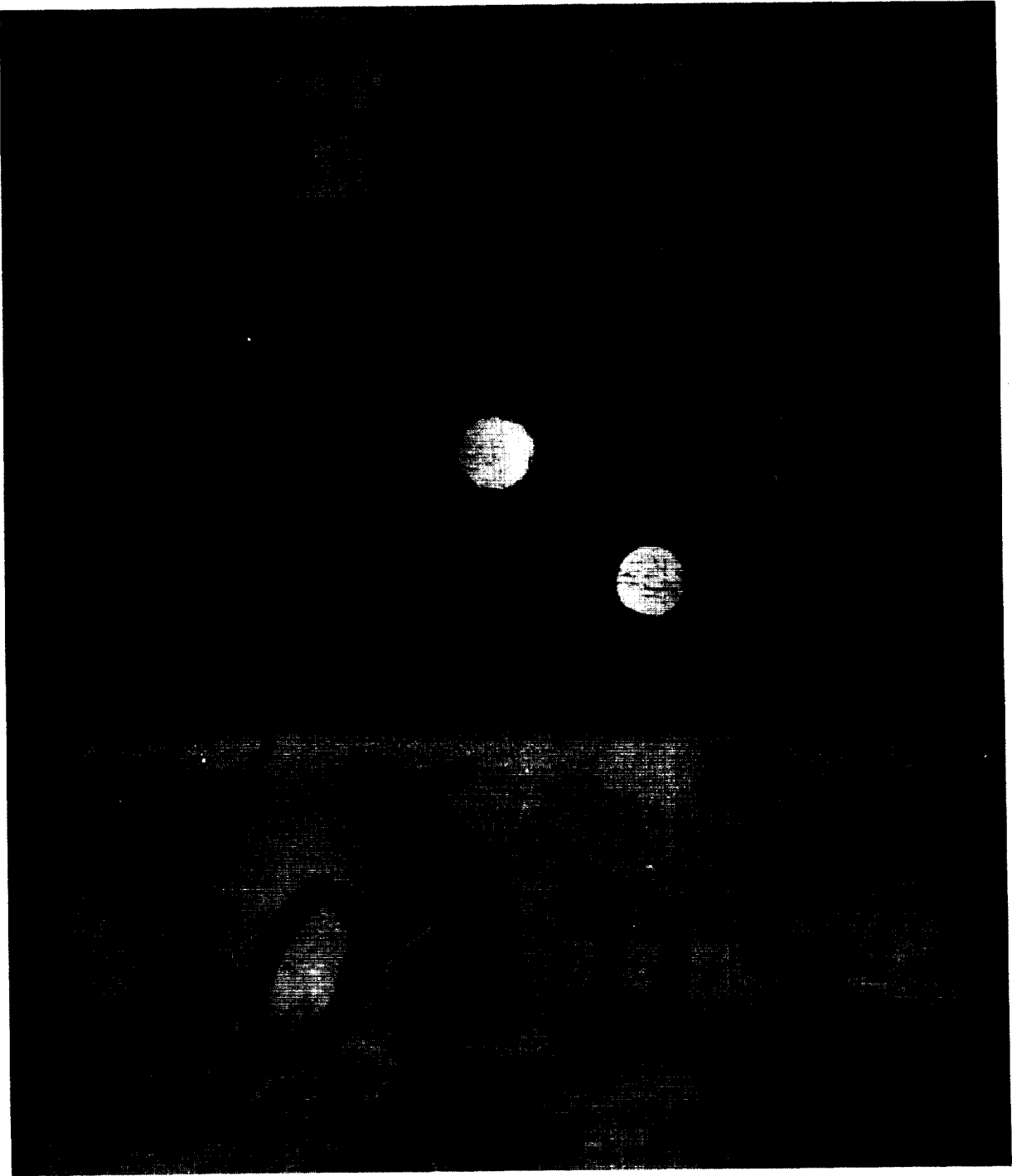
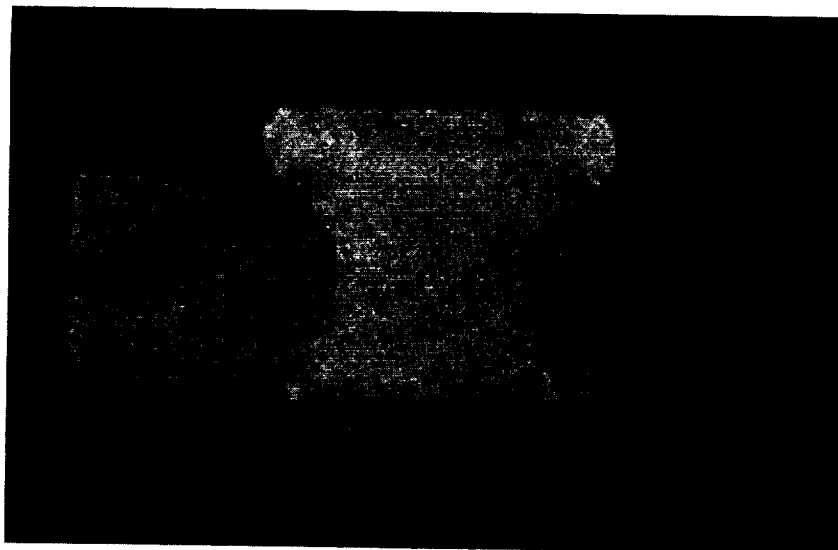
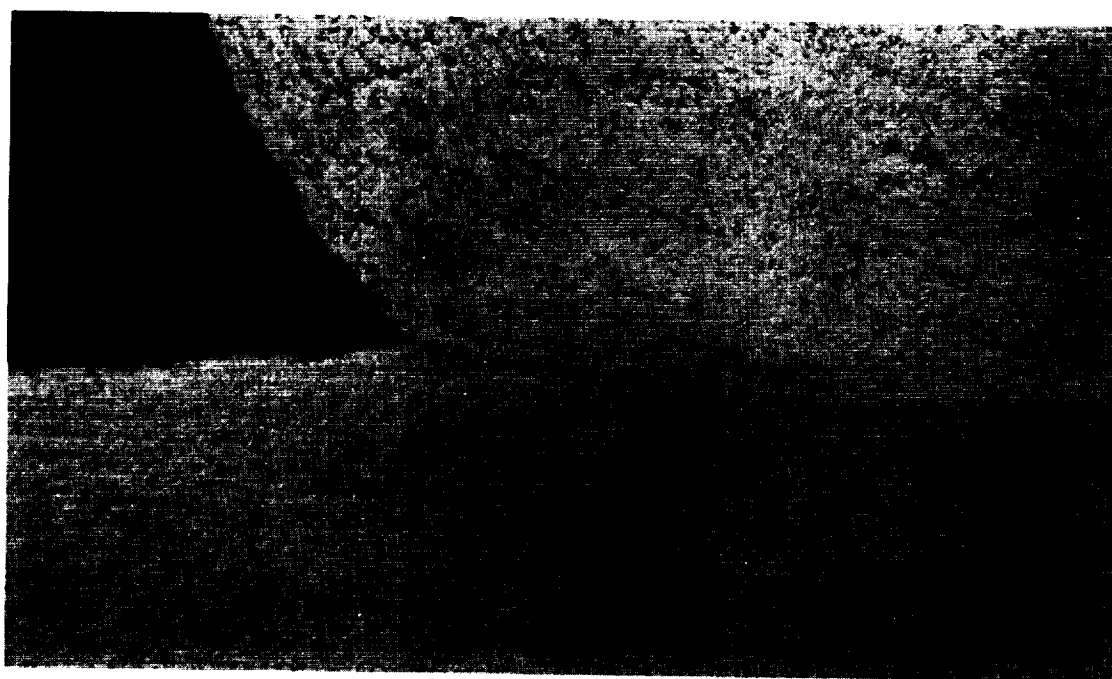


FIGURE 84. TYPE IIID SPECIMEN - COUNTERSUNK BERYLLIUM RIVETS.  
CLOSE-UP OF FLUSH GROUND RIVETS.



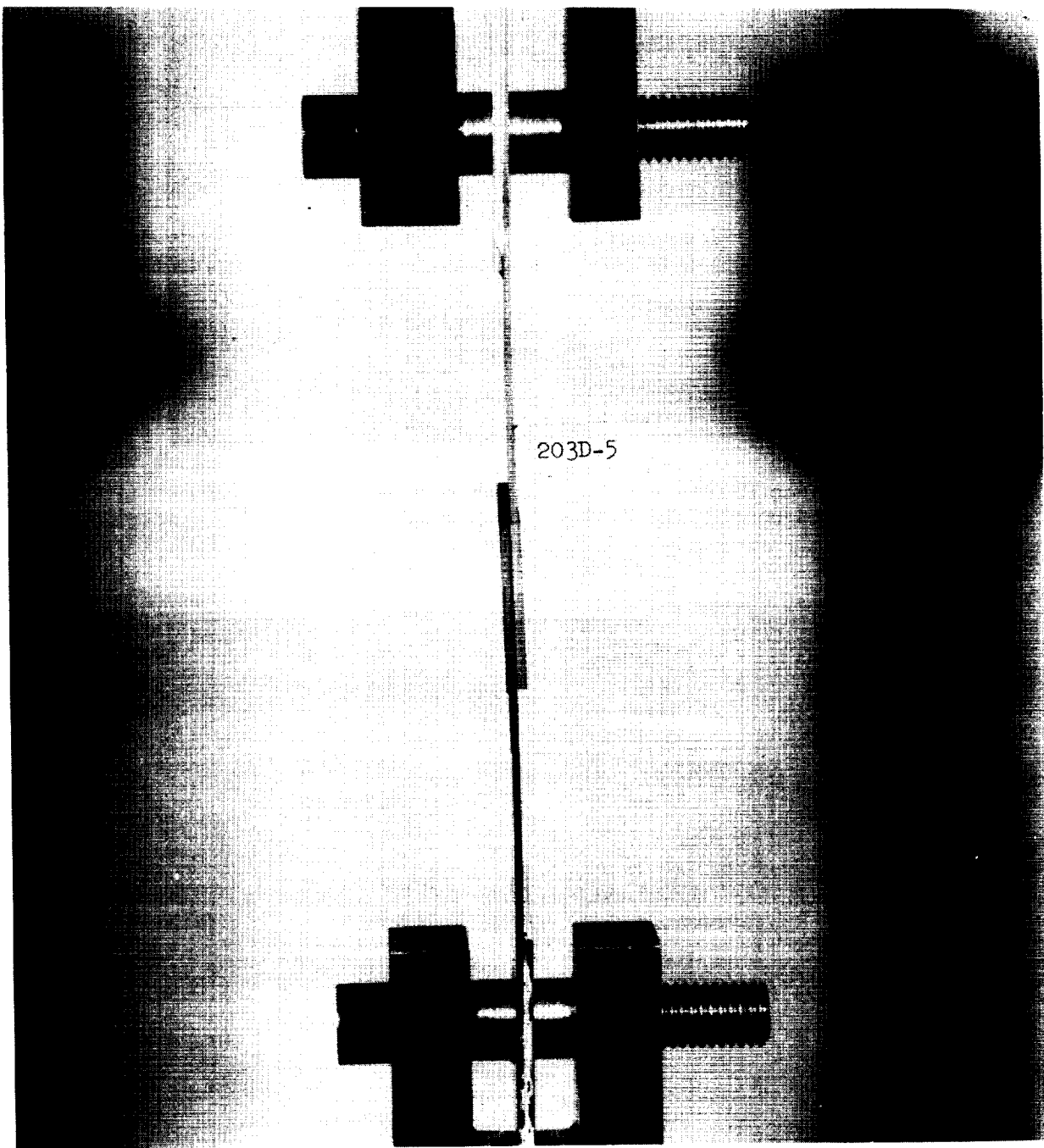
Double Countersunk Beryllium Riveted Joint - 10X  
Note completely filled countersunk areas.



Top of Double Countersunk Beryllium Rivet - 100X  
Note intimate contact and uniform grain orientation.

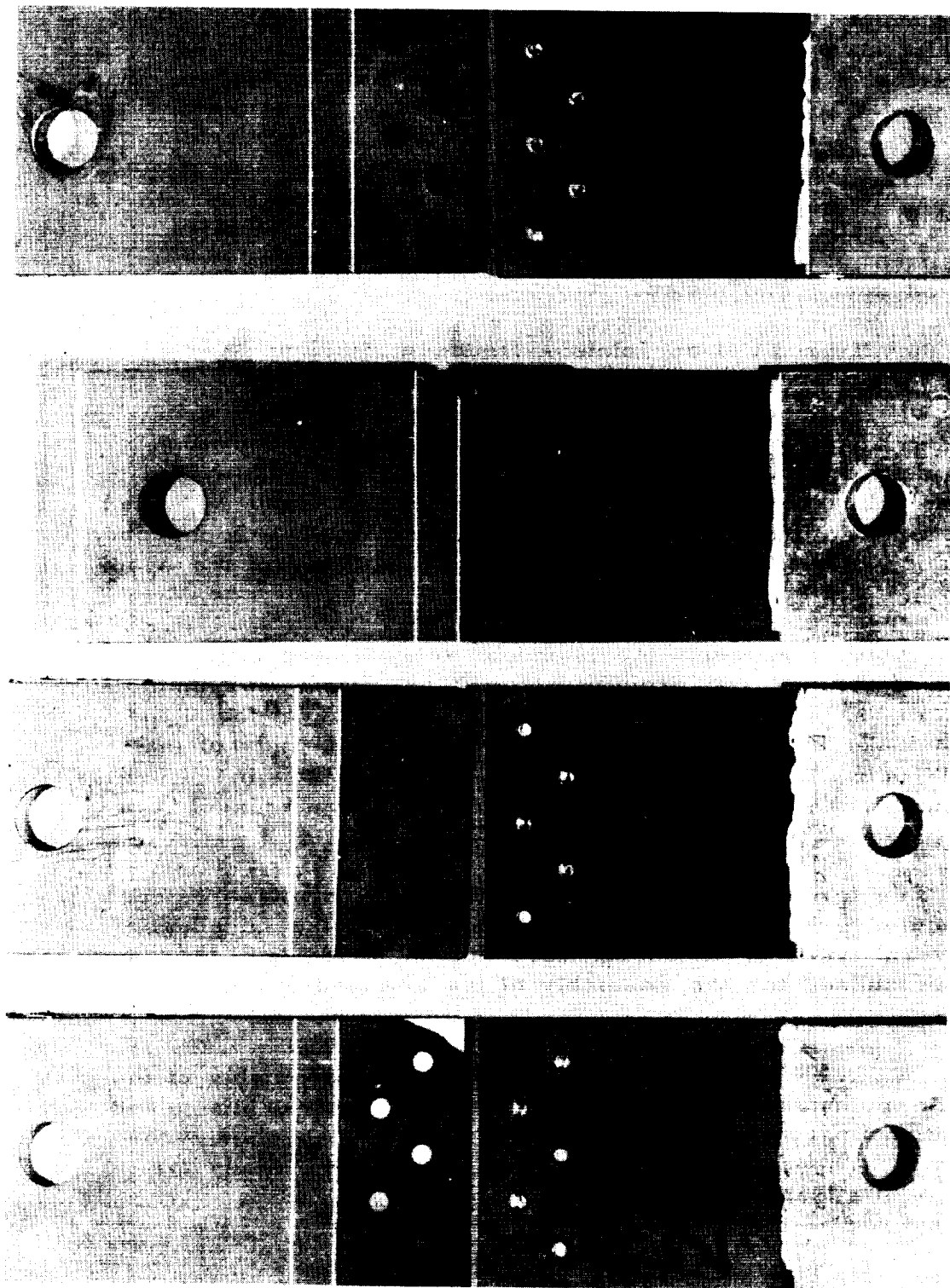
TOP OF DOUBLE COUNTERSUNK BERYLLIUM RIVET - 100X  
NOTE INTIMATE CONTACT AND UNIFORM GRAIN ORIENTATION.

FIGURE 85. TYPE IIID SPECIMEN - DOUBLE COUNTERSUNK BERYLLIUM RIVET



Fastener: Double Flush Beryllium Rivet  
Material: .090"/.075"/.060" Beryllium  
Picture taken at 3850 lbs. load  
Failure occurred at 4075 lbs. load  
Maximum Load - IIID Series: 4720 lbs.

FIGURE 86. TYPE IIID SPECIMEN - TENSILE TEST



NOTE: SPECIMENS 203D-2 AND 203D-5 JOINED WITH DOUBLE FLUSH GROUND RIVETS.  
THE RIVETS IN SPECIMENS 203D-3 AND 203D-4 WERE NOT GROUND.

FIGURE 87. TYPE IIID SPECIMENS - TYPICAL FAILURE MODE

Visual inspection of the load-deflection curves, autographically recorded during the testing of the specimens, clearly revealed a momentary load release, just prior to ultimate, during the testing of three of the specimens. It is believed that slight initial shearing of the rivets may have occurred at this point. A representative load-deflection curve, illustrated in Figure 88, clearly shows this load release point. Another load-deflection curve, recorded during the testing of one of the non-flush-ground riveted specimens, and illustrated in Figure 89, shows only a very slight break in the curve with no apparent load release. This specimen, 202D-4, was the strongest of the four counter-sunk riveted specimens tested.

6. Type IV Lap Joints - Reduced Sections with Eccentric Joint. The objective of this investigation was the evaluation of the effect of extreme eccentricity in the joint area, combined with the reduction in stress gradient afforded by the same segment configuration utilized during the Type III evaluation. The utilization of the same segment configuration, reversed during assembly, provided directly comparable data, and permitted the evaluation of the effects of the eccentric assembly of the specimens.

Table X presents the chemical analysis and mechanical properties of the material procured from The Brush Beryllium Company for the fabrication, testing, and evaluation of the Type IV mechanically fastened joints. The configuration and nominal dimensions of the "204" Type IV joints are illustrated in Figure 90. A summary of the test loads, stresses, and modes of failure is presented in Table XI.

The formation of the reduced thickness sections (steps), the subsequent preparation of the specimens, and the installation of the several types of fasteners were accomplished with the same procedures utilized for the assembly of the respective Type III specimens.

a. Type IVA - Huckbolts. The assembly of the Type IVA specimens, utilizing the procedure that was discussed in the section on Type IA - Huckbolts, was accomplished without incident. The completed Type IVA specimens, ready for testing, are illustrated in Figure 91.



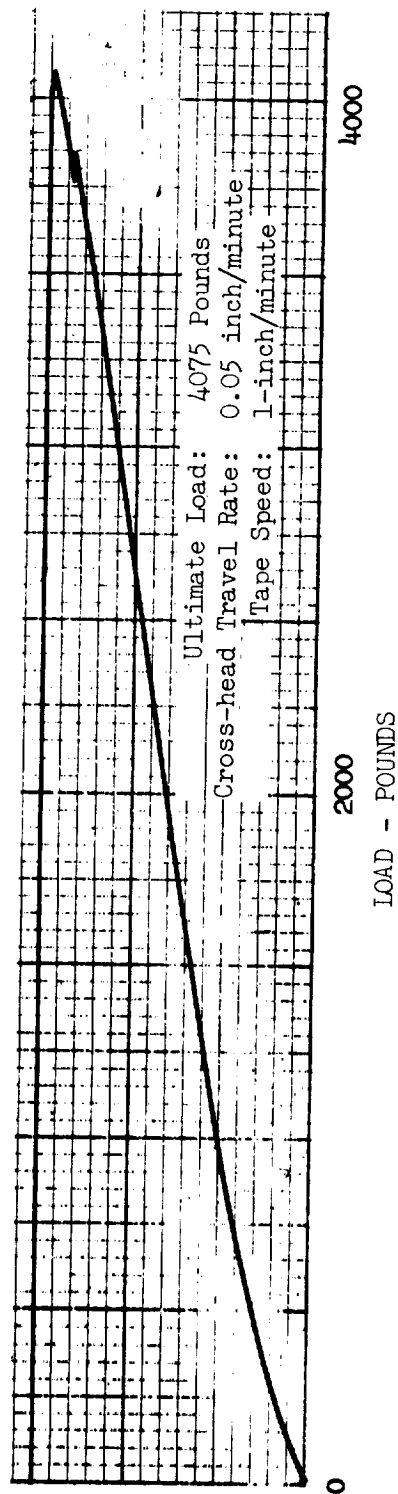


FIGURE 88. TYPE IIID LOAD-DEFLECTION CURVE - SPECIMEN 203D-5  
 DOUBLE FLUSH COUNTERSUNK BERYLLIUM RIVETS.  
 NOTE LOAD RELEASE POINT.

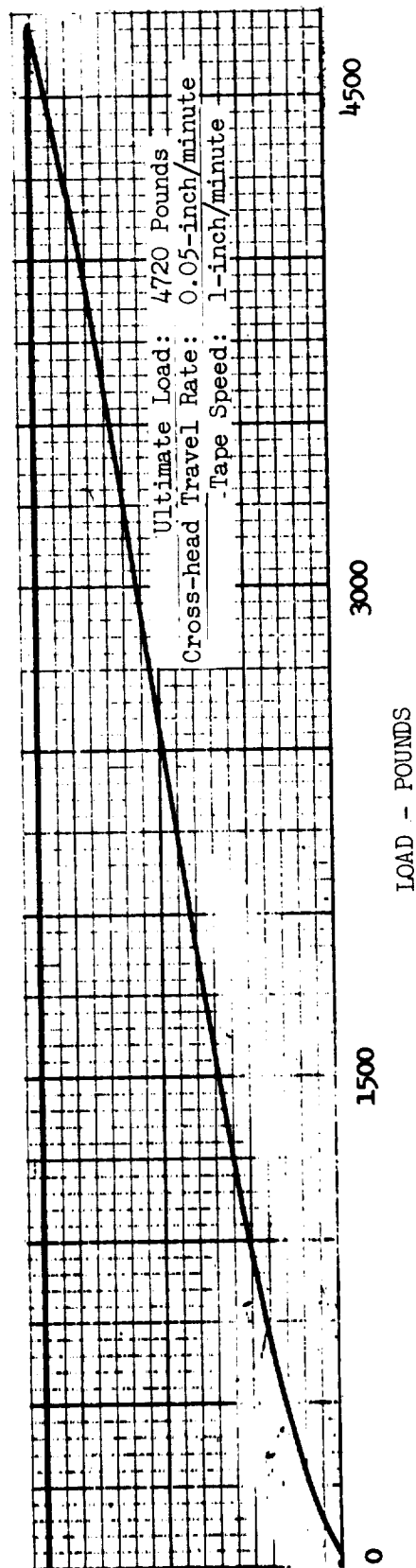


FIGURE 89. TYPE IIID LOAD-DEFLECTION CURVE - SPECIMEN 203D-4.  
 DOUBLE COUNTERSUNK BERYLLIUM RIVETS - "AS FORGED" -  
 NOT FLUSH GROUND.

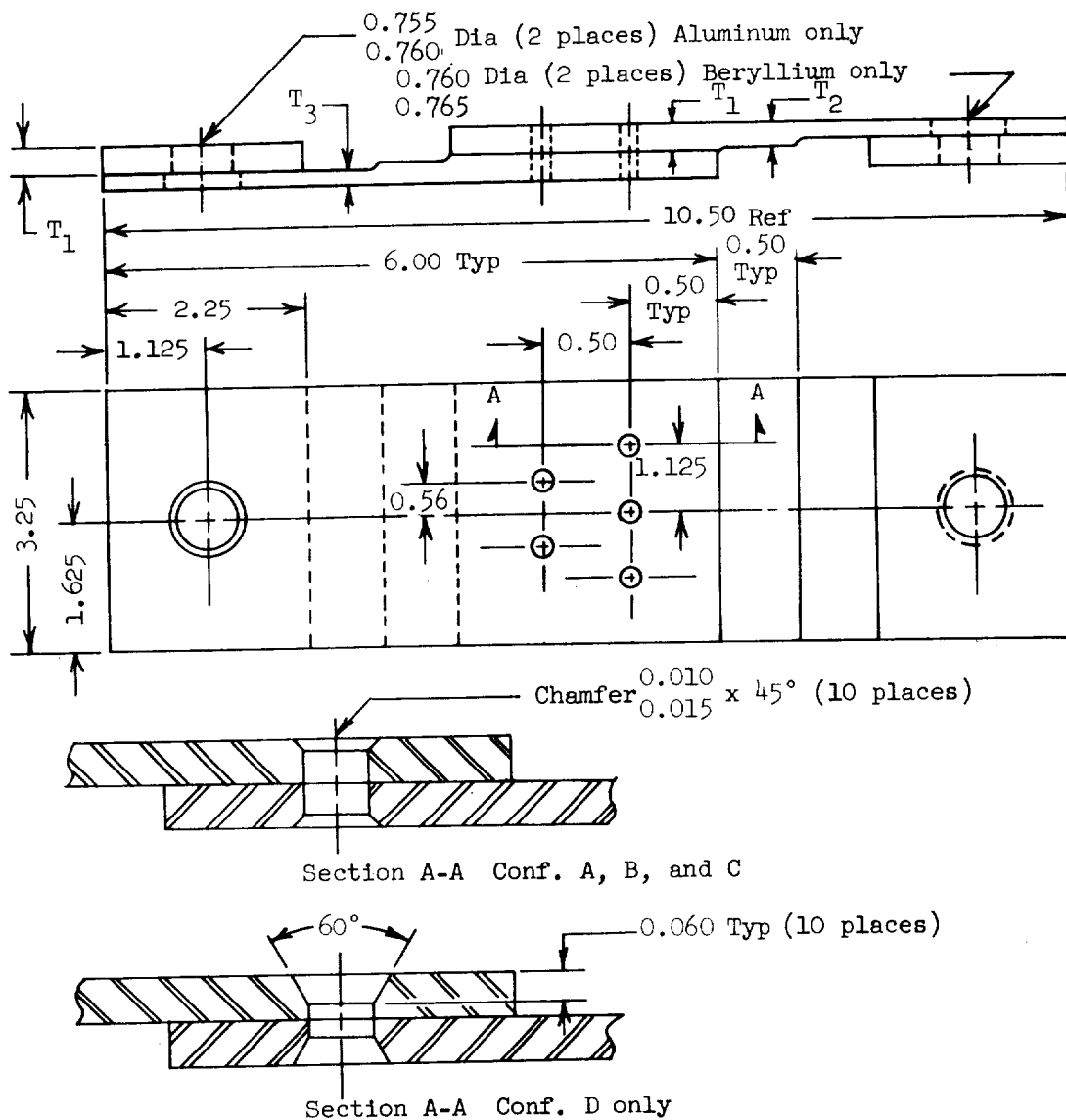
TABLE X  
CHEMICAL ANALYSIS AND MECHANICAL PROPERTIES - MATERIAL FOR TYPE IV MECHANICAL JOINTS

Vendor: The Brush Beryllium Company  
 Lot No.: 2843  
 Sheet No.: 992A

CHEMICAL ANALYSIS - %						
Be Assay	BeO	Fe	Si	Al	Mg	C
98.80	1.64	0.12	0.03	0.09	0.01	0.09

NOTE: Cr, Mn, Ni LESS THAN 0.04%

MECHANICAL PROPERTIES					
Type Joint	Gage Inch	Test Direction	F <sub>ty</sub> PSI	F <sub>tu</sub> PSI	Elongation % in 1-Inch
IVA, IVB, IVC, IVD	0.090	L	55,200	80,500	25.0
		T	54,800	80,000	17.0



Conf.	Fastener Type	Hole Dia.	Mat'l. Gage		
			T1	T2	T3
A	Huckbolt (NAS 2006-V4)	0.189-0.193	0.090	0.075	0.060
B	Jo-bolt (NAS 1671-3)	0.199-0.202	0.090	0.075	0.060
C	Cherry Rivet (MS 20600-M5)	0.158-0.164	0.090	0.075	0.060
D	Beryllium Rivet	0.160-0.164	0.090	0.075	0.060

NOTE: ALL DIMENSIONS ARE IN INCHES.  
 FIGURE 90. TYPE IV JOINT CONFIGURATION - NOMINAL DIMENSIONS

TABLE XI  
TYPE IV SPECIMENS (1) - TEST SUMMARY

Specimen No.	Sheet Thickness			Area (in <sup>2</sup> ) (2)			Load (lbs.)		Tension Stress (PSI)				Avg. Bearing Stress at Fasteners (10)	Notes	
	Full Section			Net at Fasteners	Ultimate	Per (3) Fastener	t <sub>1</sub> (8)	t <sub>2</sub> (8)	t <sub>3</sub> (8)	Net at Holes(9)					
											t <sub>1</sub>	t <sub>2</sub>			t <sub>3</sub>
204A-1	0.0940	0.0750	0.0630	0.3045	0.2429	0.2041	0.2498	10,475	2,095	34,401	43,125	51,323	41,934	117,962	5
204A-2	0.0940	0.0770	0.0640	0.3053	0.2501	0.2079	0.2509	9,725	1,945	31,854	38,884	46,777	38,760	109,516	5
204A-3	0.0935	0.0750	0.0640	0.3031	0.2432	0.2075	0.2490	8,780	1,756	28,967	36,102	42,313	35,261	99,434	5
204A-4	0.0930	0.0760	0.0630	0.3015	0.2464	0.2042	0.2477	10,480	2,096	34,760	42,532	51,322	42,309	119,362	5
204A-5	SAMPLE - NOT TESTED														4
204B-1	SAMPLE - NOT TESTED														4
204B-2	0.0935	0.0750	0.0620	0.3034	0.2434	0.2012	0.2476	10,825	2,165	35,679	44,474	53,802	43,720	116,775	5
204B-3	0.0905	0.0740	0.0610	0.2936	0.2401	0.1979	0.2392	10,575	2,115	36,018	44,044	53,436	44,210	117,893	5
204B-4	0.0920	0.0750	0.0640	0.2981	0.2430	0.2074	0.2432	10,070	2,014	33,781	41,440	48,554	41,406	110,417	5
204B-5	0.0925	0.0740	0.0640	0.3003	0.2402	0.2077	0.2450	10,160	2,032	33,833	42,298	48,917	41,469	110,796	5
204C-1	SAMPLE - NOT TESTED														4
204C-2	0.0910	0.0730	0.0640	0.2947	0.2364	0.2072	0.2425	5,400	1,080	18,324	22,843	26,062	22,268	74,176	6
204C-3	0.0955	0.0740	0.0630	0.3101	0.2403	0.2046	0.2547	6,000	1,200	19,349	24,969	29,326	23,557	78,534	6
204C-4	0.0930	0.0750	0.0640	0.3016	0.2432	0.2076	0.2477	6,070	1,214	20,126	24,959	29,239	24,505	81,586	6
204C-5	0.0920	0.0750	0.0630	0.2983	0.2432	0.2042	0.2446	6,280	1,256	21,053	25,822	30,754	25,675	84,750	6
204D-1	0.0940	0.0760	0.0620	0.3051	0.2467	0.2013	0.2603	4,150	830	13,602	16,822	20,616	15,943	55,556	6, 7
204D-2	0.0915	0.0740	0.0630	0.2969	0.2401	0.2044	0.2533	4,250	850	14,315	17,701	20,793	16,779	58,459	6
204D-3	0.0930	0.0750	0.0630	0.3016	0.2432	0.2043	0.2572	4,140	828	13,727	17,023	20,264	16,096	56,022	6
204D-4	SAMPLE - NOT TESTED														4, 7
204D-5	0.0920	0.0750	0.0630	0.2981	0.2430	0.2041	0.2539	3,700	740	12,412	15,226	18,128	14,573	50,272	6

# TABLE XI NOTES

1. The nominal dimensions of the Type IV specimens are shown in Figure 90.
2. Either the cross-sectional area of the failed segment, or if the fasteners failed, the lesser of the cross-sectional areas of the two segments is reported.
3. The fastener shear strengths are presented in Table II.
4. Sample - not tested.
5. Failed in net tension through the fastener holes - no fastener failure.
6. Fasteners sheared prior to development to full tensile potential of the beryllium segment.
7. Rivets ground flush on both sides.
8. Full Tension Stress:

$$\sigma_{ft} = \frac{P}{Wt}$$

P = Test Load; pounds

W = Specimen width; inches

t = Local beryllium thickness; inch

9. Net Tension Stress:

$$\sigma_{nt} = \frac{P}{W_n t_1}$$

P = Test Load; pounds

$W_n$  = Specimen width less diameter of three holes on common centerline; inches

TABLE XI NOTES (Cont'd)

$t_1$  = Beryllium thickness at fastener area; inch

10. Average Bearing Stress:

$$\sigma_{br} = \frac{P}{Dt_1}$$

P = Test Load; pounds

$t_1$  = Beryllium thickness at fastener area; inch

(a) Types 204A and 204B only:

D = Total average diameter of (5) fasteners; inch.

(b) Types 204C and 204D only:

D = Total diameter of (5) fastener holes; inch.

(c) Type 204D only:

Projected hole diameter utilized in computation of bearing area (60° countersink ignored).

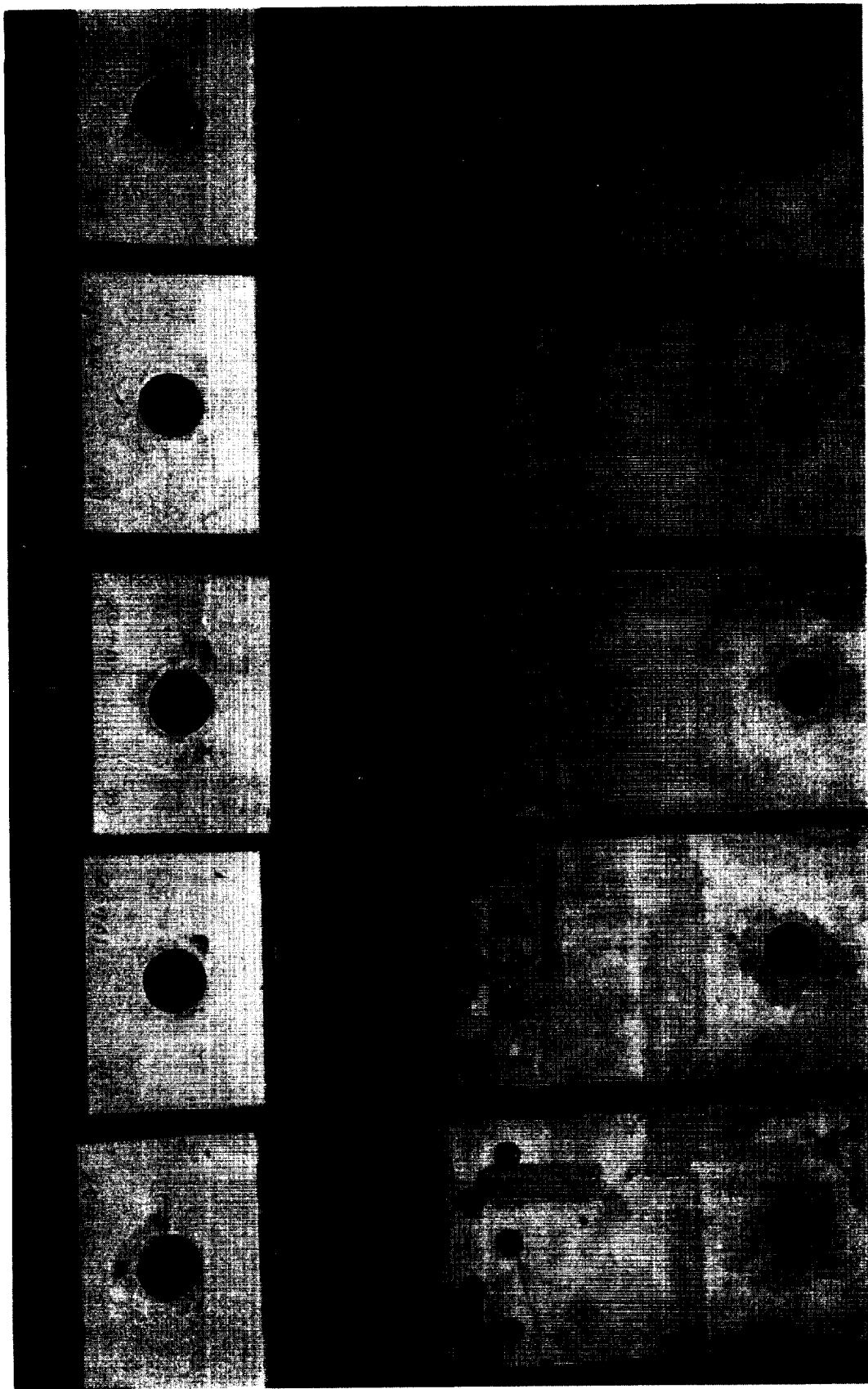


FIGURE 91. TYPE IVA SPECIMENS - HUCKBOLT FASTENERS



The testing of the Type IVA specimens was accomplished in the "Riehle" hydraulic tensile testing machine at a constant loading rate of 3000 pounds per minute. The typical bending of the material, "tilting" of the fasteners, and separation of the segments in the joint area are clearly visible in Figure 92.

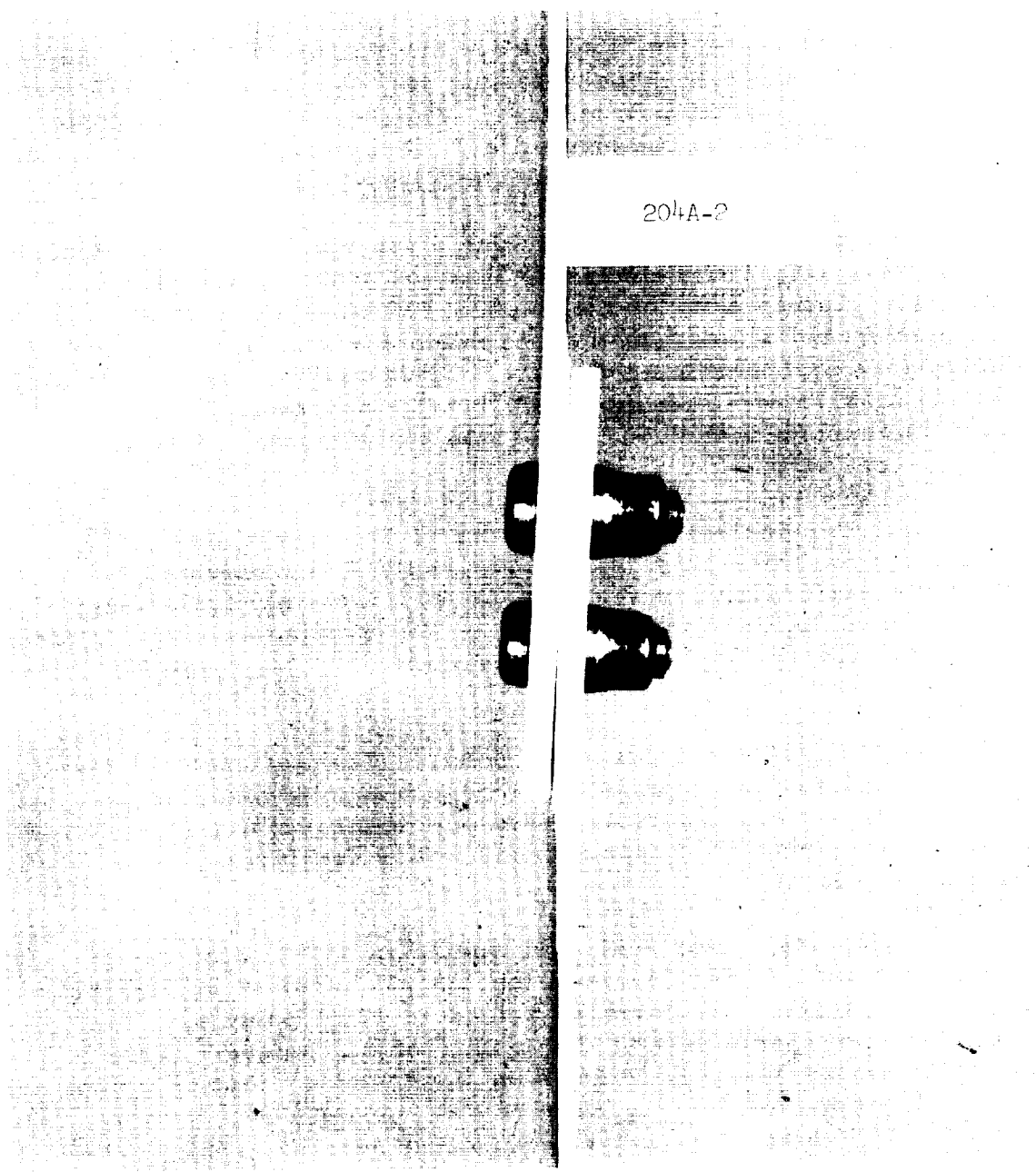
The failure mode of the Type IVA specimens, illustrated in Figure 93, was very similar to that exhibited by the Type IIIA specimens. Again, with one exception (204A-3), all of the specimens failed in net tension in the beryllium through one of more of the holes in a fastener line; the crack propagation extended through the 0.075-inch "step" into the basic 0.060-inch area in three of the four specimens tested. There was no indication of fastener failure.

The comparison of the results of the tensile tests of the Type IIIA and Type IVA specimens verified the deleterious effect of the eccentricity of the joint area. The higher bending stress resulted in the earlier failure of the specimens; the average reduction in joint strength was 1.5 percent.

b. Type IVB - Jo-bolts. The assembly of the Type IVB specimens utilizing the procedures discussed in the section on Type IB - Jo-bolts, was accomplished without incident. The completed Type IVB specimens, ready for testing, are illustrated in Figure 94.

During the initial testing of specimen 204B-4 in the "Instron" tensile testing machine, the beryllium failed in bearing at one of the loading pin holes at a load of 6120 pounds. The retesting of this specimen and the testing of the balance of the Type IVB series were performed in the "Riehle" tensile testing machine at a constant loading rate of 2500 pounds per minute. Due to the high load at which the picture was taken, the typical bending of the material, the "tilting" of the fasteners, and the separation of the segments in the joint area are clearly illustrated in Figure 95.

The typical failure mode of the Type IVB specimens, illustrated in Figure 96, was similar to that exhibited by the Type IIIB specimens. The combined effect of the high bearing stress at the fasteners and the bending stress in the material



Fastener: NAS 2006V4 Huckbolt  
Material: .090"/.075"/.060" Beryllium  
Picture taken at 8000 lbs.  
Failure occurred at 9725 lbs.  
Maximum Load - IVA Series: 10,480 lbs.

FIGURE 92. TYPE IVA SPECIMEN - TENSILE TEST



FIGURE 93. TYPE IVA SPECIMENS - TYPICAL FAILURE MODE

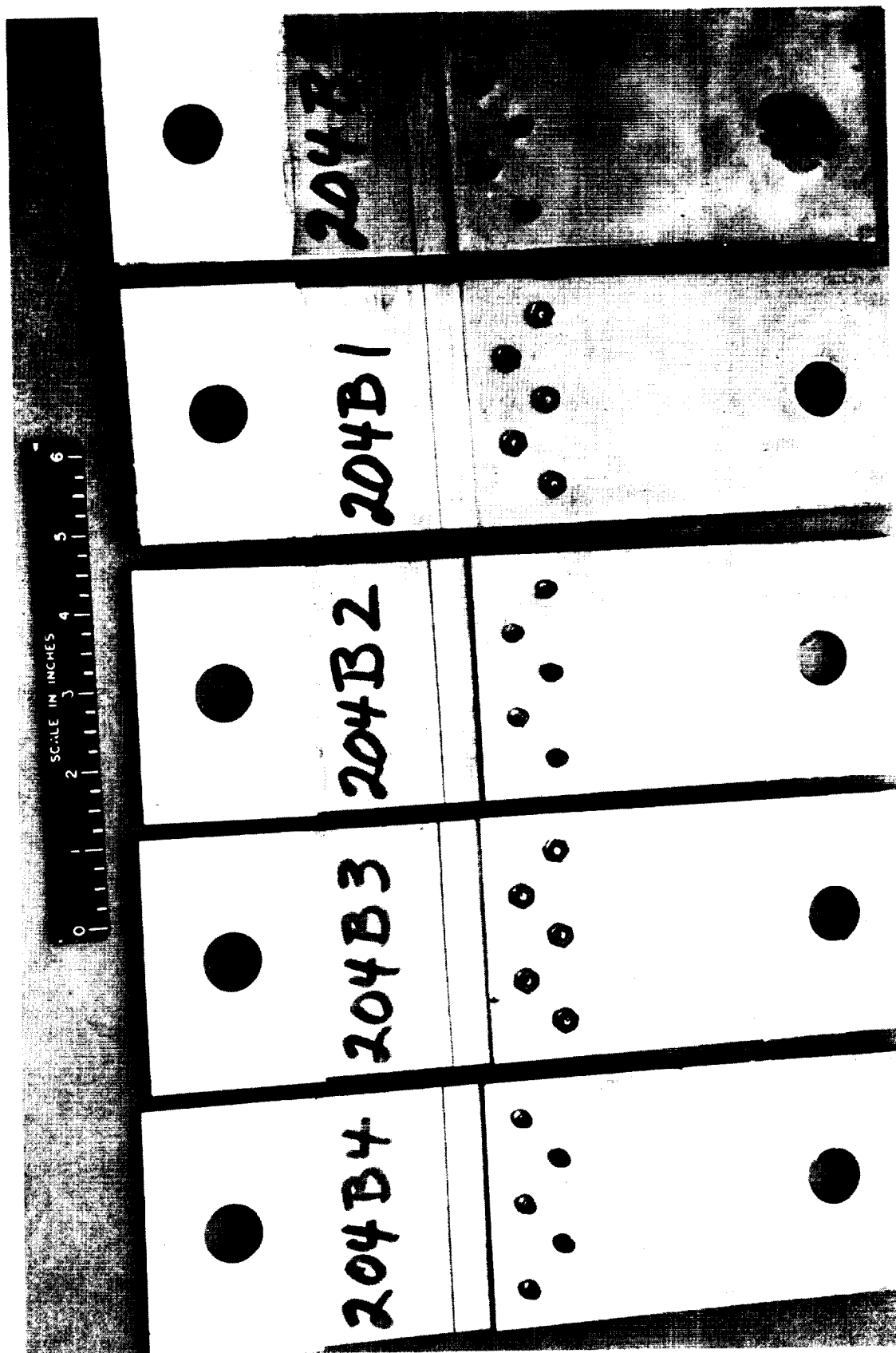
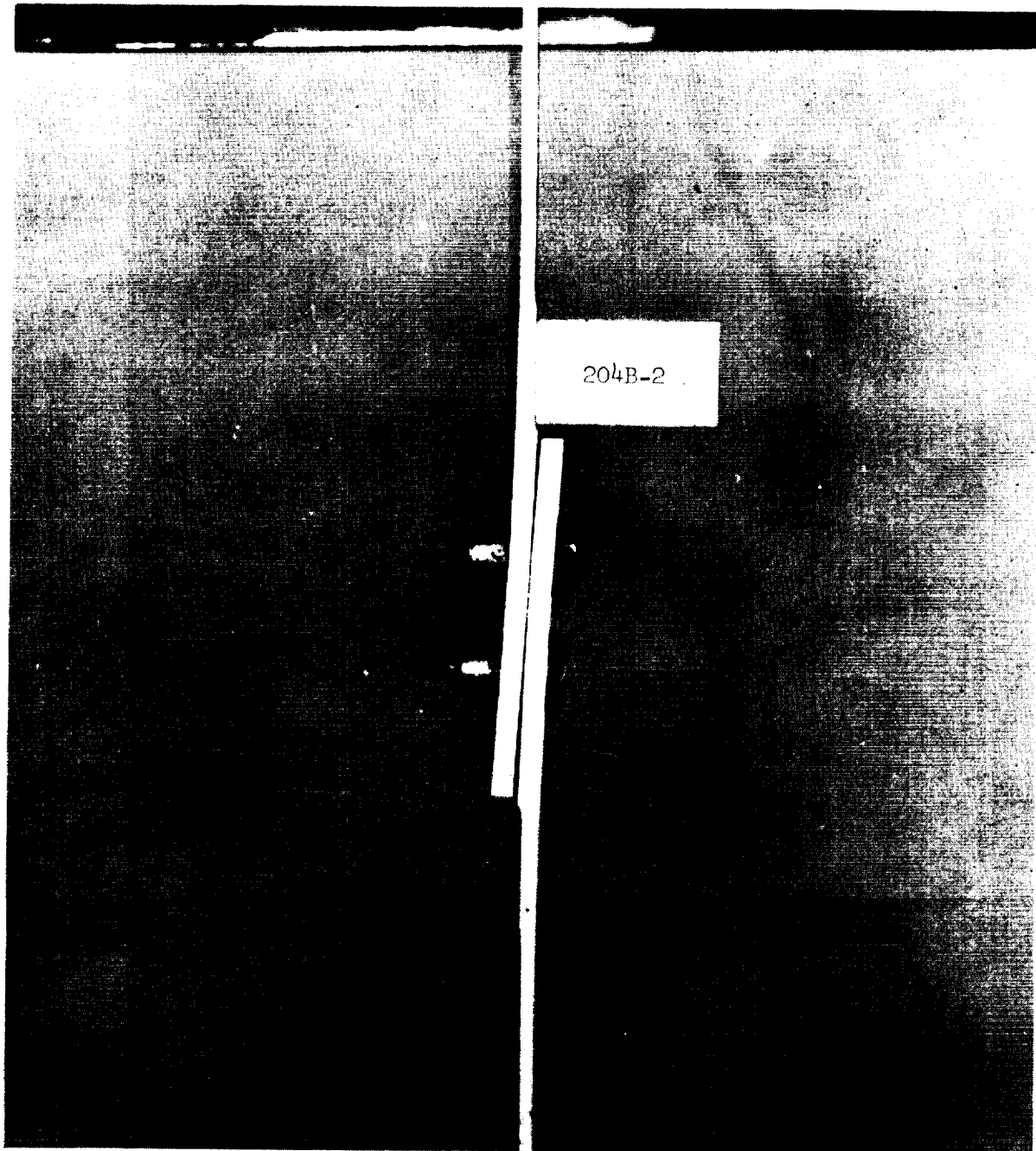


FIGURE 94. TYPE IVB SPECIMENS - JO-BOLT FASTENERS



Fastener: NAS 1671-3 Jo-bolt  
Material: .090"/.075"/.060" Beryllium  
Picture taken at 9,025 lbs.  
Failure occurred at 10,825 lbs.  
Maximum Load - IVB Series: 10,825 lbs.

FIGURE 95. TYPE IVB SPECIMEN - TENSILE TEST

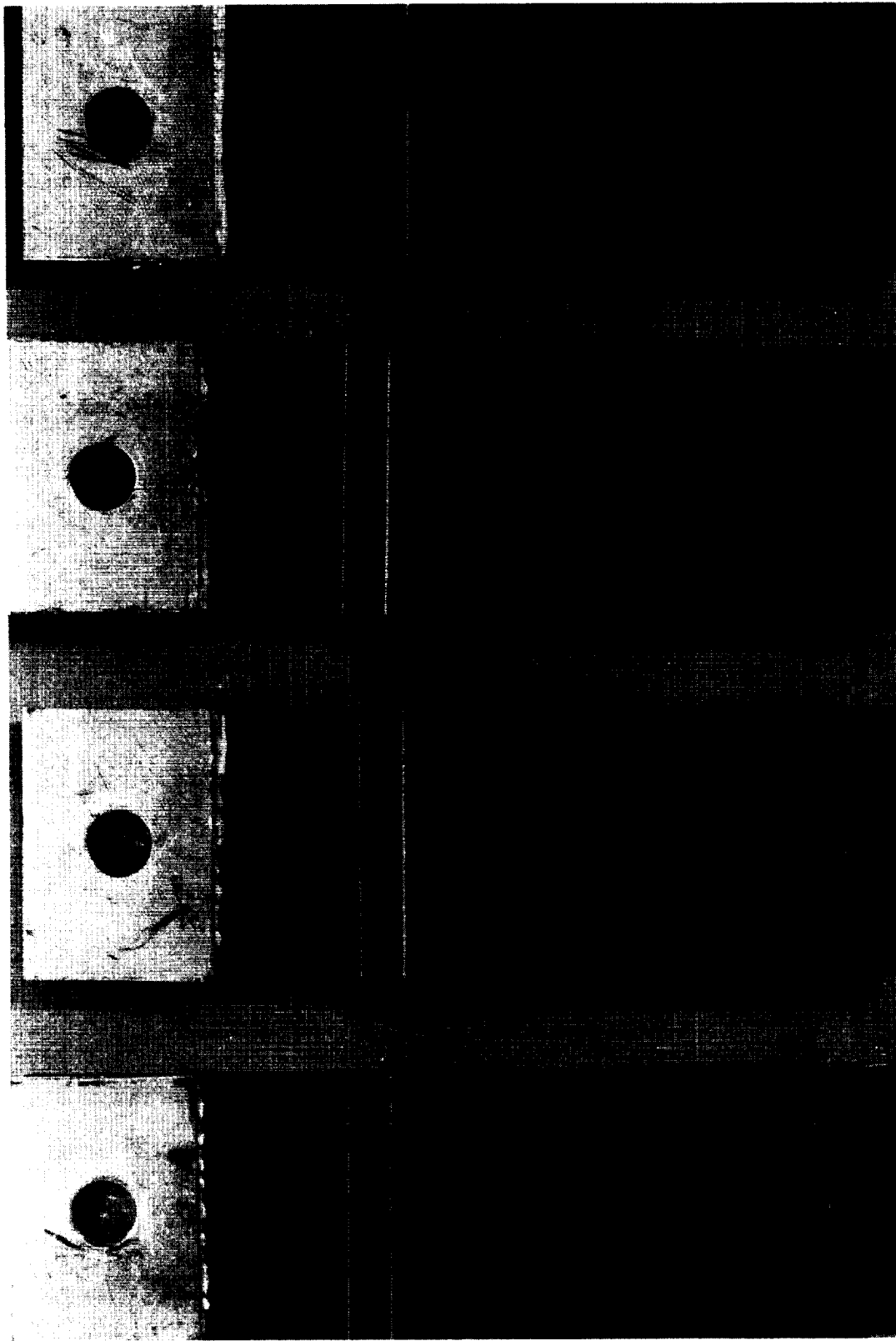


FIGURE 96. TYPE IVB SPECIMENS - TYPICAL FAILURE MODE

resulted in the failure of the joints in net tension in the beryllium material, with crack propagation extending, with one exception (204B-4), through the 0.075-inch "step" into the basic 0.060-inch material.

Contrary to the results anticipated from the previous comparison of the results of the tests of the Type IIIA and IVA specimens, there appears to be little difference in the strengths of the two types of specimens in spite of the greater eccentricity of the joint in the Type IVB specimens.

c. Type IVC - Cherry Blind Rivets. With the exception of one specimen (204C-2) in which the failure of the rivets to "pull-up" tightly resulted in a small gap between the joint faying surfaces, the assembly of the Type IVC specimens was accomplished without incident. The completed Type IVC specimens, ready for testing, are illustrated in Figure 97.

Figure 98 illustrates the testing of a typical Type IVC specimen in the "Instron" tensile testing machine at a constant cross-head travel rate of 0.05 inch per minute and an average loading rate of 3300 pounds per minute. The typical bending of the material, "tilting" of the fasteners and the separation of the segments in the joint area are clearly visible in the illustration.

The failure mode of the Type IVC specimens was very similar to that exhibited by the Type IIIC specimens. As illustrated in Figures 99 and 100, the failure of the specimens was due to the failure of the rivets. With the exception of the rivets in specimen 204C-2, all of the rivets failed in shear at the joint interface. In all cases, some deformation of the rivet holes is visible. The occurrence of some rivet slippage and yield in the joint just prior to failure, is revealed by the automatically recorded load-deflection curve for specimen 204C-2, illustrated in Figure 101. The reversal of the load just prior to the failure of the joint, but after the maximum load had been reached, indicated this slippage.

The comparison of the results of the tensile tests of the Type IIC and Type IVC specimens indicated little difference in the strengths of the two joint configurations. This consistency of results may be anticipated, as the limiting factor in both cases is the shear strength of the rivets, not the ultimate strength

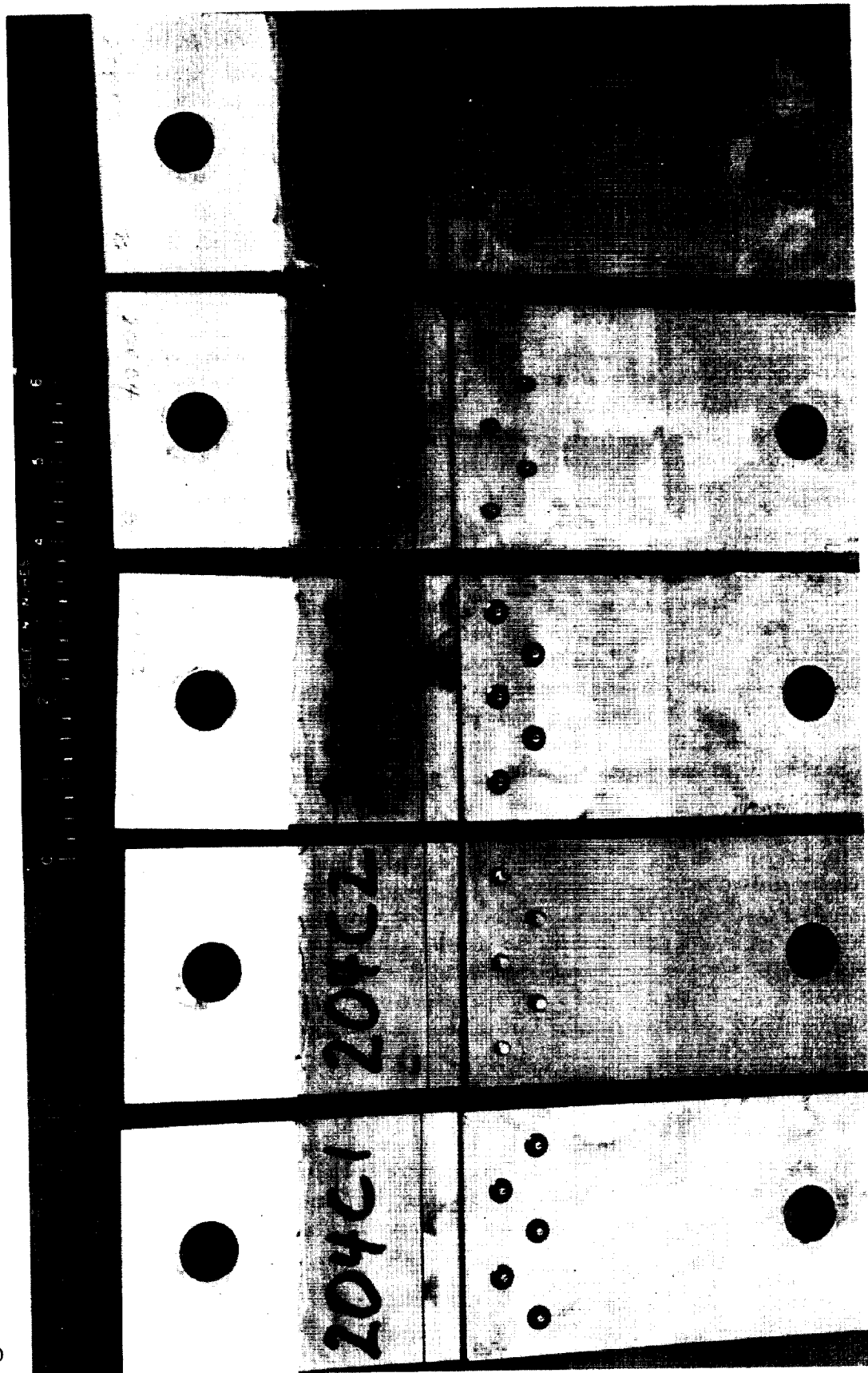
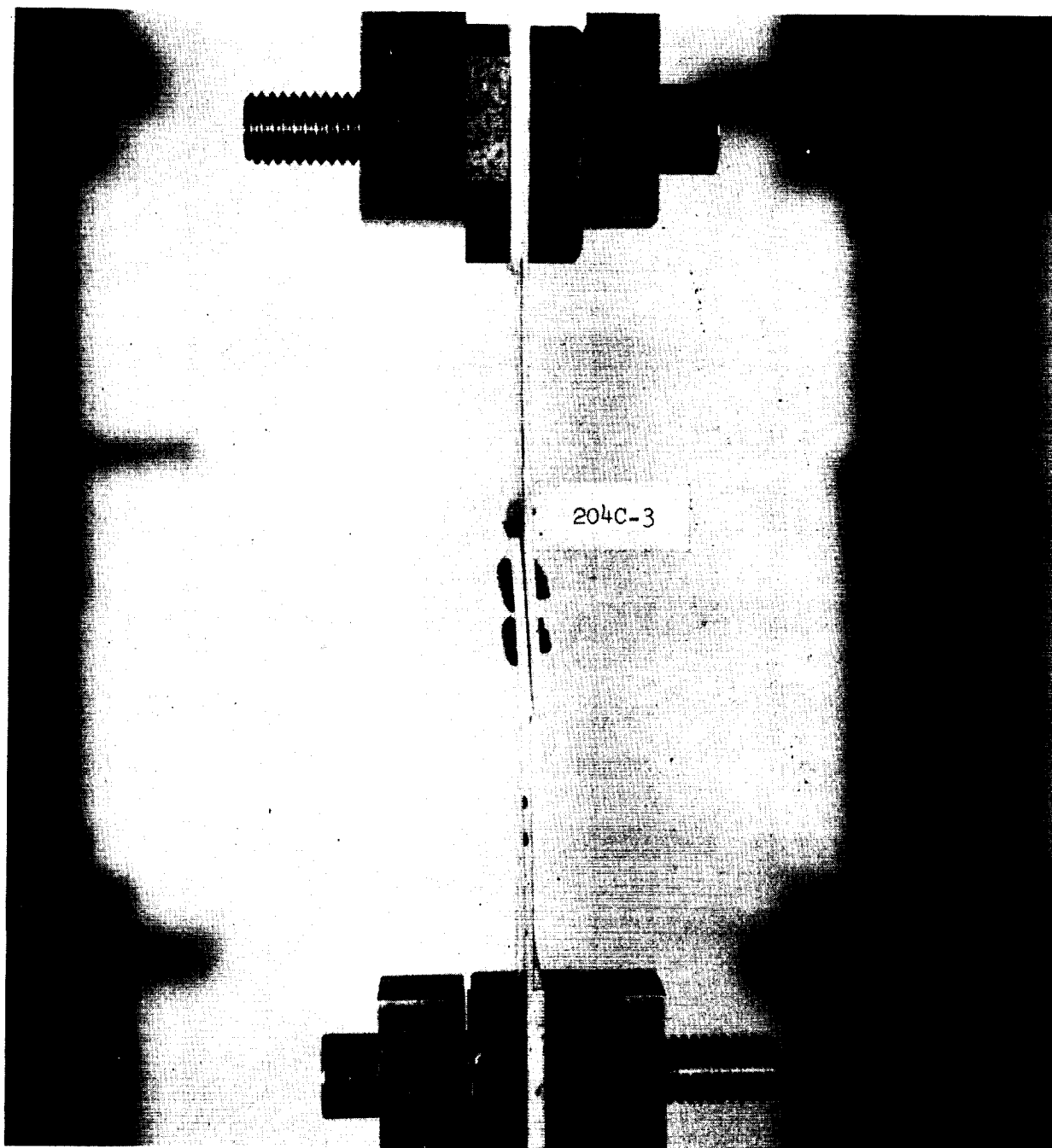


FIGURE 97. TYPE IVC SPECIMENS - CHERRY BLIND RIVETS





Fastener: MS 20600-M5 Cherry Blind Rivet  
Material: .090"/.075"/.060" Beryllium  
Picture taken at 5800 lbs.  
Failure occurred at 6000 lbs.  
Maximum Load - IVC Series: 6280 lbs.

FIGURE 98. TYPE IVC SPECIMEN - TENSILE TEST

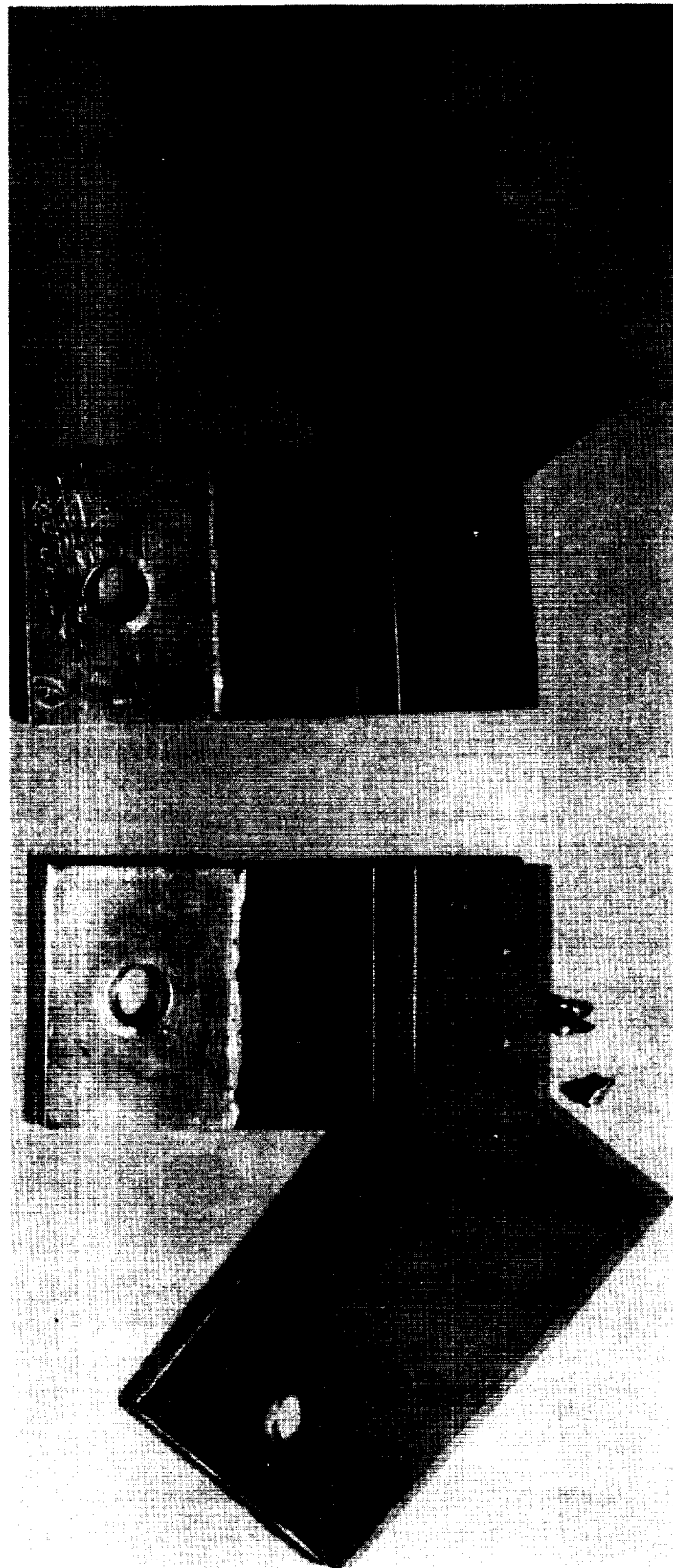


FIGURE 99. TYPE IVC SPECIMENS - TYPICAL FAILURE MODE

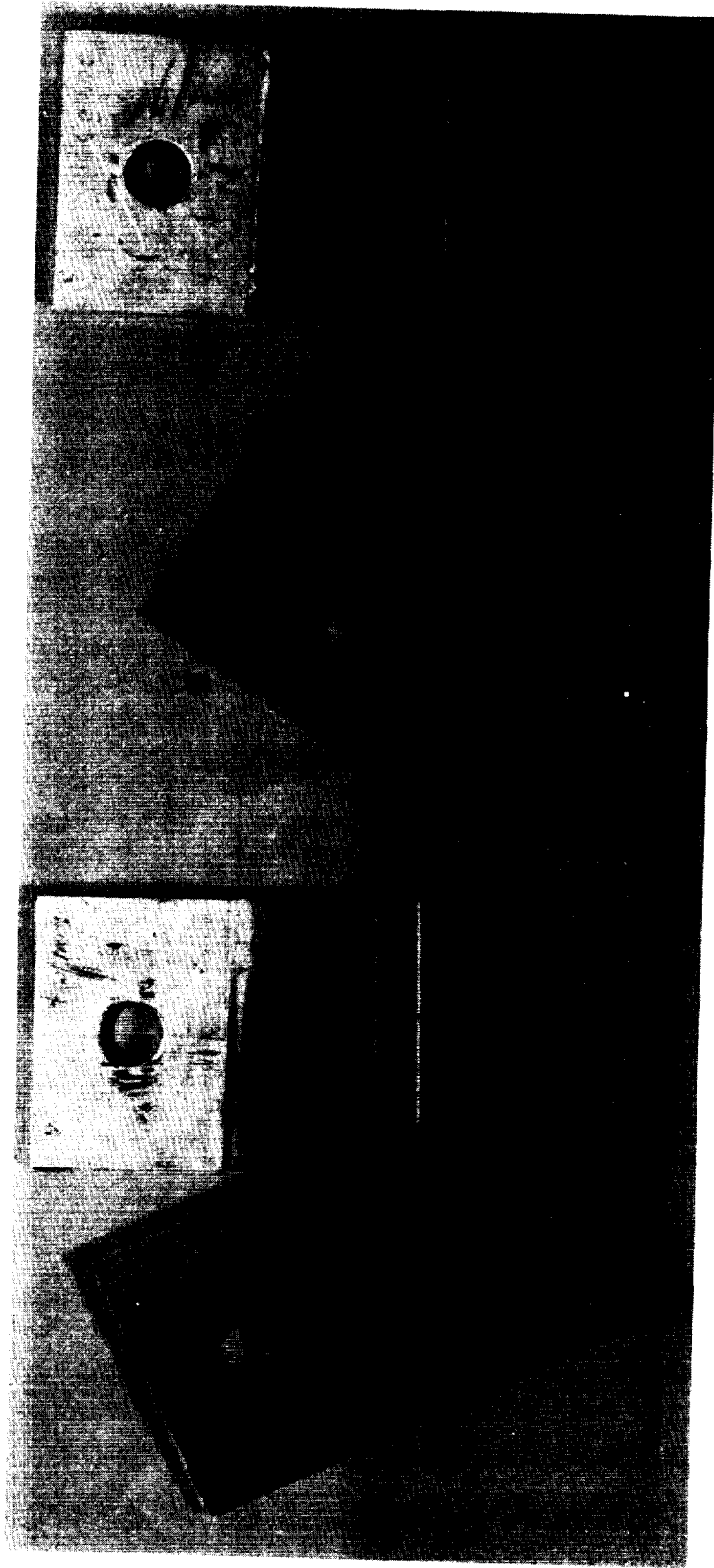


FIGURE 100. TYPE IVC SPECIMENS - TYPICAL FAILURE MODE

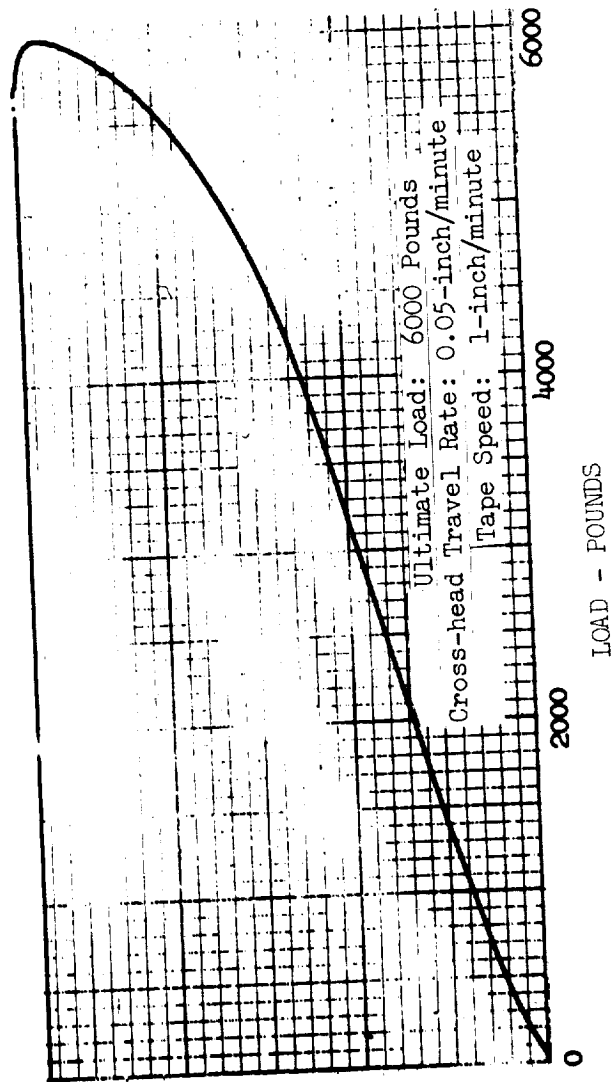


FIGURE 101. TYPE IVC LOAD-DEFLECTION CURVE - SPECIMEN 204C-3.  
 NOTE LOAD REVERSAL.

of the beryllium material. The comparison of the results of the tensile tests of these Type IVC specimens and of the Type IIC specimens (Reference Table VII), again substantiates the advantage of the "stepped" joint configuration.

d. Type IVD - Beryllium Rivets. The objectives of this investigation was the evaluation of the feasibility of joining eccentric beryllium structures with double-flush countersunk rivets. The assembly of the Type IVD specimens utilizing the "hot forging" procedure discussed in the section on the Type IIID Specimens, was accomplished without incident. Following the "forging" of the rivets, a surface grinder was used to grind the rivet heads, on two of the specimens, as nearly flush with the surface as the slight "bowing" of the material permitted. The rivet heads on the remaining three specimens were not ground or otherwise altered subsequent to the forging operation. The completed Type IVD "as forged" and "ground" specimens ready for testing, are illustrated in Figures 102 and 103, respectively. Visual examination of a close-up of the two "ground" specimens, illustrated in Figure 104, clearly reveals the complete filling of the countersunk holes. The shadow cast by the incompletely flush ground heads should not be mistaken for incomplete filling of the countersunk holes.

Figure 105 illustrates the testing of one of the specimens in the "Instron" tensile testing machine at an average loading rate of 3300 pounds per minute. Due to the decreased loads reached during the testing of these specimens, very little bending of the material or separation of the joint surfaces occurred.

As illustrated in Figure 106, the rivets in all of the specimens failed in shear at the joint interface. In addition, the secondary failure in the beryllium material that occurred during the testing of specimen 204D-5 was believed due to slightly uneven distribution of the load and progressive rather than simultaneous failure of the rivets.

Contrary to the results anticipated from the results obtained during the testing of the Type IIID specimens, there was little difference in the strengths of the two Type IVD joint configurations, i.e., the "flush ground" and the "as forged" specimens appear to be equally strong. Furthermore, in spite of the greater eccentricity of the Type IVD joints, these results

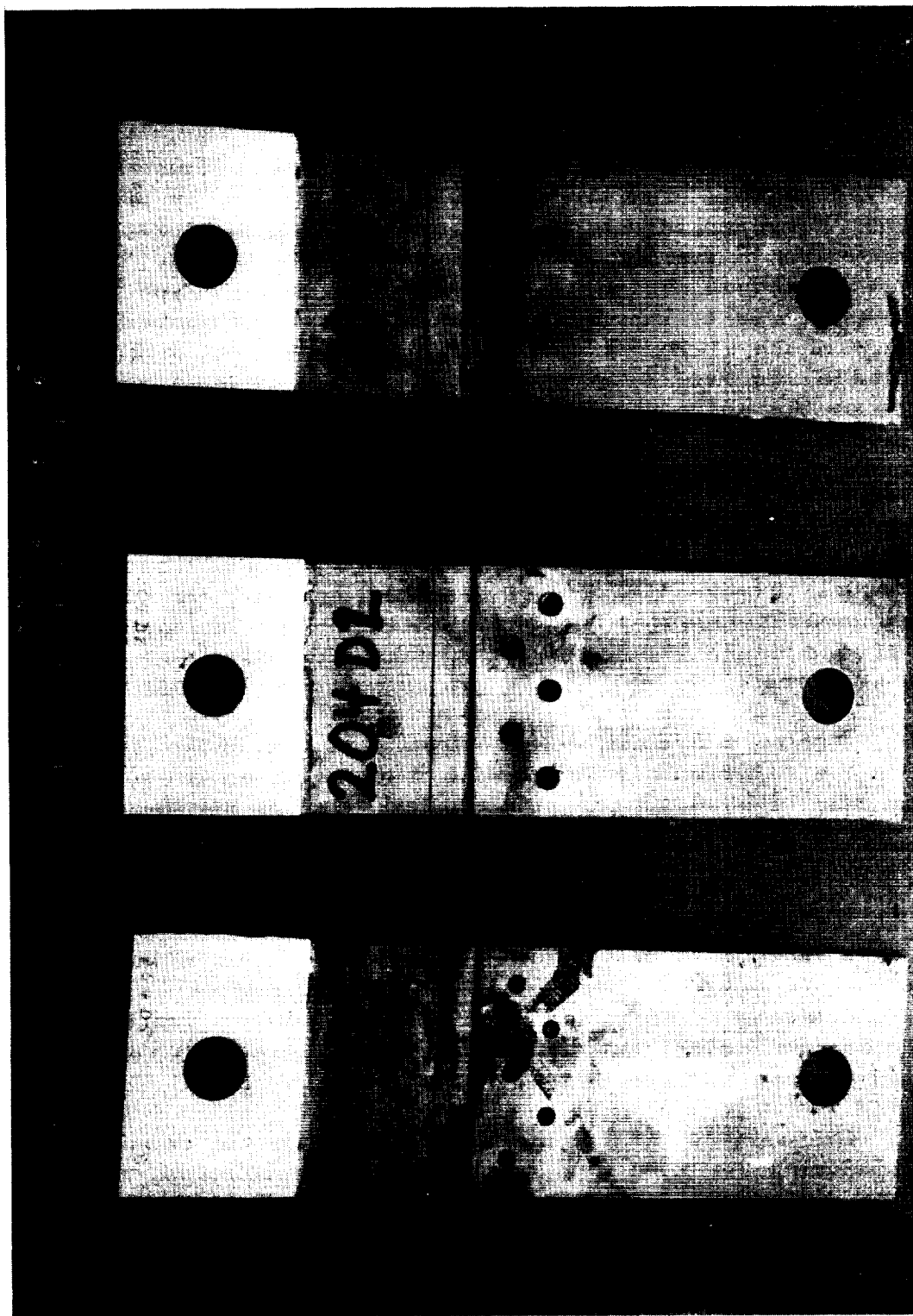


FIGURE 102. TYPE IVD SPECIMENS - COUNTERSUNK BERYLLIUM RIVETS  
"AS FORCED" RIVET HEADS

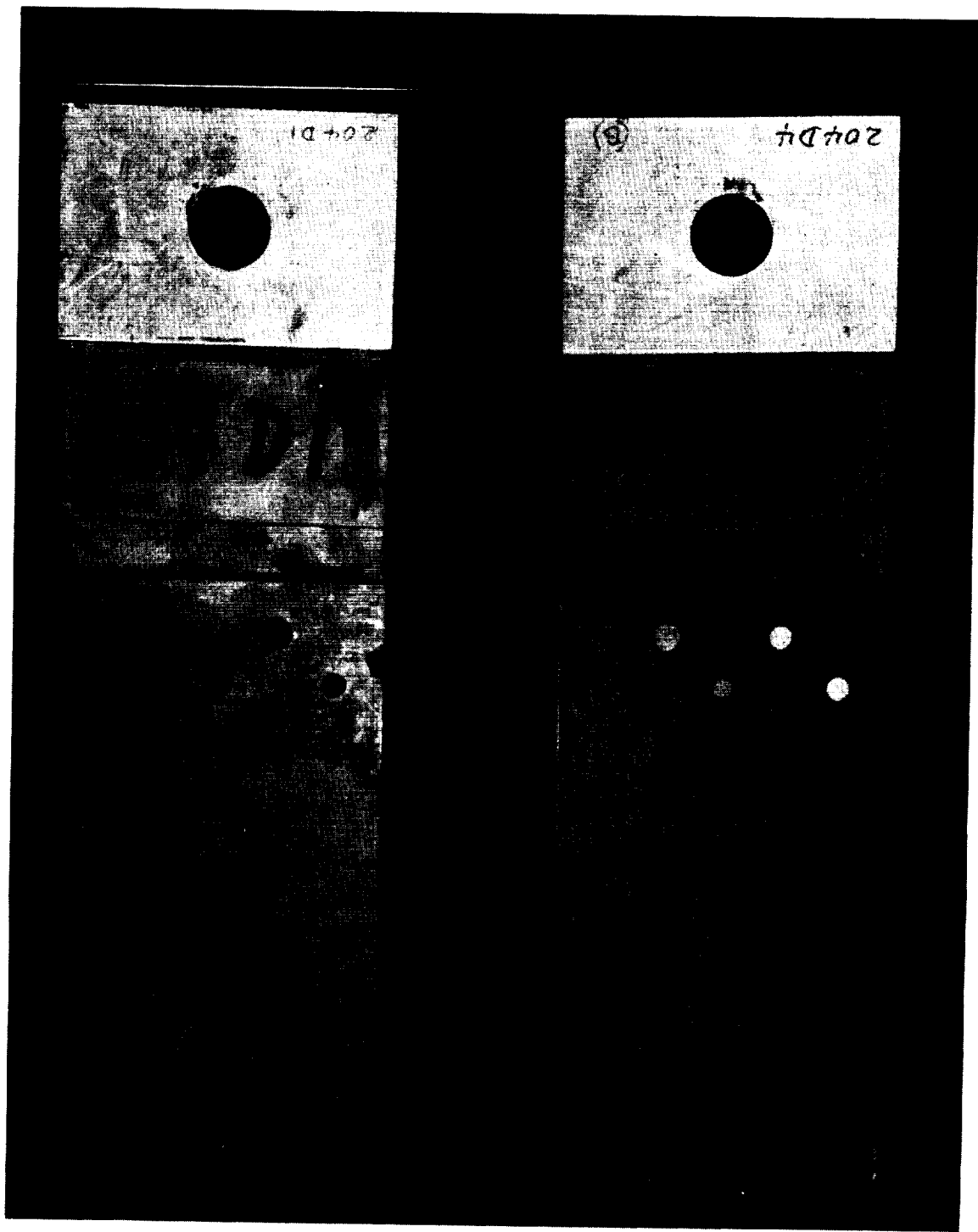


FIGURE 103. TYPE IVD SPECIMENS - COUNTERSUNK BERYLLIUM RIVETS,  
RIVETS GROUND FLUSH ON BOTH SIDES.

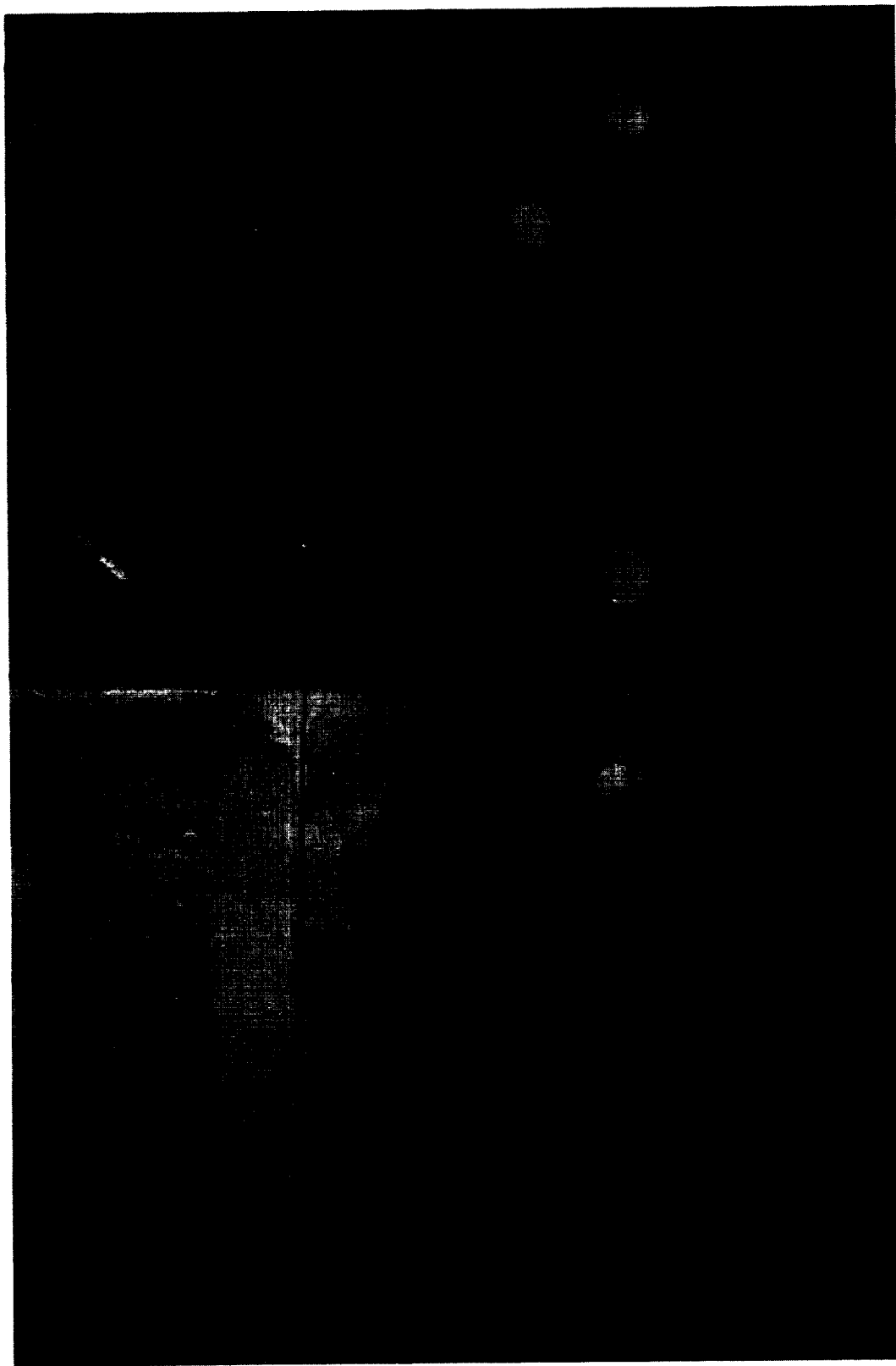
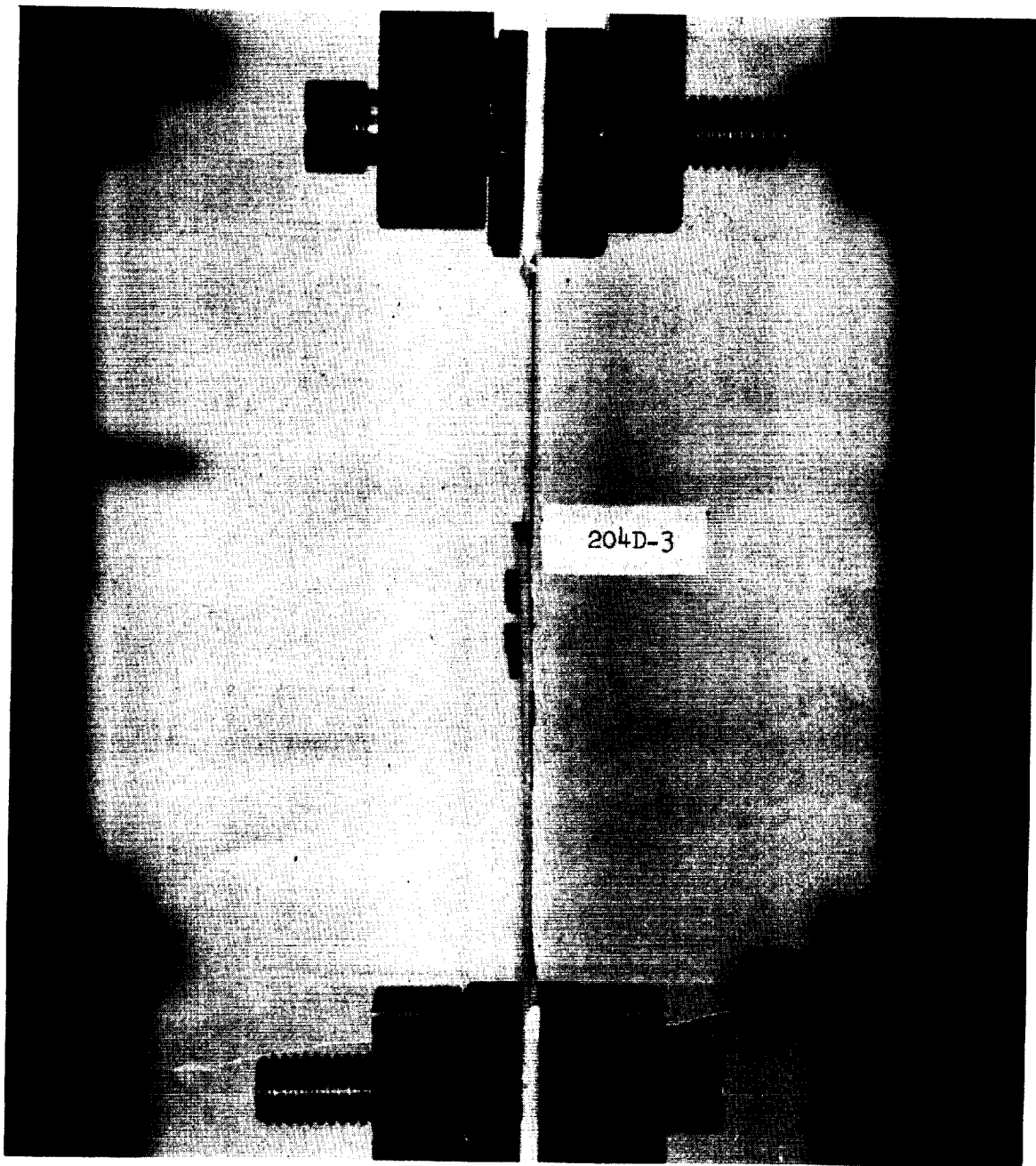


FIGURE 104. TYPE IVD SPECIMENS - COUNTERSUNK BERYLLIUM RIVETS.  
CLOSE-UP OF FLUSH GROUND RIVETS.





Fastener: "As Forged" Double Countersunk Beryllium Rivet  
Material: .090"/.075"/.060" Beryllium  
Picture taken at 3250 lbs.  
Failure occurred at 4140 lbs.  
Maximum Load - IVD Series: 4250 lbs.

FIGURE 105. TYPE IVD SPECIMEN - "AS FORGED" BERYLLIUM RIVETS -  
TENSILE TEST

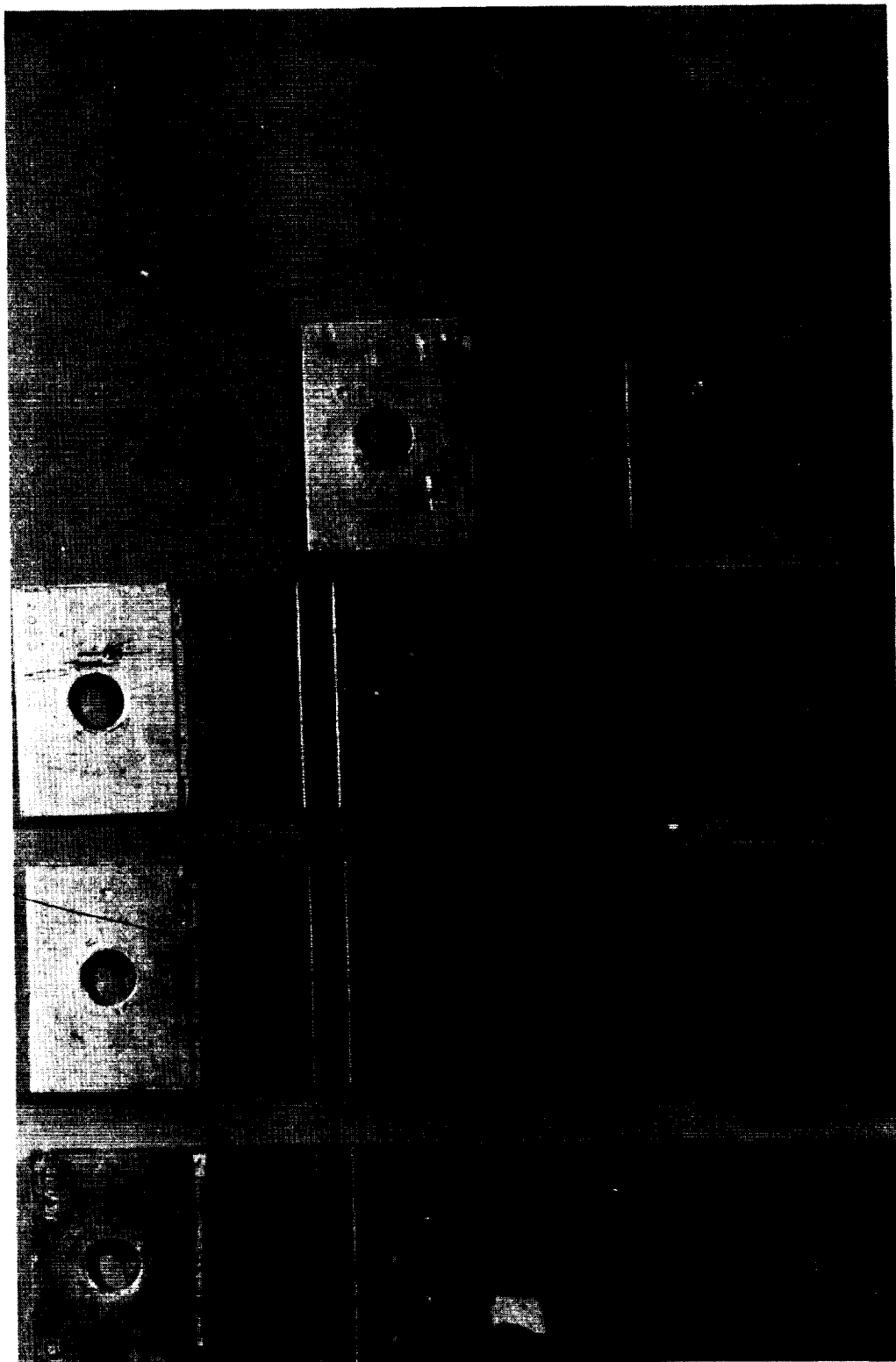


FIGURE 106. TYPE IVD SPECIMENS - TYPICAL FAILURE MODE

also were very comparable with those obtained during the testing of the Type IIID specimens. The reason for this consistency of results is unknown.

Visual inspection of a representative, autographically recorded load-deflection curve for an "as forged" specimen, 204D-3, illustrated in Figure 107, clearly reveals the lack of any indication of yield; the trace is nearly linear.

7. Mechanical Fasteners - Conclusions. The results of this evaluation indicate that all of the investigated mechanical fastening methods are feasible, that high efficiency mechanical joints can be fabricated on a routine production basis, and that large beryllium structures can be successfully assembled. The results of these investigations indicate the following conclusions:

1. Beryllium structures can be successfully assembled with high-strength fasteners, such as Huckbolts and Jo-bolts, which subject the material to an appreciable shock load during installation.
2. The configuration of the holes in which conventional fasteners, such as bolts and screws, will be installed must incorporate suitable edge clearance for the head-shank radius of the fastener to avoid a high local stress concentration. During this program, a micrometer stop 45 degree countersink was used to chamfer these holes.
3. The results of the limited investigation clearly indicated the lack of any advantage accruing from the incorporation of adhesive bonding in a mechanically fastened joint. Further development may result in improved joint characteristics.
4. The efficiency of joints assembled with either beryllium or "Lockalloy" rivets is comparable to that exhibited by joints assembled with other high-strength rivets.
5. Prior to the assembly of the joints, all holes must be etched to remove any micro-cracks, delaminations, or other surface defects.
6. A minimum radial clearance must be provided between the fastener and the hole wall.

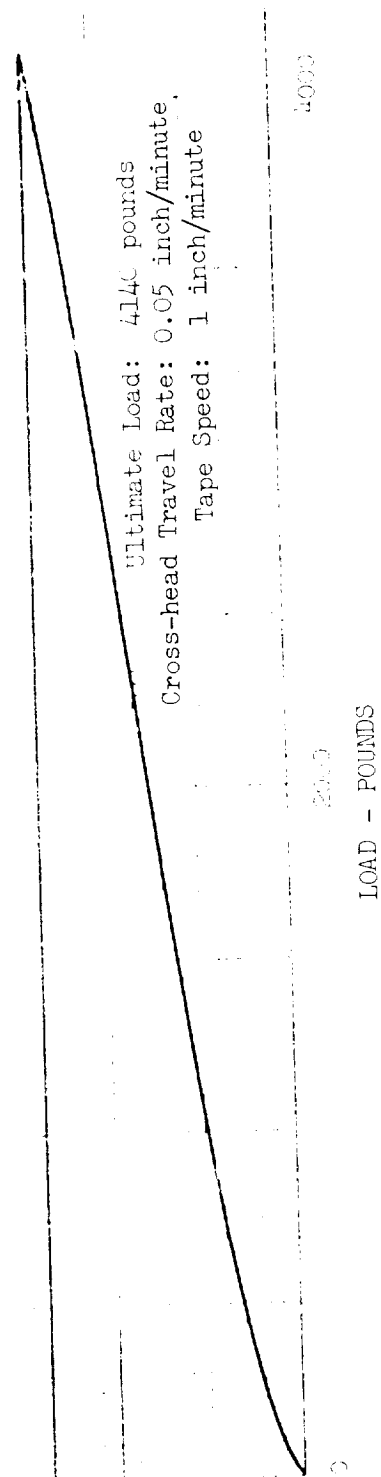


FIGURE 107. TYPE IVD LOAD-DEFLECTION CURVE - SPECIMEN 204D-3.  
 NOTE LACK OF YIELD INDICATION.

7. An interference fit between the fastener and the hole cannot be tolerated.

8. Eccentricity in the joint area has an extremely deleterious effect on joint efficiency, and should be avoided or minimized.

9. The staggered double row fastener configuration is approximately 50 percent more efficient than the single row configuration.

10. In order to avoid possible fractures due to hoop stresses, expanding types of rivets should not be used to join beryllium components less than 0.060-inch thick.

11. The designer must consider and balance the fastener shear strength, the beryllium bearing strength, and the beryllium net tensile strength in his designs to attain the maximum joint efficiency.

12. Suitable forging temperatures for the installation of beryllium and "Lockalloy" rivets appear to be 1350°F and 1000°F respectively.

## B. ADHESIVE BONDING

1. Introduction. The use of adhesive bonding as a means for joining beryllium components permits the exploitation of the excellent properties exhibited by the material, and simultaneously minimizes the inherent problems of the high notch sensitivity and low ductility. In addition, stress concentrations due to joint discontinuities, drilled holes, etc., are eliminated; this results in definite advantages for both "Design" and "Production." Furthermore, adhesive bonding may be the only practical joining method for the assembly of many types of structures, such as honeycomb panels, which incorporate very thin materials.

The several adhesives, selected for this study and used in assembling the test specimens, included both low and high temperature cure types. Table XII presents the cure cycles and shear strengths of the selected adhesives.

TABLE XII  
CURE CYCLES AND SHEAR STRENGTHS - SELECTED ADHESIVES  
VENDOR DATA

Adhesive	Vendor	Cure Cycle (1)		Shear Strength PSI (3)
		Time Hours	Temp. °F	
NARMCO 7343/7139	Narmco Material Division Whitaker Corporation Costa Mesa, Calif.	1.0	290	1600
BR-90	Bloomingdale Department American Cyanamid Co. Havre de Grace, Md.	16.0	130	5100-5600
Epon VI	Shell Chemical Company 110 West 51st Street New York, N. Y.	0.75	200	3800
FM-1000	Bloomingdale Department American Cyanamid Co. Havre de Grace, Md.	1.0	350	7000
Imidite-850	Narmco Materials Division Whitaker Corporation Costa Mesa, Calif.	1.0 1.0 6.0	430 650 750 (2)	3000
Narmco 402	Narmco Materials Division Whitaker Corporation Costa Mesa, Calif.	1.0	350	4600

**NOTES:**

- (1) VENDOR RECOMMENDATIONS FOR ALUMINUM
- (2) SEQUENTIAL CYCLE: FINAL CURE IN ARGON ATMOSPHERE
- (3) VENDOR CERTIFIED PROPERTIES FOR ALUMINUM

Due to the inherent eccentric loading, the single lap shear specimen was not considered to be suitable for this investigation. The bending moment produced in the metal not only tends to cause joint failure due to peeling action, but also precludes the development of the full tensile strength of the beryllium segments and the accurate determination of the bond efficiency. Therefore, the double lap shear type of joint was selected for this investigation.

The cleaning materials and techniques used during the preparation of the surface for bonding must be compatible with bonding agent to be used. If incompatible, minute traces of the cleaning agent in the surface of the material may vaporize or out-gas during high temperature curing cycles and inhibit the proper curing of the bonding material. Although every precaution is taken to insure the removal of all residue, the possibility of microscopic entrapment in the pores of the beryllium must be considered. Therefore, the utilization of a "neutral" or "bond compatible" cleaning process is required. A procedure found to be suitable for the cleaning of beryllium in preparation for bonding is included.

In order to obtain representative comparative data, a set of five test specimens was fabricated for each of the four material gages and six adhesives. A 60,000-pound capacity "Riehle" tensile testing machine was used for testing the joints at a constant loading rate of 600 pounds per minute in accordance with the requirements of Federal Specification No. 175; Method 1033.

Table XIII presents the chemical analyses and mechanical properties of the material procured from The Brush Beryllium Company and The Beryllium Corporation for the fabrication, testing, and evaluation of the adhesive bonded joints. The configuration and nominal dimensions of the "205" adhesive bonded joints are illustrated in Figure 108. A summary of the modes of failure is presented in Table XIV, and a summary of the test results and bond strengths is presented in Figure 109.

2. Specimen Preparation. Current standard production procedures were utilized for the production of the test specimen components. All of the segments were identified during the initial layout on full-size vellum sheets and this identification was maintained throughout the program. The layout, including the identifying numbers,

TABLE XIII  
CHEMICAL ANALYSES AND MECHANICAL PROPERTIES - MATERIAL FOR ADHESIVE BONDED SPECIMENS

Vendor Data

Vendor: The Beryllium Corporation and The Brush Beryllium Company

CHEMICAL ANALYSIS - %

Vendor	Lot No.	Be Assay	BeO	Fe	Si	Al	Mg	C
Brush	2469	98.50	1.83	0.12	0.03	0.008	0.009	0.10
Brush	3516	98.21	1.70	0.14	0.04	0.11	0.008	0.13
Brush	9967	99.29	1.66	0.138	0.05	0.095	0.011	0.12
Brush	1942	98.50	1.81	0.13	0.04	0.090	0.010	0.11
Beryllco	397D	98.22	1.91	0.134	0.05	0.083	0.027	0.10

NOTE: Cr, Mn, Ni LESS THAN 0.04% EACH

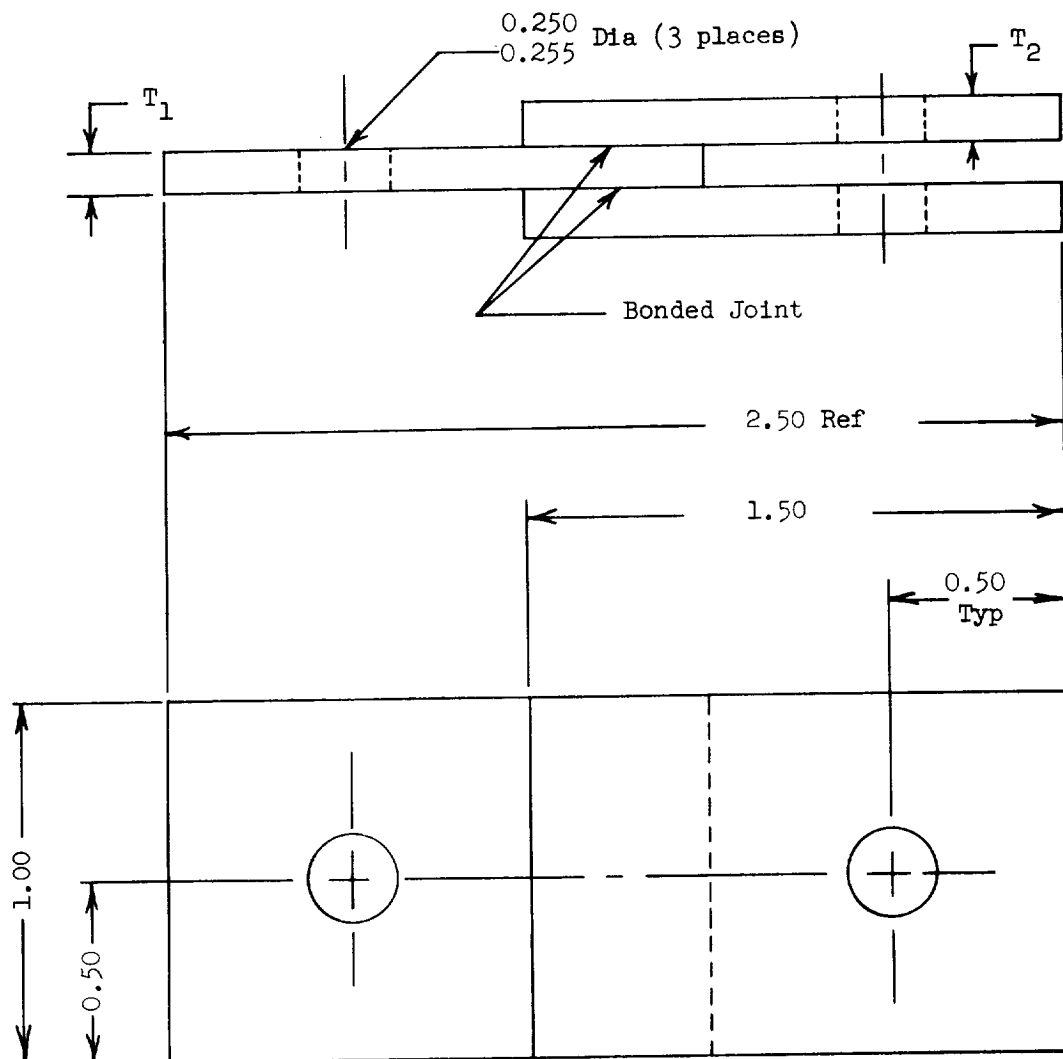


TABLE XIII (Cont.)

## MECHANICAL PROPERTIES

Vendor	Gage Inch	Lot No.	Sheet No.	Test Direction	Fty PSI	Ftu PSI	Elongation % in 1"
(1)	.020" / .030"	--	--	--	--	--	--
Brush	.060	9967	447B	L T	57,400 58,100	78,300 86,200	11.5 14.0
Brush	.060	1942	540A	L T	56,700 59,800	83,000 84,700	9.8 12.3
Brush	.060	2469	734	L T	51,300 50,300	79,700 70,000	16.5 6.5
Berylco	.060	397D	HR31-3	L T	51,200 53,000	70,600 78,400	8.0 21.0
Berylco	.060	397D	HR33-1	L T	52,700 56,600	70,400 76,900	23.0 33.0
Brush	.120	3516	1064A1	L T	63,300 60,400	85,000 82,100	16.0 18.0
Brush	.120	3516	1064A2	L T	63,300 60,400	85,000 82,100	16.0 18.0
Brush	.120	3516	1065A1	L T	61,400 60,300	81,100 82,100	10.0 18.0
Brush	.120	3516	1065B1	L T	62,200 59,700	84,600 80,300	16 15
Brush	.120	3516	1066A1	L T	60,900 58,400	84,600 80,000	18 10
Brush	.120	3516	1066A2	L T	60,900 58,400	84,600 80,000	18 10

NOTE: (1) CHEMICALLY MILLED AND CUT FROM 0.07-INCH RANDOM AVAILABLE MATERIAL. CHEMICAL ANALYSES AND CERTIFIED PROPERTIES ARE NOT AVAILABLE.



Material Gage	
T <sub>1</sub>	T <sub>2</sub>
0.020	0.020
0.030	0.030
0.060	0.060
0.120	0.120

Figure 108. Adhesive Bonded Joint Configuration - Nominal Dimensions

TABLE XIV  
Adhesive Bonded Specimens - Failure Modes

Gage	ADHESIVE TYPE AND FAILURE MODE					
	Low Temperature Cure			High Temperature Cure		
	NARMCO 7343/7139	BR-90	EPON VI	FM-1000	Imidite 850	NARMCO 402
0.020	5-Cohesive	2-Tensile in metal 2-Double bearing 1-Handling before test	5-Tensile in metal	2-Tensile in metal 3-Single bearing	5-Bearing, single & double	5-Single bearing
0.030	5-Cohesive	3-Cohesive 2-Tensile in metal	3-Tensile in metal 2-Double bearing	1-Tension 4-Adhesive (surfaces apparently contaminated)	3-Double bearing 1-Tensile in metal 1-Handling before test	2-Cohesive 2-Tensile in metal 1-Double bearing
0.060	5-Cohesive	3-Cohesive 1-Tensile in metal 1-Single bearing	4-Cohesive 1-Double bearing	1-Cohesive 2-Tension 1-Double bearing 1-Single bearing	5-Cohesive, coincident with bearing or tensile	5-Double bearing
0.120	5-Cohesive	4-Cohesive 1-Single bearing	5-Cohesive	2-Cohesive 2-Single bearing 1-Tensile in metal	3-Cohesive in single lap shear 2-Handling before test	3-Cohesive 2-Single bearing

NOTE: COHESIVE FAILURE - WITHIN THE ADHESIVE MATERIAL ITSELF  
ADHESIVE FAILURE - AT THE ADHESIVE-BERYLLIUM INTERFACE

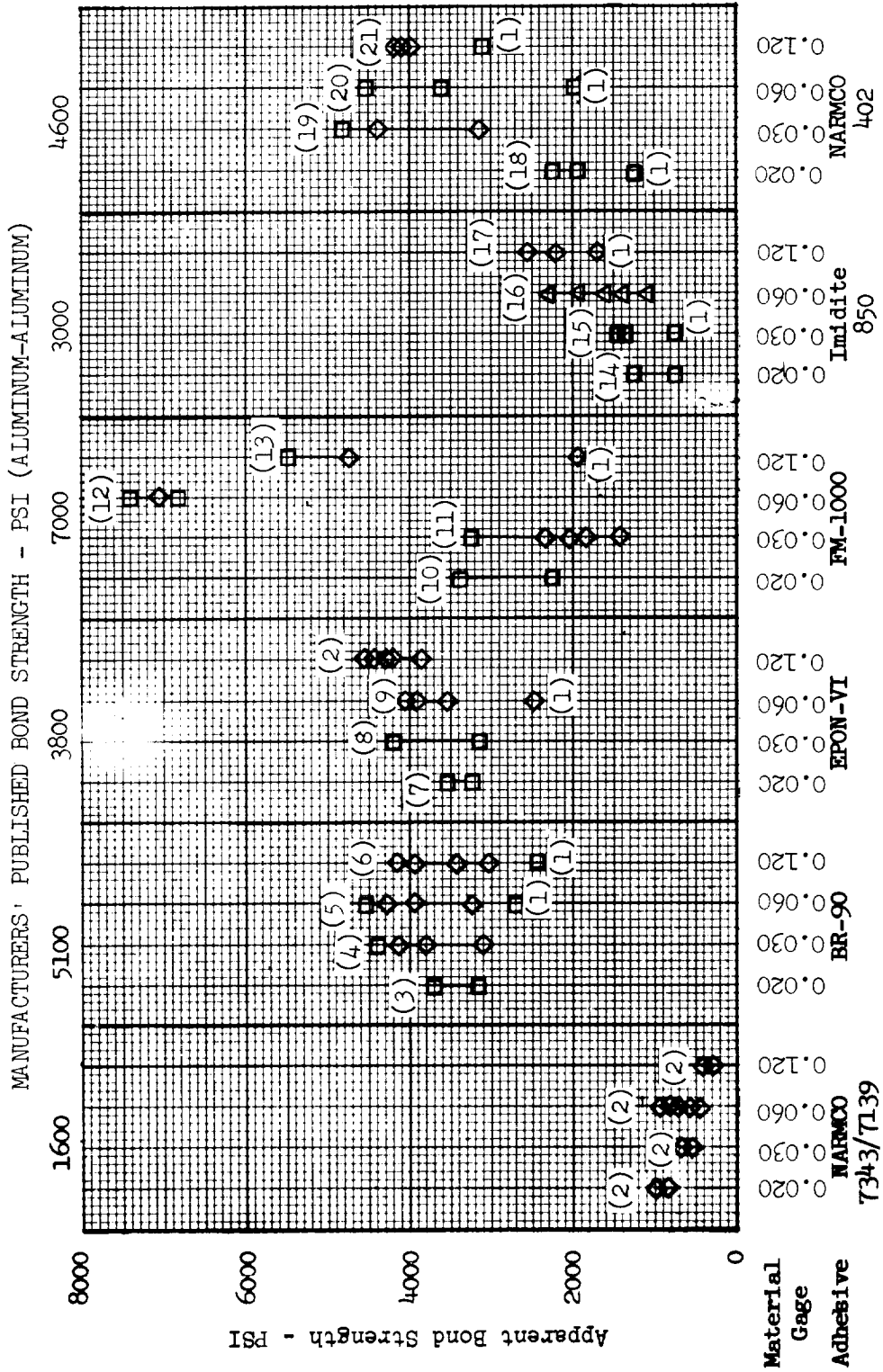


FIGURE 109. ADHESIVE BONDED JOINTS - TEST SUMMARY

## FIGURE 109 NOTES

◇ Adhesive material failures - no beryllium failure.

□ Beryllium failure - no adhesive failure.

△ Coincidental failure - adhesive and beryllium.

### FAILURE MODES:

1. Excessively low - not considered to be within normal range.
2. Cohesive shear in all test specimens.
3. Net tension in Be segment (2) - Ave: 66,670 psi bearing at loading pin hole (2) - Ave: 127,300 psi fracture during assem. (1)
4. Cohesive shear (3)  
net tension in Be segment (2) - Ave: 54,350 psi
5. Cohesive shear (3)  
net tension in Be segment (1) at 55,800 psi  
bearing at loading pin (1) - 132,700 psi
6. Cohesive shear (4)  
bearing at loading pin (1) - 88,400 psi
7. Net tension in Be segment (5) - Ave: 70,360 psi
8. Net tension in Be segment (3) - Ave: 60,890 psi  
bearing at loading pin hole (2) - Ave: 127,650 psi
9. Cohesive shear (4)  
bearing at loading pin (1) at 118,350 psi
10. Net tension in Be segment (2) - Ave: 52,380 psi  
bearing at loading pin (3) - Ave: 217,600 psi

FIGURE 109 NOTES (Cont'd)

11. Net tension in Be segment (1) at 43,870 psi  
adhesive shear (4)
12. Cohesive shear (1)  
net tension in Be segment (2) - Ave: 67,240 psi  
bearing at loading pin (2) - Ave: 147,750 psi
13. Cohesive shear (2)  
net tension in Be segment (1) at 45,480 psi  
bearing at loading pin - (2) - Ave: 152,500 psi
14. Bearing at loading pin (5) - Ave: 108,700 psi
15. Bearing at loading pin (3) - Ave: 88,035 psi  
net tension in Be segment (1) at 24,500  
during assembly (1)
16. Cohesive shear with coincident failure of Be segments in  
net tension/bearing (5).
17. Cohesive shear (3)  
Fracture during assembly (2)
18. Bearing at loading pin hole (5) - Ave: 146,780 psi
19. Cohesive shear (2)  
net tension in Be segment (2) - Ave: 60,685 psi  
bearing at loading pin hole (1) at 86,450 psi
20. Bearing at loading pin hole (5) - Ave: 116,500 psi
21. Cohesive shear (3)  
bearing at loading pin hole (2) - Ave: 117,550 psi

was transferred to the sheet material, and the parts were cut to size on the precision abrasive cut-off saw. The 0.250-inch diameter loading pin holes then were "tornetically" drilled in a drill fixture which assured the proper alignment of the holes and the subsequent control of the load path during the testing operations. After the mechanical operations were completed, all of the beryllium parts were etched in a solution consisting of 3 percent HF (hydrofluoric acid) and 45 percent HNO<sub>3</sub> (nitric acid) to remove at least 0.002 inch of material from all surfaces. This etching is mandatory; all surface imperfections such as irregularities, micro-cracks, etc., must be removed to avoid compromising the integrity of the parts.

Several sets of 0.020-inch thick segments, ready for surface cleaning and bonding, are illustrated in Figure 110. Prior to the assembly of the specimens, all of the critical dimensions were measured and recorded for later use in the calculation of the stresses. The specimens then were cleaned, in preparation for bonding, in accordance with the following procedure, detailed as follows:

1. Vapor degrease in trichloroethylene vapor.
2. Immerse the parts for three minutes in a 7.5 percent (by weight) solution of "Pre-bond 700" (Bloomington Department, American Cyanamid Company, Havre de Grace, Maryland) and water at a controlled temperature of  $200 \pm 5^{\circ}\text{F}$  for 10 minutes.
3. Remove the part from the cleaning solution tank and wash in de-ionized water.
4. Dry the part in a forced-air drying oven, equipped with air filters, at a controlled temperature of  $290 \pm 5^{\circ}\text{F}$  for  $30 \pm 5$  minutes.

NOTE: Hot forced dry air, outside an oven, may be used if no oven is available, providing suitable precautions are observed to avoid recontamination

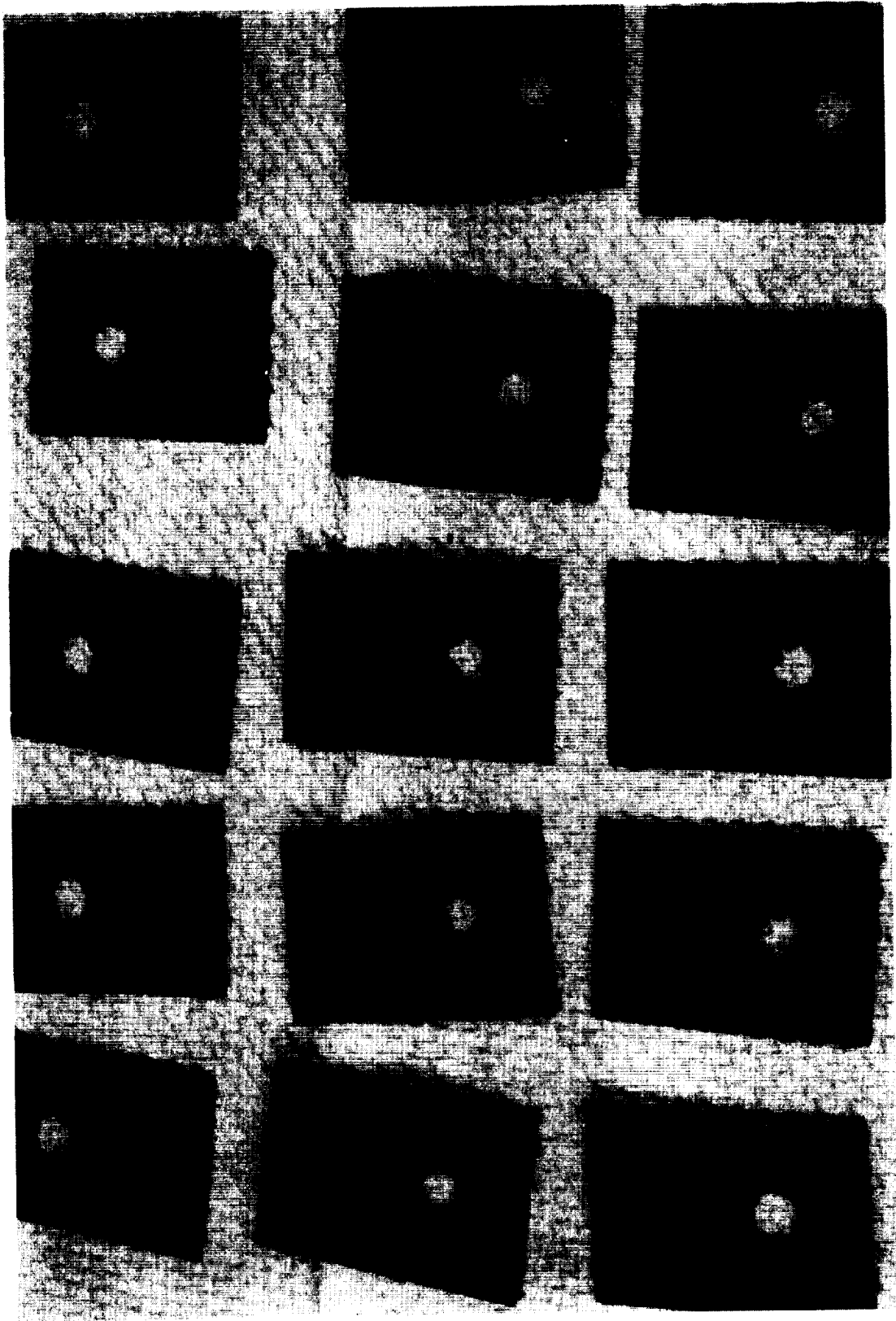


FIGURE 110. COMPLETED 0.020-INCH SEGMENTS - READY FOR CLEANING AND BONDING



of the part. The cleaned parts shall be handled only with clean dry gloves.

Following the completion of the cleaning operations, sets of specimens were assembled in a special assembly fixture consisting of a base and three sets of interchangeable shims. The selection of the desired thickness of shims permitted the assembly of all of the specimens with a minimum of tooling. The base and one of the shims are illustrated in Figure 111. It should be noted that all five specimens of a given thickness and selected adhesive may be bonded simultaneously. The use of this fixture also assured the proper alignment of the segments and the exact control of the joint overlap. The overlap at the bond line was varied from 0.200 inch to 0.500 inch, depending upon the thickness of the beryllium, to avoid exceeding the 70,000 psi ultimate strength of the material.

Prior to the assembly of each set of specimens, the fixture and the appropriate shims were treated lightly with a suitable bond release agent ("Release All," manufactured by the Release All Corporation, Fort Worth, Texas) to avoid the concurrent bonding of the specimens to the tooling. In addition, one adhesive, NARMCO 402, required the application of primer (NARMCO 402 Type II Primer) to the bond surface of the specimens prior to the application of the adhesive itself.

The sequential procedure for the assembly of the specimens, illustrated in Figures 112 through 115, is outlined as follows:

1. Place the proper shim and one segment of the double bearing end of the specimen in place on the base of the fixture as illustrated in Figure 112. Apply adhesive to the bond area.
2. Place the center segment of the specimen and the appropriate shim in place on the fixture as illustrated in Figure 113. The placement of this segment determines the overlap of the bond area. Apply adhesive to the bond area of the second segment.

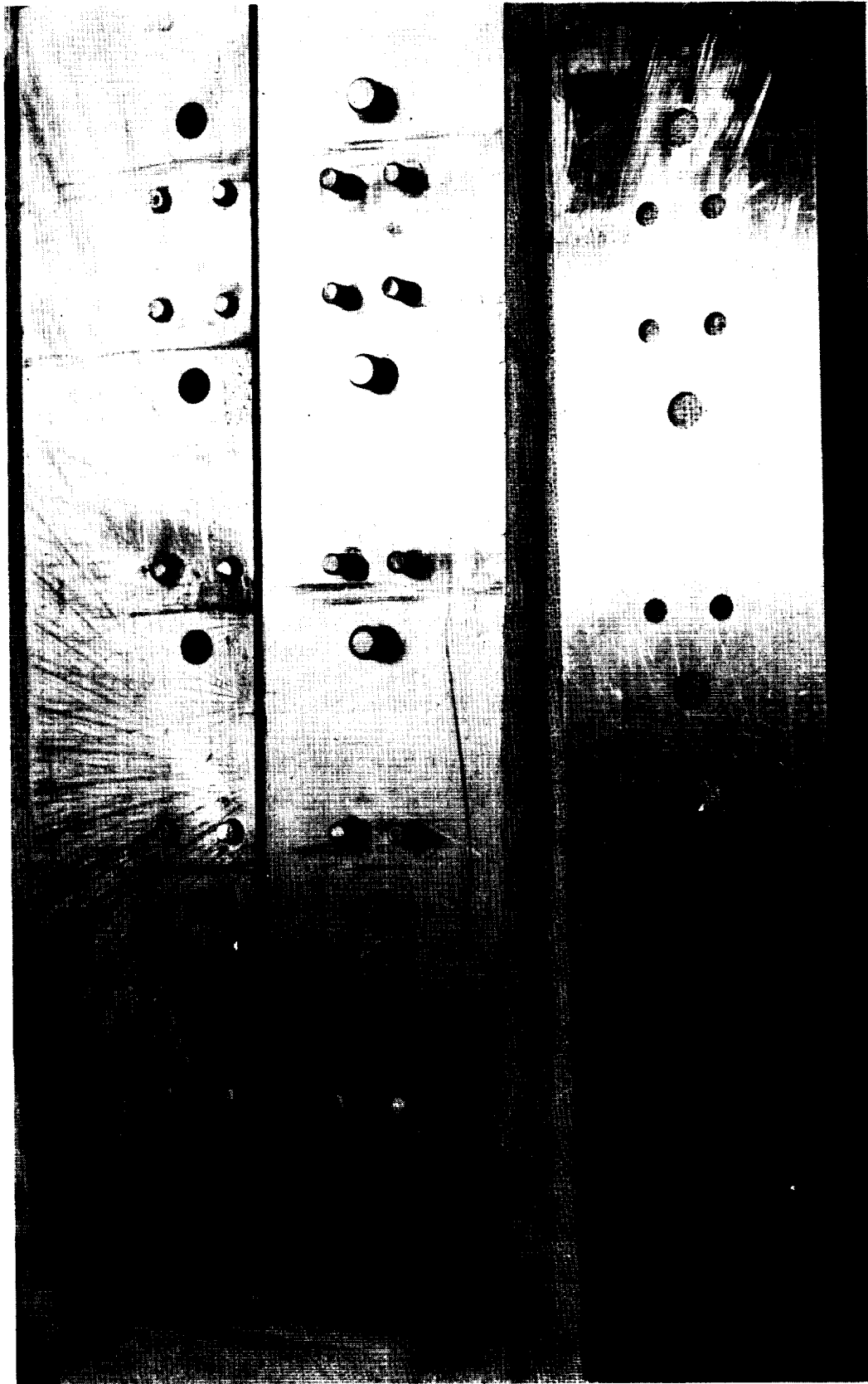


FIGURE 111. ASSEMBLY FIXTURE AND ONE SHIM.  
FIVE SPECIMENS MAY BE BONDED SIMULTANEOUSLY.

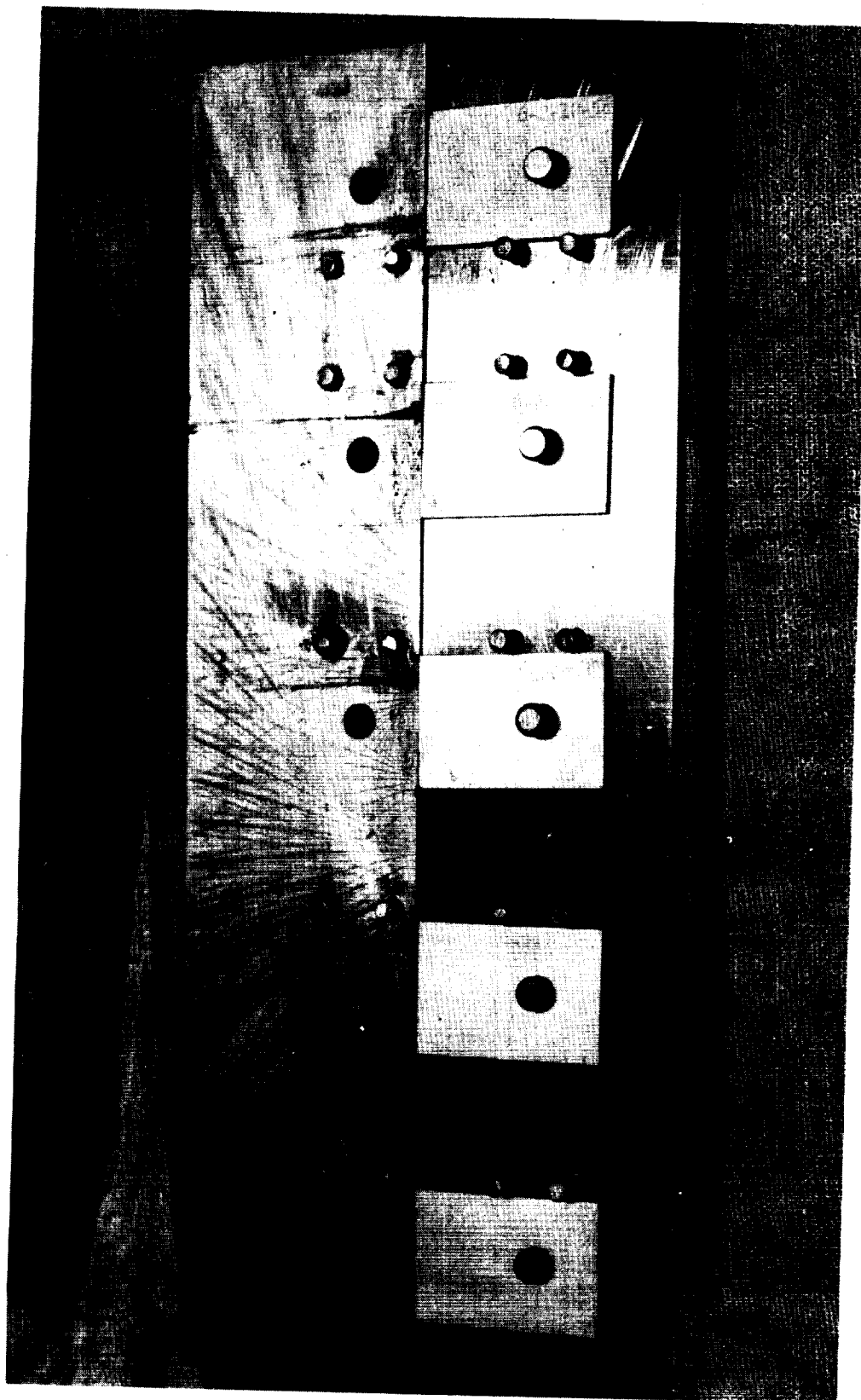


FIGURE 112. FIRST STEP IN THE ASSEMBLY OF ADHESIVE BONDED TEST SPECIMENS

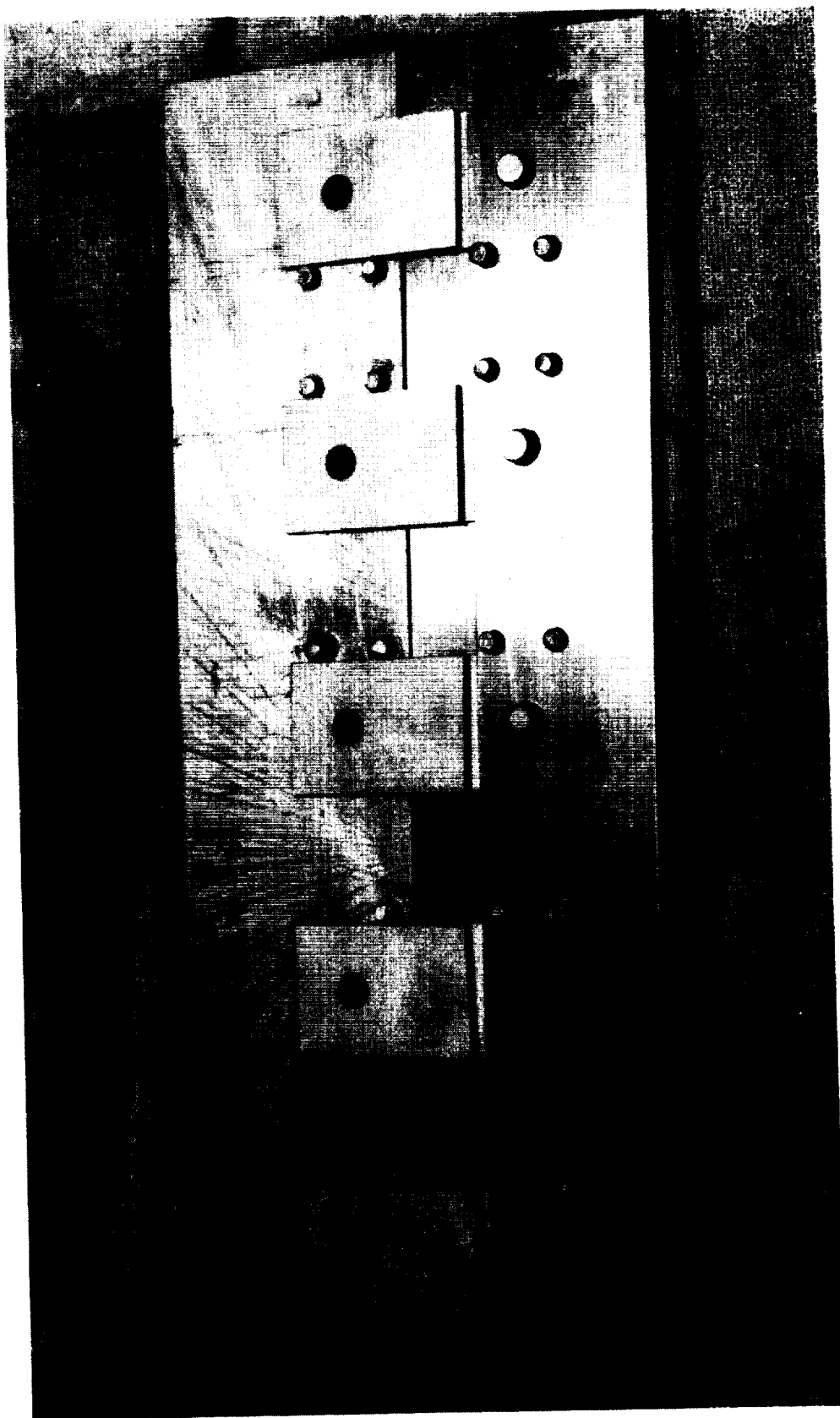


FIGURE 113. SECOND STEP IN THE ASSEMBLY OF ADHESIVE BONDED TEST SPECIMENS

3. Place the second segment of the double bearing end of the specimen (third segment) in place on the fixture as illustrated in Figure 114.
4. Place the fixture with the assembled specimens in a vacuum bag, as illustrated in Figure 115, in preparation for curing in an autoclave.

With the exception of those assembled with "Imidite 850", all of the specimens were bonded in an autoclave in a reduced atmosphere of 2.7 psia. During the heating of the autoclave, the reduced atmospheric pressure of the autoclave was supplemented with 25 psig mechanical pressure for a total effective pressure of 37 psi on the joint, for 10 minutes to insure good bond contact. The specimens then were cured, at autoclave pressure, in accordance with the vendors' recommendations outlined in Table XII. Due to the high pressure requirement of 200 psi, the "Imidite 850" specimens were not vacuum bagged, but were cured in a press in accordance with the vendors' recommendations. During the curing operation, the temperature was monitored by means of four thermocouples placed adjacent to the bond areas.

Several of the adhesive bonded specimens, ready for testing, are illustrated in Figure 116.

Due to the short overall length of the test specimens, a test fixture consisting of secondary steel straps was used to facilitate the installation of the specimens in the test machine. A spacer of appropriate thickness was inserted between the double bearing ends of the test specimen in order to reduce the potential bending moment at the bond line and thus maintain a pure shear load on the adhesive bond. The assembled fixture and a representative test specimen are illustrated in Figure 117.

During the initial testing of the specimens, the beryllium failed in bearing at the loading pin hole in the single segment end of the test specimen. In order to provide the necessary bearing at the loading pin hole, and thus avoid additional similar failures, aluminum reinforcement pads were fabricated and bonded with "Epibond 122" to both sides of the single segment ends of the 0.020, 0.030, and 0.060-inch thick test specimens. The

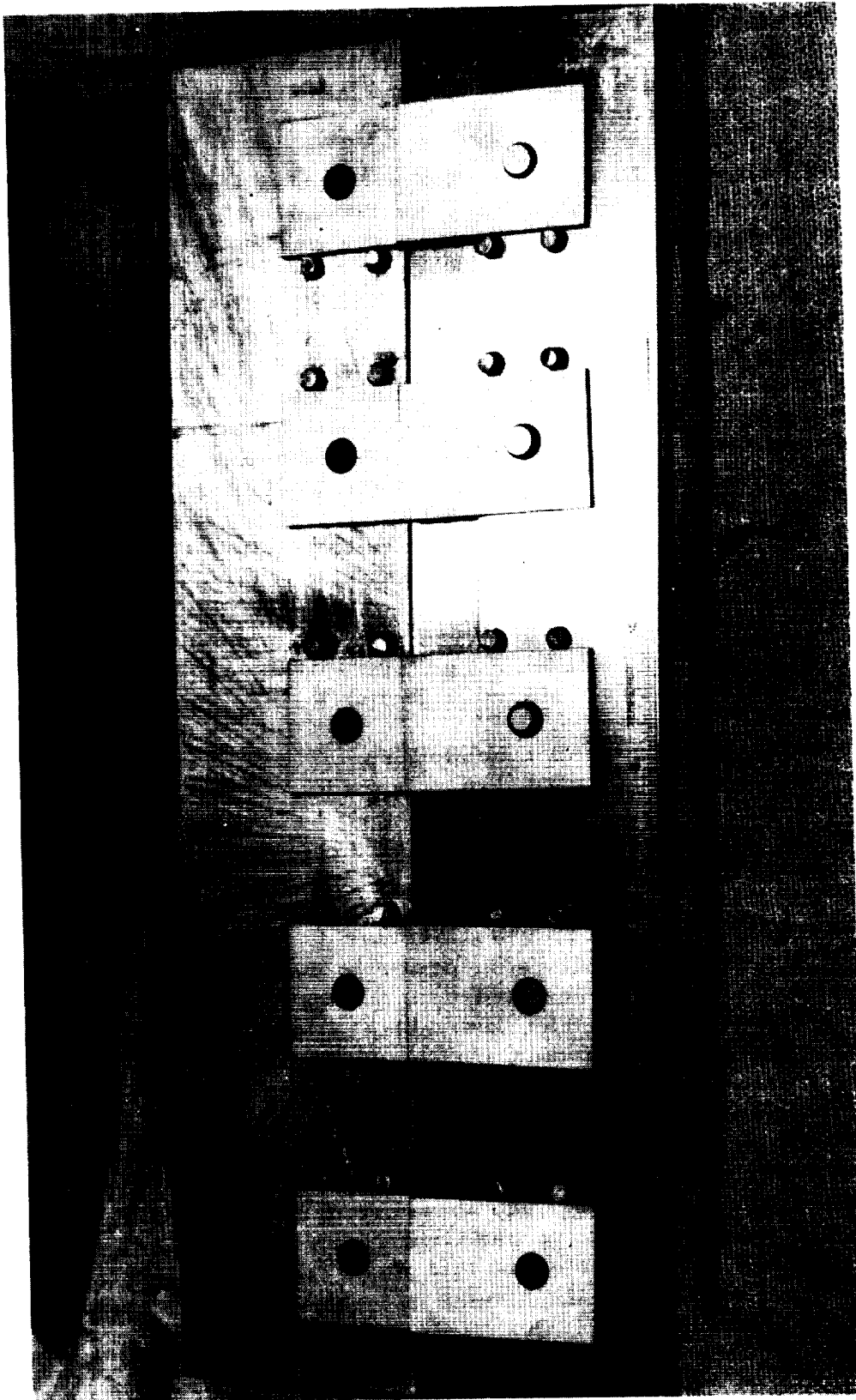


FIGURE 114. THIRD STEP IN THE ASSEMBLY OF ADHESIVE BONDED TEST SPECIMENS

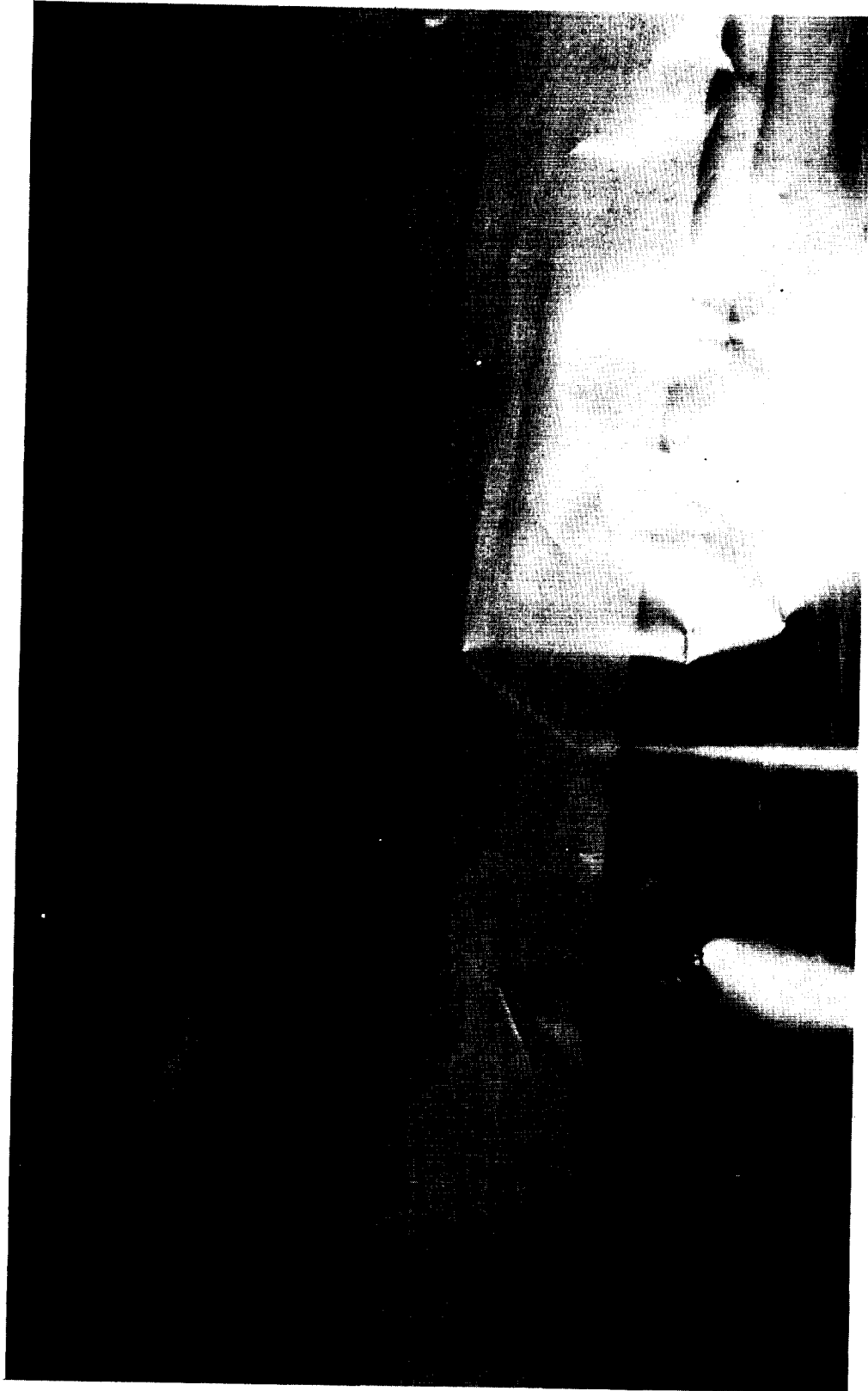
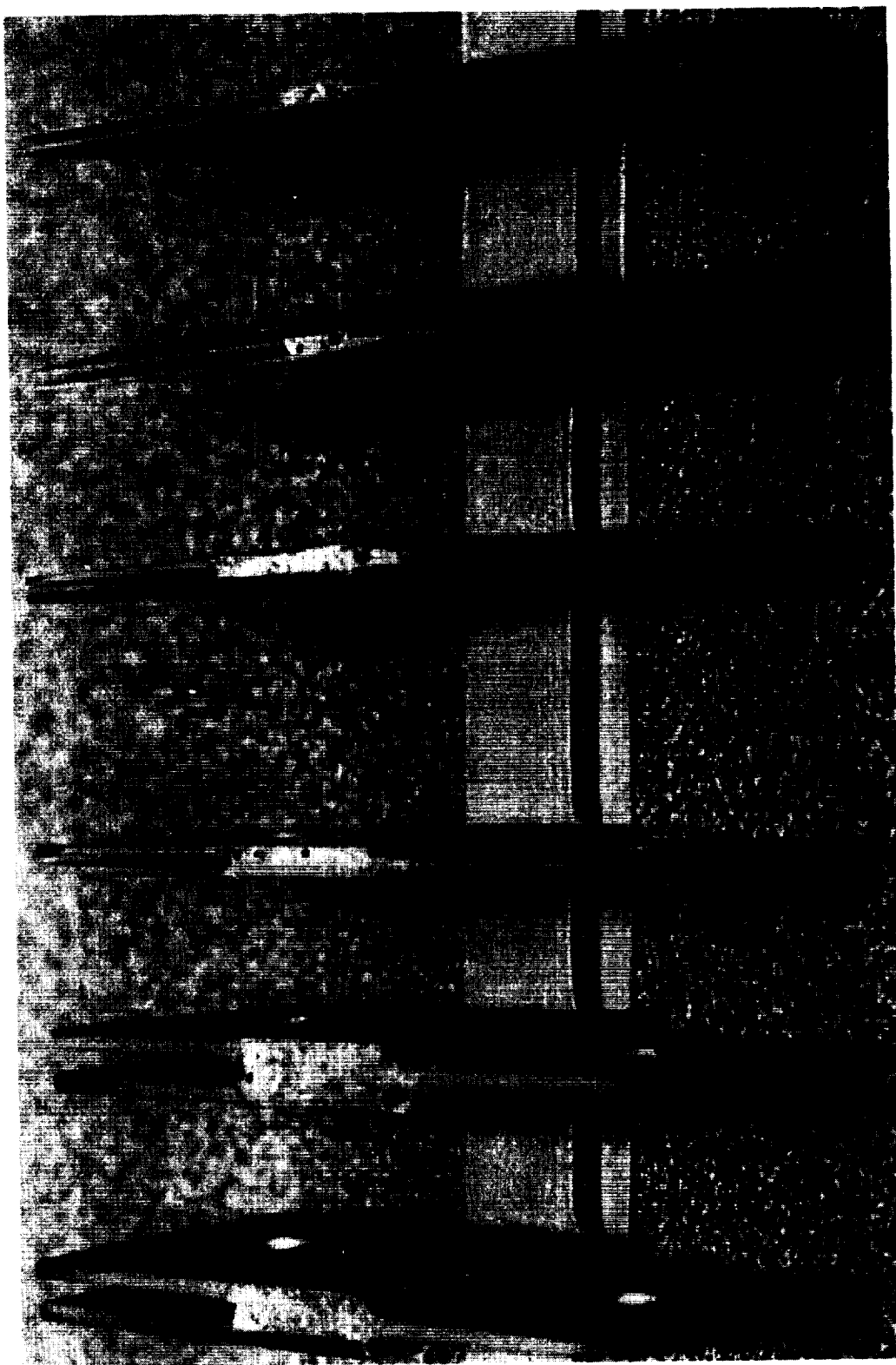


FIGURE 115. BONDING FIXTURE AND ASSEMBLED TEST SPECIMENS IN VACUUM BAG



.020

.030

.060

FIGURE 116. ADHESIVE BONDED SPECIMENS



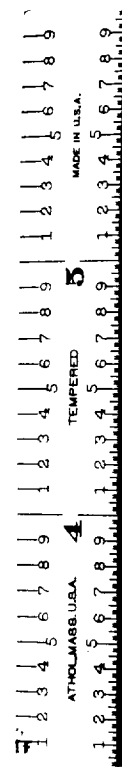
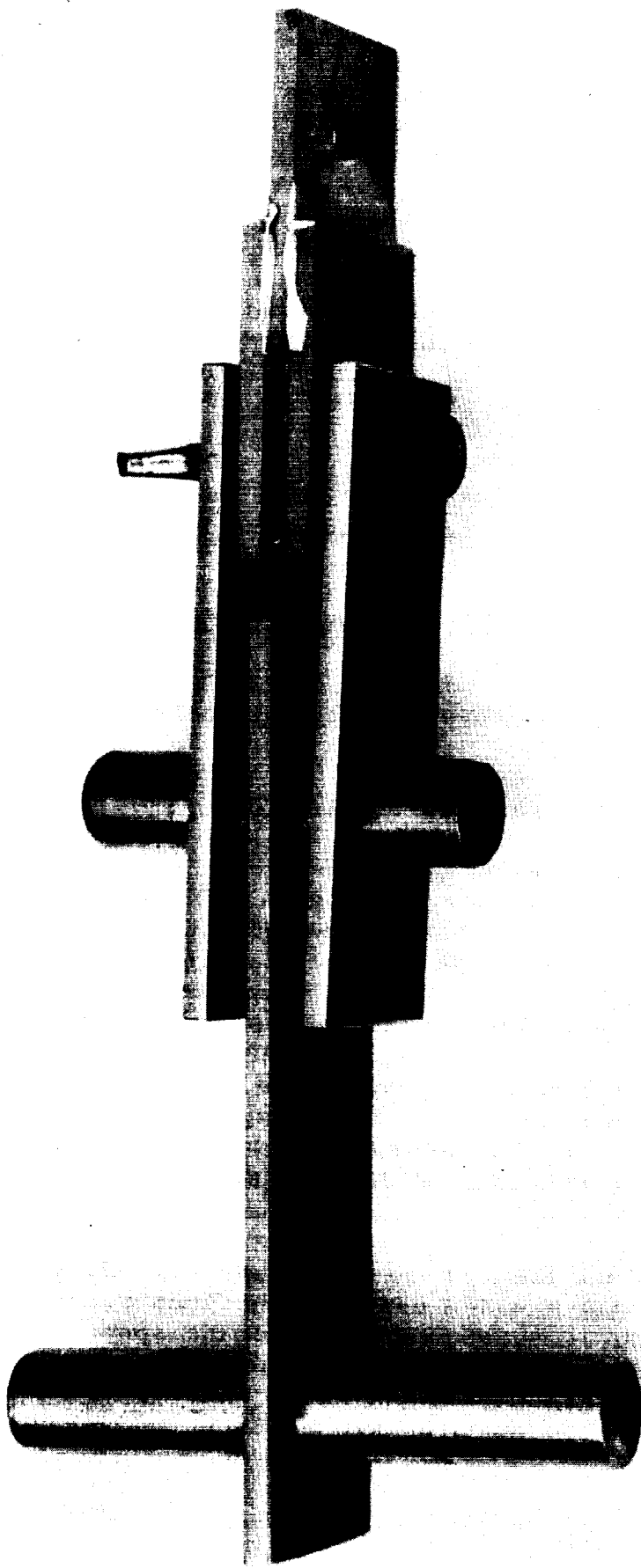


FIGURE 117. TEST FIXTURE AND ADHESIVE BONDED SPECIMEN

reinforcement of the 0.120-inch test specimens was not required; in most cases, the 0.120-inch thickness of the material provided sufficient bearing. The original group of "beryllium bearing failure" specimens also was reinforced in the same manner in order to permit retesting. Two reinforced 0.060-inch specimens and an unreinforced 0.120-inch specimen are illustrated in Figure 118.

In addition, the pin type connection was replaced by a vise grip, which spanned the full width of the specimens and thus assured even distribution of the load. Figure 119 illustrates the testing of one of the reinforced specimens in the "Riehle" hydraulic tensile testing machine

3. Results and Discussion. The three basic modes of failure observed during the testing of the adhesive bonded specimens were:

- a. Bearing failure in the single beryllium segment.
- b. Net tension failure in the single beryllium segment.
- c. Shear failure of the bond.

Approximately 45 percent of the specimens failed either in bearing or net tension in the beryllium segments; the shear strength of the bonded joint exceeded the basic tensile or bearing strength of the beryllium. It should be noted, however, that the majority of these basic material failures occurred during the testing of the thinner gage specimens; the adhesive failed during the testing of approximately 80 percent of the 0.120-inch specimens. Figure 120 illustrates the typical failure mode of the 0.120-inch specimens bonded with one of the higher strength adhesives, FM-1000. The extreme bearing deformation of the single segment loading pin holes is indicative of the high stresses in the specimens.

The results of the tests of the specimens not only were lower than anticipated, but included considerable "data scatter" within each set as well. Critical examination of the specimens indicated the variations may have been due either to random contamination of the surfaces subsequent to the cleaning operations, or to slight differences in the material properties in the segments. This variation in the test results, for each set of specimens, is

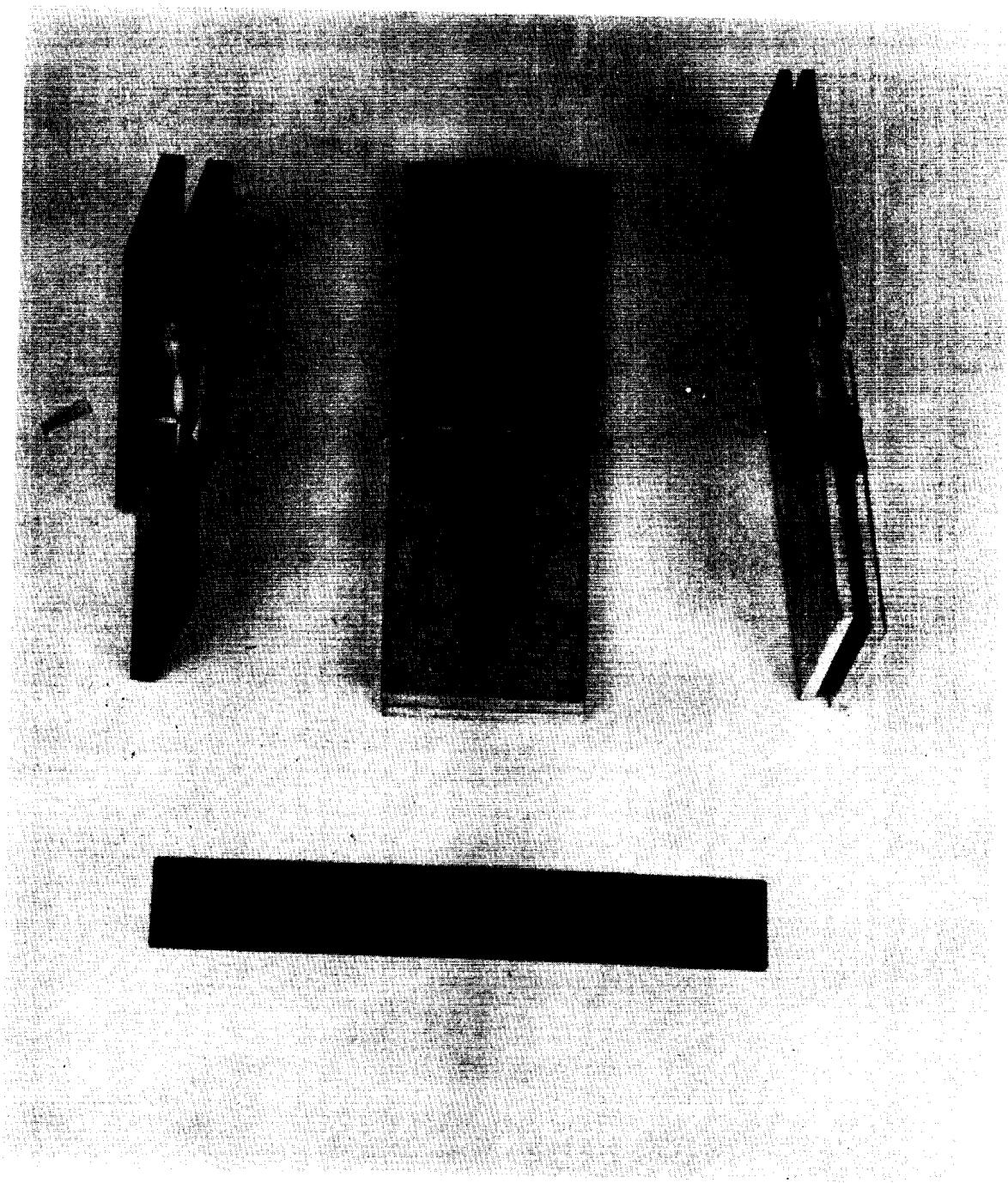


FIGURE 118. REINFORCED 0.060-INCH TEST SPECIMENS WITH AN UNREINFORCED 0.120-INCH TEST SPECIMEN

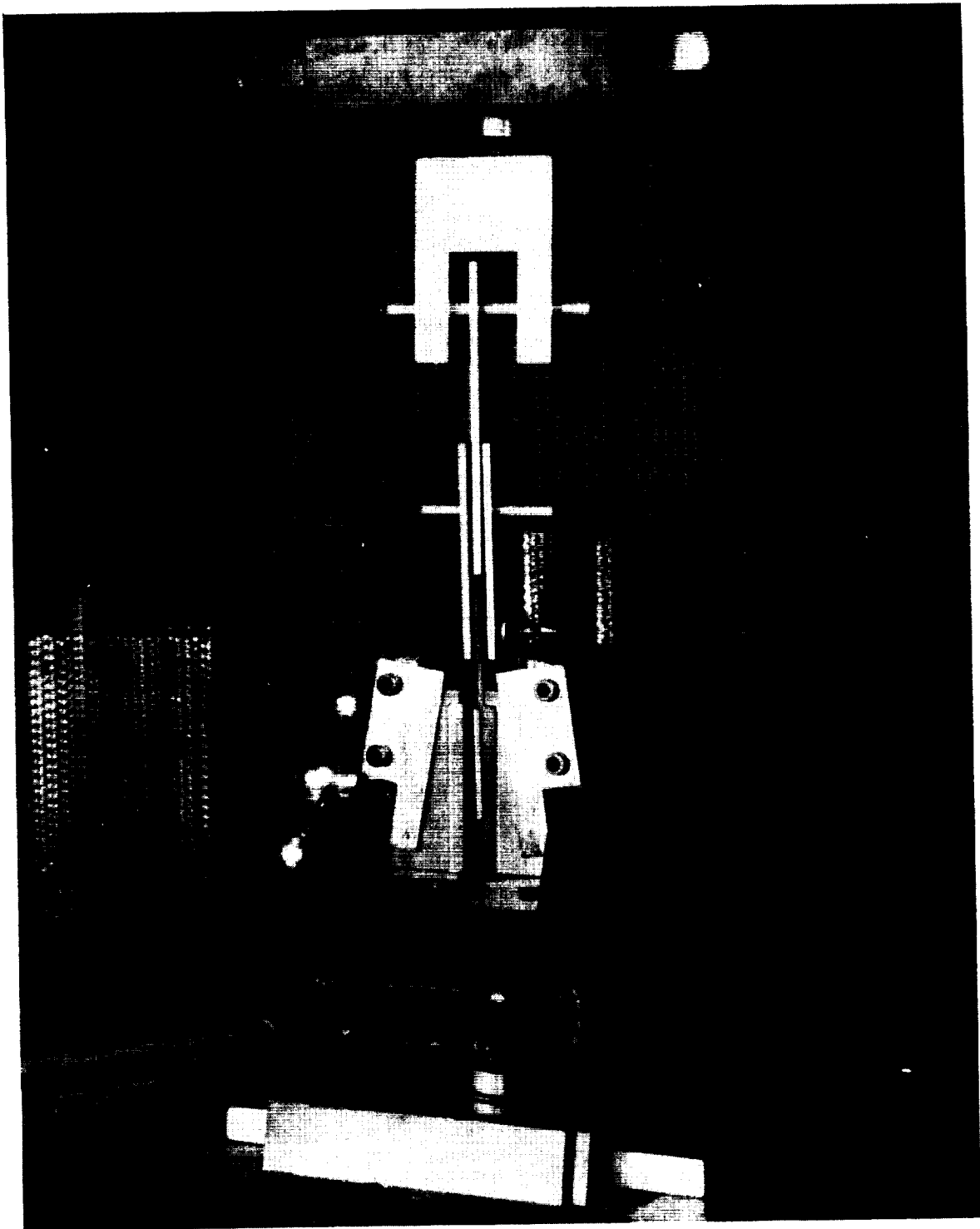


FIGURE 119. ADHESIVE BONDED SPECIMEN - TENSILE TEST

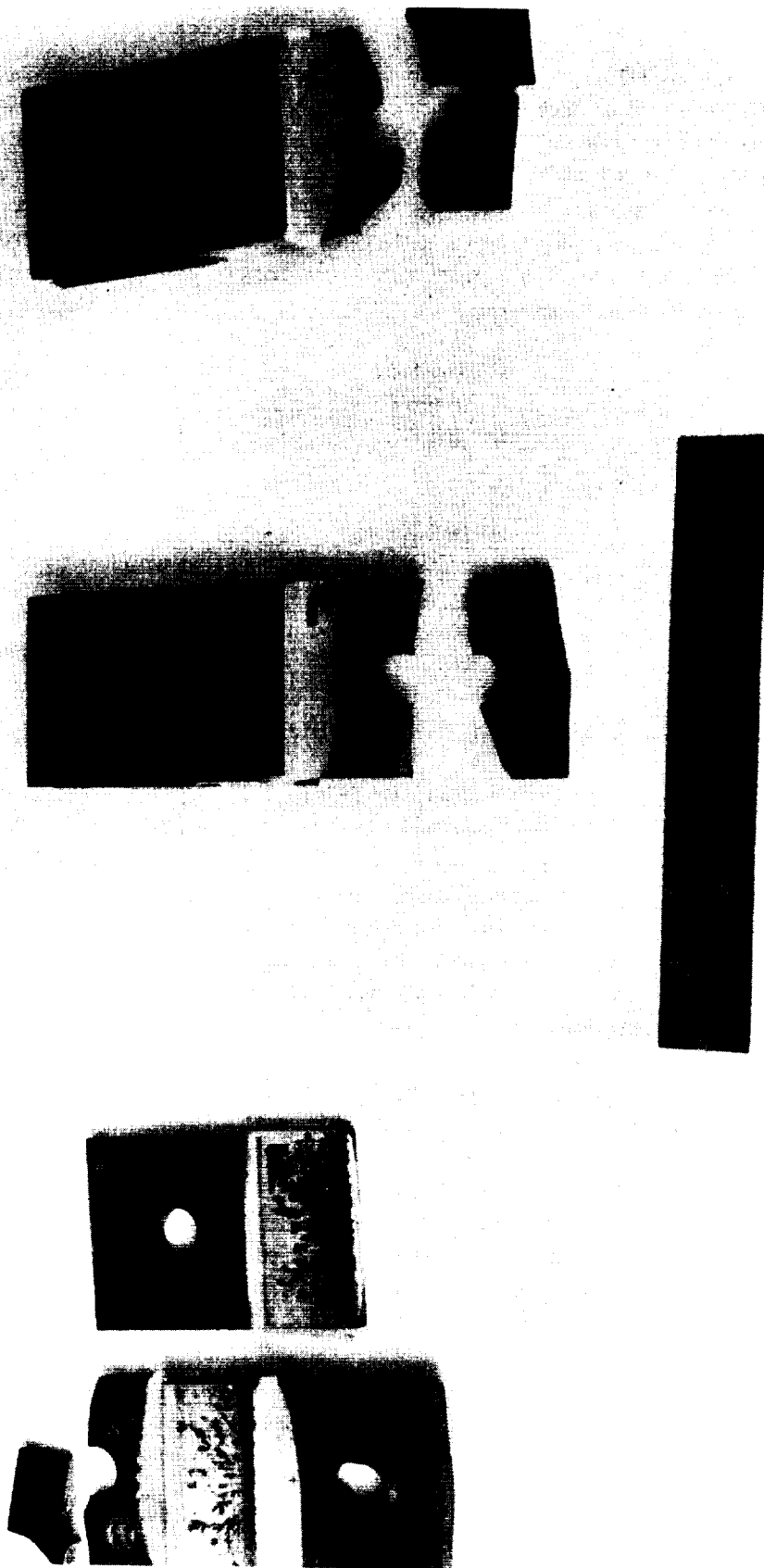


FIGURE 120 ADHESIVE BONDED SPECIMENS - FM-1000 ADHESIVE - 0.120-INCH MATERIAL -  
TYPICAL FAILURE MODE

illustrated in Figure 109. It may be noted that, with the exception of Epon VI, the average apparent bond strength of each of the adhesives tested was significantly less than the published values. However, it should be emphasized that the vendor data is based upon, and applicable to, the bonding of aluminum to aluminum; the completely different characteristics of beryllium, particularly its self-passivating nature, preclude the establishment of any valid direct comparisons.

It is believed that, in addition to the self-passivating characteristic of beryllium, the lower strength levels attained during this investigation may be attributed to one or more of the following:

- a. Inappropriate specimen dimensions, i.e., the cross-sectional area of the beryllium segments was inadequate in proportion to the shear strength of the specific adhesive being tested. The use of larger segments, relative to the bond area, will alleviate this problem.
- b. Possible recontamination of the surfaces to be bonded subsequent to the cleaning operation. The exercise of extreme care during the cleaning and handling of the specimens, and the reduction of the time interval between the cleaning and the bonding operations, will avoid the recontamination problem.
- c. Possible unanticipated incompatibility of the cleaning material and the adhesive. Careful analyses of the compositions of the involved materials may not reveal an obscure effect. As new adhesives become available, additional test work may be required to resolve this potential problem.

4. Adhesive Bonding - Conclusions and Recommendations. The limited scope of this investigation, conducted to establish the feasibility of adhesive bonding as an assembly method

for beryllium, did not permit the optimization of the processes and procedures. However, the optimization of the processes, including the development of exact controls, will insure the production of high strength bonded joints.

In conclusion, additional adhesive bonding development work is recommended. Although satisfactory beryllium to beryllium adhesive bonding has been accomplished on a laboratory scale, further investigation and refinement of the processes are required. In addition, due to the developmental nature of this work, the establishment of routine production procedures has not yet been initiated.

### C. BRAZING

1. Introduction. Brazing is one of the more versatile and desirable methods for joining components of either the same or dissimilar metals. It is, theoretically, an ideal method for joining notch sensitive materials, such as beryllium, and the disadvantages inherent in the discontinuities normally present in a mechanical joint can be avoided.

However, due to the characteristics of beryllium, particularly the almost immediate formation of an extremely thin, very tenacious surface layer of beryllium oxide upon the exposure of the surface to normal atmosphere, the fabrication of successful brazed joints does present several problems. Many of the more commonly utilized brazing alloys are unacceptable for one or more of the following reasons:

- a. The brazing material alloys with the surface of the beryllium form an extremely brittle, and therefore weak and unacceptable, interface.
- b. Chemical reactions between the beryllium and elements of the brazing material result in deleterious effects on the beryllium.
- c. The excessively high temperatures required for the brazing material result in grain growth in the beryllium with consequent reductions in

the mechanical properties, particularly in wrought products, i.e., sheets, forgings, extrusions, etc.

- d. Insufficient or no "wetting" action, which results in weak and low grade joints.

An investigation of these problems, and the development of acceptable processes, therefore, was included in this program. Due to the limited nature of this phase of the program comprehensive analyses and evaluations of the many cleaning agents, brazing filler metals and fluxes, and the optimization of processes and procedures could not be accomplished. This effort, therefore, was directed toward the development of those processes and procedures deemed most promising. Maximum use was made of the existing information and data, in order to avoid the duplication of previous investigations.

The scope of this investigation was arbitrarily limited to the consideration of low and medium temperature range brazing alloys, as it was believed these alloys were most applicable for the fabrication of large space vehicle components and assemblies.

Zinc was selected as the filler metal to be utilized during the investigation and evaluation of low temperature brazing. An alloy of silver, copper, zinc, cadmium, conforming to the requirements of standards ASTM B-260-56T and AWS A5 8-56 and sold under various trade names, was utilized as the filler metal during the performance of the medium temperature brazing investigation. Due to the dissimilar nature of the respective brazing processes, the performance of the tasks was accomplished independently and the results are reported separately.

2. Low Temperature Zinc Brazing. This type of brazing normally is used for the assembly of components whose operational environment will not exceed 350°F. Specific advantages of zinc, as the filler metal, include good wetting characteristics and relative ease of application.

- a. Experimental Procedures. The first phase in the investigation of zinc brazing as a joining method, prior to the fabrication of tensile test specimens and the determination of the mechanical properties of the brazed joints, consisted of the evaluation of the flow characteristics of zinc on beryllium. The determination of the flow characteristics, as a function of the contact angle formed between the beryllium and the zinc at the junction, was accomplished as follows:



1. Remove the lubricants, dust, and similar surface contaminants by wiping with MEK.
2. Etch the specimens in a solution consisting of 3 percent HF (hydrofluoric acid) and 45 percent  $\text{HNO}_3$  (nitric acid), plus water at a controlled temperature of  $90 \pm 5^\circ\text{F}$  for a period of 1-2 minutes.
3. Rinse the parts in clear water (if available, use de-ionized water) and oven dry at a temperature of  $180^\circ\text{F}$  -  $200^\circ\text{F}$  for 30 minutes to remove all moisture.
4. Coat the surface of the beryllium with a proprietary flux (nominal composition: 25 percent  $\text{ZnCl}$ , 75 percent  $\text{NH}_4\text{Cl}$ , by weight).
5. Place a piece of zinc on the prepared beryllium and attach a thermocouple to the blank.
6. Place the test item in a furnace preheated to a temperature of  $860^\circ\text{F}$ . Allow sufficient time for the temperature of the test item to stabilize within the range of  $840^\circ\text{F}$  -  $860^\circ\text{F}$ ; hold for 4 minutes.

NOTE: The nominal total time in the furnace is approximately 13 minutes.

7. Remove the assembly from the furnace and allow it to cool to room temperature.
8. Remove the residual flux by scrubbing the test unit in de-ionized water with a stainless steel bristle wire brush.

In order to provide sufficient support for the zinc during the preparation of the specimen for micrographic analysis, a copper strike and a 0.004-inch thick nickel plate then were applied to the test specimen as follows:

1. The test item was transferred into a cyanide copper strike solution consisting of:

Dupont Elchem 1469	50 gm/liter
NaF	20 gm/liter
NaCO <sub>3</sub>	45 gm/liter
NaKC <sub>4</sub> H <sub>4</sub> O <sub>6</sub> ·4H <sub>2</sub> O	20 gm/liter

This operation was conducted at a temperature of 135°F, adjusted with KOH to a pH of 10.5, with a current density of 50-150 asf, for one minute.

2. The test item then was transferred immediately (no intermediate step) into the following nickel plating solution:

NiSO <sub>4</sub> ·7H <sub>2</sub> O	300 gm/liter
NiCl <sub>2</sub> ·6H <sub>2</sub> O	35 gm/liter
H <sub>3</sub> BO <sub>4</sub>	43 gm/liter
*WA7	1 gm/liter

The solution was maintained at a temperature of 120°F and a pH of 3.2, and the plating operation was continued until approximately 0.004 inch of nickel had been deposited.

The specimen then was sectioned, mounted, and polished for micrographic examination to permit the determination of the contact angle between the zinc and the beryllium. As indicated by the extremely small contact angle of 2-4 degrees, illustrated in Figure 121, the flow characteristics of zinc on beryllium are

---

\*Proprietary wetting agent



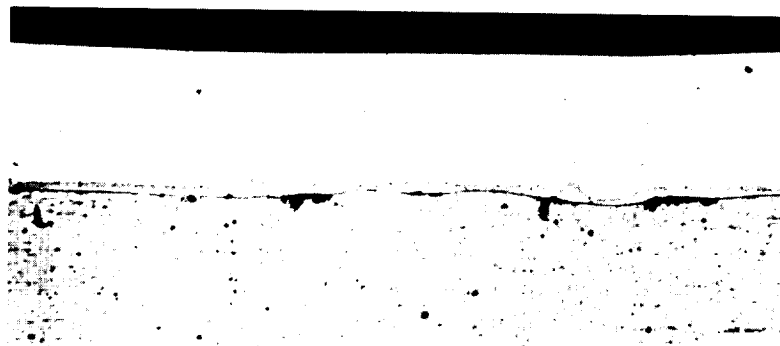
NICKEL

COPPER STRIKE  
ZINC

BERYLLIUM

200X

FIGURE 121. CONTACT ANGLE AT JUNCTION - ZINC ON BERYLLIUM  
NICKEL-COPPER-ZINC-BERYLLIUM INTERFACE



NICKEL

COPPER STRIKE  
ZINC

BERYLLIUM

200X

FIGURE 122. PLATED BERYLLIUM CROSS-SECTION  
NICKEL-COPPER-ZINC-BERYLLIUM INTERFACE

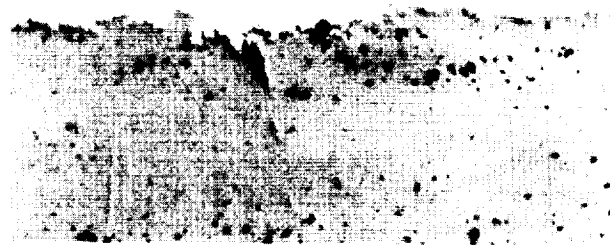
very good. The dark spots visible in the layer of zinc are believed to be BeO inclusions.

The dark discontinuities in the beryllium-zinc interface, illustrated in Figure 122, are believed to be entrapped residue from the etching process. Even the most thorough washing, subsequent to the etching process, occasionally may fail to remove all traces of the residues. The presence of such contaminants results in the bridging of the zinc over the inclusion.

The interface of the zinc and beryllium was critically examined to ascertain the degree of diffusion of the zinc into the beryllium that resulted from the time-temperature schedule used for the application of the zinc onto the beryllium. The excellent adhesion, with no evidence of diffusion or alloying, is clearly visible in Figures 123 and 124.

Following the completion of the flow characteristic investigation, five standard 2-inch by 0.500-inch tensile test specimens were fabricated of nominal 0.060/0.070-inch material. Following the completion of the machining operations, the specimens were etched to remove all surface imperfections. Both ends of the specimens were identified, the specimens were cut into two pieces midway in the test section, and the test section ends of the segments were cleaned and prepared for brazing as previously outlined. The specimens then were brazed as described in the following sequence:

1. Coat the surfaces to be joined with flux.
2. Heat the ends of the segments and add zinc; continue heating until the zinc flows over the entire area to be joined.
3. Allow the segments to cool to room temperature and remove the residual flux by scrubbing with a stainless steel wire brush and de-ionized water.
4. Coat the zinc surfaces to be joined with flux.

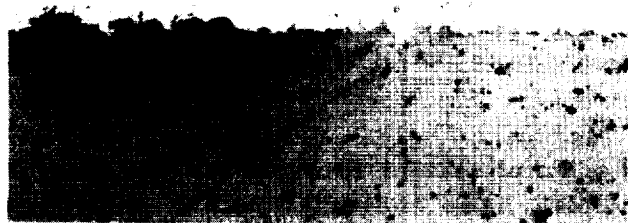


ZINC

BERYLLIUM

1040X

FIGURE 123. ZINC-BERYLLIUM INTERFACE



ZINC

BERYLLIUM

1040X

FIGURE 124. ZINC-BERYLLIUM INTERFACE

5. Place the specimen segments on a holding fixture to maintain the desired lap dimensions.
6. Heat the segments until the zinc flows; press the ends of the segments together and allow the assembled specimen to cool to room temperature.

CAUTION: Do not use high pressure, or insufficient zinc will remain in the bond area to produce a good joint.

The edges of the specimens then were lightly ground to remove the excess zinc filler metal, and the final pertinent joint dimensions were determined and recorded. One of the completed specimens, ready for testing, is illustrated in Figure 125. A 60,000-pound capacity "Riehle" tensile testing machine, equipped with vise grips, was used for the testing of the joints.

As all of this first group of five test specimens failed in the beryllium rather than in the brazed joint, four larger specimens were fabricated of nominal 0.090/0.095-inch material in an effort to determine the strength of the brazed joint. The "Riehle" tensile testing machine again was utilized for the testing of these specimens. However, the vise grips were applied to the specimens as close to the joint area as possible (approximately 3/8 inch from the lap area) rather than at the ends. All of this second group of specimens also failed in the beryllium rather than in the joint area.

b. Results and Discussion. A summary of the specimen dimensions, test loads, and stresses is presented in Table XV.

It should be emphasized that all of the specimens failed in tension in the beryllium base material rather than in the brazed joint. Three of the failures occurred at stresses approaching the known tensile strength (approximately 35,000-40,000 pounds) of the material when subjected to the combined effect of tensile and bending loads.

Thus, it may be concluded that the overlap area of the brazed area resulted in a joint strength exceeding the limit of the

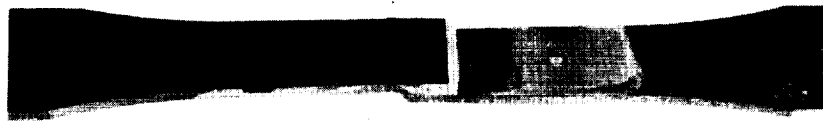
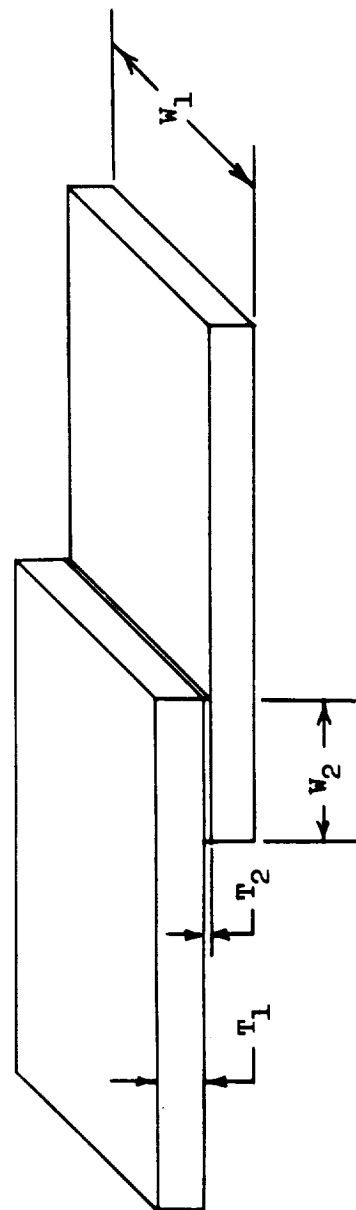


FIGURE 125. ZINC BRAZED LAP SHEAR JOINT - TEST SPECIMEN

TABLE XV  
Brazed Specimens - Low Temperature Zinc Brazing - Test Summary

Specimen Group	No.	Net Dimensions - Inch				Area - Square Inches		Load Pounds	Apparent Stress - PSI	
		$t_1$	$t_2$	$W_1$	$W_2$	Braze	Be X-Section		Be	Braze
I	1	0.072	0.009	0.498	0.245	0.122	0.036	1200	33,300	9,800
	2	0.073	---	0.498	0.260	0.129	0.036	1100	30,600	8,500
	3	0.062	0.011	0.490	0.240	0.118	0.030	1065	35,500	9,000
	4	0.067	0.005	0.491	0.250	0.123	0.033	820	24,800	6,700
	5	0.062	0.010	0.491	0.240	0.118	0.030	860	28,700	7,300
II	6	0.093	0.002	0.762	0.204	0.155	0.071	1850	26,000	11,900
	7	0.094	0.002	0.761	0.216	0.164	0.072	1470	20,400	9,500
	8	0.092	0.005	0.785	0.227	0.178	0.072	1760	24,400	9,900
	9	0.094	0.005	0.761	0.211	0.160	0.072	1980	27,500	12,400

NOTE: ALL SPECIMENS FAILED IN THE BERYLLIUM BASE METAL.





basic cross-sectional area of the beryllium.

The testing of the second group of specimens, with the vise grips adjacent to the joint area, resulted in lower net tensile stresses in the beryllium and apparently higher stresses in the brazed joint. These apparently inconsistent results, particularly when compared with the results of the tests of the first group of specimens, were due to the attachment of the vise grips adjacent to the single lap brazed joints rather than at the ends of the specimens. This "close gripping" limited the bending capability of the specimen and resulted in premature failure of the beryllium. The greater cross-sectional area of the beryllium segments (approximately double) permitted substantially higher total loads, and thus the shear strength of the brazed joint appeared to be substantially higher.

Critical metallographic examinations of the joints, subsequent to the tensile testing, revealed discontinuities in the zinc filler metal. Microphotographs of the discontinuous areas, visible in the cross-section of a representative zinc brazed joint illustrated in Figure 126, are presented in Figures 127 and 128. An excellent, completely brazed area is illustrated in Figure 127. The intimate contact of the zinc and the beryllium, with no voids or discontinuities, is clearly visible. The discontinuous area, illustrated in Figure 128, consists of voids, minute scattered bits of zinc, and loose beryllium particles. It is believed the loose beryllium particles resulted from partial shear failure that occurred during the tensile tests. The irregular fracture lines around the partially separated beryllium particles substantiate this hypothesis.

3. Medium Temperature Alloy Brazing. The results of previous investigations have indicated the difficulty of brazing bare beryllium to itself, or to other metals, at medium to high temperatures. The self-passivating nature of beryllium, i.e., the almost immediate formation of an extremely thin surface layer of beryllium oxide upon the exposure of the surface to normal atmosphere, is accelerated at elevated temperatures. Thus the accomplishment of satisfactory high temperature brazing is extremely difficult. A vacuum of approximately  $10^{-4}$  Torr is required to maintain equilibrium between beryllium and its oxides, and even the rare gases cannot be so highly purified.



FIGURE 126. ZINC BRAZED LAP SHEAR JOINT - APPROXIMATELY 14X

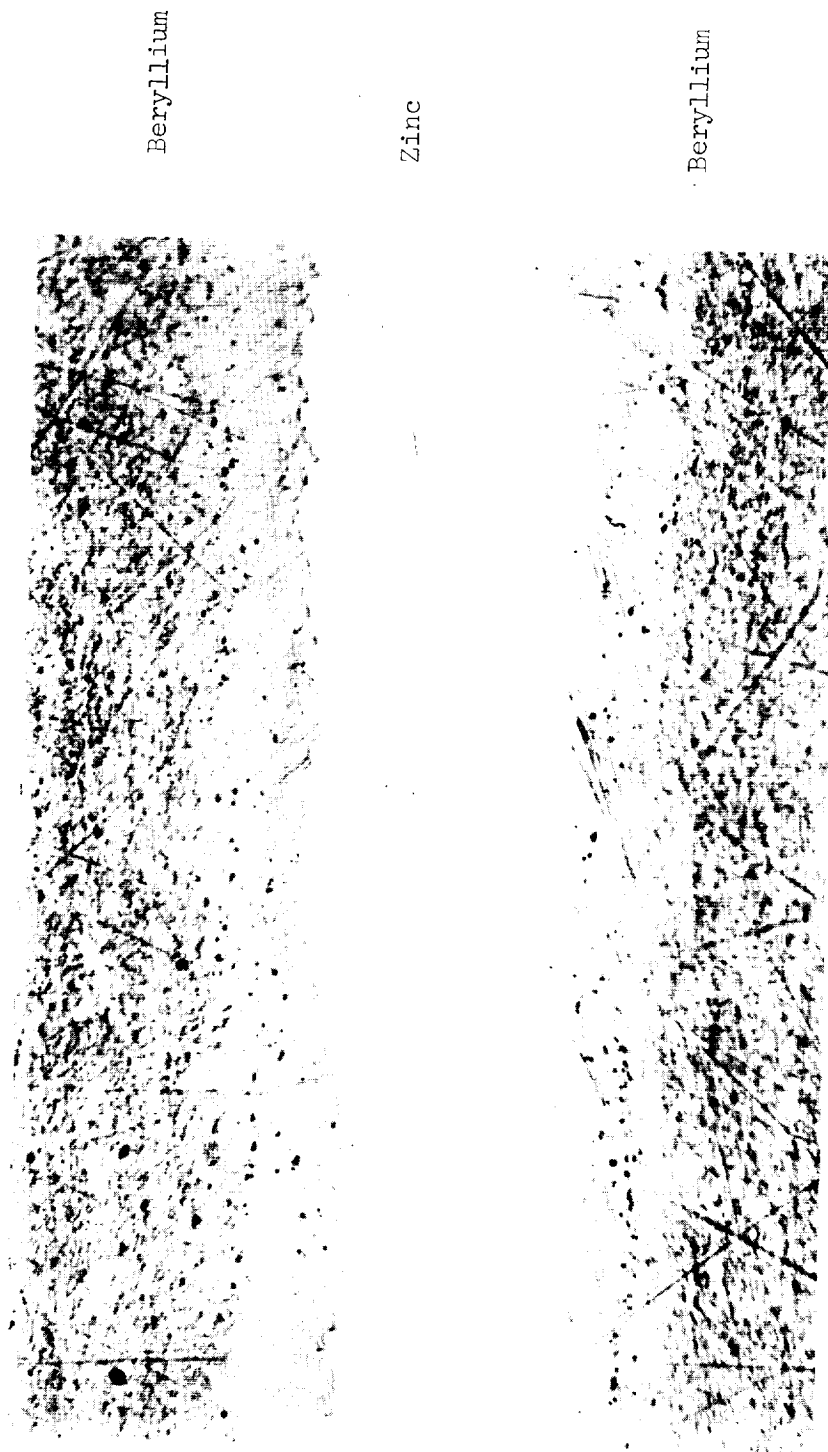


FIGURE 127. ZINC-BERYLLIUM INTERFACE - SOUND BRAZE AREA

BERYLLIUM

VOIDS: MINUTE  
SCATTERED BITS  
OF ZINC: LOOSE  
BERYLLIUM PARTICLES

BERYLLIUM



FIGURE 128. ZINC-BERYLLIUM INTERFACE - DISCONTINUOUS BRAZE AREA

The application of flux to the surfaces to be joined is an alternate solution, but due to the active chemical nature of these materials, severe pitting can result from improper use. Therefore, the use of plating, as the substrate for subsequent brazing, appeared to present definite advantages.

a. Plating Investigation - Substrate for Brazing.

The most important facets in the selection of the candidate plating materials were first, the ease of plating; second, reasonably high melting points which would avoid the rapid diffusion of the plating material at brazing temperatures; and finally, the material must produce reliable joints when brazed with flux, or in an inert gas atmosphere, using commercially available filler alloys. The initial choice, based upon the ease of brazing and the relatively slow diffusion rate of nickel in silver based brazing alloys, was nickel, plated directly onto the beryllium. Since nickel is quite active with beryllium, forming intermetallics at temperatures as low as 1100°F - 1200°F, a modification of this process appeared to be desirable. Therefore, the process was changed to include an initial silver plate followed by the overplate of nickel. However, the application of silver directly onto beryllium resulted in poor adhesion due to blisters. The substitution of copper for the silver then was proposed; but the results of earlier experiments had clearly indicated that the plating of copper and nickel directly onto beryllium resulted in low shear strength adhesion. Therefore, the plating process was modified to include the plating of a thin layer of zinc directly onto the beryllium, followed by a copper strike and finally the nickel plate. This final method resulted in the maximum adhesion of the plate to the base material. The zinc coating is so thin that it cannot be detected by ordinary methods after the plating has been completed.

It was determined, during the investigation, that the successful plating of beryllium was dependent upon the best possible preparation of the surface. In an effort to provide a more uniform and economical pre-cleaning method, vapor blasting was tried. The resulting surfaces appeared to be completely free of the contamination which had caused severe pitting during earlier experiments. Vapor blasting now has been adapted as the standard process for the cleaning of surfaces in preparation for direct brazing, and for all beryllium plating processes. It should be noted that this plating development work was accomplished subsequent to the work previously reported in the "Surface Treatment" portion of this final report.

The procedure found to be the most suitable for the cleaning and plating of beryllium in preparation for brazing is outlined as follows:

1. Wet abrasive blast (80 grit at 80 psi).
2. Immerse in 10 percent sulfuric acid (by volume) for 10 seconds and rinse.
3. Immerse for 3 minutes in:

Solution -

Sodium Hydroxide                      500 gm

Zinc Oxide                              100 gm

Water                                      to 1000 ml

4. Rinse
5. Strip zinc with 33 percent nitric acid (by volume) and rinse.
6. Re-immerses in solution of step 3 for 1 minute. Rinse rapidly and thoroughly.
7. Copper strike:

Solution -

Sodium Copper Cyanide    5 oz/gal

Free Sodium Cyanide      0.5 to 0.6 oz/gal

Sodium Carbonate              1 oz/gal

Current Density              25 amps/sq ft  
   first minute

   12 amps/sq ft  
   10 minutes

NOTE: Parts to be introduced into bath connected to cathode and with current on.

8. Rinse
9. Dip in 3 percent Phosphoric acid; rinse.
10. Copper pyrophosphate plate

Temperature:	120°F ± 3°F
Time:	30 minutes
Current Density:	20 ASF
11. Rinse
12. Acid Dip, rinse
13. Nickel sulfamate plate:

Solution -	
Density	29 to 31° Be
pH	3.0 to 3.6
Chloride	low
Temperature:	130 ± 3°F
Time:	15 minutes
Current Density:	50 ASF
Agitation:	Cathode Rocker
Filtration:	Continuous
14. Rinse and dry.

b. Experimental Procedures. Following the completion of the plating investigation, 42 tensile test specimens were fabricated and tested. The beryllium material used during the brazing process development phase, specimens 1 through 37, was salvaged cross-rolled sheet material, conforming to the standards for space vehicles. Since much of this material was refurbished after being partially worked during prior fabrication, it was not entirely representative of virgin sheets; however, for the purpose of process development, it was entirely satisfactory. Later, parts were produced from the lots of material, purchased specifically for the contract and machined to standard tensile coupons. These coupons were cut into two equal halves for joining to the stainless steel strips as illustrated in Figure 129.

The braze filler metal consisted of an alloy of silver, copper, zinc, and cadmium. It is sold under various trade names and conforms to ASTM B-260-56T and AWS A5.8-56T, with analysis requirements for both specifications designated BAg 1a. The filler metal also conforms to Federal Specifications QQ-S-561d grade 4, and to AMS 4770. The alloy exhibits a melting range of 1160°F to 1175°F. This alloy was selected because it has good "as brazed" strength, it melts below the temperature range which might result in deleterious effects on the beryllium, and it wets easily and flows well on nickel. This is the most easily used alloy for a wide variety of joint configurations; a wide latitude in fit-up tolerances is acceptable, and it can be utilized either with the "flux" or the "inert atmosphere" brazing process. The filler metal can be preformed and pre-placed in the joint prior to assembly, or can be placed at the joint edge and fed into the braze area by gravity and capillary flow. The latter method was used for this development due to the simple lap shear joint configuration which permitted capillary flow from one side. The entrapment of flux or gas is easily avoided when this very fluid filler metal is used for the assembly of a joint of this type.

The beryllium segments were prepared for brazing by vapor blasting and nickel plating in the manners previously outlined.

The mating stainless steel segments were cut from 0.08-inch sheets of Type 304 material in the form of 3/4-inch by 4-inch strips. After nickel plating, the stainless steel and beryllium



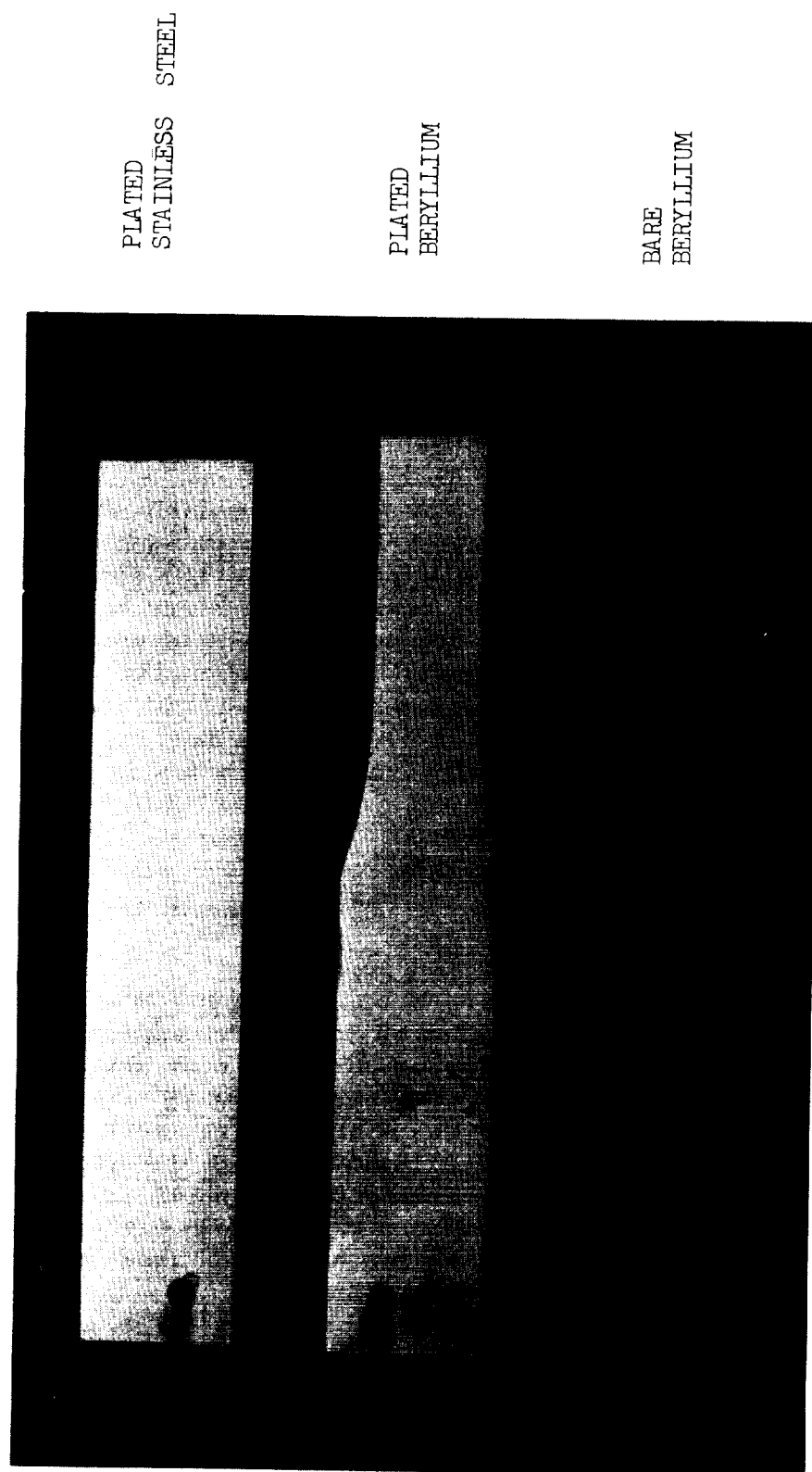


FIGURE 129. BERYLLIUM AND STAINLESS STEEL TEST SEGMENTS

parts were stored in individual plastic bags until needed.

Various diffusion treatments were performed on selected test coupons to determine whether the adherence of the plating on the beryllium could be improved by low temperature diffusion. A temperature level of 400°F was selected for the diffusion treatment to avoid extensive formation of the copper-beryllium compounds prior to brazing, and to remain within the temperature zone where the solubilities of copper into beryllium and nickel were appreciable.

The brazing was accomplished by clamping a beryllium and stainless steel specimen in a fixture, illustrated in Figures 130 and 131, which assures the proper alignment, and suitable lap spacing for the filler alloy. The entire assembly then was coated with flux\* and the filler metal wire was pre-placed adjacent to the joint. The fixture and parts were immediately placed into the furnace and heated to the braze temperature of 1220°F, which was 40°F to 50°F above the melting point of the braze alloy. Thermocouples attached to the entire assembly indicated that the fixture and coupons, completely covered with flux, required heating for approximately 20 minutes to achieve the desired braze temperature. When the parts were run through the furnace at a rapid rate, more time was required for preheating in order to obtain a successful braze. This was determined by examining the test specimen to verify the melting of the filler alloy. An additional 5 minutes of heating was incurred when melting was not evident.

After the test parts were properly joined, the fixture was removed from the furnace and allowed to cool to approximately 900°F. The parts then were forced-air cooled to about 300°F in approximately 5 minutes, followed immediately by water cooling to tap water temperature. The flux then was removed in running water and the brazed coupon was removed from the fixture. Following the completion of the brazing development, additional specimens (38 through 42), of new material, were prepared and brazed. A standard tensile testing machine was used for testing all of the beryllium stainless steel specimens. After the tensile testing was completed, metallographic specimens were prepared

---

\*Easy Flux was used with Easy Flow alloy throughout this program.

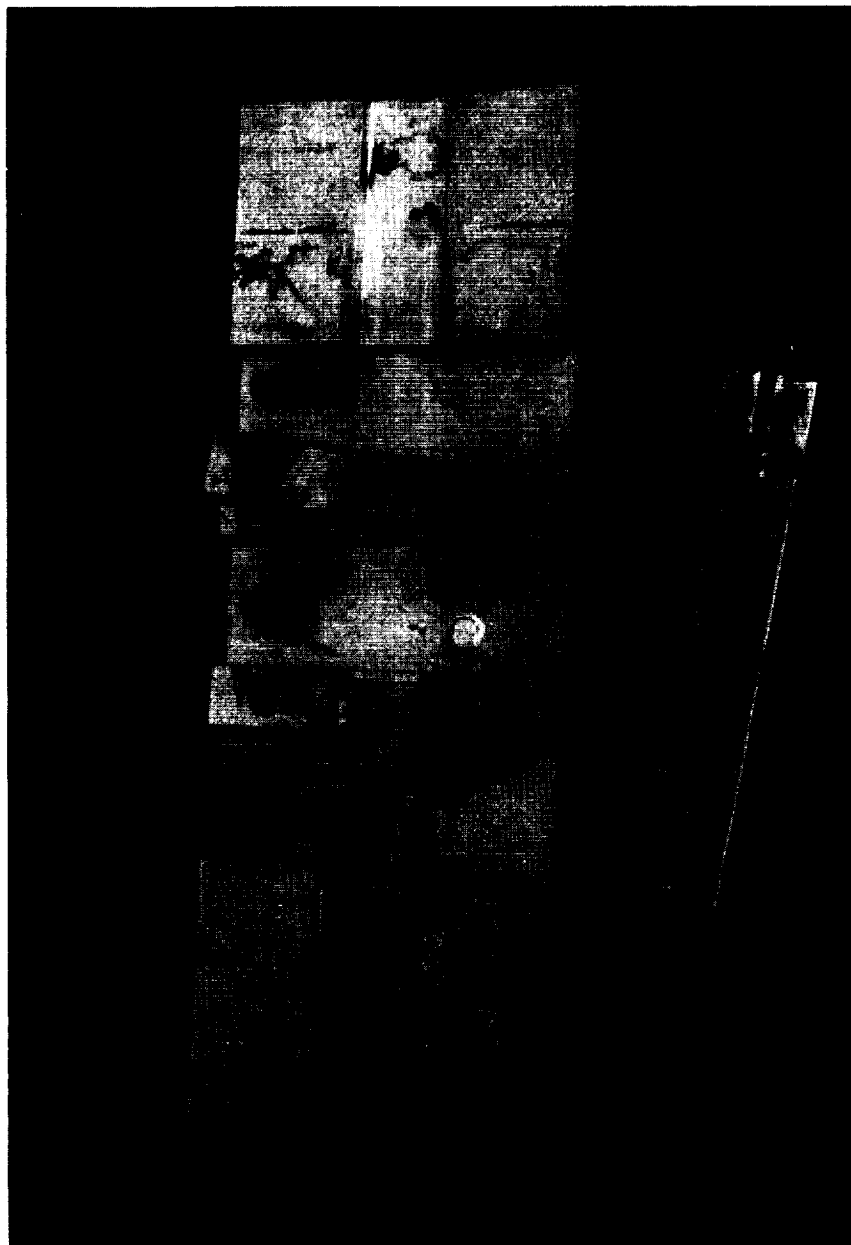


FIGURE 130. BRAZING FIXTURE AND LAP GAGE

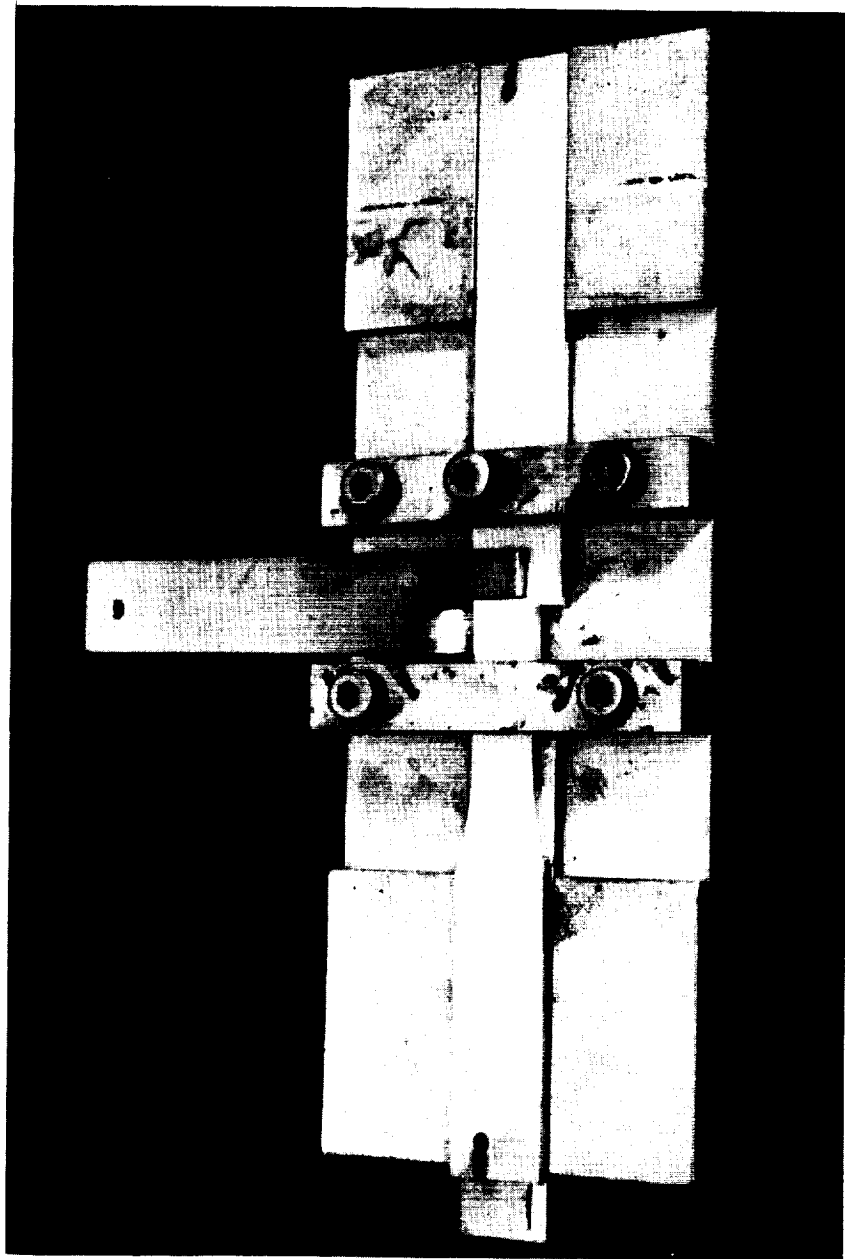


FIGURE 131. BRAZING FIXTURE AND SPECIMEN SEGMENTS.  
LAP GAGE IN USE.

to permit the examination and evaluation of the quality of the plating and of the brazed joint.

c. Results and Discussion. A summary of the brazing development tests including the diffusion treatments, the failure modes, and the stresses is presented in Table VXI. Examination of this test data indicates the definite progress that had been made during this development program. The strength of the brazed joints increased from low, inconsistent values of approximately 3000-8000 psi to reasonably consistent values of approximately 20,000 psi. In addition, it should be noted that these final specimens (39 through 42) broke in the parent material, thus a true indication of the actual joint strength itself could not be obtained.

Critical metallographic examination of these joints, subsequent to the tensile testing, revealed the uniformly good adhesion between the beryllium and the plating. This uniformity is clearly visible in Figure 132. The particles at the beryllium to copper interface are the slight inclusions typically found throughout the beryllium. It should be noted that the Kirdendall effect will move all inclusions, within a band representing the entire volume of beryllium reacting with the copper, to new locations at the surface of the compounds. This indicates that the precleaning process is satisfactory and that no further gains in the adhesion of the plating can be expected.

4. Brazing - Conclusions and Recommendations. The results of this investigation clearly demonstrate the feasibility of brazing as a method for joining beryllium. Simultaneously, the difficulties associated with the attainment of consistently reliable results also are obvious.

The careful observance of all cleaning and surface preparation precautions will result in the production of uniform zinc brazed joints of reasonable strength suitable for low temperature applications.

Consistent, reliable procedures for plating beryllium, as the substrate for brazing, have been developed which will make possible the assembly of high-strength brazed joints.

TABLE XVI

Braze Specimens - Lap Shear Braze on Nickel Plated Beryllium - Test Summary

SPECIMEN NO. (1)	DIFFUSION TREATMENT		MODE OF FAILURE	OVERLAP INCHES	MAXIMUM STRESS PSI
	TIME HRS.	TEMPERATURE °F			
1		none	Plate peel	0.175	N11
2		"	" "	0.216	5,560
3		"	" "	0.175	2,600
4		"	" "	0.175	1,320
5		"	" "	0.175	3,170
6		"	" "	0.175	3,150
7		"	" "	0.175	4,000
8		"	" "	0.175	6,500
9	14	500	" "	0.175	8,200
10	2.5	750	" "	0.175	8,580
11	15	400	" "	0.084	15,900
12	17	400	" "	0.275	7,400
13	20	400	" "	0.078	10,300
14	17	440	" "	0.18	10,000
15	15	400	" "	0.18	2,000
16		none	" "	0.18	7,000
17		"	" "	0.18	1,000
18		"	" "	0.18	690
19		"	" "	0.18	N11
20		"	Plate peel, blistered	0.18	N11
21		"	Broke parent metal	0.18	12,900
22		"	" " "	0.090	20,700
23		"	Broke at Cu Plate	0.056	7,000
24	62	400	Plate Peel	0.100	7,600
25	63	400	Broke Parent Metal	0.100	18,400
26	1.5	400	Plate Peel	0.093	9,300
27	1	400	Blistered Parent Metal	0.100	11,700

TABLE XVI (Cont.)

Brazed Specimens - Lap Shear Brazes on Nickel Plated Beryllium - Test Summary

SPECIMEN NO. (1)	DIFFUSION TREATMENT		MODE OF FAILURE	OVERLAP INCHES	MAXIMUM STRESS PSI
	TIME HRS.	TEMPERATURE °F			
28	1	400	Badly Blistered	0.100	11,800
29	1	400	Broke Parent Metal	0.090	20,700
30	1	400	Badly Blistered Plate Peel	0.080	11,300
31		none	Badly Blistered Plate Peel	0.60	N11
32		"	Blistered - Broke in Parent Metal	0.100	16,000
33	1	400	Parent Metal	0.100	20,200
34	1	400	" "	0.075	24,800
35	1	400	Plate Peel	0.070	17,400
36	1	400	Parent Metal	0.062	25,500
37	1	400	" "	0.050	27,000
38 (2)		none	Be Delaminated	0.060	6,800
39 (2)	1	400	Parent Metal	0.060	33,000
40 (2)	1	400	" "	0.060	25,200
41 (2)	1	400	" "	0.060	14,000
42 (2)	1	400	" "	0.060	30,800

- (1) ALL SPECIMENS BRAZED WITH EASY FLO SILVER SOLDER AT 1220 F, WITH A TOTAL TIME IN THE FURNACE OF 20 MINUTES.
- (2) BERYLLIUM 1/8-INCH SHEET IN THESE TESTS, WAS NEW MATERIAL MACHINED TO HALF TENSILE SPECIMENS, AND BRAZED TO 3/4-INCH + 0.062-INCH STAINLESS SHEET TYPE 304.

NICKEL

COPPER

BERYLLIUM



1000X

FIGURE 132. PLATED BERYLLIUM - READY FOR BRAZING



It should be emphasized that, although these processes did result in the production of joints of reasonable strength, their total reliability has not been established and that the procedures have not progressed beyond the laboratory stage. Therefore, although the feasibility has been established, further work is recommended.

Future work should be directed, first, toward the reduction of the thickness of the copper plate and, by adjusting braze time and temperature, hopefully reduce compound layer thickness to a minimum. Following the successful completion of this approach, other methods which may eliminate the copper, or substitute other metals that do not form brittle intermetallics at the brazing temperature, should be investigated. The principal objective of this investigation has been met; i.e., to braze beryllium with alloy fillers which exhibit useful strength while remaining within the temperature range which does not affect the properties of beryllium sheet.

Although the plating parameters developed for this study are known to be repeatable for producing sound brazes, the associated costs of plating beryllium could be reduced by the application of additional attention to the reduction of the thickness of the nickel plate and the amount or type of copper undercoating required. Copper was most convenient for this development due to the great deal of experience available from previous work on plating aluminum. It does, however, form intermetallics with beryllium; therefore, other metals should be investigated which will result in the production of more ductile joints.

The minimum permissible thickness of nickel was not determined and, although a standard thickness of 0.50 mil was used, it is possible that as little as 0.2 mil would be sufficient.

#### D. DIFFUSION BONDING

1. Introduction. The objective of this phase of the program was the demonstration of the feasibility of joining beryllium to beryllium by means of solid state diffusion bonding at temperatures below those required for brazing the metal by conventional means. The results of previous work discussed in Reference 3, have shown that certain metals diffuse rapidly in beryllium at temperatures well below their melting points, or

the melting points of the eutectics which may form. This information, and available thermo-mechanical data on beryllium, provided the foundation for the work described in this report.

2. Background. The three variables of primary importance in solid state diffusion bonding are temperature, time, and pressure. The first two control the intensity and extent of the diffusion, respectively, as described by the classical diffusion equations. Pressure does influence diffusion coefficients to some extent, but of greater importance in this case, is the effect on the completeness of the interfacial contact, particularly since the components will be joined with no liquid present. Clearly, the greater the pressure, the more intimate the contact will be until ultimately all of the points on opposite surfaces touch. Furthermore, interfacial voids, caused by surface irregularities, will result, under low pressure, in unbonded areas which can close only by a process similar to sintering. The lower the pressure, the greater will be the total unbonded area, and the longer will be the time required to effect a bond of maximum strength since, in principle, only a minute amount of diffusion is required to produce a strong bond.

Surface preparation and the method of applying the diffusion metal also will influence the process. However, these were not included as variables in this brief study.

The specific conditions for the proposed solid-state diffusion bonding of beryllium were determined from the available data, with due consideration of the deleterious effects that might result from the process. The time-temperature relationship could not be such as to produce noticeable grain growth; the temperature-pressure relationship was to be the maximum that would not result in noticeable deformation of the beryllium during the bonding cycle. The selection of the other parameters was based primarily on convenience.

The results of previous work discussed in Reference 3, indicated that, from the standpoint of kinetics, copper was a very efficient diffusing metal. Seven mils of copper, sandwiched between pieces of high purity beryllium, were completely dissolved in 100 hours at 1520°F. The resulting beryllium to beryllium bond is illustrated in Figure 133. It was anticipated that an adequate joint could be made in a much shorter time at a lower temperature, providing the bond between the beryllium and the copper was not weakened by intermediate phases.



INTERFACE

500X

FIGURE 133. BERYLLIUM-TO-BERYLLIUM SOLID-STATE DIFFUSION

The results of the previously referenced study on the diffusion of copper in beryllium indicated that a bond could be formed at temperatures of approximately 932°F or above. For long duration cycles, however, temperatures approaching 1500°F might cause grain growth and thus alter the properties of the beryllium. Therefore, the temperatures selected for this study were 932°F, 1022°F and 1112°F.

3. Experimental Procedures. A duplex pressure cycle was used at each temperature due to the plastic-creep characteristics of the hot-pressed QMV beryllium block, used in lieu of sheet material for this study, in this temperature range. The thermal-mechanical characteristics of hot-pressed QMV beryllium block are illustrated in Figure 134. It is evident that excessive deformation of the beryllium would occur during the first hour of the thermal treatment at temperatures as low as 1000°F and pressures in the range of 10,000 psi. A pressure of 8,000 psi was selected for the first phase of the 1112°F cycles, with time periods of 3 minutes for one specimen and 6 minutes for another. The application of the initial high pressure for a short time was to insure the maximum interfacial contact without deformation of the parent metal. Two additional specimens were bonded; one at 1022°F with an initial pressure of 12,000 psi applied for 6 minutes, and one at 930°F with an initial pressure of 15,000 psi also applied for 6 minutes.

A constant pressure of 3200 psi was applied during the second phase of each test cycle. It was presumed that this procedure will cause no noticeable creep in any of the selected time-temperature combinations. Approximately 20 minutes were required to heat the test specimens up to the selected diffusion temperature. Consequently, a nominal pressure of 1000 psi was applied to all specimens until the desired cycle temperature was attained. The pressure then was increased to the desired first-phase level, maintained for the specified time period, then decreased to the second level for the completion of the process. The subsequent cooling of the specimens was by radiation in a vacuum, and by conduction through the loading bar and the support. Approximately one hour was required for the specimens to cool to room temperature.

4. Specimen Preparation. Three methods of applying the intermediate metal (copper) were considered: placement

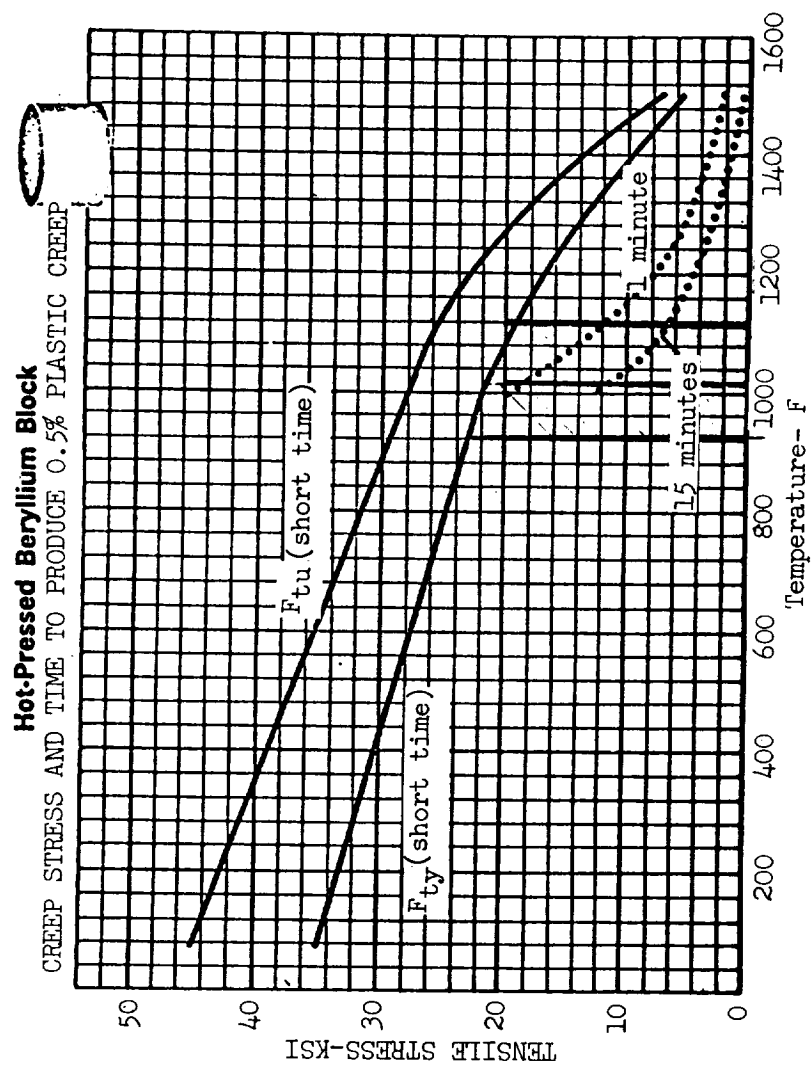


FIGURE 134. THERMAL-MECHANICAL CHARACTERISTICS OF HOT-PRESSED QMV BERYLLIUM BLOCK

of the foil or thin sheet between the components, coating the faying surfaces with copper either by electro or electroless plating, or by vapor deposition in vacuum. The first method was selected since the use of either of the others would have involved corollary experiments of indefinite duration which would have delayed the initiation of the diffusion bonding study.

All of the mating surfaces were prepared by mechanical grinding and polishing with no oil to contain the abraded particles and to prevent surface oxidation, followed by an alcohol rinse immediately prior to the assembly of the components.

Hot-pressed beryllium block material was machined into lap-shear specimens as illustrated in Figure 135. The specimens were 3/8-inch thick, except at the bond area where 3/16 inch was machined from one side in order to locate the joining plane on the tensile axis and thus produce as nearly a true shear condition as possible. The overlap could be varied from 0 to 1/4 - inch; the latter dimension was used for these tests. A small hole was drilled into the side of the specimen near the faying surface to provide a firm anchor for spot welding a thermocouple.

All of the diffusion bonding experiments were accomplished in a water-cooled brass vacuum chamber designed to heat the specimen by radiation from a nichrome heater wound inside a stainless steel reflector surrounding the specimen. A bellows in the chamber cover permitted the application of force to the joint from the hydraulic press in which the entire chamber was mounted.

Temperatures were controlled to within  $\pm 5^{\circ}\text{F}$  by means of an on-off type of controller-indicator connected to the heater power supply and to the thermocouple junction spot-welded to the specimen. The joint pressure was calculated from the force indicated by the gage connected to the hydraulic pressure line of the press, divided by the previously measured faying area of the specimen.

The vacuum within the chamber was produced by means of a mechanical pump connected to the chamber in a series with a liquid nitrogen trap.

The pressure was indicated by means of a thermocouple vacuum gage connected to a sensor mounted in the chamber wall. The best vacuum obtained during this study, subsequent to the initial outgassing, was approximately  $200 \times 10^{-3}$  Torr.

The two specimen halves, with the copper foil in place, were clamped in a stainless steel fixture, designed to maintain the alignment of the test segments during the loading and diffusion operations. The entire assembly then was placed within the chamber and held in position by light pressure from the press.

Following the completion of the bonding operations, the specimens were tested to failure. A 10,000-pound capacity "Instron" research tensile testing machine was used to test the specimens at a constant strain rate of 0.01 inch per minute. The alignment of the specimens insured essentially pure shear in the bonding plane.

5. Results and Discussion. A summary of the Time-Temperature-Pressure Cycles, and ultimate shear stresses is presented in Table XVII. As may be noted in the table, specimens A, B, and C, illustrated in Figure 135, bonded successfully. The specimen surfaces were oxidized during the high-temperature portion of each cycle, but the bright appearance of the surfaces under the loosely fitting holding fixture (the light bands on each side of the joint) indicated that the faying surfaces were unaffected. The extent of the surface oxidation is considered to be comparable to that which normally occurs during brazing at the higher temperatures. The fourth specimen, D, was not bonded because of excessive oxidation that occurred due to an air leak that developed in the vacuum system.

TABLE XVII

Time-Temperature-Pressure Cycles  
Diffusion Bonded Beryllium

<u>Specimen</u>	<u>Phase</u>	<u>Temp.</u> °F	<u>Pressure</u> psi	<u>Duration</u> minutes	<u>Ult. Shear</u> psi
A	1	1112	8,000	3	
	2	1112	3,200	240	11,200

TABLE XVII (Cont'd)

Time-Temperature-Pressure Cycles  
Diffusion Bonded Beryllium

<u>Specimen</u>	<u>Phase</u>	<u>Temp.</u> °F	<u>Pressure</u> psi	<u>Duration</u> minutes	<u>Ult. Shear</u> psi
B	1	1112	8,000	6	
	2	1112	3,200	480	9,400
C	1	1022	12,000	6	
	2	1022	3,200	1,080	8,480
D	1	932	15,000	6	
	2	932	3,200	1,080	0

As may be noted in Table XVII, Specimen A, the strongest, failed at 11,200 psi in joint shear, due to bending in the beryllium adjacent to the bonded area. Specimen B failed at 9,400 psi joint shear at the copper-beryllium interface. In this case, only one half of the available area was bonded; the bond strength was based on the actual bonded area. Marks made by the loading member on the end of the specimen indicated that the load was asymmetrically applied. The failure mode of Specimen C was very similar to that of B, except at a lower load of 8,480 psi.

Following the completion of the tensile testing, Specimen A, which had remained intact, was sectioned and prepared for metallographic examination of the joint area. The 500X microphotograph of this representative area is illustrated in Figure 136. The copper, in the center, is bonded to the beryllium on either side with two intermediate layers. This thick, bright layer on the copper side is the beta-primed phase; the thin, dark layer on the beryllium side is the delta phase. This structure is clearly visible in the high magnification, 3000X. microphotograph illustrated in Figure 137. The copper is visible at the bottom of the illustration, followed in order by the thick, bright beta-primed phase, the thin, dark delta phase, and the





SPECIMEN "A"



SPECIMEN "B"



SPECIMEN "C"

FIGURE 135. DIFFUSION BONDED QW BERYLLIUM TEST SPECIMENS

BERYLLIUM

COPPER

BERYLLIUM



FIGURE 136. SPECIMEN A - BERYLLIUM SOLID-STATE DIFFUSION BONDED AT 1112°F

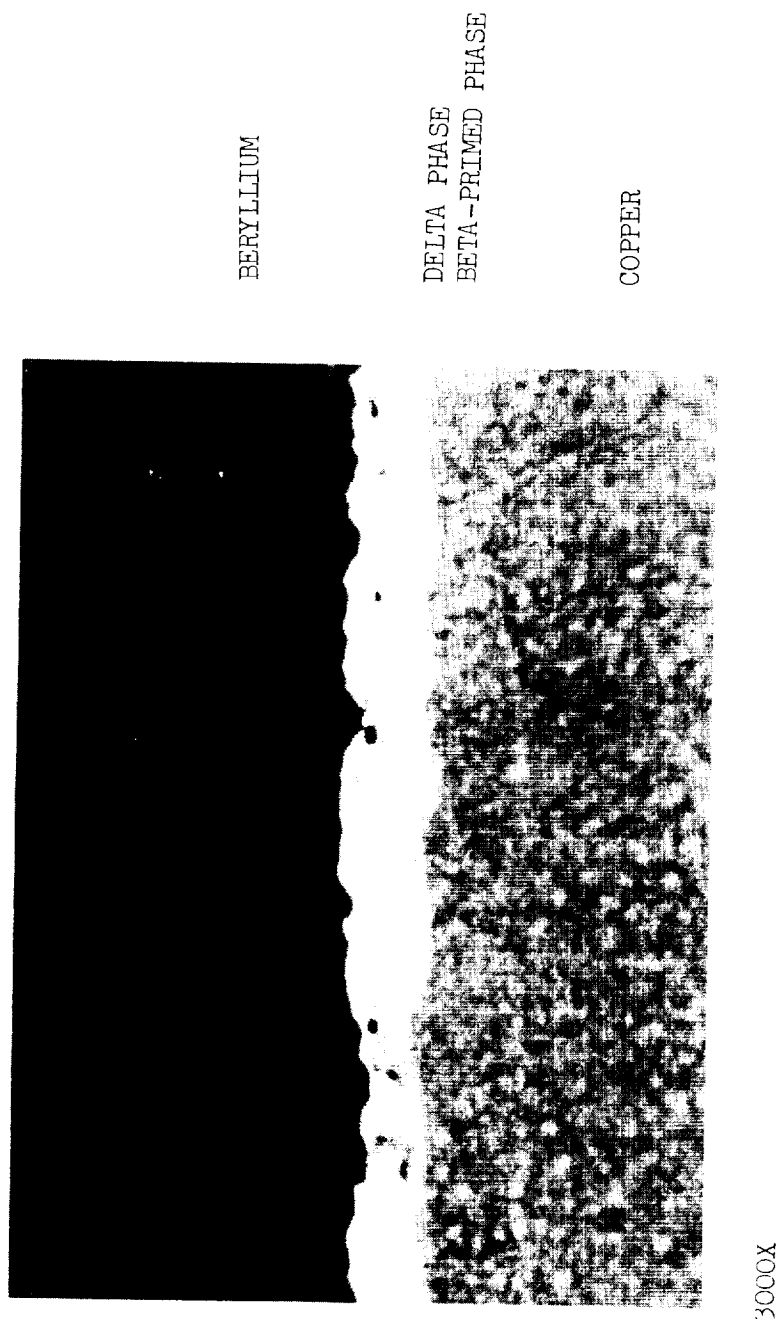


FIGURE 137. SPECIMEN A - SHOWING PRODUCTS OF THE INTERFACIAL REACTION BETWEEN BERYLLIUM AND COPPER

beryllium at the top.

Critical examination of the microphotographs revealed areas with no interfacial diffusion or bonding. As illustrated in Figure 138, the copper-beryllium contact was adequate in the left side portion of the interface, but not in the right. The absence of an intermediate phase on the right may have been caused by a geometric separation, thin surface oxides, or by other impurities that were not removed during the surface preparation of the beryllium. The presence of such impurities will impede the diffusion of the copper.

6. Diffusion Bonding - Conclusions and Recommendations. The results of this limited investigation have demonstrated the feasibility of solid state diffusion bonding of beryllium. The kinetics of copper diffusion in beryllium are sufficient to permit the use of the metal for this purpose at temperatures of approximately 1,000°F; with a duplex cycle consisting of a first phase pressure of approximately 10,000 psi applied for approximately 4.5 minutes, followed by the second phase pressure of 3200 psi for at least 4 hours.

No specific reason was determined for the low strength or failure of the specimens that failed in the joint. It appears possible, however, that the ultimate failure may have been caused by the presence of a weak intermediate phase.

Uniform joint pressure is mandatory for copper diffusion bonding of beryllium; unbonded areas may occur if the pressure is too low. Objectives to be considered in the further development of the diffusion bonding process include:

1. Determine the minimum cycle temperature.
2. Determine the minimum cycle pressure.
3. Determine the minimum cycle time.
4. Determine whether a single cycle is feasible.
5. Determine the optimum combination of parameters to obtain the maximum bond strength.



FIGURE 138. SPECIMEN A - ADJACENT BONDED AND UNBONDED AREAS

The selection of the proper combination of temperature, pressure, intermediate diffusion material, and cycle time will result in the production of joints of maximum strength. However, the maximum available bond strength is dependent upon the proper selection of other factors. The five factors considered to be of greatest importance are:

1. Surface preparation .
2. Method of applying the diffusion metal.
3. Surface activators, e.g., titanium.
4. Proper selection of diffusion metal.
5. Ambient atmospheric control.

Mechanical grinding and polishing, chemical etching, vapor blasting, and electropolishing are four possible methods of surface preparation which may affect the average bond quality. The application of the diffusion metal layer may be by the physical placement of a sheet of foil, by electro or electroless deposition, or by vapor deposition in a vacuum. Other metals suitable for consideration include silver and aluminum. The effects of inert gasses and higher vacuums should be investigated.

It is imperative that, during any development program which may follow this feasibility study, a large number of specimens be produced under the most optimum conditions possible. The specimens should be representative of production assemblies. Only through the accomplishment of an adequate statistical sampling can the effects of small variations in processing be confidently determined. This knowledge is necessary if products of consistently high quality are to be produced.

#### SECTION IV. CONCLUSIONS AND RECOMMENDATIONS

The results of this investigation verified the feasibility of utilizing high-strength, mechanical fasteners, adhesive bonding, brazing, and diffusion bonding for the joining of beryllium components. Large beryllium structures can be successfully fabricated if the details of the joint geometry and of the assembly processes are carefully observed.

The results of the several investigations indicate the following conclusions:

#### A. MECHANICAL FASTENERS

1. Beryllium structures can be successfully assembled with high-strength fasteners such as Huckbolts and Jo-bolts.

2. The holes in which conventional fasteners will be installed must incorporate suitable clearance for the head-shank radius, must provide a minimum radial clearance, and must be etched to remove any surface defects.

3. An interference fit between the fastener and the hole cannot be tolerated.

4. Eccentricity in the joint area has an extremely deleterious effect on the joint efficiency, and should be avoided or minimized.

5. The efficiency of joints assembled with either beryllium or "Lockalloy" rivets is comparable to that exhibited by joints assembled with other high-strength rivets.

6. Suitable forging temperatures for the installation of beryllium and "Lockalloy" rivets appear to be 1350°F and 1000°F, respectively.

7. There appears to be no advantage in incorporating adhesive bonding in mechanically fastened joints.

#### B. ADHESIVE BONDING

1. Satisfactory beryllium to beryllium adhesive bonding has been accomplished on a laboratory scale; the feasibility of adhesive bonding as an assembly method for beryllium has been demonstrated.

2. The cleaning materials and techniques used during the preparation of the surface for bonding must be compatible with the bonding agent to be used.

3. In order to avoid recontamination of the cleaned beryllium parts, the bonding operation should be initiated as soon as possible subsequent to the cleaning operation.

4. Additional adhesive bonding development work is recommended. Although the feasibility of adhesive bonding as an assembly method has been demonstrated, further investigation and refinement of the processes are required. The optimization of the processes, the development of exact controls, and the establishment of routine production procedures have not yet been accomplished.

### C. BRAZING

1. Uniform zinc brazed joints of reasonable strength suitable for low temperature applications can be produced consistently.

2. All cleaning and surface preparation precautions must be observed if good joints are to be consistently produced.

3. Consistent, reliable procedures for plating beryllium, as the substrate for brazing, have been developed which make possible the assembly of high-strength brazed joints.

4. Additional brazing development work is recommended. Although joints of reasonable strength have been produced, the development of the processes beyond the laboratory stage and the establishment of routine production procedures have not yet been accomplished.

### D. DIFFUSION BONDING

1. The diffusion bonding of beryllium has been accomplished on a laboratory scale; the feasibility of diffusion bonding as an assembly method for beryllium has been demonstrated.

2. Additional diffusion bonding development work is recommended. Although diffusion bonded joints have been assembled on a laboratory scale, the development of preparation processes and procedures, the evaluation of various suitable intermediate materials, the investigation of the effects of various



inert gases and higher vacuums, the determination of firm parameters, and the establishment of routine bonding procedures have not yet been initiated.

## REFERENCES

1. Burns, A. B., R. F. Crawford, "Strength, Efficiency and Design Data for Beryllium Structures," USAF, Aeronautical Systems Division, Technical Report 61-692, February 1962.
2. Ingels, S., L. Riedinger, E. Schuette, "Development of Beryllium Structure for Space Vehicles," as presented at the Second International Conference on Beryllium Technology, Franklin Institute, Philadelphia, Pennsylvania, October 15-17, 1964.
3. Jacobson, M. I., M. L. Hammonds, "The Beryllium Rich End of Five Binary Systems," Lockheed Missiles and Space Company Report Number 2-53-64-2, July 15, 1964.
4. King, Bryce, "A Review of Advances in Beryllium Applications since the 1961 International Conference on the Metallurgy of Beryllium," as presented at the Second International Conference on Beryllium Technology, Franklin Institute, Philadelphia, Pennsylvania, October 15-17, 1964.
5. Rebholz, M., G. Wolff, "Beryllium Design and Development Summary Report," Lockheed Missiles and Space Company Report Number A701583, September 1964.
6. Sherman, P. G., Diffusion in Solids, McGraw - Hill, 1963.
7. Turner, H. C., "The Structural Application of Beryllium to the Gemini System," as presented at the Second International Conference on Beryllium Technology, Franklin Institute, Philadelphia, Pennsylvania, October 15-17, 1964.

## DISTRIBUTION

### INTERNAL

R-ME-DIR		R-P&VE-S
Mr. Kuers		Mr. Kroll
Mr. Wuenschel		
R-ME-A		R-P&VE-SA
Mr. Berge		Mr. Blumrich
R-ME-M		R-P&VE-SAE
Mr. Orr		Mr. Colley
Mr. Schwinghamer		R-P&VE-SAF
Mr. Holland	(5)	Mr. Garrett
R-ME-MM		R-P&VE-M
Mr. Wilson		Mr. Kingsbury
Mr. Brown		
R-ME-MMP		R-P&VE-MM
Mr. Schuerer		Mr. Cataldo
R-ME-MMS		R-P&VE-MMJ
Mr. Davis		Mr. Olsen
R-ME-MW		R-ASTR
Mr. Parks	(4)	R-ASTR-P
		Mr. Angele
R-ME-D		R-ASTR-M
Mr. Eisenhardt		Mr. Boehm
R-ME-T		R-TEST-DIR
Mr. Franklin		Mr. Heimborg
R-ME-TP		
Mr. Chesteen		MS-IP
R-P&VE-DIR		MS-IPL
Dr. Lucas		(8)
		MS-H

## THE FABRICATION OF BERYLLIUM - VOLUME VI.

## JOINING TECHNIQUES FOR BERYLLIUM ALLOYS

The information in this report has been reviewed for security classification. Review of any information concerning Department of Defense or Atomic Energy Commission Programs has been made by the MSFC Security Classification Officer.

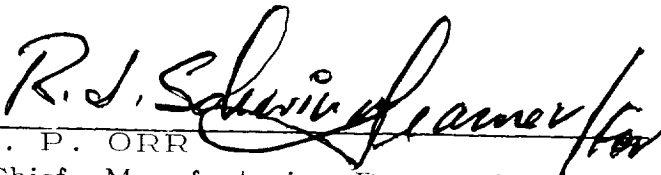
This report, in its entirety, has been determined to be unclassified.



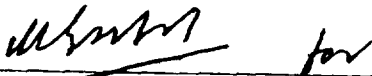
---

W. A. WILSON

Chief, Methods Development Branch



---

J. P. ORRChief, Manufacturing Research and  
Technology Division

---

WERNER R. KUERSDirector, Manufacturing Engineering  
Laboratory